

The leukaemogenic fusion protein
MOZ-TIF2 inhibits
Nuclear Receptor-mediated transcription
and mislocalises CBP

Thesis submitted for the degree of
Doctor of Philosophy
at the
University of Leicester

by

Philip J. F. Troke B.Sc. (Hons) (Leeds)
Department of Biochemistry
University of Leicester

December 2003

UMI Number: U601344

All rights reserved

INFORMATION TO ALL USERS

The quality of this reproduction is dependent upon the quality of the copy submitted.

In the unlikely event that the author did not send a complete manuscript and there are missing pages, these will be noted. Also, if material had to be removed, a note will indicate the deletion.



UMI U601344

Published by ProQuest LLC 2013. Copyright in the Dissertation held by the Author.
Microform Edition © ProQuest LLC.

All rights reserved. This work is protected against
unauthorized copying under Title 17, United States Code.



ProQuest LLC
789 East Eisenhower Parkway
P.O. Box 1346
Ann Arbor, MI 48106-1346

Declaration

Unless otherwise acknowledged, the experimental work in this thesis has been carried out by the author in the Department of Biochemistry at the University of Leicester between October 1999 and September 2003. The work has not been submitted, and is not presently being submitted, for any other degree at this or any other university.

Signed: 

Date: 28/11/03

Philip John Frank Troke

Department of Biochemistry,
University of Leicester,
University Road,
Leicester.
LE1 7RH.

copyright 2003

by

Philip John Frank Troke

**The leukaemogenic fusion protein MOZ-TIF2
inhibits Nuclear Receptor-mediated
transcription and mislocalises CBP**

Philip J. F. Troke

Synopsis

Chromosomal rearrangements associated with the M4/M5 subtype of Acute Myeloid Leukaemia include fusions of the gene encoding the histone acetyltransferase (HAT) MOZ with genes encoding the transcription factor coactivators TIF2, CBP or p300. The physiological roles of MOZ *in vivo* remain to be established. However, TIF2 functions to recruit the HATs CBP/p300 to ligand-bound Nuclear Receptors (NR), thus leading to transcription activation. Studies investigating the role of NRs and their ligands in haematopoiesis suggest that they aid the regulation of myeloid cell differentiation. The research described in this thesis therefore investigated the effect of the MOZ-TIF2 fusion protein on NR-mediated transcription. Expression of MOZ-TIF2 resulted in an inhibition of ligand-dependent transcription by the Retinoid X Receptor α , Retinoic Acid Receptor α and Estrogen Receptor α in the COS1 cell line. Further studies showed that MOZ-TIF2 also inhibited transcription mediated by endogenous NRs in the haematopoietic cell line U937. Investigation of protein interactions demonstrated that MOZ-TIF2 bound CBP through its Activation Domain 1 (AD1) and that deletion of this region resulted in the inability of the protein to inhibit NR transcription. Immunofluorescence analysis showed that MOZ-TIF2 formed a mesh-like nuclear pattern in contrast to the speckled nuclear localisations of MOZ, TIF2 and CBP. In addition, in cells expressing MOZ-TIF2, but not the AD1 deletion mutant, endogenous CBP displayed a diffuse staining pattern. Thus, the experiments described here show that MOZ-TIF2 inhibits NR-mediated transcription and mislocalises CBP, and that both of these activities are dependent upon its AD1. Further experiments investigating the effect of MOZ-TIF2 on p53 and AML1 -mediated transcription have indicated that MOZ-TIF2 also has the ability to affect the function of transcription factors in addition to NRs. Thus, expression of the MOZ-TIF2 fusion protein may result in the formation of leukaemia through the misregulation of normal haematopoietic transcription.

**Dedicated to my parents
Chris and Peter,
and my sister, Sarah**

Acknowledgements

The completion of this Ph.D. thesis would not have been possible without the hard work, advice and support of a large number of people. My most grateful thanks go to David, my supervisor, whose commitment to this work and to me made it all possible, and to Karin, for her friendship and her immeasurable help and advice with so many areas of the research described, in particular the immunofluorescence and co-immunoprecipitation studies. My thanks also to Sachiko for her assistance with the U937 transfection experiments, and to Hilary, Billy and Vic for their advice and friendship.

I would also like to thank a special group of people that have supported me through my life, and in particular the last four years. Firstly, my parents Chris and Peter and my sister Sarah, whose undying love and support have helped me achieve all that I have done. To Rich, whose ability to survive so many long journeys and hours in cold halls has meant so much to me; to Steph, for reminding me what it is all about these last eighteen months; to Bec and Richard for keeping the sherry replenished and the camp-bed to hand; and to Ann and Jo for letting me talk them into saying yes so often. Finally my thanks to all those in Birmingham and Leicester, and from planet Thanet, whose names are too long to list but who have been there whenever I have asked.

Abbreviations

9- <i>cis</i> RA	9- <i>cis</i> retinoic acid
AD1/2	p160 protein family Activation Domain 1/2
AF1/2	nuclear receptor Activation Function 1/2
AIB1	p160 protein Altered in Breast cancer 1
AML	Acute Myeloid Leukaemia
ANOVA	ANalysis Of VAriance
APL	Acute Promyelocytic Leukaemia
AT-RA	all <i>trans</i> retinoic acid
bHLH	basic-Helix-Loop-Helix motif
bp	base pairs of DNA
CBP	CREB-Binding Protein
cds	coding sequence
DBD	DNA-Binding Domain
DCSS	dextran-charcoal stripped serum
DNA	deoxyribonucleic acid
E2	17 β -oestradiol
ER	Estrogen Receptor
FCS	foetal calf serum
FITC	fluorescein isothiocyanate
GRIP1	p160 protein Glucocorticoid Receptor Interacting Protein 1
HAT	histone acetyltransferase
HBO1	Histone acetyltransferase Binding to Origin recognition complex 1
HDAC	histone deacetylase
HRE	hormone response element
HRP	horse-radish peroxidase
IVT	<i>In vitro</i> transcribed and translated
kb	kilobase pairs of DNA
LB	Luria Bertani
LBD	Ligand-Binding Domain
MORF	Moz Related Factor
MOZ	Monocytic Leukaemia Zinc Finger Protein

MOZ-TIF2	MOZ-TIF2 fusion protein
MOZ-TIF2mAD1	MOZ-TIF2 fusion protein containing a mutated AD1 (LLL-AAA)
MOZ-TIF2 Δ AD1	MOZ-TIF2 fusion protein containing a deletion of the AD1
MYST	MOZ, YBF2, SAS2, TIP60 protein family
NCoR	Nuclear Receptor Co-Repressor
NR	Nuclear Receptor
NID	Nuclear receptor Interaction Domain
p/CAF	p300/CBP Associated Factor
PAS	Per Arndt Sim homology domain
PCR	polymerase chain reaction
PHD	plant homeodomain
Pol.II	Polymerase II enzyme
PPAR	Peroxisome Proliferator Activated Receptor
PPRE	PPAR Response Element
RA	retinoic acid
RAR	Retinoic Acid Receptor
RARE	Retinoic Acid Receptor response Element
RLA	relative luciferase activity
RLU	relative light units
rpm	revolutions per minute
RXR	Retinoid X Receptor
R.T.	room temperature
SDS-PAGE	sodium dodecyl sulphate-polyacrylamide gel electrophoresis
S.E.M.	Standard Error of the Mean
SID	SRC1 Interaction Domain
SMRT	Silencing Mediator for Retinoid and Thyroid hormone receptor
SRC1	Steroid Receptor Coactivator 1
TF	Transcription Factor
TIF2	p160 protein Transcriptional Intermediary Factor 2
TRITC	tetramethyl rhodamine isothiocyanate
UTR	untranslated region of DNA

Table of Contents

Title Page	<i>i</i>
Declaration	<i>ii</i>
Copyright	<i>iii</i>
Synopsis	<i>iv</i>
Dedication	<i>v</i>
Acknowledgements	<i>vi</i>
Abbreviations	<i>vii</i>
Table of Contents	<i>ix</i>
Chapter One: Introduction	1
1.1 General introduction	2
1.2 Structure of DNA	2
1.3 Regulation of cell processes by chromatin structure	4
1.4 The covalent modification of chromatin	5
1.5 The histone code hypothesis	8
1.6 The Nuclear Receptor superfamily	10
1.7 The structure of Nuclear Receptors	10
1.8 Activation of transcription by Nuclear Receptors	15
1.9 Structure of the p160 coactivator family	21
1.10 CBP/p300 structure and function	27
1.11 Transcription factors and leukaemia	31
1.12 The role of RAR α and other NRs in haematopoiesis and Acute Myeloid Leukaemia	34
1.13 NR coactivators in haematopoiesis and AML	36
1.14 The structure and function of MOZ	38
1.15 The MOZ-CBP and MOZ-TIF2 leukaemogenic fusion proteins	42
1.16 Other MYST domain proteins	46
1.17 Research Aims	49

Chapter Two: Materials and Methods	50
2.1 General reagents	51
2.2 Tissue culture	51
2.2.1 Media, supplements and reagents	51
2.2.2 Cell line maintenance	51
2.2.3 Freezing down cells for liquid Nitrogen stocks	51
2.2.4 Thawing cells from liquid Nitrogen stocks	53
2.2.5 Stripped FCS for nuclear receptor transfections	53
2.2.6 Calcium phosphate-mediated transfection of adherent cells	53
2.2.7 Electroporation of suspension cells for reporter assays	55
2.3 Bacterial Manipulations	55
2.3.1 Bacterial strains	55
2.3.2 Liquid growth media	56
2.3.3 Solid growth media	56
2.3.4 Antibiotics	56
2.3.5 Sterilisation	56
2.3.6 Preparation of competent <i>E. coli</i> DH5 α cells	57
2.3.7 Transformation of DH5 α cells	57
2.3.8 Transformation of SURE [®] 2 bacterial cells	58
2.4 Molecular Biological Techniques	58
2.4.1 General reagents	58
2.4.2 Solutions	58
2.4.3 Small-scale plasmid purification from bacterial cells	61
2.4.4 Large- scale plasmid purification from bacterial cells	61
2.4.5 Caesium chloride purification of plasmid DNA	61
2.4.6 Phenol / chloroform extraction of DNA	62
2.4.7 Ethanol precipitation of DNA	62
2.4.8 Determination of nucleic acid concentration	63
2.4.9 Agarose gel electrophoresis	63
2.4.10 Isolation and purification of DNA from agarose gels	63
2.4.11 Oligonucleotides	63

2.4.12	Polymerase Chain reaction (PCR)	64
2.4.13	Recovery of DNA from PCR reactions	64
2.4.14	Generation of mutations / deletions by recombinant PCR	64
2.4.15	Annealing of single-stranded oligonucleotides	66
2.4.16	Polynucleotide Kinase treatment of DNA	66
2.4.17	Restriction enzyme digestion	66
2.4.18	Alkaline Phosphatase treatment of DNA	66
2.4.19	DNA ligation	66
2.4.20	Colony PCR screening	67
2.4.21	DNA sequencing	67
2.5	Biochemical Techniques	67
2.5.1	Solutions and buffers	67
2.5.2	Radiolabelled chemicals	69
2.5.3	Antibodies	69
2.5.4	Harvesting adherent cells for reporter assays	69
2.5.5	Harvesting suspension cells for reporter assays	70
2.5.6	Assay of transfected cells	70
2.5.7	Preparation of cells for immunofluorescence	71
2.5.8	Capturing of immunofluorescence images	71
2.5.9	Preparation of whole cell lysates	71
2.5.10	Protein co-immunoprecipitation	72
2.5.11	Protein concentration determination	72
2.5.12	Sodium Dodecyl Sulphate-Polyacrylamide Gel Electrophoresis	72
2.5.13	Coomassie staining of SDS-PAGE gels	73
2.5.14	Preservation of SDS-PAGE gels	73
2.5.15	Protein transfer to nitrocellulose membrane	73
2.5.16	Western blotting and immunodetection	73
2.5.17	Stripping membranes for re-probing	74
2.5.18	Small-scale bacterial expression of GST-tagged proteins	74

2.5.19	Large-scale bacterial expression of GST-tagged proteins	74
2.5.20	Purification of GST-tagged proteins	75
2.5.20	<i>In vitro</i> transcription and translation of expression vector -encoded cDNAs	75
2.5.22	GST-pulldown of <i>in vitro</i> translated protein	76
2.5.23	Fixing and amplifying radioactive SDS-PAGE gels	76
2.5.24	Exposure of radioactive gels to x-ray film	76
2.6	Construction of epitope-tagged MOZ and MOZ-TIF2 plasmids	77
2.6.1	Construction of the vector pcDNA3.0PT	78
2.6.2	pcDNA3.0PT:tag-MOZ	80
2.6.3	pcDNA3.0PT:tag-MOZ-TIF2	84
2.7	Yeast Experimental Materials and Methods	85
2.7.1	Yeast strain	85
2.7.2	Solutions	85
2.7.3	Yeast growth medium	85
2.7.4	Solid growth medium	85
2.7.5	Yeast transformations	86
2.7.6	Preparation of a yeast cell-free lysate	86
2.7.7	Antibodies	87
2.7.8	β -galactosidase assay for LacZ expression in yeast	87
2.8	Construction and analysis of LexA-MOZ fusion proteins	87
2.8.1	Construction of LexA expression vectors that span the entire MOZ sequence	88
2.8.2	Expression analysis of LexA-MOZ fusions in the <i>S. cerevisiae</i> strain L40	89
2.8.3	β -galactosidase assays to determine the auto-activation ability of the LexA-MOZ fusions in the L40 strain	91

Chapter 3: MOZ-TIF2 inhibits Nuclear Receptor AF2-mediated transcription	96
3.1 Introduction	97
3.2 The sub-nuclear distribution of MOZ-TIF2 is distinct from that of MOZ or TIF2	100
3.3 9- <i>cis</i> retinoic acid-dependent activation of a GAL4-responsive reporter by a GAL4-RXR α fusion reporter	105
3.4 TIF2 acts as a coactivator for GAL4-RXR α	110
3.5 GAL4-RXR α transcriptional activity is not enhanced by MOZ	110
3.6 MOZ-TIF2 does not enhance GAL4-RXR α -mediated transcription	110
3.7 MOZ-TIF2 acts as a dominant inhibitor of GAL4-RXR α :TIF2-mediated transcription	114
3.8 MOZ does not inhibit GAL4-RXR α :TIF2-mediated transcription	118
3.9 Inhibition of GAL4-ER α and GAL4-RAR α by MOZ-TIF2 but not MOZ	118
3.10 Chapter Summary	121
Chapter Four: The MOZ-TIF2 AD1 domain is essential for inhibition of GAL4-RARα-mediated transcription	124
4.1 Introduction	125
4.2 TIF2, but not MOZ nor MOZ-TIF2, interacts with NRs in a ligand -dependent manner <i>in vitro</i>	127
4.3 TIF2 and MOZ-TIF2 interact strongly with the CBP SID <i>in vitro</i>	131
4.4 Deletion of the MOZ-TIF2 AD1	136
4.5 Mutation of the MOZ-TIF2 AD1	138
4.6 Deletion of the MOZ-TIF2 AD1 results in loss of inhibition of GAL4-RAR α -mediated transcription	139
4.7 Deletion of the AD1 domain from MOZ-TIF2 results in a MOZ-like subnuclear localisation	141
4.8 Construction of truncated MOZ and MOZ-AD1 expression plasmids	145
4.9 Expression of a MOZ-AD1 fusion does not result in a MOZ-TIF2-like inhibition of GAL4-RAR α -mediated transcription	148
4.10 Truncated MOZ and MOZ-AD1 localise to nuclear foci	150
4.11 Statistical analysis of the inhibition of GAL4-RAR α by MOZ, MOZ-TIF2 and derivatives	153

4.12	Deletion of the MOZ-TIF2 AD1 abolishes <i>in vitro</i> binding to the CBP SID	153
4.13	TIF2 and MOZ-TIF2 interact with full-length CBP <i>in vitro</i>	157
4.14	MOZ-TIF2, but not MOZ-TIF2 Δ AD1, binds CBP in co-immunoprecipitation experiments	160
4.15	TIF2, but not MOZ, colocalises with CBP speckles	164
4.16	MOZ-TIF2 expression results in the loss of CBP speckles	165
4.17	Deletion of the MOZ-TIF2 AD1 prevents the fusion protein-mediated loss of CBP foci	170
4.18	Chapter Summary	176
Chapter Five: Effect of MOZ-TIF2 on transcription activation by endogenous Nuclear Receptors in U937 cells, and on exogenously expressed p53, ETS-2 and AML1		181
5.1	Introduction	182
5.2	Activation of RARE and PPRE luciferase reporters by endogenous NRs in the U937 haematopoietic cell line	185
5.3	MOZ-TIF2 inhibition of NR-mediated transcription in the U937 cell line is dependent upon the AD1 domain	186
5.4	Activation of luciferase reporter gene expression by p53	192
5.5	Inhibition of p53-mediated transcription of the IRGC-E4-Luc luciferase reporter by MOZ-TIF2	197
5.6	Activation of luciferase reporters by the ETS-2 transcription factor	197
5.7	MOZ-TIF2 does not appear to inhibit ETS2-mediated reporter gene transcription	202
5.8	Activation of the luciferase reporter pT109-Luc by AML1	202
5.9	CBP, but not MOZ nor MOZ-TIF2, activates AML1-mediated transcription	205
5.10	Co-transfection of MOZ-TIF2 with CBP results in potentiation of AML1/CBP-mediated transcription	209
5.11	MOZ does not enhance AML1/CBP-mediated transcription	212

5.12	MOZ-TIF2 enhancement of AML1/CBP-mediated transcription requires the AD1 domain	212
5.16	Chapter Summary	214
Chapter Six: Discussion		217
6.1	Function of MOZ	218
6.2	TIF2, Nuclear Receptors and a potential role in haematopoiesis	218
6.3	Effect of MOZ-TIF2 on Nuclear Receptor-mediated transcription	219
6.4	Role of the AD1 in MOZ-TIF2 function	220
6.5	The mechanism of MOZ-TIF2 inhibition of NR transcription correlates with the ability of the fusion protein to immortalise haematopoietic cells	222
6.6	MOZ-TIF2 forms a mesh-like nuclear localisation pattern and mislocalises CBP	224
6.7	Effect of MOZ-TIF2 expression on transcription activation by p53 and ETS-2	226
6.8	Summary Model for the effect of MOZ-TIF2 expression on NR- and p53- mediated transcription	228
6.9	MOZ-TIF2 as a coactivator for AML1-mediated transcription	230
6.9	Concluding remarks	231
Appendix One: Oligonucleotides		233
Appendix Two: Statistical analysis of GAL4-RARα inhibition		236
A2.1	Introduction	237
A2.2	Univariate Analysis of Variance	237
A2.2.1	Between-subjects factors	237
A2.2.2	Levene's test of equality of error variances	238
A2.2.3	Test of between-subjects effects	238
A2.3	<i>Post hoc</i> Bonferroni statistical test	239
A2.4	Conclusions	240
Bibliography		241

Chapter One:

Introduction

1.1 General introduction

The evolution of complex multi-cellular organisms has required the close cooperation of large numbers of specialised cells. These cells perform specific functions, which are carried out by the proteins they express. However, all cells of a multi-cellular organism are derived from a single egg and are thus, in theory, capable of expressing every protein the organism requires. Therefore, the coordinated regulation of gene expression to generate specific proteins in specialised cells is a key requirement for complex multi-cellular life. It is only with the development of modern biochemical and molecular biological techniques that the sophistication and complexity of these cellular control processes has become apparent. Our understanding, limited though it currently is, was made possible with the determination of the structure of deoxyribonucleic acid (DNA), and the breaking of the genetic code, fifty years ago (Watson and Crick, 1953b; Watson and Crick, 1953a).

1.2 The structure of DNA

Studies prior to 1953 had shown that DNA was made up of linked nucleotides, each of which was comprised of a deoxyribose sugar residue, a phosphoryl group and one of four possible bases: adenine, thymine, guanine and cytosine (Figure 1.1a). However, the structure of DNA, and its role in the cell was unknown. These questions were answered when Watson and Crick showed that the chains of nucleotides formed two anti-parallel DNA strands that wound around a common axis with a right-handed twist to form a $\sim 20\text{\AA}$ -diameter double helix (Watson and Crick, 1953b; Watson and Crick, 1953a). This arrangement resulted in the sugar-phosphate backbone coiling around the bases, which formed the core of the helix (Figure 1.1b). Thus the gross structure of the α -helix was unaffected by the sequence of the bases, allowing it to form a stable, relatively unreactive molecule, ideal for the passage of genetic information from one generation to the next. The bases on one strand interacted with the bases on the other through specific hydrogen bonding that only permitted an interaction between adenine and thymine, and one between guanine and cytosine. This meant that the anti-parallel DNA strands were complimentary and therefore, that both strands could be utilised during the synthesis of new DNA.

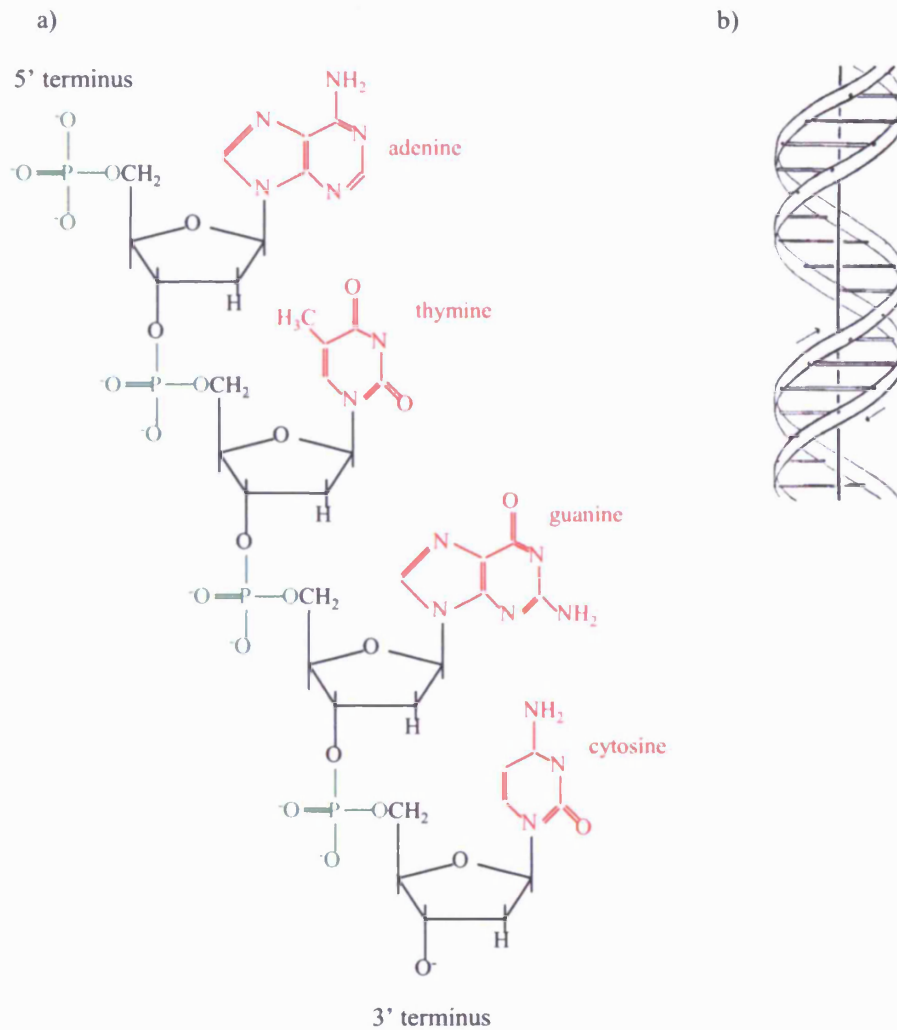


Figure 1.1: Schematics showing the structure of DNA

a) The structure of deoxyribonucleotides in a single DNA polymer is shown, with each nucleotide represented once. The sugar-phosphate nucleoside backbone of the molecule is shown in black and blue respectively and the four bases in red. With the exception of the hydrogen that denotes the molecules as deoxyribonucleotides, the ring carbon and hydrogen atoms are not shown. b) The original Watson and Crick schematic (1953a) of the helical structure of the DNA molecule. Arrows indicate the 5'-3' direction of the two strands, horizontal lines represent hydrogen-bonded base pairs and the vertical line, the central axis of the molecule.

The determination of the helical structure of DNA was only the first step in the path to understanding how DNA is packaged in a cell and utilised to encode life. Human DNA is ~1 m in length and yet fits into a ~10 μm cell nucleus. It must therefore be condensed in an ordered manner to allow access to specific regions as it is required. At the gross level, eukaryotic DNA is split into chromosomes, of which humans have 46. Each chromosome is packaged into chromatin through the interaction of proteins with the DNA. The basic unit of chromatin is the nucleosome (Kornberg and Lorch, 1999), which is made up of 147 base pairs of DNA wound 1.7 times around an octamer of the histone proteins H2A, H2B, H3 and H4 (Luger, 2003). This octamer is comprised of a tetramer core of two H3 and two H4 histones with an H2A:H2B dimer on either side. The DNA makes contacts with the nucleosome every 10 bases through the phosphodiester backbones of the strands. Thus the DNA sequence plays no direct role in its packaging. Between each nucleosome is a 10-60 bp length of linker DNA, thus giving rise to a basic repeating “beads on a string” nucleosome structure. The linker DNA is bound by the histone protein H1 at the point where it meets the nucleosome. The role of histone H1 is to further package the DNA into higher order structures through interactions with adjacent H1 proteins and nucleosomes. The first of these structures is the 30 nm helical “solenoid” chromatin fibre, whereby the string of nucleosomes coils to form a filament. However, the mechanism by which this process occurs, and the subsequent steps that result in further condensation of the DNA in interphase nuclei, are not well understood (Horn and Peterson, 2002). It is likely though, that these putative chromatin superstructures play a significant role in limiting protein access to the DNA. Thus, in addition to the genetic code, there is an epigenetic (or histone) code that is fundamentally important to the regulation of gene expression and other cellular processes involving DNA.

1.3 Regulation of cell processes by chromatin structure

Following mitosis, the high degree of chromatin condensation essential for metaphase is no longer required. Therefore as the cell enters interphase, regions of DNA are decondensed resulting in the formation of two distinct types of chromatin known as euchromatin and heterochromatin. Euchromatin is the most decompacted form and is gene-rich, acting as the site for the vast majority of gene transcription. In contrast, heterochromatin, which is predominantly gene-poor, remains densely packaged and thus is visible as darker stained

areas within the nucleus. The functions of heterochromatin will not be discussed here, but have been reviewed recently (Dillon and Festenstein, 2002).

Despite the decompaction of chromatin that occurs during the formation of euchromatin in the interphase nucleus, the higher order structures that remain are still repressive to many cellular processes such as gene transcription. Initially believed to be a hindrance to the cell, this repression of gene transcription in fact allows a very tight regulation of both global and individual gene expression. In order to overcome the repressive nature of chromatin structure and initiate gene transcription, two mechanisms are employed by the cell. The first is nucleosome remodelling, whereby nucleosomes are moved locally in an ATP-dependent manner to allow interaction of specific factors with the DNA. These ATP-dependent remodellers, which include the SWI/SNF, NURF and CHRAC complexes, will not be discussed in this thesis. However, two extensive reviews of the current research in this field have been published recently (Becker and Horz, 2002; Tsukiyama, 2002). The second mechanism, discussed below, is through the post-translational modification of the histones present in nucleosomes (Strahl and Allis, 2000; reviewed in Berger, 2002; Iizuka and Smith, 2003).

1.4 The covalent modification of chromatin

Histones are comprised of a globular central domain that forms a characteristic “histone fold” and mediates predominantly histone-histone interactions, and an N-terminal “tail”. These tails are not resolved in nucleosome crystal structures as they emanate out from the protein core and are exposed to the solvent (Luger, 2003) (Figure 1.2). As a result they are accessible to proteins that associate with nucleosomes or DNA. This allows them to be covalently modified. At least five such methods of post-translational modification of histones have been identified: acetylation, methylation, phosphorylation, ubiquitination and ADP-ribosylation, and enzymes that add or remove these groups are continually being documented. Histone acetylation is currently the most well understood form of chromatin modification. The addition of acetyl groups to lysine residues in the histone N-terminal tails is carried out by histone acetyltransferase enzymes (HATs) (Roth *et al.*, 2001).

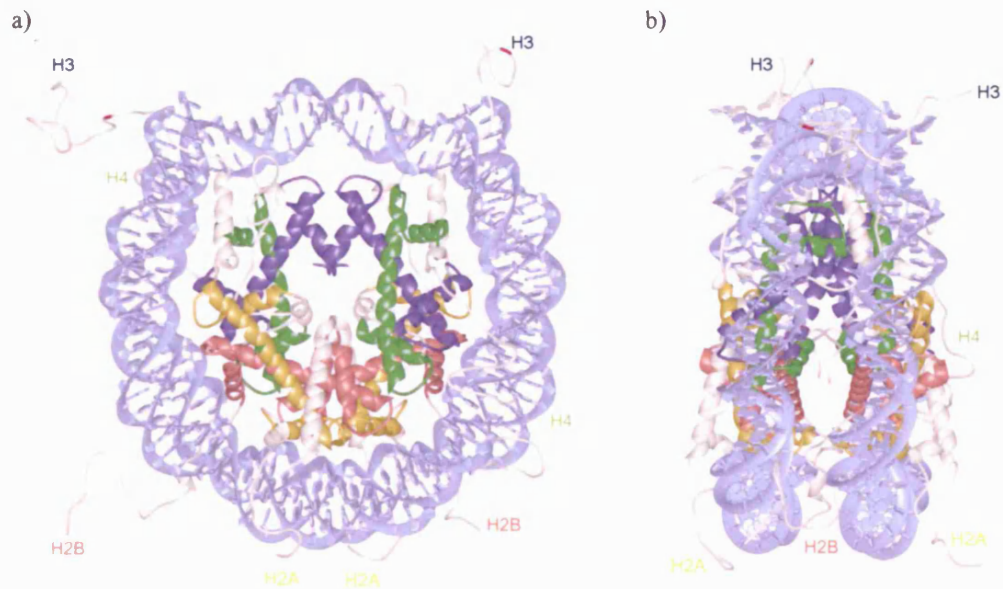


Figure 1.2: Structure of the nucleosome core particle

a) View down the superhelical axis of a nucleosome core particle (reproduced from Luger, K. (2003)) with the double-stranded DNA helix in light blue. The central histone fold domains are shown: H2A histones in red; H2B histones, yellow, H3 histones, dark blue; H4 histones, green. The histone tails, which emanate out from the central core, are indicated. b) Side view of the core particle (Luger, K. (2003)) resulting from a 90° rotation of Figure a) about the vertical axis. The coil of the DNA around the histone proteins is clearly visible.

In higher eukaryotes hyper-acetylation of histones is generally accepted as being associated with DNA that is actively being transcribed. In contrast, the removal of acetyl groups by histone deacetylases (HDACs) results mainly in repression and silencing (Cress and Seto, 2000). There are a number of families of HATs, often present in large multi-subunit complexes, which function in histone deposition, transcription regulation and DNA repair and synthesis (reviewed in Roth *et al.*, 2001). Two families of HATs, the CBP/p300 family and MYST family are discussed in greater detail below (Sections 1.10 & 1.16 respectively).

The importance of chromatin methylation by histone methyltransferases (HMTs) has also become apparent during the last five years. However, in contrast to acetylation, the correlation between methylation and transcriptional activation is less clear. Methylation of histone tails has been shown to be involved in both transcriptional silencing and activation. It appears that the effect of methylation is dependent upon the particular residue being methylated (arginine or lysine), its exact location within the histone tail and even the number of methyl groups (1-3) that are covalently attached (reviewed in Kouzarides, 2002; Bannister *et al.*, 2002). For example, methylation of Histone H3 lysine 9 functions to silence gene expression through both suppressing serine 10 phosphorylation and preventing acetylation of lysine 9 on Histone H3. In contrast, addition of a methyl group to Histone H3 lysine 4 or to arginine 17 (the latter by the NR coactivator CARM1; Section 1.9) is associated with active chromatin.

The roles of the three remaining histone modifications have been less extensively studied. However, recent publications suggest all play a role in the regulation of chromatin structure and thus function. The importance of histone phosphorylation was first identified in the condensation of chromatin during mitosis (discussed in Hans and Dimitrov, 2001). Subsequent studies have suggested that histone phosphorylation also plays a role in the activation of transcription, with high levels of phosphorylation of serine-10 on histone H3 associated with histone acetylation and actively transcribed genes (Featherstone, 2002 and references therein; Li *et al.*, 2002). The roles of ubiquitination and ADP-ribosylation of histones in the regulation of chromatin structure remains to be clarified but studies suggest ADP-ribosylation is also involved in transcriptional activation (Kraus and Lis, 2003). The role of ubiquitination in transcriptional regulation has not yet been confirmed, though it has

been hypothesised to act as another chromatin signalling mechanism as the high level of ubiquitination of histones H2A and H2B seen *in vivo* appears to have surprisingly little effect on overall chromatin folding (reviewed in Jason *et al.*, 2002).

The chromatin modifying proteins that add and remove covalent groups to and from histones, and the remodelling proteins mentioned in Section 1.3, are not DNA binding factors themselves. Rather they are coactivators and corepressors, known collectively as coregulators, that are recruited to the DNA by transcription factors (Lemon and Tjian, 2000). This separation between sequence-specific DNA binding and modification of chromatin structure allows a significant increase in the flexibility of transcription regulation. On the one hand, it increases complexity by allowing a single transcription factor to interact with multiple, often-opposing coregulators in a temporal manner, as determined by numerous signalling pathways. On the other, it allows some redundancy in that different transcription factors may recruit the same coregulator to achieve similar goals, such as the activation of transcription. This diversity of recruitment is further enhanced by the presence of coregulators in large complexes. Thus, some non-enzymatic coactivators that bind transcription factors in response to a particular signal act as platforms for recruitment of a number of chromatin modifiers. This is exemplified by the activation of gene transcription by nuclear receptors, as will be discussed in greater detail below.

1.5 The Histone Code Hypothesis

The covalent modification of histone residues was originally postulated to act by modulating histone-DNA and histone-histone interactions. Thus, bulk changes such as large-scale acetylation, which would result in an increased negative charge of the nucleosome, were postulated to weaken the interaction between the nucleosomes and DNA and open up the chromatin structure. However, this did not explain the huge diversity of possible modifications and complex nature of their arrangement, both globally and on individual histone tails. As a result a new theory was proposed (Strahl and Allis, 2000) that attempted to explain the complex nature of the covalent modifications found on histone H3. Strahl and Allis (2000) suggested that, rather than causing relatively large-scale changes to nucleosome structure, the modifications resulted in the alteration of particular

surfaces of the nucleosome. These changes were postulated to affect the binding of specific factors to the nucleosome, resulting in the dissociation of some and recruitment of others. In effect the modifications on nucleosomes covering a single gene promoter could be 'read' by the binding of these associated proteins, and depending on which were associated, the gene would be transcribed or silenced. This theory has been expanded as it has become clear that the presence of particular modifications on a tail can be read by other chromatin modifying enzymes and lead to either their recruitment to the chromatin and addition of more groups, or preclude additional modifications (Li *et al.*, 2002). Furthermore, in addition to the idea of cross-talk between modifications in a single histone tail, evidence is now emerging of cross-talk in *trans* as modifications on one histone tail have been shown to affect the addition of groups to another, both in the same nucleosome and on adjacent ones (reviewed in Fischle *et al.*, 2003).

Combining the hypothesis of a histone code with the findings of other studies describing the activation of gene expression, the cascade of events leading to transcription of a previously silent gene may be summarised in very general terms as follows: activation of a specific transcription factor by a signalling pathway causes an alteration of its structure that results in binding DNA (if not already bound), the dissociation of corepressors and the recruitment of coactivator proteins. The chromatin remodelling coactivators alter the position of the nucleosomes covering the gene promoter to enhance transcription activation while the recruited chromatin modifying coactivators remove covalent groups that signal the gene as silent and add new groups that signal the gene is active. The presence of these highly specific covalent modifications in conjunction with the bound coactivator complexes results in the recruitment of the basal transcription machinery in the form of the RNA Polymerase II complex and general transcription initiation factors (Reese, 2003), which then initiate gene transcription. A schematic showing these steps as envisaged for transcription activation by the Class II Nuclear Receptors is shown in Figure 1.5 and is discussed in Section 1.8.

The considerable complexity provided by coregulator proteins (Lemon and Tjian, 2000) has meant that the relative impact and order of recruitment of the various mechanisms controlling chromatin structure has been a major source of interest (Featherstone, 2002). In an attempt to answer these questions, studies have investigated the transcription of

individual genes by specific transcription factors. Due to the ease with which they can be activated by addition of ligand, Nuclear Receptor (NR) transcription factors provide an ideal system with which to investigate the role of different protein complexes in the initiation of transcription

1.6 The Nuclear Receptor superfamily

Lipophilic hormones such as the steroid and thyroid family are released by endocrine glands, which include the gonads, thyroid glands and adrenal cortex. They play a crucial role in both tissue development / differentiation and normal metabolic processes. Such hormones control gene expression through binding to, and activation of, a large group of transcription factors known as the Nuclear Receptors (NRs). This superfamily is comprised of over 150 members present in both vertebrates and invertebrates (Mangelsdorf *et al.*, 1995; Aranda and Pascual, 2001). Classification through differing DNA-binding and dimerisation properties has allowed division into four broad sub-groups. The steroid receptors form Class I, and bind the steroid hormones, which include oestrogen and androgen. These receptors bind as homodimers to palindromic DNA sequences known as hormone response elements (HREs) present in the promoters of responsive genes. Class II is made up of the non-steroidal nuclear receptors, the majority of which bind DNA as heterodimers, with the Retinoid X Receptor (RXR) as the common dimerisation partner. This family is made up of the NRs that bind the thyroid, retinoid, fatty acid and prostaglandin hormones. The members of Class II bind palindromic, direct repeat or inverted palindromic response elements. The final two families, Classes III and IV, are the “orphan” nuclear receptors (Giguere, 1999), many of which still have no identified ligand. Class III preferentially bind direct repeats as homodimers, while Class IV preferentially bind to extended core sequences as monomers.

1.7 The structure of Nuclear Receptors

Our understanding of the mechanism of transcriptional activation by nuclear receptors has been greatly aided by structural analysis of individual NR domains (reviewed in Moras and Gronemeyer, 1998; Renaud and Moras, 2000). Nuclear receptors share a common basic

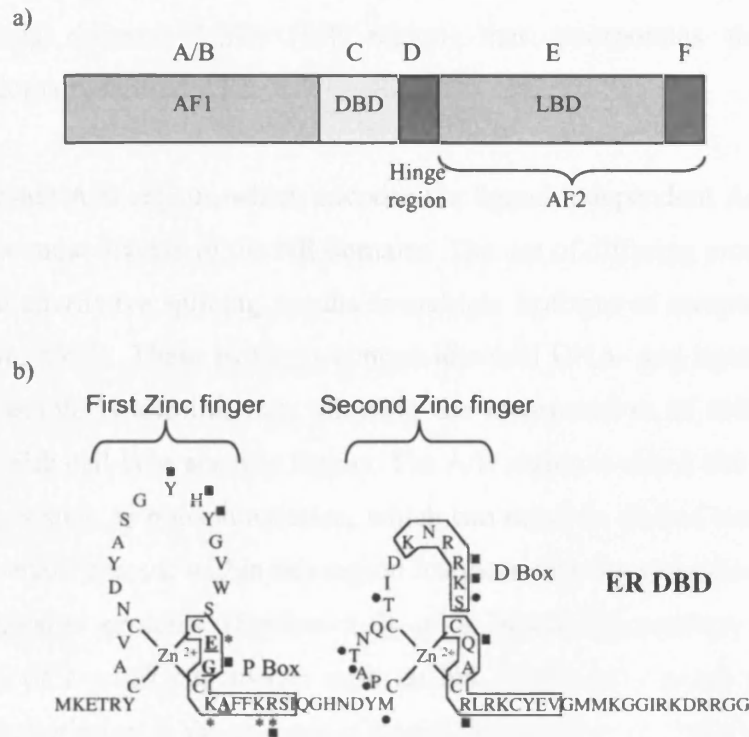


Figure 1.3: Schematic of the overall domain structure of NRs and of their DNA-binding domain

a) The domain (A-F) structure of NRs is shown with their function indicated. AF1, ligand-independent Activation Function-1; DBD, DNA-binding domain; LBD, ligand-binding domain; AF2, ligand-dependent Activation Function-2. b) Schematic showing the amino-acid sequence and zinc-fingers of the ER α DNA-binding domain (reproduced from Renaud and Moras (2000)). Residues forming α -helices are boxed; the P-box residues that direct half-site specificity are underlined; squares indicate residues making contacts with the phosphate groups of the DNA backbone; asterisks, those making contacts with nucleotide bases; circles, residues involved in mediating receptor dimerisation.

structure made up six regions (Figure 1.3a): the N-terminal A/B region that incorporates the (ligand-independent) activation domain, AF1; a central DNA-binding domain (DBD) or region C; a hinge (D) region containing the nuclear localisation signal; and a C-terminal ligand-binding domain (LBD) (E/F region) that incorporates the ligand-dependant activation domain, termed AF2.

The N-terminal A/B region, which encodes the ligand-independent Activation Function-1 (AF1), is the most diverse of the NR domains. The use of differing promoters and initiation codons, and alternative splicing, results in multiple isoforms of receptors such as the RAR (Leroy *et al.*, 1991). These isoforms contain identical DNA- and ligand- binding domains but very variable N-termini, thus allowing the incorporation of cell-specificity through interaction with cell-type specific factors. The A/B region is also a site of post-translational modifications such as phosphorylation, which can result in altered transcriptional activity. The AF1 domain present within this region interacts with the glutamine-rich domain of the p160 coactivator proteins (Section 1.9) in a ligand-independent manner. Thus, co-transfection of a p160 coactivator with an NR results in a small potentiation of NR-mediated transcription in the absence of ligand (Sheppard *et al.*, 2001). However, mutation of the SRC1 (Sheppard *et al.*, 2001) or TIF2 (Voegel *et al.*, 1998) LXXLL motifs that mediate the ligand-dependent interaction with NRs (Sections 1.8 and 1.9) results in a drastic reduction in ligand-mediated transcription activation whereas deletion of the glutamine-rich region has a negligible effect. Thus, this AF1 interaction appears to play only a minor role in ligand-dependent activation by ER. Studies investigating the interaction of the p160 coactivator family with other NRs suggest that the importance of the AF1 domain varies with the receptor and coactivator investigated, and the cell type and promoter examined. However, for the significant majority of NRs, with the notable exception of the Androgen Receptor (AR) (Ma *et al.*, 1999), the AF1 domain appears to function predominantly as a secondary stabilising interaction site for the p160 coactivators, rather than as a primary mechanism for coactivator recruitment to active NR complexes.

Crystal and NMR structures of several NR DBDs have been determined (reviewed in Renaud and Moras, 2000) and these have characterised the DNA-Binding Domain (DBD) as the most structurally conserved of the nuclear receptor domains. It contains two α -helices, each incorporating a zinc finger motif coordinated by four highly conserved

cysteine residues (Figure 1.3b). The first “recognition” helix binds in the DNA major groove. At its C-terminal end is a motif known as the “P-Box”. This short sequence is located at the base of the first zinc finger and determines the DNA-binding specificity through specific contacts with individual bases. The second α -helix is involved in NR dimerisation and is orientated at 90° to the first. Present within this zinc finger structure is the “D Box”, which is involved in determining dimerisation specificity. In addition to the sequence encoding the two α -helices and zinc finger motifs, the DBD of the Class II NRs contains a C-terminal Extension (CTE). This region encodes two further motifs, the “T-Box” and “A-Box”. The A-Box contacts the nucleotide bases flanking the core recognition sequence and is important for the high affinity binding to the DNA of thyroid hormone receptor (TR) monomers and homodimers, though not for receptors such as RXR and RAR. For these receptors, the T-box appears to be more important for dimerisation and high affinity binding.

The hinge region, also known as the D domain, is not particularly well conserved between different NRs. It acts as a flexible linker between the DNA-binding and ligand-binding domains, thus allowing rotation of the LBD relative to the DBD. Most NRs contain a nuclear localisation signal within this domain.

The E Region acts as the Ligand-Binding Domain (LBD) of the NR with Region F forming a short C-terminal extension to it. The LBD is relatively conserved structurally, though the F region is more variable. The interface between the E and F regions forms the surface utilised during recruitment of coactivators and corepressors, and therefore the domain formed by these two regions is termed the Activation Function 2 (AF2) domain. Thus the AF2 functions as the ligand-dependent transactivation module. In addition, it provides the predominant interaction surface for heat shock proteins and is also involved in receptor dimerisation (reviewed in Moras and Gronemeyer, 1998). The crystal structures of several ligand-binding domains have been solved (Renaud and Moras, 2000 and references therein) and highlight the similarities in the overall structure of the domain between different NRs.

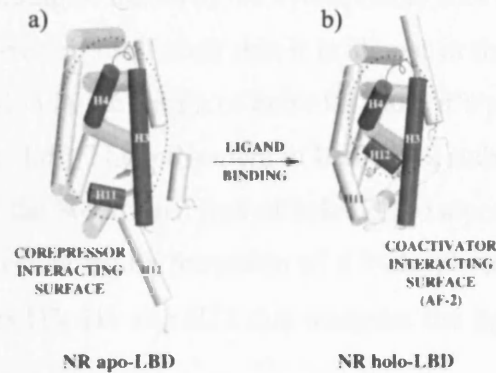


Figure 1.4: Structure of the NR Ligand Binding domain

The α -helical ligand-binding domain (LBD) structures of the RXR (a) and RAR (b) nuclear receptors are shown in the absence (apo-NR) and presence (holo-NR) of ligand respectively (reproduced from Renaud and Moras (2000)). The dotted ovals indicate the interacting surfaces for co-repressors in the apo-NR structure and coactivator proteins in the holo-NR structure. The repositioning of Helix H12 upon binding of ligand is clearly visible, and results in the increased specificity of the LBD for coactivators over corepressors.

The ligand-binding domain (LBD) is comprised of twelve α -helices and one β -turn that form an anti-parallel three-layered structure with the ligand-binding pocket at the centre. Figure 1.4 (modified from Renaud and Moras, 2000) shows the LBD in the non-liganded (a: apo-RXR LBD) and ligand-bound (b: holo-RAR LBD) conformational states. In the absence of ligand (apo-receptor) α -helix H12 “floats” clear of the rest of the structure and a relatively large hydrophobic binding surface for corepressor proteins is formed by helices H3, H4 and H11. The binding of ligand in the hydrophobic core of the domain causes helix H11 to lengthen and reposition itself such that it is almost in the plane of helix H10. This in turn results in a reduction in the length of helix H12 and its positioning over the ligand-binding pocket to form a “lid”. The movement of helix H12 stabilises binding of the ligand and allows movement of the N-terminal part of helix H3 to a position under helix H6. This conformational change results in the formation of a hydrophobic binding cleft comprised of the NR LBD α -helices H3, H4 and H12 that mediates the ligand-dependent interaction with coactivator proteins.

1.8 Activation of transcription by Nuclear Receptors

In the absence of ligand the Class II family of NRs such as RAR and PPAR are bound to the DNA in complex with the corepressor proteins “Silencing Mediator for Retinoid and Thyroid hormone receptors” (SMRT) and “Nuclear Receptor CoRepressor” (N-CoR) (reviewed in Jones and Shi, 2003). Interaction of SMRT and NCoR with NRs is mediated by NR binding motifs present in their C-termini, which form amphipathic α -helices similar to those found in NR coactivators such as the p160 family (Section 1.9). At their N-termini, SMRT contains four N-terminal repression domains and NCoR three. These mediate recruitment of histone deacetylases (HDACs), both through direct interactions and through binding of the corepressor to the platform protein Sin3, which in turn associates with HDACs. The recruitment of HDACs to the DNA-bound NR complex results in the removal of acetyl groups from the histone N-termini in the vicinity of the complex. This leads to the repression of basal transcription, thus allowing a greater induction of transcription upon ligand binding and coactivator recruitment. In contrast, the Class I Steroid Receptors are not bound to the DNA in the absence of ligand. Instead, these NRs are found in cytoplasmic complexes with heat shock proteins such as hsp90 (reviewed in Cheung and Smith, 2000).

For both Class I and Class II Nuclear Receptors, the binding of their cognate ligand results in a conformational change in the NR LBD (discussed in Section 1.7) that causes the dissociation of bound proteins. For the Steroid Receptors, this means the dissociation of the chaperone complex that mediates sequestration of the NR in the cytoplasm, thus allowing translocation to the nucleus and binding to HRE's in responsive genes. Class II NRs are in some cases known to be already present on the DNA and thus hormone binding results in the dissociation of the associated corepressor protein complexes. In addition to mediating the dissociation of these proteins, the conformational change induced by the binding of ligand promotes the association of coactivator complexes (Aranda and Pascual, 2001; McKenna and O'Malley, 2002). These proteins alter the chromatin structure surrounding the NR-bound promoter of the responsive gene. This in turn allows the association of the general transcriptional machinery and the initiation of transcription.

Studies investigating the activation of individual promoters have identified distinct coactivator complexes that play a role in NR-mediated transcription. The most studied NR coactivator complex is the p160 CBP/p300 complex. The p160 proteins (Leo and Chen, 2000) are a family of coactivators that act as non-enzymatic bridging factors to recruit enzymes with chromatin modification properties such as CBP/p300 and the histone methyltransferases CARM1 and PRMT1. The interaction of the p160 proteins with the NR complex is mediated by binding of leucine-rich "LXXLL" motifs (Heery *et al.*, 1997) present in the p160 NR Interaction Domain (NID) to the NR LBD (Section 1.9). This motif forms an amphipathic α -helix that sits in the hydrophobic cleft generated by the ligand-induced conformational change in the LBD. A second complex related to the yeast Mediator complex has also been shown to interact with ligand-bound NRs through the use of LXXLL motifs. The interaction of this multi-subunit complex, termed the TRAP (Thyroid Receptor Associated Protein), DRIP (vitamin D Receptor Interacting Protein) or metazoan Mediator complex (reviewed in Rachez and Freedman, 2001) with NRs is mediated by the TRAP220 / DRIP205 subunit, which binds the hydrophobic cleft in the ligand-bound LBD via two LXXLL motifs (Coulthard *et al.*, 2003). Though no enzymatic activity has been shown for this complex, it appears to function as a bridging factor between the active NR complex and the general transcriptional machinery.

One of the first studies describing coactivator recruitment to endogenous promoters was carried out using chromatin immunoprecipitation (ChIP) analysis of ER activation of the Cathepsin D and *pS2* promoters in the human breast cancer cell line MCF-7 (Shang *et al.*, 2000). ER α , AIB1 (a member of the p160 family) and the TRAP220 protein were found to be recruited to these promoters within 15 min of oestradiol addition. The presence of the p160 protein results in the rapid recruitment of p300, which correlates with histone acetylation and the opening-up of the chromatin. This allows the recruitment of the Pol.II complex and transcription initiation. Concurrent with this, the Pol.II C-terminal domain is phosphorylated, p300 dissociates and CBP is recruited. Associated with CBP is a second HAT P/CAF (p300/CBP Associated Factor) (Yang *et al.*, 1996). The activity of these two proteins further increases the acetylation level of the histones surrounding the promoter. CBP also functions to acetylate the p160 protein (Chen *et al.*, 1999b) resulting in the dissociation of the ER α p160 complex. This complete process appears to take approximately 90 minutes. However, further time points indicated that ER α activation of these promoters is a cyclical process. Additional rounds of transcription occur in a manner nearly identical to the first. However, p300 does not appear to be required for these subsequent cycles, possibly due to the level of histone acetylation between rounds not dropping to the basal level seen before the first round of transcription.

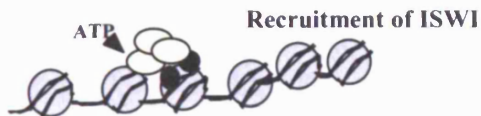
The seminal work by Shang *et al.* (2000) describing coactivator recruitment by a ligand-bound NR has been extended by a number of papers that have investigated the interplay of chromatin modifying coactivator proteins in NR-mediated transcription. Phosphorylation of histone H3 serine-10 has been shown to enhance acetylation of histone H3 (Li *et al.*, 2000), while the methyltransferase CARM1, which is recruited to the *pS2* promoter following acetylation of histone H3, acts as an NR coactivator through methylation of H3 arginine-17 (Daujat *et al.*, 2002). Thus, activation of transcription by NRs involves the coordinated modification of histones by a number of coactivator proteins.

In addition to the studies describing the interplay of different chromatin modifications, the roles of the TRAP complex and chromatin remodelling enzymes have been investigated. Though it is still unclear as to whether they are recruited concomitantly (Sharma and Fondell, 2002), the TRAP and p160 CBP complexes have both been shown to stimulate the formation of the first Pol.II pre-initiation complex (Shang *et al.*, 2000; Acevedo and Kraus, 2003). In contrast to the p160 CBP complex however, the TRAP complex appears to have an additional role in promoting reassembly of the Pol.II complex during subsequent rounds of transcription (Acevedo and Kraus, 2003). Evidence is also emerging for the role of chromatin remodelling enzymes in the activation of transcription by NRs (Huang *et al.*, 2003) and has resulted in the proposal of a multi-stage model (described in Dilworth and Chambon, 2001) of transcription activation by NRs (Figure 1.5). Investigations into the temporal recruitment of HAT and remodelling complexes by NRs suggest that remodelling complexes are first required prior to any activation steps in order to strengthen the weak ligand-independent binding of Class II NR dimers to the DNA. Once bound, the apo-NR dimer recruits corepressors to silence basal transcription. Binding of ligand, which acts to initiate the transcriptional activation process, results in the dissociation of the corepressors and the immediate recruitment of histone acetyltransferases and methyltransferases by the p160 proteins. The HAT activity of these coactivators is required for the efficient recruitment of the Pol.II pre-initiation complex by the Mediator/TRAP complex, suggesting that histone acetylation is likely to be a prerequisite for further stages in gene expression. Remodelling complexes then appear to be recruited a second time in order to remodel the proximal promoter to permit tight binding of the basal transcription factors and the activation of transcription. Thus, transcription activation by NRs appears to be a complex process involving a wide range of coactivator proteins in order to facilitate the recruitment of the basal machinery and the initiation of transcription. Central to this process however, is the recruitment of HAT enzymes by the non-enzymatic p160 coactivator family.

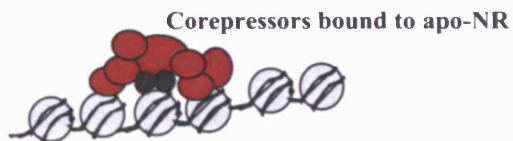
Figure 1.5: Multi-stage model describing transcription activation by NRs

A schematic is shown of the stages that appear to be required for the activation of transcription by NRs. In the absence of ligand, Class II NRs such as the RAR/RXR dimer associate weakly with their response elements. However, recruitment of the ISWI remodelling complex results in the remodelling of the chromatin surrounding the promoter and an increase in the strength of binding. The DNA-bound NR dimers recruit corepressor proteins and associated histone deacetylase and DNA methylase enzymes that modify the histones and DNA, thus leading to the inhibition of basal transcription. Upon addition of ligand the corepressor proteins dissociate and the p160 coactivator complex binds. The presence of the histone acetyltransferases CBP/p300 and P/CAF in this complex, and the subsequent recruitment of the methyltransferases CARM1 and PRMT1 results in histone acetylation and methylation, thus opening up the chromatin structure. CBP-mediated acetylation of the p160 then causes the dissociation of this complex, allowing the recruitment of Mediator/TRAP. Interactions between this complex and components of the Pol.II holoenzyme results in its association before a further round of chromatin remodelling by the SWI/SNF complex leads to the initiation of transcription.

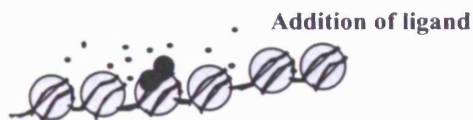
**Chromatin remodelling
allows tight NR binding**



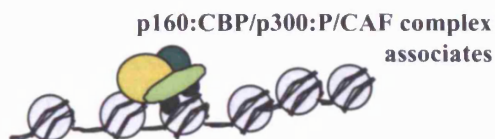
**Histone deacetylation
and DNA methylation**



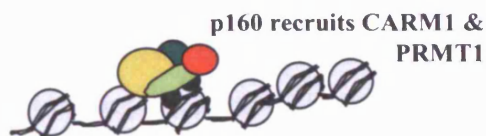
Corepressor displacement



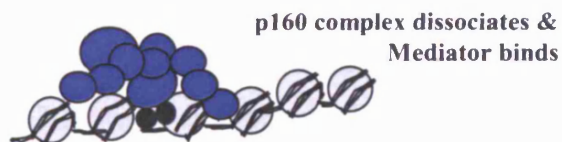
Histone acetylation



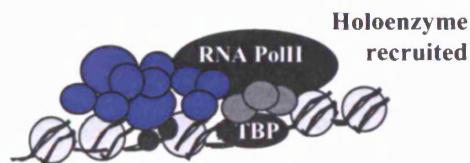
Histone methylation



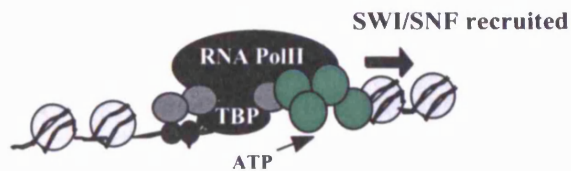
Mediator assembly



PIC assembly



**Chromatin remodelling
allows transcription initiation**



1.9 Structure of the p160 coactivator family

Steroid Receptor Coactivator 1 (SRC1), the first member of the p160 coactivator family to be identified (reviewed in Leo and Chen, 2000; Xu and Li, 2003), was isolated in a yeast 2-hybrid screen for human proteins that interact with the LBD of the Progesterone Receptor (PR) and shown to act as a coactivator for all the steroid receptors (Onate *et al.*, 1995). Subsequent work identified the related murine protein GRIP1 (GR-Interacting Protein 1) (Hong *et al.*, 1997), while the human homologue of GRIP1, TIF2 (Transcription Intermediary Factor 2), was isolated in a far-western screen for RAR and ER-binding proteins (Voegel *et al.*, 1996). The final member of the family was identified simultaneously by several groups and called: ACTivator for Thyroid and Retinoid hormone receptors (ACTR) (Chen *et al.*, 1997), p300/CBP Co-integrator-associated Protein (p/CIP) (murine homologue) (Torchia *et al.*, 1997), Amplified In Breast cancer 1 (AIB1) (Anzick *et al.*, 1997), Receptor Associated Coactivator 3 (RAC3) (Li *et al.*, 1997) and Thyroid Receptor Activator Molecule 1 (TRAM-1) (Takeshita *et al.*, 1997).

All three members of the p160 family share a common domain structure (Figure 1.6). At their N-terminus is the basic-Helix-Loop-Helix-Per-ARNT-Sim (bHLH-PAS) domain, which shows the highest degree of conservation between the family members. Though the p160 coactivators were originally thought to act purely as NR-specific coactivators, these two protein interaction regions have recently been shown to mediate binding to, and coactivation of, the four members of the Transcription Enhancer Factor (TEF) family of proteins (Belandia and Parker, 2000). TEFs act as developmentally regulated transcription factors that play important roles in both organogenesis and central nervous system development (Jacquemin *et al.*, 1996). Present in the N-terminus of the p160 family member SRC1, following the bHLH-PAS domain, is a region that mediates interaction with the STAT3 transcription factor (Giraud *et al.*, 2002). STAT3 is a member of the cytoplasmic STAT family of proteins that translocate to the nucleus following phosphorylation. They function to activate genes that regulate progression from G1 to S phase of the cell cycle. Expression of responsive genes by STAT3 requires the recruitment of CBP, and the study by Giraud *et al.* (2002) suggests that it is through the enhancement of this recruitment that SRC1 functions.

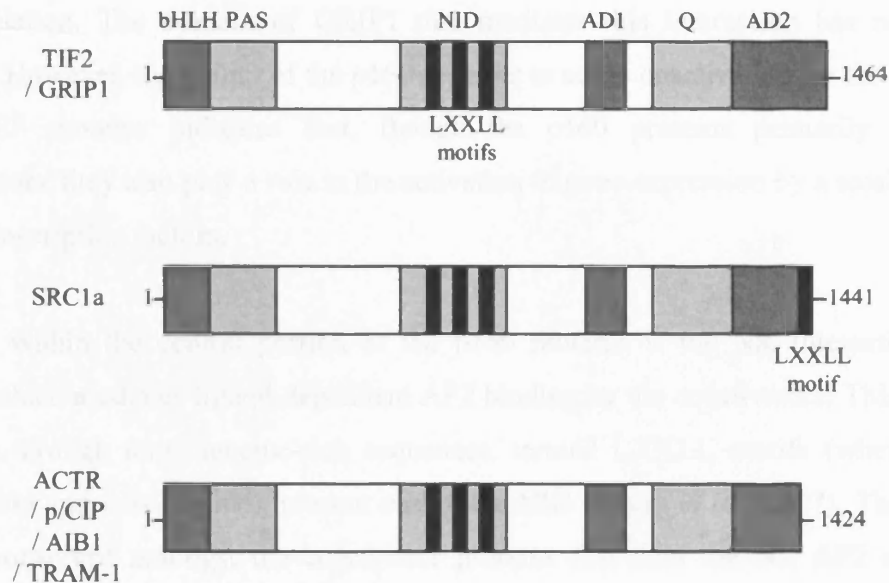


Figure 1.6: Domain structure of the p160 coactivator proteins

Domain structure schematics of the p160 coactivators TIF2/GRIP1, SRC1e and ACTR/pCIP/AIB1/TRAM-1 are shown. A basic-Helix-Loop-Helix (bHLH) domain and a Per-Arndt-Sim (PAS) domain are present in the N-terminus. The central Nuclear Receptor Interaction Domain (NID) mediates ligand-dependent interaction with Nuclear Receptors through three LXXLL (L, leucine; X, any amino acid) motifs (shown in black). The C-terminus contains the AD1 (Activation Domain 1) that mediates interaction with CBP, the glutamine-rich (Q) domain that acts as a secondary ligand-independent NR interaction domain, and the AD2 (Activation Domain 2) through which the p160 binds the methyltransferases CARM1 and PRMT1. In addition, SRC1a contains a fourth LXXLL motif at its extreme C-terminus. SRC1 also binds STAT3 via an extended region in its N-terminus. “Numbers” indicate the lengths of the proteins in amino acids.

The p160 protein GRIP1 has been shown to act as a coactivator for the MEF2C protein (Chen *et al.*, 2001). This transcription factor is a member of the Myocyte Enhancer Factor 2 family that cooperates with the MyoD transcription factors to control muscle cell differentiation. The domain of GRIP1 that mediates this interaction has not yet been defined. However, the ability of the p160 proteins to act as coactivators for the TEF, STAT and MEF proteins indicates that, though the p160 proteins primarily act as NR coactivators, they also play a role in the activation of gene expression by a small number of other transcription factors.

Located within the central portion of the p160 proteins is the NR Interaction Domain (NID), which mediates ligand-dependent AF2 binding by the coactivators. This interaction is made through three leucine-rich sequences, termed LXXLL motifs (where X is any amino acid and L is leucine), present within the NID (Heery *et al.*, 1997). The motifs are highly conserved amongst the coactivator proteins that bind the NR AF2 domain in a ligand-dependent manner. However, Class I and II NRs do display some specificity for the three p160 proteins (Ding *et al.*, 1998; Kalkhoven *et al.*, 1998). In addition, a broad, though not universal ability of NRs to bind particular LXXLL motifs in each of the p160 coactivators (McInerney *et al.*, 1998), coupled with the finding that a single p160 protein is able to bridge the two AF2 domains present within an NR dimer (Nolte *et al.*, 1998), suggests that the p160 protein may be orientated in a particular manner relative to the NR dimer. The LXXLL motif forms an amphipathic α -helix with the leucine residues projecting into the groove formed when the NR LBD α -helix H12 moves over the ligand-binding pocket in response to ligand binding (Section 1.7). This coactivator NR interaction is further strengthened by a charged clamp involving highly conserved lysine and glutamate residues present within the NR, and the backbone amides and carbonyl groups of the coactivator's helical LXXLL motif. The minimal core coactivator sequence required for NR binding has been mapped to 8 residues spanning positions -2 to +6 relative to the first conserved leucine within the LXXLL motif (Heery *et al.*, 2001). However, recent work has shown that the selectivity of LXXLL-containing coactivators, such as TRAP220, for NRs involves an extended 13 amino acid sequence rather than the minimal 8 residues that mediate binding (Coulthard *et al.*, 2003).

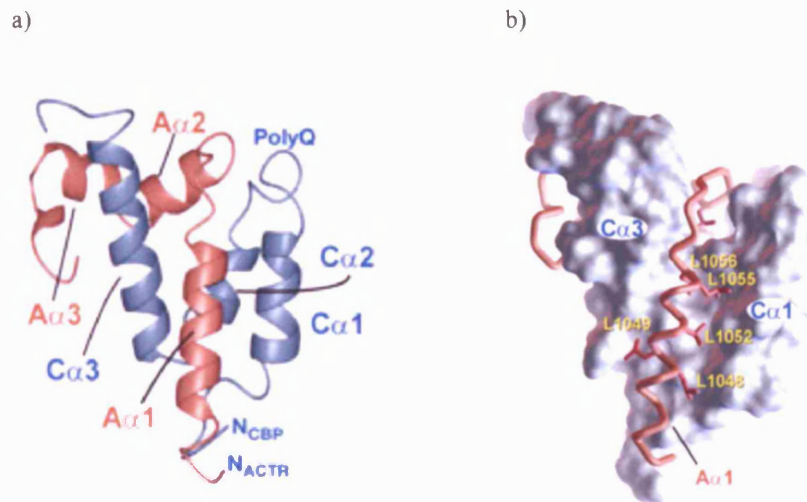


Figure 1.7: Solution structure of a complex of the ACTR AD1 and CBP SID

The NMR structure of the complex of the ACTR Activation Domain 1 (AD1) and CBP SRC1 Interaction Domain (SID), reproduced from Demarest *et al.* (2002) is shown with ACTR in pink and CBP in blue. a) Ribbon diagram denoting the secondary structure of the two interacting domains. The α -helices from each domain are labelled: A α 1-3 for ACTR and C α 1-3 for CBP. b) Ribbon structure of ACTR shown bound to a surface representation of CBP to indicate the extensive interaction of the amphipathic ACTR A α 1 helix with the CBP helices C α 2 and C α 3. The leucine residues in ACTR that make contacts with the CBP helices are indicated with amino acid numbers.

Present within the C-terminal half of the p160 proteins are two autonomous Activation Domains, known as AD1 and AD2, separated by a glutamine-rich region that mediates a ligand-independent interaction with the NR N-terminus (Section 1.7). Three motifs, termed A, B and C, have been identified in the glutamine-rich domain (Christiaens *et al.*, 2002). Of these, motifs A and B have been shown to be required for SRC1 interaction with the AF1 domain of the Androgen Receptor. The role of this Q-rich domain interaction with NRs varies depending upon the NR examined. However, for the majority of Class I and II receptors, with the notable exception of the AR (Bevan *et al.*, 1999), the glutamine-rich region appears to provide a secondary mechanism for NR binding that acts to stabilise the crucial NID interaction with the NR LBD.

Initial studies investigating the role of the p160 AD1 region indicated that it mediated transcription activation through the recruitment of the global coactivators p300/CBP as these two functions could not be separated (Voegel *et al.*, 1998; Kalkhoven *et al.*, 1998). More recent work has mapped the minimal sequences from SRC1 and CBP required for this interaction to residues 926-960 and 2058-2130 respectively (Sheppard *et al.*, 2001). This study also showed that, in a transient transfection system, an SRC1 construct comprised solely of the NID and AD1 domains was sufficient to coactivate ER α activity to a level equivalent to the full-length SRC1 protein. Thus, under these experimental conditions, the bHLH-PAS and AD2 domains were not required for full coactivation of ligand-dependent transcription activation by ER α , suggesting that the p160 recruitment of CBP to active NR complexes provides the predominant mechanism of transcription coactivation by this family. Structure predictions of the interacting regions of SRC1 and CBP suggested the binding would involve amphipathic α -helices in a manner similar to the ligand-dependent interaction of the p160 family with NRs (Sheppard *et al.*, 2001). Confirmation of this hypothesis was provided by the recent publication of a solution structure for a CBP ACTR complex (Demarest *et al.*, 2002). This complex was formed by residues 2059-2117 of CBP and 1018-1088 of ACTR, and involved the cooperative folding of the two protein domains as both were found to be intrinsically unstructured in isolation. The resulting domain complex was α -helical, with three being provided by each partner (Figure 1.7). The CBP α -helices were found to pack into a bundle resulting in the formation of a hydrophobic groove between α -helices C α 1 and C α 3, into which the ACTR A α 1 helix was docked. The second ACTR helix, A α 2, also slotted tightly into the CBP

structure, between the loop separating the C α 1 and C α 2 helices and the C α 3 helix. The final ACTR helix packed against the hydrophobic face of the C α 3 helix. As a result, the ACTR helices almost completely surround the CBP C α 3 helix, which appears to provide the majority of the critical residue interactions that formed the complex. In addition to the large leucine-rich hydrophobic core, a number of polar groups contribute to the binding. In particular, the aspartate residue 1068 in the ACTR α -helix A α 2, which is completely conserved within the p160 family, forms a buried salt bridge to arginine 2105 in CBP helix C α 3. This, coupled with a number of interactions formed by hydrogen bonds ensures the correct positioning of the helices.

Transient transfection studies investigating the role of the SRC1 AD1 indicated that expression of a construct comprised of solely the NID and AD1 was sufficient for coactivation of ER α to a level equivalent to that seen upon expression of full-length SRC1 (Sheppard *et al.*, 2001). Thus, it appears that the predominant function of the p160 proteins is to mediate recruitment of CBP to active NR complexes. Further evidence for this hypothesis has recently been provided by the finding that a TIF2 protein comprised solely of the NID and AD1 was able to mediate transcription activation of the *pS2* promoter by TR β /RXR α to a level equivalent to that seen with full-length ACTR in *in vitro* chromatin assembly experiments (Lee *et al.*, 2003). However, in addition to the AD1 a second activation domain, AD2, has been identified in the p160 proteins and studies investigating its role have shown that it mediates binding to the methyltransferase enzymes CARM1 (Chen *et al.*, 1999a) and PRMT1 (Koh *et al.*, 2001), which can potentiate NR-mediated transcription. These methyltransferases are able to preferentially methylate histone H3 and H4 respectively, in addition to other non-histone proteins. They appear to function synergistically with each other suggesting that the methylation of a number of distinct substrates is required (Koh *et al.*, 2001). In addition, cross-talk between CARM1-mediated methylation and CBP-mediated acetylation of histone H3 has been shown (Daujat *et al.*, 2002). These experiments investigated the ordered recruitment of coactivators to the *pS2* promoter in the MCF-7 (breast cancer) cell line upon addition of oestrogen. At this promoter histone H3 acetylation appears to precede, and is required for, efficient H3 methylation. This is mediated in part through the increased association of CARM1 directly with acetylated nucleosomal histone H3, which likely follows its initial recruitment to the *pS2* promoter by the NR-bound p160 proteins. The inter-play between the role of CBP and

CARM1 in NR-mediated transcription has been further extended by the finding that CARM1 can methylate arginine residues both in the KIX domain, thus inhibiting the interaction of CBP with CREB (Xu *et al.*, 2001), and also in a region of CBP between residues 685 and 774 (Chevillard-Briet *et al.*, 2002). Methylation in this second region appears to stimulate CBP's potentiation of steroid receptor-mediated transcription through an as yet undetermined mechanism. Therefore, this methylation of CBP appears to be required for full NR transcription activation involving the p160 proteins. However, further studies are required to decipher the exact mechanisms involved.

The p160 family members ACTR and SRC1 have both been described as histone acetyltransferase proteins (Chen *et al.*, 1997; Spencer *et al.*, 1997). However, in experiments in our laboratory SRC1 HAT activity was not detected under conditions where CBP and P/CAF HAT activities were readily demonstrable (unpublished observations). In addition, no HAT activity for TIF2 has been identified (Voegel *et al.*, 1998). Given the lack of identified substrates that are efficiently acetylated by SRC1 and ACTR, and the current lack of published data showing that mutation of the proposed HAT domains results in a reduced ability to enhance NR transcription, the physiological role of any SRC1 or ACTR HAT activity must still be clarified.

1.10 CBP/p300 structure and function

CREB-Binding Protein (CBP) was first identified as a protein that bound the transcription factor CREB (cAMP response element binding protein) and enhanced its transcriptional activity (Chrivia *et al.*, 1993), while p300 was isolated as a cellular factor bound by the adenovirus E1A protein (Eckner *et al.*, 1994). p300 and CBP (reviewed in Chan and La Thangue, 2001; Janknecht, 2002; Blobel, 2002) are close homologues that in many instances appear interchangeable. They are ubiquitously expressed in all higher eukaryotes, though no homologues have been found in yeast or bacteria, and have now been shown to act as coactivators for over 100 different transcription factors, including Nuclear Receptors (Chakravarti *et al.*, 1996). As a result they have been termed "global coactivators". The recruitment of CBP/p300 appears to result in the enhancement of transcription activation through a number of mechanisms. Once associated with the promoter-bound transcription factor complex, CBP/p300 act as a scaffold for the formation of complexes that enhance

transcription activation (Merika *et al.*, 1998) and the recruitment of other coactivators such as the histone acetyltransferase P/CAF (p300/CBP Associated Factor) (Yang *et al.*, 1996). They also act as bridging factors between the DNA-bound transcription factor and the basal transcription machinery (Nakajima *et al.*, 1997). In addition to these structural roles, CBP and p300 possess acetyltransferase activity (Ogryzko *et al.*, 1996). Initially identified as being histone acetyltransferases (Bannister and Kouzarides, 1996; Ogryzko *et al.*, 1996), they have since been shown to also mediate their transcriptional effects through the acetylation of a number of non-histone proteins. The effects of this acetylation appear to be dependent upon the protein that is modified. Acetylation of the transcription factor p53 results in an enhancement of its transcriptional activity (Barlev *et al.*, 2001), whereas acetylation of the NR coregulator ACTR results in the dissociation of the ACTR from the NR complex and a shutting-off of the transcriptional signal (Chen *et al.*, 1999b).

The ability of CBP and p300 to bind such a diverse range of proteins (reviewed in Chan and La Thangue, 2001; Janknecht, 2002) is due to their modular structure (Figure 1.8). A number of specific regions, which are especially well conserved between the two proteins, have been identified that mediate these protein-protein interactions. These are the N-terminus region; three cysteine/histidine-rich zinc finger domains (termed C/H1, C/H2, and C/H3); a region designated the KIX domain (through which it binds CREB) (Parker *et al.*, 1996); a bromodomain (mediates binding to acetylated lysine residues) (Dhalluin *et al.*, 1999) and the SID domain, which mediates binding to the p160 coactivators (Sheppard *et al.*, 2001). The N-terminus has been shown to contain two LXXLL motifs that mediate direct binding of CBP/p300 to both the Class I and Class II NRs (Heery *et al.*, 1997). However, these interactions with NRs are much weaker than those seen between the p160 coactivators and NRs (Sheppard *et al.*, 2001; Heery *et al.*, 2001), suggesting that recruitment of CBP/p300 to active NR complexes occurs predominantly through recruitment by the NR-bound p160 coactivators (Sheppard *et al.*, 2001; Lee *et al.*, 2003). As discussed in Section 1.9, this interaction between the p160 coactivators and CBP/p300 is mediated by the SID (SRC1 Interaction Domain) present in the C-terminus of the global coactivators (Sheppard *et al.*, 2001). The solution structure of a complex of the CBP SID with the AD1 of ACTR, an SRC1 homologue (Figure 1.7) has recently been solved (Demarest *et al.*, 2002).

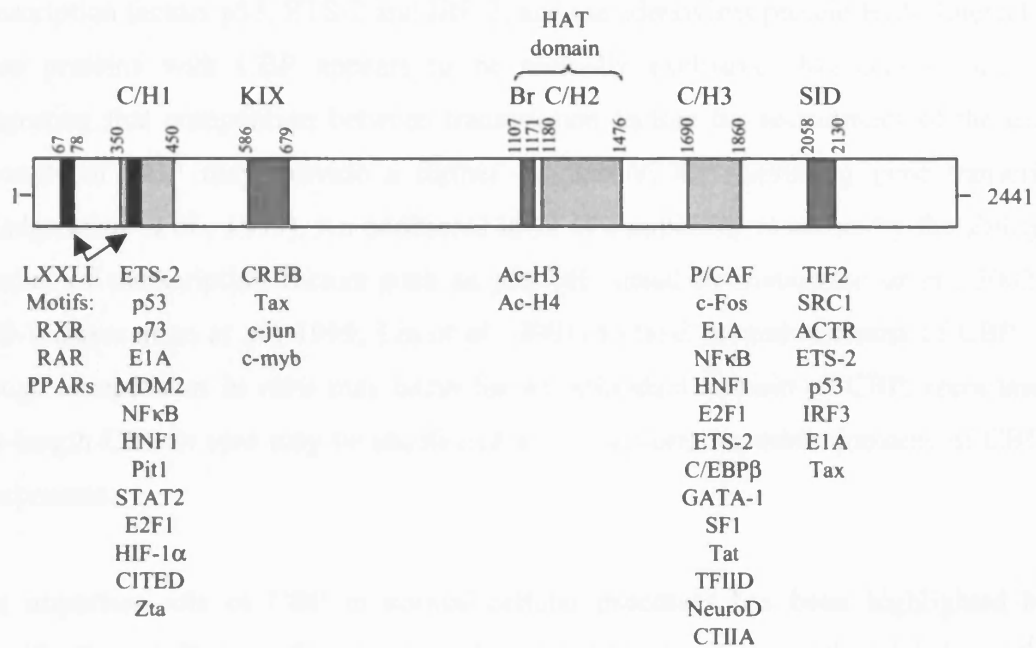


Figure 1.8: Domain structure of CBP

A schematic detailing the domain structure of CBP is shown. Numbers indicate approximate amino acid boundaries of each domain. At its N-terminus CBP contains two LXXLL (L, leucine; X, any amino acid) motifs that mediate NR interaction, the second of which is contained within the first cysteine/histidine-rich (C/H) domain. The second C/H domain coupled with the bromodomain, which mediates interaction with acetylated (Ac-) histone H3 and H4, forms the histone acetyltransferase (HAT) domain. CBP also contains a third C/H domain and the SRC1 Interaction Domain (SID) in its C-terminus. A small number of the proteins that interact with CBP are listed beneath the domain(s) to which they bind.

Studies of the SID in conjunction with other domains of CBP/p300 have highlighted another important factor in the recruitment of the global coactivators by transcription factor complexes. In addition to binding the p160 coactivator proteins, the SID binds a number of other proteins (Lin *et al.*, 2001; Matsuda *et al.*, 2003). These include the human transcription factors p53, ETS-2 and IRF-3, and the adenovirus protein E1A. Interaction of these proteins with CBP appears to be mutually exclusive (Matsuda *et al.*, 2003), suggesting that competition between transcription factors for recruitment of the limiting amounts of CBP may provide a further mechanism for regulating gene transcription (Wadgaonkar *et al.*, 1999). An additional level of complexity is added by the ability of a number of transcription factors such as p53 (discussed in Livengood *et al.*, 2002) and ETS-2 (Jayaraman *et al.*, 1999; Lin *et al.*, 2001) to bind several domains of CBP. Thus, though competition *in vitro* may occur for an individual domain of CBP, recruitment of full-length CBP *in vivo* may be unaffected as interactions via other domains of CBP may compensate.

The important role of CBP in normal cellular processes has been highlighted by the identification of diseases that appear to be caused by alterations in the global coactivator. These include Rubenstein Taybi Syndrome (RTS) (Petrij *et al.*, 1995), which leads to mental retardation and craniofacial abnormalities. RTS been shown to result from the heterozygous mutation of CBP leading to haplo-insufficiency, suggesting that the level of CBP protein in the cell is critical to normal cell function. In addition, sequestration of CBP has been reported to occur in Huntington's disease (Nucifora *et al.*, 2001). This neurodegenerative disorder is one of a number that appear to result due to the expansion of polyglutamine sequence, which leads to the formation of protein aggregate inclusions. The mutant Huntington protein co-aggregates CBP, but not p300, in these inclusions and this inhibits CBP-activated gene transcription. Interestingly, the associated neuronal toxicity can be rescued by over-expression of CBP, suggesting that the sequestration of CBP, rather than formation of the inclusion, may be the critical factor affecting the normal function of the cell (Nucifora *et al.*, 2001). Finally, both CBP and p300 have been identified as targets of chromosomal alteration resulting in haematopoietic malignancies, which is discussed further in Section 1.13.

1.11 Transcription factors and leukaemia

The importance of tight regulation of gene expression has been highlighted by the identification of cancers that arise from genetic alterations affecting transcription factors and their coregulators. Such changes have particularly pronounced effects on tissues that require high levels of cell proliferation for normal function. This is due to the absolute requirement for correct gene expression patterns to regulate proliferation versus differentiation decisions in these cells. The haematopoietic system provides one such example. Due to the limited lifespan of blood cells, the production of as many as one trillion new cells is required each day (Hoffman, 2000). In the adult, these cells are derived from approximately 2×10^4 identical primitive pluripotent haematopoietic stem cells (HSCs) located in the bone marrow. Thus, haematopoiesis (the formation and development of blood cells) not only requires cell proliferation on a huge scale, but also carefully regulated differentiation in order to produce the required number of each type of mature blood cell.

The initial stages in haematopoietic cell generation involve the limited differentiation, termed commitment (Enver and Greaves, 1998), of self-renewing pluripotent haematopoietic stem cells to give rise to multi-potent lymphoid or myeloid stem cells. These two stem cells provide the first defined stages of the two haematopoietic cell lineages (Figure 1.9). The lymphoid lineage gives rise to the T and B -lymphocytes, while differentiation of the myeloid lineage stem cell results in the generation of basophils, eosinophils, erythrocytes, megakaryocytes (platelets), monocytes, and neutrophils. The mechanism by which the initial differentiation pathway, or commitment, of a pluripotent stem cell is selected remains to be elucidated. However, the process by which stem cells differentiate along the specific lymphoid and myeloid lineages and then mature to give rise to terminally differentiated cells appears to be a result of coordinated lineage-specific gene expression. This is controlled, at least in part, by lineage-specific growth factors such as cytokines, which promote proliferation and differentiation along particular pathways (Zhu and Emerson, 2002), though many of the regulatory pathways and transcription complexes are still to be identified.

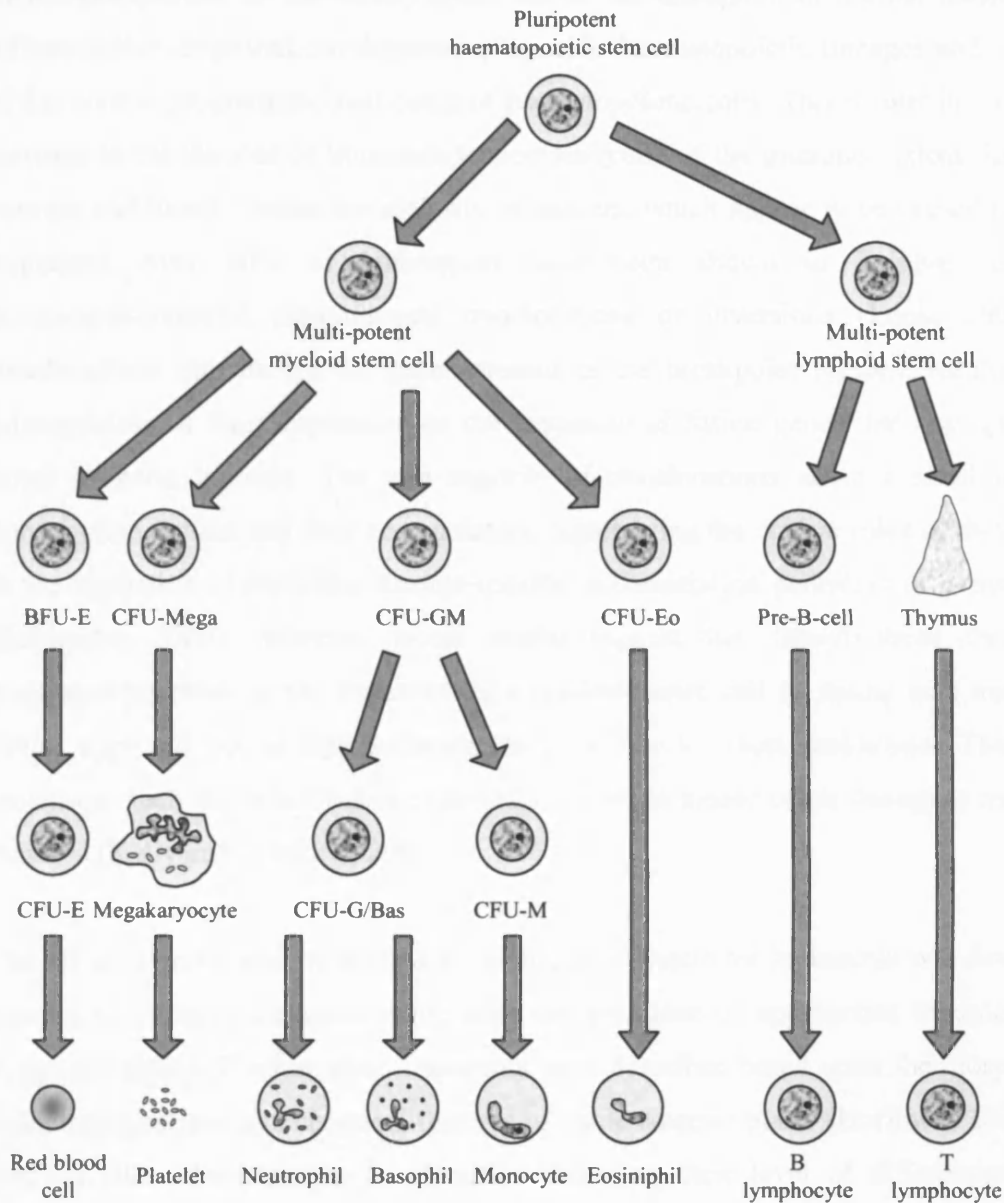


Figure 1.9: Schematic showing the haematopoietic stem cell hierarchy

The hierarchy that results from the differentiation of pluripotent haematopoietic stem cells is shown with selected stages indicated. The initial differentiation step results in commitment to either the myeloid or lymphoid lineage. Further steps delineate the particular mature haematopoietic cell that will arise. CFU, colony forming unit; BFU, burst forming unit; Bas, basophil; E, erythroid; Eo, eosinophil; G, granulocyte; M, monocyte; Mega, megakaryocyte.

Leukaemia (cancer of the blood) arises due to the disruption of normal haematopoietic differentiation, impaired development of specific haematopoietic lineages and / or failure of the normal programmed cell death of haematopoietic cells. This results in an abnormal increase in the number of immature leucocytes (cells of the immune system) in the bone marrow and blood. Unlike the majority of cancers, which appear to be caused by random mutations, over 60% of leukaemias have been shown to involve non-random somatically-acquired chromosomal translocations or inversions (Look, 1997). Such translocations can disrupt the genes present in the breakpoint regions, resulting in the misregulation of their expression or the formation of fusion genes that may give rise to novel chimeric proteins. The vast majority of translocations affect a small number of transcription factors and their co-regulators, highlighting the critical roles of these proteins in the regulation of particular lineage-specific differentiation pathways in haematopoiesis (Bohlander, 2000). However, recent studies suggest that, though these chromosomal translocations result in the formation of a pre-leukaemic cell by acting as a transforming event, they are not always sufficient to give rise to overt leukaemia. Thus, further mutations, such as the activation of the FLT3 tyrosine kinase or ras oncogene may also be required (Kelly and Gilliland, 2002).

The French-American-British (FAB) classification system for leukaemia was devised in an attempt to improve diagnosis and enable the provision of appropriate treatments. Eight subgroups (M0-M7) of myeloid leukaemia were described based upon the morphological, immunological and cytochemical features of the leukaemic blasts (Hoffman, 2000). These features allow the blasts to be classified according their level of differentiation along particular lineages. As the genes present at the breakpoints of leukaemic chromosomal translocations are identified, it is becoming clear that individual genes are associated with particular subtypes of leukaemia. This suggests that alterations of that gene affect further differentiation beyond the point reached by the blast cells, and further implicates that gene product as possibly essential to haematopoiesis. The retinoic acid receptor α (see below) provides one such example as translocations involving this gene predominantly result in the M3 subtype of myeloid leukaemia.

1.12 The role of RAR α and other NRs in haematopoiesis and Acute Myeloid Leukaemia

The retinoic acid receptor alpha (RAR α) has been identified as a major target of specific chromosomal translocations that result in the M3 sub-type of Acute Myeloid Leukaemia (AML) termed Acute Promyelocytic Leukaemia (APL) (Melnick and Licht, 1999; Zelent *et al.*, 2001). These chromosomal rearrangements all result in the formation of proteins comprised of the N-terminus of the partner protein fused to regions B-F of RAR α (Section 1.7). Over 70% of APL patients have been shown to harbour the translocation t(15;17)(q22;q11-23), which results in the fusion of the PML gene to RAR α (Melnick and Licht, 1999; Zelent *et al.*, 2001). PML is a predominantly nuclear protein that forms nuclear structures termed PML bodies, also known as PODs (PML oncogenic domains), ND10s (nuclear domain 10) or Kramer bodies. A significant number of proteins, including the NR coactivators CBP and GRIP1 / TIF2 (Doucas *et al.*, 1999; Boisvert *et al.*, 2001; Baumann *et al.*, 2001), associate with these nuclear bodies, and the expression of the PML-RAR α fusion, which disrupts their formation, results in the mislocalisation of all associated proteins (Melnick and Licht, 1999; Zelent *et al.*, 2001). Though the exact role of PML remains to be clarified, it has been implicated in transcription, RNA processing / transport, DNA repair and DNA replication (discussed in Melnick and Licht, 1999; Borden, 2002).

The PML-RAR α fusion protein has been shown to bind to retinoic acid response elements (RAREs) as a homodimer, in contrast to wild-type RAR α , which binds as a heterodimer with RXR. In the absence of retinoic acid, the PML-RAR α homodimer recruits the NCoR / SMRT corepressor complex with far greater affinity than wild-type RAR α /RXR heterodimers (reviewed in Guidez and Zelent, 2001). As a result, it represses transcription from genes containing RAREs to a much greater extent. Addition of physiological doses of retinoic acid does not result in the dissociation of the tightly-bound co-repressors and thus, the repression cannot be overcome. It appears likely that this inability to de-repress transcription may play an important role in the transformation of a normal differentiating promyelocyte into an APL leukaemic blast. APL patients expressing the PML-RAR α fusion however, may be treated successfully by the administration of pharmacological doses of all-*trans* retinoic acid (AT-RA) in combination with HDAC inhibitors. The PML-RAR α protein has also been shown to inhibit transcription by other NRs, such as the

VDR and PPAR, suggesting that it may also function to sequester RXR and / or NR coactivators.

Given the importance of RAR α in APL, Parrado *et al.* (1999) investigated whether mutations in the RAR α gene are present in non-APL human leukaemia. Their finding that RAR α mutations could be detected in a low percentage of such patients provides further evidence for a possible role of this NR transcription factor in haematopoiesis. In addition, a number of studies have been carried out investigating the effects of retinoids and retinoic acid receptors in normal haematopoiesis (reviewed in Collins, 2002). Analysis of RAR α mouse knock-outs indicated that while RAR α was dispensable for granulopoiesis, it played a modulatory role in haematopoiesis as RAR α ^{-/-} granulocyte precursors differentiated more rapidly *in vitro* (Kastner *et al.*, 2001). Thus, unliganded RAR α appears to inhibit differentiation and the ability of retinoic acid to overcome this is required for normal haematopoiesis. The retinoid X receptor (RXR) has also been shown to play a role in haematopoiesis through myeloid cell-targeted expression of a dominant negative RXR β gene in the mice (Sunaga *et al.*, 1997). RXR acts as the dimerisation partner for all Class II NRs and thus this dominant negative protein would be expected to inhibit transcription by NRs in addition to RAR α .

Interestingly, translocations involving other NRs have not as yet been identified in human leukaemia. However, studies investigating the effects of vitamin D and PPAR ligands suggest that they play a role in haematopoietic differentiation. The U937 cell line (Sundstrom and Nilsson, 1976) in particular has been used as a model system in which to test the effects of leukaemogenic fusion proteins and NR ligands on terminal myeloid cell differentiation. U937 cells phenotypically resemble monocytic blasts and can be induced to terminally differentiate into monocytes through the addition of several Class II NR hormones. Addition of retinoic acid (Liu *et al.*, 1996a) and vitamin D (Liu *et al.*, 1996b) to the growth medium results in the induction of p21 expression and terminal differentiation of U937 cells, while PPAR γ ligands cause growth arrest, and the induction of differentiation in combination with an RXR or RAR ligand (Asou *et al.*, 1999). These findings, coupled with those investigating the mechanism of leukaemogenesis of the PML-RAR α fusion suggest that NR ligands play an important role in promoting myeloid

differentiation, both through the de-repression of gene expression, and through activation of specific genes such as the cell cycle regulator p21.

1.13 NR coactivators in haematopoiesis and AML

The role of the global coactivator CBP and p300 in haematopoiesis (reviewed in Janknecht, 2002) has been investigated through studies of CBP knock-out mice (Kung *et al.*, 2000). Though the double knockout of either CBP or p300 is embryonic lethal, heterozygous knockout mice survive. CBP^{+/-} mice show the craniofacial abnormalities and growth retardation that are characteristic of the human Rubenstein Taybi syndrome. In addition, when analysed haematologically, they show reduced levels of all haematopoietic stem cells, and with increasing age, the onset of haematological malignancies. Thus, it appears that two wild-type alleles of CBP are required for normal haematopoietic differentiation. In contrast however, p300^{+/-} mice do not show any haematopoietic abnormalities, providing one of the few examples where a physiological difference in the function of CBP and p300 has been identified.

The role of NR coactivators in haematopoiesis has also been highlighted by the identification of leukaemic chromosomal translocations that involve their genes. The most commonly involved NR coactivator is CBP, which has been identified in fusions with the genes MOZ and MLL. The fusion of CBP to MLL (Mixed Lineage Leukaemia) by the chromosomal translocation t(11;16)(q23;p13) is associated with therapy-related acute leukaemia. The MLL gene (Ernst *et al.*, 2002) is a common target for chromosomal translocations associated with human acute leukaemia, with over 30 distinct partner proteins currently identified. Such translocations appear to result in a gain of MLL function that affects early stages of haematopoietic development. Interestingly however, the myeloid cell-line SN-1, which was generated from a patient with T-cell acute lymphoblastic leukaemia resulting from in the MLL-CBP fusion is completely unresponsive to differentiation mediated by retinoic acid or vitamin D3, but not actinomycin D (inhibits RNA transcription) or sodium butyrate (HDAC inhibitor) (Hayashi *et al.*, 2000). Thus the fusion of MLL to CBP, in addition to its effects on normal MLL function, may also inhibit NR-mediated differentiation.

The first leukaemic fusion involving CBP to be identified was the t(8;16)(p11;p13) chromosomal translocation, which was present in myeloid blast cells from a patient with the M4/5 subtype of AML (Borrow *et al.*, 1996). A novel protein they termed monocytic leukaemia zinc finger protein (MOZ) was identified as the fusion partner. RT-PCR analysis identified the presence of a MOZ-CBP mRNA with the correct open reading frame maintained, thus allowing the generation of a full-length MOZ-CBP protein. However, though an mRNA for the reciprocal CBP-MOZ gene fusion was also identified, it contained intronic DNA sequence that served to place the CBP-MOZ fusion out-of-frame. Therefore, the critical fusion product appeared to be encoded by the MOZ-CBP fusion. The MOZ-CBP translocation defines a subtype of AML with distinct clinicopathological features (Borrow *et al.*, 1996; Sun and Wu, 2001) that has now been shown to include a number of other chromosomal translocations. The first such variant identified, inv8(p11;q13), was shown to result in the fusion of the MOZ gene to the p160 coactivator, TIF2 (Carapeti *et al.*, 1998a; Liang *et al.*, 1998). Subsequent analyses of patients presenting similar clinical features have also identified the fusion of p300, the CBP homologue, to MOZ (Chaffanet *et al.*, 2000), and CBP to MORF (MOZ related factor), a human MOZ homologue (Panagopoulos *et al.*, 2001). In addition, a recent study has identified the MOZ gene as one fusion partner in the chromosomal translocation t(2;8)(p23;p11), though the gene located on chromosome 2 was not identified. Given the location of SRC1 to 2p23 (Carapeti *et al.*, 1998b) however, it is interesting to speculate that this translocation might result in a MOZ-SRC1 fusion.

The functions of MOZ and MORF are only now beginning to be elucidated (Champagne *et al.*, 2001; Kitabayashi *et al.*, 2001a; Pelletier *et al.*, 2002; Bristow and Shore, 2003), while CBP and p300 are global coactivators utilised by many transcription factors including NRs (reviewed in Chan and La Thangue, 2001; Janknecht, 2002; Blobel, 2002). However, TIF2 is predominantly an NR-specific coactivator that functions to recruit CBP to transcriptionally active NR complexes (Voegel *et al.*, 1998; Kalkhoven *et al.*, 1998). Thus it appeared possible given the similarities in the leukaemogenic phenotypes of these fusions, and the important role of NRs in haematopoiesis, that the fusion proteins might affect NR-mediated myeloid differentiation.

1.14 The structure and function of MOZ

The protein domain structure of MOZ is shown as a schematic in Figure 1.10. MOZ encodes a 2004 amino acid, 225kDa nuclear protein originally identified through its fusion to CBP in a patient with the Acute Myeloid Leukaemia. The MOZ gene is comprised of 17 exons that span approximately 80kb of DNA with the MOZ protein encoded by exons 2 to 17 (Panagopoulos *et al.*, 2003). All the MOZ fusions identified thus far have resulted in the replacement of the C-terminal part of the acidic domain and all the residues downstream of it with the fusion partner. The acidic domain is encoded by exons 15-17, with exon 17 encoding residues 1117-2004. Thus, given that the majority of MOZ fusions involve the replacement of MOZ residues 1118-2004 with the residues from the fusion partner, it appears that the predominant site of the translocation breakpoints is the MOZ intron 16 (Panagopoulos *et al.*, 2003).

Six domains have been identified in the MOZ protein through homology searches. At its N-terminus (residues 52-166), MOZ contains a region (the H15-like domain) that shows homology to the linker histone H1 and its variant, histone H5, suggesting that it might function to stabilise an interaction of MOZ with nucleosomes. In addition, this domain has been shown recently to play a role in the subcellular localisation of exogenously expressed MOZ (Kitabayashi *et al.*, 2001a). Following the H15-like domain are two C4HC3 zinc fingers that together form a region known as a plant homeodomain (PHD) or leukaemia-associated-protein (LAP) domain. The PHD zinc finger motif is found in a number of nuclear proteins, including CBP/p300 (where it is located within the HAT region), and is believed to act as a protein interaction domain. The N-terminus regions of both MORF (Champagne *et al.*, 1999) and MOZ (Kitabayashi *et al.*, 2001a) have been shown to function as transcription repressors when fused to the DNA binding domain (DBD) of GAL4. C-terminal to the PHD domain, Borrow *et al.* (1996) identified an atypical Cys-X₁₂-Cys-X₁₂-His-X₃-Cys (C2HC) zinc finger which, along with ~190-residues downstream, showed homology to a number of other proteins. Contained within this domain was a region that had been previously identified as an acetyltransferase signature, suggesting that proteins containing this domain might acetylate other molecules. Based upon the proteins that were initially identified as containing this novel domain (MOZ, YBF2, SAS2, TIP60), it was named the MYST domain (discussed in Section 1.16).

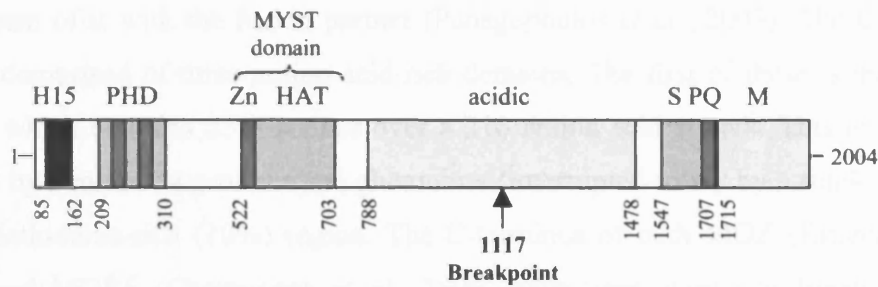


Figure 1.10: Domain structure of MOZ

A schematic detailing the domain structure of MOZ is shown. Numbers indicate approximate amino acid boundaries of each domain. At its N-terminus MOZ contains a histone H15-like domain and two zinc fingers present within the Plant Homeodomain (PHD). The central MYST domain that functions to acetylate proteins is comprised of an N-terminal zinc finger and ~190 additional residues. The C-terminus of the protein is made up of an acidic domain, and serine (S), proline/glutamine (PQ) and methionine (M) - rich regions. The predominant breakpoint occurring in leukaemic translocations results in the generation of a protein containing the N-terminus of MOZ up to residue 1117 and the C-terminus of the fusion partner.

A large acidic domain comprised of 28% aspartic acid and glutamic acid residues is located in the central region of MOZ. The function of this domain is unclear, though acidic domains are often associated with transcription activation and protein interactions. When fused to the GAL4 DBD however, the MOZ acidic domain was found to repress, rather than activate, transcription (Kitabayashi *et al.*, 2001a). All the MOZ fusions thus far have involved the replacement of the C-terminal portion of the acidic domain and the sequence downstream of it with the fusion partner (Panagopoulos *et al.*, 2003). The C-terminus of MOZ is comprised of three amino acid-rich domains. The first of these is the serine-rich domain, which contains 25% serines over a 216 amino acid stretch. This is immediately followed by a run of 54 prolines and glutamines (interrupted solely by a single alanine) and then a methionine-rich (10%) region. The C-terminus of both MOZ (Kitabayashi *et al.*, 2001a) and MORF (Champagne *et al.*, 1999) have been shown to function as strong transcription activation domains. This activity has been mapped to residues 1517-1948 in MOZ, with further deletions into the methionine-rich region of this construct resulting in a loss of activation. MORF does not contain the proline/glutamine-rich region and thus its C-terminus differs somewhat from that of MOZ. However, comparison of the transcription activational activities of MORF constructs containing either both the serine and methionine-rich regions, or solely the methionine-rich region, suggests that at least some portion of the serine-rich domain is also required.

Borrow *et al.* (1996) identified MOZ as a possible acetyltransferase protein through homology searches in 1996. However, it was not until 2001 that the ability of its MYST domain to acetylate histones was confirmed (Champagne *et al.*, 2001). The MOZ C-terminus was also shown in the same study to act as a transcription activation domain suggesting that the protein might function as a transcriptional coactivator. This hypothesis was confirmed later in 2001 when MOZ was identified as an AML1-binding protein (Kitabayashi *et al.*, 2001a). AML1 (Runx1, CBFa2) is a transcription factor that is essential in early definitive haematopoiesis and has been identified as the most frequent target of chromosomal translocations resulting in leukaemia (Lutterbach and Hiebert, 2000; Skalnik, 2002; Michaud *et al.*, 2003; Look, 1997). It is one of three members of the RUNX family of transcription factors that dimerise with the CBF β protein to activate gene transcription. The three RUNX members contain a RUNT domain that mediates both interaction with CBF β and DNA binding. In addition they contain C-terminal

transactivation and repression domains. AML1 has been shown to interact with p300 and CBP (Kitabayashi *et al.*, 1998) in addition to MOZ, suggesting the recruitment of multiple coactivators is required for maximal transcription activation.

The interaction of MOZ with AML1 is mediated by two regions in the MYST protein (Kitabayashi *et al.*, 2001a). The N-terminal binding site was mapped to residues 312-664, while the second site corresponded to the serine-rich domain in the C-terminus of the protein. The binding site in AML1 was identified as the activation domain located between residues 291 and 371, suggesting that MOZ might act as a coactivator for AML1. Indeed, transfection studies indicated that co-expression of MOZ with AML1 resulted in a potentiation of AML1-mediated transcription of a myeloperoxidase (MPO; lysosomal enzyme present in myeloid cells) promoter luciferase construct. Interestingly, the MOZ MYST domain, and thus HAT activity, was not required for this activity, though MOZ was shown to acetylate AML1 *in vitro*. The histone H15-like domain, N-terminal portion of the acidic domain and the C-terminal activation domain were essential however. During the preparation of this thesis a second study investigating the ability of MOZ to act as a coactivator of AML1-mediated transcription was published (Bristow and Shore, 2003). MOZ was shown to enhance AML1-mediated transcription of MIP1 α , a pro-inflammatory cytokine that also functions to inhibit haematopoietic stem cell and progenitor cell proliferation. Thus, MOZ functions as a coactivator for AML1-mediated transcription, which is essential for the early steps in adult haematopoietic differentiation.

In addition to acting as a coactivator for AML1, MOZ, has been shown to enhance Runx2-mediated transcription, though this coactivation was not as strong as was seen with the MOZ homologue MORF (Pelletier *et al.*, 2002). Runx2 is the second of the three RUNX family of proteins and appears to function primarily in the control of osteoblast differentiation and bone formation. The MOZ C-terminus was shown to bind two separate regions in the N-terminus of Runx2, thus resulting in its association with active Runx2 complexes and potentiation of transcription of a Runx2-responsive luciferase reporter. Thus, both MOZ and its close homologue MORF appear to function as coactivators for the RUNX family of transcription factors.

1.15 The MOZ-CBP and MOZ-TIF2 leukaemogenic fusion proteins

The domain structures of the MOZ, TIF2 and CBP proteins, and the longer MOZ-TIF2 fusion and predominant form of the MOZ-CBP proteins are shown in Figure 1.11. The majority of the MOZ fusions identified thus far result in the replacement of the MOZ residues 1118-2004 with the fusion partner protein sequence (Carapeti *et al.*, 1998a; Liang *et al.*, 1998; Chaffanet *et al.*, 2000; Panagopoulos *et al.*, 2000b; Panagopoulos *et al.*, 2000a; Panagopoulos *et al.*, 2003). This consistent amino acid breakpoint has been shown to result from multiple breakpoints within intron 16 of the MOZ sequence (Panagopoulos *et al.*, 2003 and references therein). In CBP/p300 the majority of the breakpoints associated with the fusion to MOZ have been mapped to intron 2, in contrast to those found upon fusion to MLL (Panagopoulos *et al.*, 2003). Interestingly, one exception to this MOZ-CBP fusion breakpoint is provided by the first MOZ-CBP translocation identified. The study by Borrow *et al.* (1996) identified a fusion resulting in a protein containing residues 1-1546 from MOZ and 266-2040 of CBP. In this case, both breakpoints occurred within exons, with two incorporated guanine nucleotides of unknown origin maintaining the appropriate reading frame. The position of these breakpoints in MOZ and CBP are indicated (labelled Borrow) in Figure 1.11.

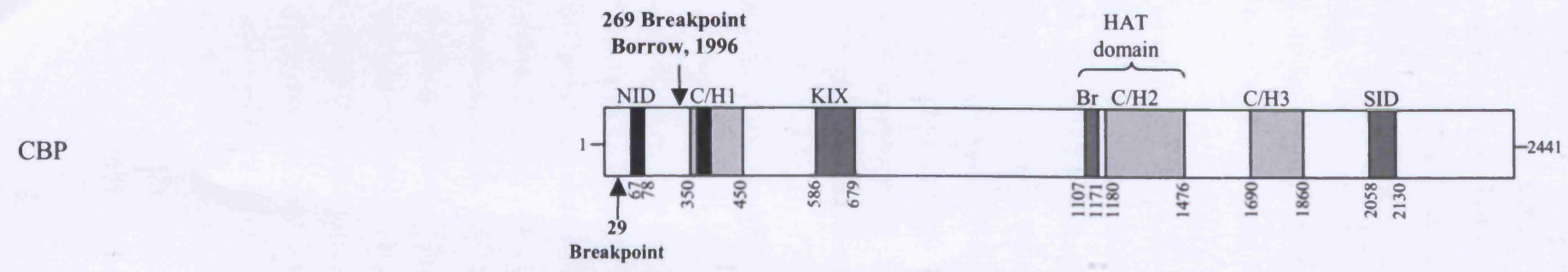
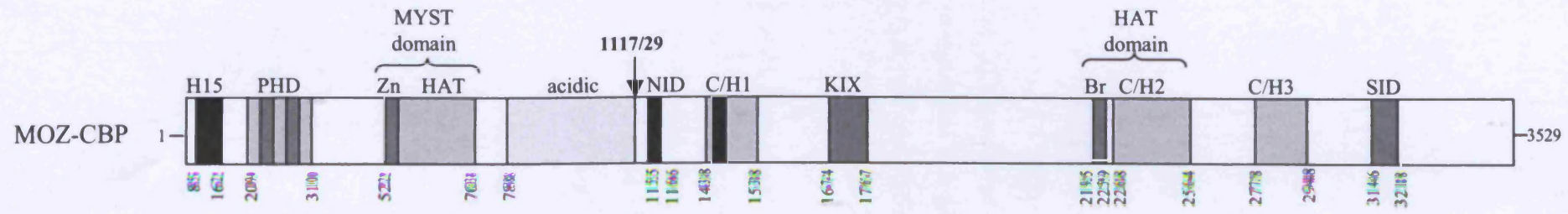
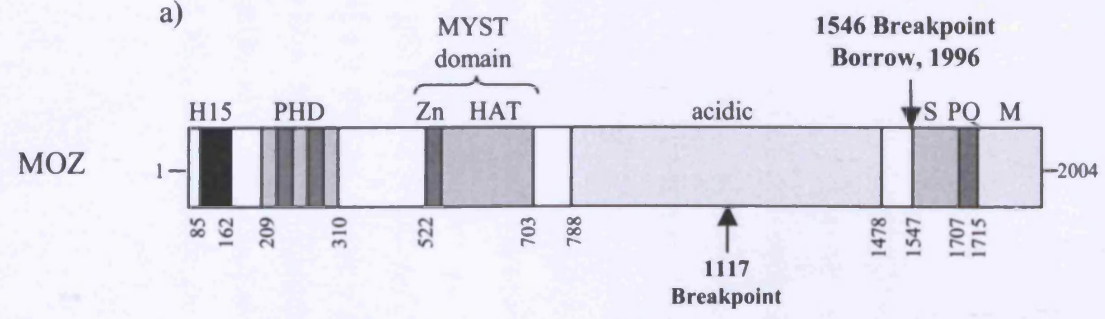
The predominant MOZ-CBP translocation event results in the generation of a MOZ-CBP protein that contains the MOZ sequence from residues 1 to 1117 N-terminal to the CBP residues 29-2040. Thus, the histone H15-like, PHD and MYST domains and N-terminal part of the acidic domains of MOZ are coupled to almost the entire sequence of CBP. The predominant MOZ-CBP fusion protein therefore has the potential to bind any proteins that interact with the N-terminus of MOZ, or almost the entire CBP sequence. Though no studies have as yet been published investigating the effects of expression of this form of the MOZ-CBP fusion, Kitabayashi *et al.* (2001) have investigated the effect of expression of the Borrow *et al.* (1996) MOZ-CBP protein on AML1-mediated transcription. This fusion contains an additional 429 residues of the MOZ acidic domain, but lacks the first 265 (rather than just 30) amino acids of CBP. Co-expression of this MOZ-CBP fusion construct resulted in the inhibition of AML1-mediated transcription (Kitabayashi *et al.*, 2001a). This inhibition was shown to be dependent upon the bromo- and HAT domains of CBP but not the PHD finger or MYST domains of MOZ. CBP/p300 functions as a coactivator of AML1 transcription (Kitabayashi *et al.*, 1998) and therefore Kitabayashi *et*

al. (2001) investigated whether the MOZ-CBP fusion inhibited transcription activation by GAL4 DBD fusions of either MOZ or CBP. Interestingly, expression of the fusion protein appeared to have no effect on transcription mediated by GAL4-MOZ but resulted in inhibition of GAL4-CBP transactivation, suggesting that the fusion protein might sequester additional factors required by CBP during transactivation. Consistent with the ability of MOZ-CBP to inhibit GAL4-CBP-mediated transcription, CBP was found to be unable to potentiate AML1-mediated transcription in the presence of the MOZ-CBP fusion. Further work is required however to determine the exact mechanism of inhibition.

The study by Kitabayashi *et al.* (2001) also investigated the effect of MOZ-CBP expression on the differentiation of the M1 mouse myeloid cell line. M1 cells can be induced to differentiate into monocytes/macrophages by the addition of Interleukin-6. However, stable expression of MOZ-CBP, but not a mutant MOZ-CBP construct lacking the CBP sequences C-terminal to the bromodomain, resulted in an inability of the cells to differentiate in response to this cytokine. Thus, expression of MOZ-CBP is sufficient to block differentiation of myeloid cells, and the regions of CBP downstream of the bromodomain are required for this inhibition.

Two different amino acid breakpoints have been identified in TIF2, thus resulting in two MOZ-TIF2 fusion proteins. These two MOZ-TIF2 proteins are derived from nucleotide breakpoints present in intronic sequences either side of an alternatively spliced-exon in TIF2. The structure of the MOZ-TIF2 fusion containing the alternatively spliced-exon is shown, with the “Liang”-labelled arrow indicating the TIF2 breakpoint in the MOZ-TIF2 fusion that does not contain the exon. As with the MOZ-CBP protein, the histone H15-like, PHD and MYST domains, along with part of the acidic domain, are retained in the fusion protein. The AD1, glutamine-rich and AD2 domains of TIF2 are present in MOZ-TIF2 and thus the fusion protein might be expected to interact with TIF2’s downstream binding partners CBP and CARM1. Though the glutamine-rich region is present in MOZ-TIF2, the nuclear receptor interaction domain (NID) is absent. For the majority of NRs the NID appears to play the predominant role in mediating ligand-dependent NR binding with the glutamine-rich domain making a secondary, possibly stabilising interaction. Therefore, it appears unlikely that the MOZ-TIF2 fusion protein can interact directly with NRs in a ligand-dependent manner.

a)



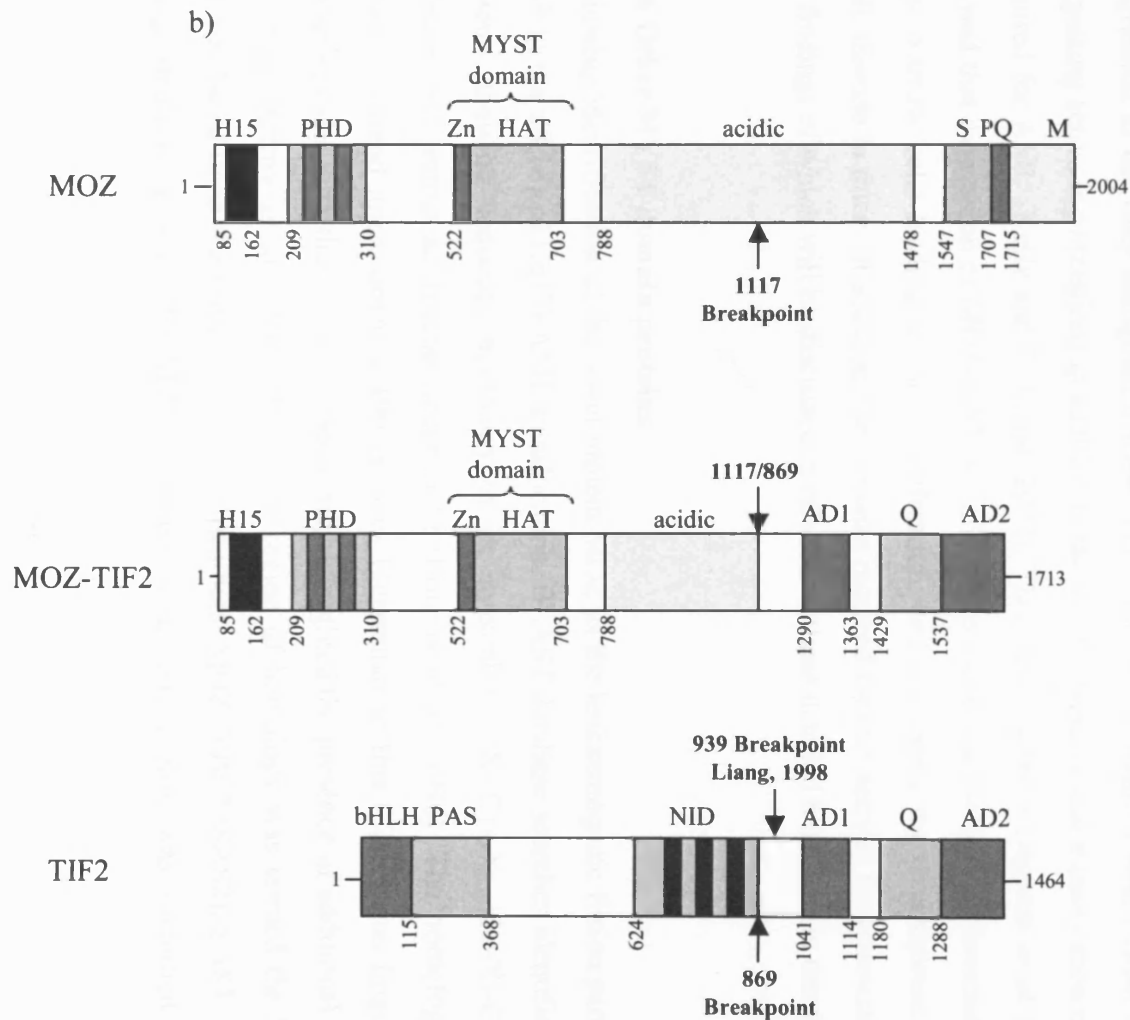


Figure 1.11: Domain structure of the MOZ-CBP and MOZ-TIF2 fusion proteins

Schematic detailing the locations of the breakpoints with respect to domain structure in the MOZ-CBP (a) and MOZ-TIF2 (b) fusion proteins. The predominant MOZ, CBP and TIF2 breakpoint fusions are shown, with the additional breakpoint sites also indicated in the wild-type proteins by first author and year. MOZ domains: H15, histone H15-like; PHD, Plant Homeodomain; MYST, histone acetyltransferase domain; acidic, acidic-rich; S, serine-rich; PQ, proline/glutamine-rich; M, methionine-rich. CBP domains: NID, Nuclear Receptor interaction domain; C/H, cysteine/histidine-rich; Br, bromodomain; HAT, histone acetyltransferase domain; SID, SRC1 Interaction Domain. TIF2 domains: bHLH, basic-Helix-Loop-Helix domain; PAS, Per-Armdt-Sim zinc finger motifs; NID, Nuclear Receptor interaction domain; AD1, Activation Domain 1; Q, glutamine-rich domain; AD2, Activation Domain 2.

During the preparation of this thesis a study of the leukaemogenic properties of the MOZ-TIF2 fusion was published (Deguchi *et al.*, 2003). Murine bone marrow cells were retrovirally transduced with MOZ-TIF2 and studied both *in vitro* and in mouse models. Serial replating experiments indicated that MOZ-TIF2-transduced cells were able to form hundreds of colonies beyond the first round of plating in contrast to the normal vector-transduced cells that were unable to proliferate. In addition, cells transduced with MOZ-TIF2 were found to be capable of sustained growth in suspension culture in the presence of Interleukin-3. Thus, expression of MOZ-TIF2 results in the immortalisation of murine bone marrow cells, though this process initially requires activation of the IL-3 signalling pathway. In addition to these *in vitro* studies, *in vivo* analysis of the MOZ-TIF2 fusion was carried out in mice. Transplantation of MOZ-TIF2-transduced bone marrow cells into irradiated mice was shown to result in the development of a fatal haematological disease. When the bone marrow from these mice were transplanted into a secondary recipient the disease latency was reduced, suggesting secondary mutations may be required for progression to the fully malignant disease. This finding is consistent with human studies suggesting activating mutations in addition to the initial chromosomal translocation may be required for AML (Kelly and Gilliland, 2002). Thus, this study by Deguchi *et al.* (2003) showed that expression of MOZ-TIF2 is sufficient to mediate a block in differentiation of bone marrow cells leading to their proliferation, and ultimately the development of an AML disease in mice. In addition, the domains required for this activity were investigated, the findings of which will be discussed in relation to those detailed here later in this thesis.

1.16 Other MYST domain proteins

Following identification of the novel protein MOZ as the leukaemogenic fusion partner of CBP in the t(8;16)(p11;q13) AML translocation, BLAST database searches identified five proteins showing sequence homology to its atypical Cys-X₂-Cys-X₁₂-His-X₃-Cys (X indicates any amino acid) zinc finger motif (Borrow *et al.*, 1996). The homology was shown to extend approximately 190 residues C-terminal to this C2HC zinc finger, and further analysis with this secondary sequence highlighted the presence of additional family members (Borrow *et al.*, 1996). The entire region of homology was termed the MYST domain, based upon the initially identified members: MOZ, YBF2 (SAS2), SAS3, TIP60. Using small regions of the MYST domain, a discrete region was identified as an

acetyltransferase signature, suggesting that the MYST domain may function to acetylate proteins (Borrow *et al.*, 1996).

In all, 12 members of the MYST family have now been isolated as functional proteins (reviewed in Utley and Cote, 2003), with additional putative orthologues identified in *C.elegans*, *D.melanogaster* and *H.sapiens* giving a total of at least twenty probable members (Sanjuan and Marin, 2001). With the exception of the *S.cerevisiae* SAS2p (something about silencing) and *H.sapiens* HBO1 (histone binding to origin recognition complex), which appear to only be active when complexed with other proteins, all purified MYST-containing proteins have been shown to acetylate free histones in vitro, and this activity is mediated by the common MYST domain. In addition, several members (Utley and Cote, 2003) including MOZ (Kitabayashi *et al.*, 2001a) have also been shown to acetylate non-histone proteins.

The functions of the MYST proteins determined to date are diverse (reviewed in Utley and Cote, 2003). The *H.sapiens* MYST family member HBO1 is one of two MYST proteins that have been shown to interact with NRs and modulate their activity. Full-length HBO1 interacts with the androgen receptor (AR) in a ligand-enhanced manner and represses AR-mediated transcription (Sharma *et al.*, 2000). HBO1 does not contain an LXXLL motif (Section 1.8) and does not inhibit TR or ER-mediated transcription, suggesting it may specifically bind and regulate the AR through a novel mechanism. TIP60 (TAT interacting protein, 60 kDa), the second protein shown to interact with NRs, was first identified as a protein that bound the human immunodeficiency virus (HIV) TAT protein. It appears to act as a coregulator for a diverse range of transcription factors in addition to NRs (reviewed in Utley and Cote, 2003). The ability of TIP60 to interact with NRs was first shown with the AR (Brady *et al.*, 1999). Subsequent work indicated that this interaction is mediated through a single LXXLL motif present at the extreme C-terminus of the protein. This motif is necessary and sufficient for AR binding and allows a TIP60 construct lacking the N-terminal seventy amino acids to act as a coactivator for the Class I Nuclear Receptors (Gaughan *et al.*, 2001). However, the study investigating the effect of HBO1 on AR-mediated transcription found that full-length TIP60 acted as a repressor of AR (Sharma *et al.*, 2000). Thus, the exact role of this MYST family member in NR-mediated transcription remains to be elucidated.

The *S.cerevisiae* TIP60 homologue, ESA1 (essential SAS2-related acetyltransferase), has been shown to be an essential component of the NuA4 complex that acetylates lysine residues in the N-terminal tail of histone H4 (Allard *et al.*, 1999). The complex appears to be responsible for both the global acetylation of histone H4, which plays an as yet undetermined non-transcriptional role, and the specific transcription of subsets of genes, including ribosomal proteins, in response to signals such as nutrient availability (Reid *et al.*, 2000; Rohde and Cardenas, 2003). Both TIP60 (Ikura *et al.*, 2000) and ESA1p (Bird *et al.*, 2002) have also been shown to play an essential role in DNA double-strand break repair.

The first MYST protein identified in *D.melanogaster* was MOF (males absent on the first). MOF is present in a complex termed MSL (male specific lethal), which shows significant sub-unit homology to the ESA1p-containing NuA4 complex found in *S.cerevisiae*. The MSL complex plays an essential role in X chromosome dosage compensation in male flies, acting to increase transcription of the single male X chromosome two-fold. Males harbouring a mutation in MOF that inactivates its HAT activity show a lack of X chromosome-specific acetylation of histone H4 Lys16. This results in a compaction of the X chromosome that is repressive to transcription and prevents this required two-fold increase in expression. Thus, as with ESA1p, MOF acts in a global manner to activate transcription.

A number of the MYST family proteins have been shown to be involved in transcriptional silencing, contrary to the considered “standard” role of HATs as transcriptional coactivators. The *S.cerevisiae* proteins SAS2p and SAS3p mediate gene silencing at telomeres and at the HML locus, which is involved in mating-type switching (Reifsnyder *et al.*, 1996). In addition, SAS2p plays a role in the re-establishment of appropriate epigenetic marks after replication through interaction with the chromatin assembly factor 1 (ASF1p) (Osada *et al.*, 2001), while SAS3p, the catalytic sub-unit of the NuA3 complex, is involved in transcription elongation (John *et al.*, 2000). The *D.melanogaster* SAS2p homologue Chameau is also involved in silencing, in this case through mediating Polycomb silencing of Hox gene expression during larval development, and also for suppression of position effect variegation (PEV) effects. PEV is the term used to describe

epigenetic repression by pericentric heterochromatin, which is due to the position of the gene near the centrosome. Proteins such as Chameau are said to be suppressors of PEV because they prevent this position-dependent transcription.

In conclusion, the MYST family of proteins exhibit a wide range of roles, affecting normal cell signalling, proliferation and differentiation. Some members are regulators of transcription initiation and elongation, while others are involved in DNA synthesis and repair, acting in concert with cell cycle checkpoints to control proliferation. The finding that MOZ and MORF bind the RUNX family of transcription factors suggests that they likely play an essential role in proliferation, highlighting their importance to cell growth and survival, as is clearly the case for the yeast MYST proteins. Further evidence for this is provided by the identification of both MOZ and MORF at the sites of leukaemic translocations. Further study of the roles of these proteins in normal cellular processes is thus crucial to the understanding of how such leukaemias arise.

1.17 Research Aims

The chromosomal translocations t(8;16)(p11;p13), t(8;22)(p11;q13) and inv8(p11,q13) identified in patients with the M4/5 subtype of Acute Myeloid Leukaemia have been shown to result in the fusion of the MOZ gene to the coactivator proteins CBP, p300 and TIF2 respectively. CBP and p300 are global coactivators utilised by a large number of transcription factors, including Nuclear Receptors, during transcription activation. TIF2 however, is predominantly a Nuclear Receptor coactivator. The identification of the Retinoic Acid Receptor α gene as a target of chromosomal translocations resulting in AML, and the ability of NR ligands to induce differentiation of myeloid cells suggests that NRs play an important role in haematopoiesis. Therefore, the research described in this thesis was undertaken in order to determine whether the MOZ-TIF2 fusion protein might function to inhibit NR-mediated transcription in both a model system and in a myeloid cell line. In addition, given the role of TIF2 in recruiting CBP to active NR complexes, studies were undertaken in order to determine whether the MOZ-TIF2 protein could interact with CBP, and investigate whether this interaction might affect CBP function as a transcriptional coactivator for a small number of selected transcription factors.

Chapter Two:

Materials & Methods

2.1 General reagents

General reagents were analytical grade and purchased from Fisher Scientific (Loughborough, Leicestershire), Sigma (Poole, Dorset) and Oxoid Ltd. (Basingstoke, Hampshire).

2.2 Tissue culture

2.2.1 Media, supplements and reagents

DMEM and RPMI-1640 media, 200 mM L-glutamine, 10,000 U/ml Penicillin/Streptomycin, foetal calf serum (FCS) and Trypsin-EDTA were purchased from GIBCO, c/o Invitrogen Corporation (Paisley, Strathclyde). PBS tablets were purchased from Oxoid Ltd.

2.2.2 Cell line maintenance

The cell lines indicated in Table 2.1 were maintained in the appropriate growth medium in sterile plasticware (TPP, c/o Helena Biosciences, Tyne and Wear) or glass cell culture stirrer flasks (Techne, Cambridge) at 37 °C and 5% CO₂. Suspension cells were maintained at concentrations of 1x10⁵-1x10⁶ cells/ml. Adherent cells were grown to confluence in 10 cm dishes, harvested using 1x Trypsin/0.5 mM EDTA (GIBCO), diluted in fresh medium and plated at 2-4x10⁵ cells/dish.

2.2.3 Freezing down cells for liquid Nitrogen stocks

1-4x10⁶ cells were washed twice with 1x PBS and harvested by trypsinisation (adherent cells) or centrifugation (suspension cells). They were resuspended in the appropriate full medium (as described in Table 2.1) containing 10% DMSO. They were frozen gradually by incubation at -20 °C for 1 hr and -80 °C overnight. The cells were then transferred to liquid nitrogen for long-term storage.

Cell Line	Origin	Growth Medium
COS-1	African Green Monkey Kidney, SV40 transformed	DMEM + 2 mM L-Glutamine + 1% Penicillin/Streptomycin + 10% FCS
HEK293	Human Embryonal Kidney, adenovirus 5 transformed	DMEM + 2 mM L-Glutamine + 1% Penicillin/Streptomycin + 10% FCS
HeLa	Human Negroid cervix epitheloid carcinoma; HPV-16 positive	DMEM + 2 mM L-Glutamine + 1% Penicillin/Streptomycin + 10% FCS
U937	Human Caucasian histiocytic lymphoma	RPMI-1640 + 2 mM L-Glutamine + 1% Penicillin/Streptomycin + 10% FCS

Table 2.1: Mammalian Cell lines

The mammalian cell lines utilised in the research described in this thesis are shown with information detailing their origin and the composition of their growth medium. DMEM: Dulbecco's modified eagle medium (GibcoBRL); RPMI-1640: Roswell Park Memorial Institute 1640 medium (GibcoBRL).

2.2.4 Thawing cells from liquid Nitrogen stocks

Adherent cells to be recovered from liquid nitrogen storage were thawed by placing in a 37 °C water-bath for 5 minutes before addition to 10 ml pre-equilibrated (37 °C, 5% CO₂) full medium. They were incubated overnight (37 °C, 5% CO₂) to allow them to attach to the plate before the medium was replaced and the cells grown and passaged as described previously. Suspension cells were washed in 10 ml pre-equilibrated full medium once thawed (as described for adherent cells), collected by centrifugation (1500 rpm, 3 min, R.T.) and resuspended in fresh full medium. They were grown and passaged as described.

2.2.5 Stripped FCS for nuclear receptor transfections

One litre foetal calf serum (FCS) was stripped twice using a dextran-charcoal mix (10 g charcoal, 1 g Dextran T70, 10 ml 1 M Tris-HCl pH 7.4, made up to 1 litre with deionised water). 125 ml dextran-charcoal mix was added to each of eight 250 ml bottles and centrifuged (8,000 rpm, 20 min). The supernatant was carefully removed to leave the dextran-charcoal pellet and the 1 litre FCS split between four of the bottles. After careful mixing the FCS-charcoal-dextran solution was transferred to a 2 litre conical flask and incubated at 55 °C for 30 min with shaking. The mix was then returned to the four 250 ml bottles and centrifuged (8,000 rpm, 20 min, 4 °C). The supernatant was carefully removed and added to the remaining four bottles containing dextran-charcoal mix pellets for the second round of stripping. The FCS-dextran-charcoal solution was mixed, incubated, and centrifuged, as already described. To remove trace charcoal from the DCSS (dextran-charcoal stripped serum), the solution was drawn through a 0.8 µm filter under vacuum. It was then transferred to a tissue culture hood, passed through a 0.2 µm filter, aliquoted into sterile plasticware in 25 ml volumes and frozen at -20 °C.

2.2.6 Calcium phosphate-mediated transfection of adherent cells

For reporter assays, adherent cells were seeded at $1-2 \times 10^5$ cells/well in 6-well plates 24 hours prior to transfection (TPP, c/o Helena Biosciences) with 2 ml phenol red-free DMEM (GIBCO) supplemented with 5% DCSS. Unless otherwise stated, the quantities of transfected plasmids per well were as follows: 100 ng β-galactosidase reporter pCH110, 500 ng luciferase reporter, 100 ng expression vectors for transcription factors and other

proteins of interest. Empty vector (pcDNA3.0PT) was used to standardise the quantity of DNA in each well in the experiment. For immunofluorescence, COS-1 cells were seeded in 6-well plates ($1-2 \times 10^5$ cells/well) containing glass coverslips (BDH, c/o VWR International, Poole, Dorset) and grown in 2 ml 10% FCS-containing DMEM. Where appropriate, they were transfected with up to 1 μ g expression vector for each protein of interest. Co-immunoprecipitation experiments were carried out using HEK293 cells seeded in 10 cm dishes at a density of 1.5×10^6 cells/dish. They were transfected with a 10 μ g epitope-tagged expression construct and 10 μ g pSG5-CBP. For control dishes, empty pcDNA3.0PT was used in place of the tagged construct and empty pSG5 vector in place of CBP, as appropriate.

1-4 hr prior to transfection, cells were washed with sterile 1x PBS and fresh medium was added (2 ml for 6-well plate experiments, 12 ml for co-immunoprecipitations). Transfections were carried out using the CalPhosTM Mammalian Transfection Kit (Clontech, Basingstoke, U.K.) with some modifications:

For 6-well plate experiments, a 100 μ l/well DNA mastermix containing sterile water, DNA and 12.5% (v/v) 2 M calcium chloride solution was prepared for each transfection condition. This was added dropwise to an equivalent volume 2x HEPES Buffered Saline (HBS) solution while vortexing gently. After a 20 min incubation at room temperature the solution was mixed by pipetting and 200 μ l was added dropwise to the 2 ml medium present in each well. 8-16 hr later the medium was removed, the cells were washed twice with 1x PBS and fresh medium was added. For experiments involving Nuclear Receptors, 24 hours post-transfection the medium was replaced with medium containing the appropriate ligand (10^{-7} M; GAL4-ER α : 17- β oestradiol; GAL4-RXR α : 9-*cis* retinoic acid; GAL4-RAR α : all *trans* retinoic acid) or vehicle, and the cells incubated for 24 hr before harvesting. For 10 cm dish transfections, mastermixes of 600 μ l/dish were set up, combined with an equal volume 2x HBS as described and 1.2 ml added dropwise to each 10 cm dish.

2.2.7 Electroporation of suspension cells for reporter assays

U937 cells were collected by centrifugation (1500 rpm, 5 min, R.T.), washed once with 1x PBS and resuspended in RPMI-1640 supplemented with 0.1% glucose to a concentration of 1×10^8 cells/ml. 200 μ l cells were electroporated (Biorad Gene Pulser[®] II, 300 V, 950 μ F, max. capacitance) with 1 μ g pEF-BOS (β -galactosidase reporter), 4 μ g pRep4-RARE or p(PPRE)₃-tk-Luc (RAR and PPAR γ luciferase reporters respectively) and expression vectors for MOZ-TIF2 or MOZ-TIF2 Δ AD1. The total amount of DNA used was standardised at 10 μ g using pcDNA3.0PT. Post-electroporation, cells were recovered by addition of 800 μ l RPMI-1640 containing 10% DCSS. After a 3 hr incubation a further 1 ml RPMI-1640 containing 10% DCSS and either ligand (10^{-7} M; pRep4-RARE: all-*trans* retinoic acid and 9-*cis* retinoic acid; p(PPRE)₃-tk-luc: rosiglitazone and 9-*cis* retinoic acid) or equivalent volume vehicle was added. Cells were harvested after a further 21 hr. Duplicate electroporations were carried out for each condition.

2.3 Bacterial Manipulations

2.3.1 Bacterial strains

The *Escherichia coli* strains DH5 α and SURE[®] 2 (Stratagene, Texas, USA) were used for DNA manipulations and protein expression. They were separated to single colonies by streaking onto agar plates containing the appropriate antibiotics and incubation at 37°C overnight. Bacteria remained viable on agar plates stored at 4°C for several weeks. Liquid cultures were grown from a single colony (picked from an agar plate) at 37°C in sterile universal screw-top tubes (Bibby Sterilin, Stone, Staffordshire) or conical flasks containing the appropriate medium. Antibiotics were added as required. For long-term storage, 700 μ l of an overnight culture was mixed with 300 μ l 50% (v/v) sterile glycerol, snap frozen in liquid nitrogen and stored at -20 °C.

2.3.2 Liquid growth media

Luria Bertani medium: 10 g/l tryptone (Oxoid Ltd.), 5 g/l yeast extract (Oxoid Ltd.), 10 g/l NaCl (Fisher Scientific), in deionised water. pH 7.0.

NZY⁺ medium: 10g NZamine (casein hydrolysate), 5 g yeast extract, 5 g NaCl, adjusted to pH 7.5 with NaOH, in 965ml deionised H₂O. NZY⁺ medium was supplemented with filter-sterilised 12.5 ml 1 M MgCl₂, 12.5 ml 1 M MgSO₄ and 10 ml 20% (w/v) glucose following sterilisation by autoclaving.

2.3.3 Solid growth media

For LB agar plates 1 litre of LB medium was supplemented with 15 g bacto-agar (Oxoid Ltd.) prior to sterilisation. 20-25 ml of molten agar medium was poured into each Petri dish and allowed to solidify. Plates were dried for 20 minutes at 37 °C and stored at 4 °C.

2.3.4 Antibiotics

Antibiotics were added to liquid medium immediately to use, and to molten LB agar medium once it had cooled to <65 °C.

Ampicillin 1,000x stock solution: 100 mg/ml in 50% ethanol

Kanamycin 1,000x stock solution: 50 mg/ml in H₂O

2.3.5 Sterilisation

Glassware was sterilised by heating to 60 °C overnight. Growth media and heat stable solutions were sterilised in an autoclave at 121 °C for 20 minutes. Other solutions, such as antibiotics, were sterilised by filtration through a 0.2 µm filter (Millipore, Watford, Hertfordshire).

2.3.6 Preparation of competent *E.coli* DH5 α cells

E.coli DH5 α were made competent for DNA transformation using the Calcium Chloride Method. Briefly, a single colony from an overnight LB plate was picked and transferred to 5 ml LB medium. After 16 hours growth at 37 °C the culture was diluted 1 in 100 in LB medium and grown at 37 °C to an Optical Density (at 600 nm) of 0.5. Following a 10 min incubation on ice in pre-chilled 50 ml Falcon tubes the cells were harvested by centrifugation (10 min, 2400 rpm, 4 °C). The cell pellets were resuspended gently on ice in 20 ml each of ice-cold Buffer 1 (30 mM KCl; 100 mM RbCl; 10 mM CaCl₂, 50 mM MgCl₂, 15% glycerol; adjusted to pH 5.8 using 0.2 M filter-sterilised glacial acetic acid). After a second centrifugation (10 min, 2400 rpm, 4 °C) each cell pellet was resuspended in 2 ml ice-cold Buffer 2 (10 mM MOPS; 75 mM CaCl₂, 10 mM RbCl, 15% glycerol; adjusted to pH 6.5 using 1 M filter-sterilised KOH) and the cell suspensions combined. Microfuge tubes were placed in dry ice to allow snap freezing of 200 μ l cell suspension aliquots. Competent cells were stored at -80 °C. Transformation efficiency was checked using pSG5 vector and the transformation serially diluted to allow determination of number of transformants: 1 μ g DNA should give $\sim 1 \times 10^6$ transformants.

2.3.7 Transformation of DH5 α Cells

Competent cells were removed from -80 °C and defrosted on ice. A cell suspension volume of 50 μ l was used for each transformation. DNA (10-500 ng) was added to the competent cells and the tubes incubated on ice for 15 min. The cells were heat-shocked for 90 seconds at 42 °C before returning to ice for 2 min. After the addition of 950 μ l LB medium, the cells were incubated at 37 °C for 1 hr. For standard transformations, 100 μ l transformation culture was plated out onto LB agar plates containing the appropriate antibiotic. For ligation transformations the cells were collected by centrifugation (5,000 rpm, 5 min), 900 μ l supernatant was removed and the cells were resuspended in the remaining LB medium before plating. Bacteria spread on LB agar plates were incubated overnight at 37 °C.

2.3.8 Transformation of SURE[®]2 bacterial cells

The *E.coli* SURE[®]2 strain was purchased (Stratagene, Texas, USA) as supercompetent cells and transformed as recommended by the manufacturer: cells (100 µl/transformation) were thawed on ice and aliquoted into pre-chilled 15ml Falcon tubes to which was added 2 µl (/transformation) 1.25 M β-mercaptoethanol (provided by manufacturer). The tubes were swirled gently every 2 min during a 10 min incubation on ice before the addition of 1-50 ng plasmid DNA. After a further 30 min on ice the cells were heat shocked (42 °C, 30 sec) and placed back on ice for 2 min. A 0.9 ml volume of pre-warmed (42 °C) NZY⁺ medium was added and the tubes incubated (37 °C, 1 hr, 220 rpm) before plating of 100 µl onto LB agar containing the appropriate antibiotic.

2.4 Molecular Biological Techniques

2.4.1 General reagents

Molecular biological products were purchased from Amersham Biosciences (Little Chalfont, Buckinghamshire), Fisher Scientific (Loughborough, Leicestershire), Invitrogen Corporation (Paisley, Strathclyde), New England Biolabs (Hitchin, Hertfordshire), Perkin Elmer (Zaventem, Belgium), Promega (Southampton, Hampshire), Qiagen (Crawley, Sussex), and Roche (Lewes, Sussex).

2.4.2 Solutions

1x TE Buffer: 10 mM Tris-HCl (pH 7.4), 1 mM EDTA

0.5x TBE: 45 mM Tris-base, 45 mM boric acid, 0.5 mM EDTA

4x DNA loading dye: 30% glycerol, 0.25% bromophenol blue

Cell Lysis Solution I: 25 mM Tris-HCl pH 8.0, 50 mM glucose, 10 mM EDTA pH 8.0, 10 µg/ml RNase

Cell Lysis Solution II: 0.2 M NaOH, 1% SDS

Cell Lysis Solution III: 60 ml 5 M potassium acetate, 11.5 ml glacial acetic acid, 28.5 ml H₂O

Table 2.2 Origin of Plasmids

Plasmids utilised during the research described in this thesis were obtained as detailed.

Plasmid	Source
pcDNA3	Invitrogen
pSG5	Stratagene
pCH110	Pharmacia Biotech, (c/o Amersham Biosciences)
pEF-BOS	Dr. C Bevan, Imperial College, London
p(Gal4) ₅ -E1b Δ -Luc	Dr. P. Shaw, University of Nottingham
GAL4-ER α	Dr. M. Parker, Imperial College, London
GAL4-RAR α	Dr. M. Parker, Imperial College, London
GAL4-RXR α	(Folkers and van der Saag, 1995)
pSG5:HA-GRIP1	Dr. M. R. Stallcup, University of Southern California, U.S.A.)
pSG5-TIF2	Dr. C. Bevan, Imperial College, London
pcDNA3-MOZ	Dr. D. G. Gilliland, Harvard University, U.S.A.
pcDNA3-MOZ-TIF2	Dr. D. G. Gilliland, Harvard University, U.S.A.
pSG5-CBP	constructed by J. Harries, University of Leicester
pSG5-FLAG-SRC1e	(Kalkhoven <i>et al.</i> , 1998)
GST-ER α :AF2	(Heery <i>et al.</i> , 1997)
GST-RXR α :AF2	Dr. K. Chatterjee, University of Cambridge
pGex2TK	Pharmacia (c/o Amersham Biosciences)
GST-CBP:SID	(Sheppard <i>et al.</i> , 2001)
GST-CBP full-length	Dr. A Harel-Bellan, Centre National de la Recherche Scientifique, Villejuif, France
pRep4-RARE	Dr. A. Zelent, Institute of Cancer Research
p(PPRE) ₃ -tk-Luc	Dr. S. Ali, Imperial College, London
pcDNA3-p53	Dr. X. Liu, University of California, Riverside, USA
p21P-Luc	(Datto <i>et al.</i> , 1995)
IRGC-E4-Luc	Dr. X. Liu, University of California, Riverside, USA
FNpcDNA3:ETS-2	Dr. M. Ostrowski, Ohio State University, USA
E.18-Luc	Dr. M. Ostrowski, Ohio State University, USA
UPA-Luc	Dr. M. Ostrowski, Ohio State University, USA
pSG5-AML1	Dr. A Zelent, Institute of Cancer Research, London
pT109-Luc	Dr. A Zelent, Institute of Cancer Research, London
pBTM116mod.	(Sheppard <i>et al.</i> , 2001)

2.4.3 Small-scale plasmid purification from bacterial cells

For small-scale plasmid DNA preparation, 1-3 ml *E.coli* culture (grown overnight at 37 °C and 220 rpm) was centrifuged and the supernatant removed by aspiration. The plasmid DNA was purified from the bacterial pellet using the microcentrifuge protocol from the Qiaprep Spin Miniprep Kit (Qiagen). Sterile water was used to elute the DNA from the Qiaprep column.

2.4.4 Large-scale plasmid purification from bacterial cells

For large-scale plasmid DNA preparation (200 ml overnight *E.coli* culture grown at 37 °C and 220 rpm) the Qiagen Plasmid Maxi Protocol was used with the following modifications: cells were lysed in the 250 ml bottles in which they were harvested. Thus, following the 20 min incubation on ice after Buffer 3 addition, centrifugation was for 30 min at 15,000 g and 4 °C. The supernatant was then immediately transferred to a 35 ml Sorvall tube (Kendro, Bishop's Stortford, Hertfordshire) and centrifuged (21,000 g, 15 min, 4 °C) before pipetting onto the Qiagen column. The final DNA pellet was resuspended in 500 µl sterile water and its concentration determined as described. If required, the DNA was diluted to 1 µg/µl.

2.4.5 Caesium chloride purification of plasmid DNA

To obtain large quantities of pcDNA3:MOZ and pcDNA3:MOZ-TIF2 DNA for cloning caesium chloride DNA purification was used.

An overnight 400 ml culture of transformed *E.coli* SURE[®]2 was harvested by centrifugation (15 min, 4,000 g, 4 °C). The cell pellet was resuspended in 10 ml Cell Lysis Solution I before addition of 20 ml Solution II and a five-minute incubation on ice. 15 ml ice-cold Solution III was then added to neutralize the alkali lysis and the suspension incubated on ice for 10 minutes. The plasmid-containing supernatant was collected by centrifugation of the cellular DNA and debris (12,000 g, 15 min, 4 °C), transferred to a fresh tube and precipitated using 50 ml ice-cold isopropanol. The DNA was collected by a further centrifugation (12,000 g, 15 min, 4 °C) and resuspended in 5.5 ml TE after air-drying for 30 minutes. A 500 µl volume of 5 mg/ml ethidium bromide and 6 g CsCl₂ were

added and, once the latter had dissolved completely, the solution was centrifuged (4,000 g, 5 min, R.T.) and the supernatant pipetted into a new tube. In order to balance the CsCl₂-containing DNA solutions, they were weighed, tared and then 100µl was removed. A reduction in weight of 0.155-0.156 g was required. If the reduction was less than 0.155 g, 1.1 mg/ml CsCl₂ in 1x TE was added and the procedure repeated. If a weight greater than 0.156 g was measured, 1x TE was added. Once balanced, the solutions were pipetted into quick-seal tubes (Beckman Coulter Ltd., High Wycombe, Buckinghamshire), heat sealed and centrifuged (100,000 rpm, overnight, 20 °C). The lower (supercoiled) plasmid band was removed from the gradient using a 21 gauge needle and the ethidium bromide removed by repeated extraction with equal volumes of caesium-saturated isopropanol. The solution was then diluted with two volumes H₂O and the DNA precipitated with ethanol. Following three washes with 70% ethanol the DNA was resuspended in 500 µl sterile H₂O.

2.4.6 Phenol / chloroform extraction of DNA

Contaminating protein was removed from solutions of DNA by increasing the aqueous volume to 300 µl with sterile H₂O followed by addition of 300 µl phenol, vigorous shaking and centrifugation (10,000 rpm, 5 min). After repetition of the phenol step, two equal-volume chloroform extractions were carried out in the same manner to remove trace phenol. The DNA was then collected by ethanol precipitation.

2.4.7 Ethanol precipitation of DNA

DNA was precipitated using 0.1 volumes of 3M sodium acetate pH 5.2 and 3 volumes ethanol. The precipitate was recovered by centrifugation (13,000 rpm, 4 °C, 15 min). To remove excess salt ions, 70% (v/v) ethanol was added and the centrifugation repeated. After a second 70% ethanol wash the DNA pellet was air-dried and resuspended in sterile H₂O.

2.4.8 Determination of nucleic acid concentration

DNA and oligonucleotide concentrations were determined by optical density measurement (Eppendorf Biophotometer, Cambridge, U.K.) at 260 nm in quartz cuvettes (Perspec Service, Newbold Verdon, Leicestershire). For uncut DNA plasmids, 1 μg was then run on a 0.8% agarose gel to allow estimation of the ratio of supercoiled to nicked DNA.

2.4.9 Agarose gel electrophoresis

DNA fragments were separated on the basis of molecular size by agarose gel electrophoresis. Agarose (Fisher Scientific) was dissolved in 0.5x TBE to a concentration of 0.8% (w/v) by heating. Once the solution had cooled to $<65\text{ }^{\circ}\text{C}$ ethidium bromide was added (final concentration 5 $\mu\text{g}/\text{ml}$), the agarose poured into an appropriate electrophoresis tray and a comb inserted. Once set, the gel was submerged in 0.5x TBE in a horizontal electrophoresis tank and the comb removed. DNA samples were mixed with 4x DNA loading dye and pipetted into the wells in the gel. DNA bands were separated at up to 5 V/cm. After electrophoresis, DNA bands were visualised by UV transilluminator.

2.4.10 Isolation and purification of DNA from agarose gels

DNA bands to be purified were cut from the agarose gel with a minimal amount of agarose after separation by electrophoresis. The DNA was purified using the QIAquick Gel Extraction Kit vacuum microcentrifuge protocol (Qiagen) and eluted in 30-50 μl sterile H_2O .

2.4.11 Oligonucleotides

Oligonucleotides were purchased from the Protein and Nucleic Acid Laboratory (PNAAL, University of Leicester, U.K.) as lyophilised and desalted pellets. They were resuspended in sterile H_2O to a concentration of approximately 100 μM and stored at $-20\text{ }^{\circ}\text{C}$. Appendix 1 describes the oligonucleotides used during this work.

2.4.12 Polymerase Chain Reaction (PCR)

PCR reactions were carried out in a total volume of 100 μ l containing 1 μ l Elongase (Invitrogen), 10 μ l each Elongase Buffers A and B (provided by manufacturer), 10 μ l 2 mM dNTP mix (Amersham), 2 μ l 10 ng/ μ l template (or H₂O for control PCR), 1 μ l each primer (of 100 μ M stock) and 65 μ l sterile H₂O. Reactions were covered by Nujol mineral oil (Perkin Elmer) and performed using a Perkin Elmer DNA Thermal Cycler 480. Initial denaturation (2 min, 94 °C) preceded 30 cycles of: denaturation (1 min, 94 °C), annealing (1 min, temperature calculated by lowest primer T_m minus 5 °C), elongation (time calculated as 30 sec + 30 sec per 1 kb DNA in region to be amplified, 68 °C). Once completed, 10 μ l PCR reaction was separated by agarose gel electrophoresis to determine whether appropriately-sized DNA fragments had been generated.

2.4.13 Recovery of DNA from PCR reactions

Oil and salt were removed from PCR reactions by chloroform extraction and ethanol precipitation. Briefly, 150 μ l sterile H₂O was added to the PCR reaction, followed by 250 μ l chloroform. The mixture was shaken vigorously and centrifuged (10,000 rpm, 5 min). The top layer was carefully collected and the chloroform extraction repeated. After the second extraction the DNA was ethanol precipitated as described previously

2.4.14 Generation of mutations / deletions by recombinant PCR

To mutate / delete specific nucleotides within a DNA sequence four oligonucleotides were designed and used as primers for PCR as shown in Figure 2.1. Primers 3 and 4 spanned existing restriction enzyme sites 5' and 3' respectively to the nucleotides to be mutated/deleted. Primers 1 and 2 were complimentary, spanned the region to be mutated/deleted and either a) contained the nucleotide mutations or b) were complimentary to the region either side of the sequence to be deleted.

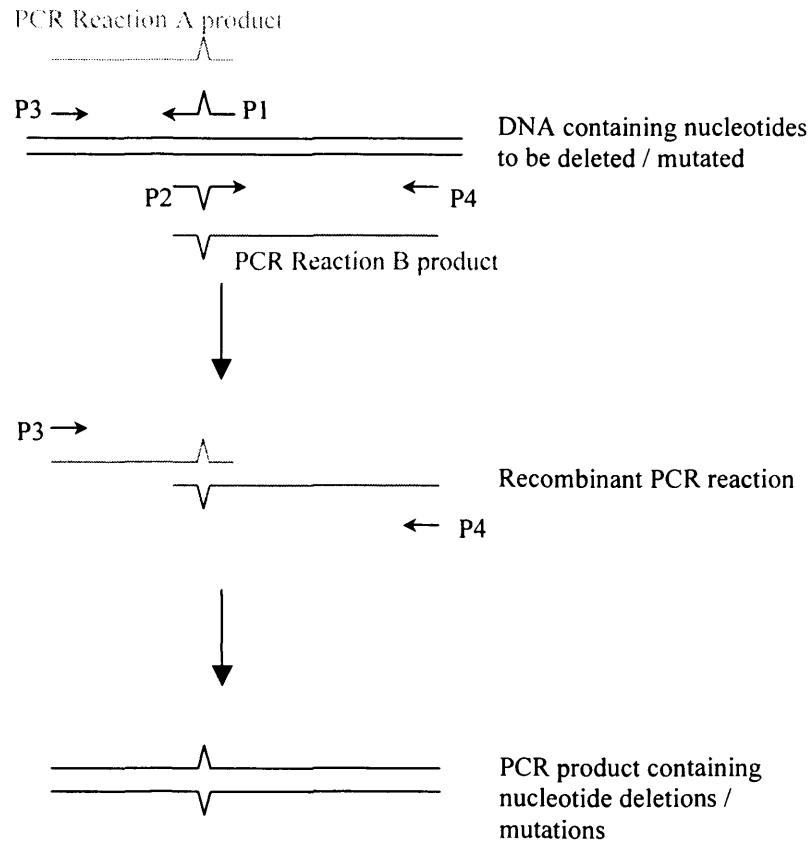


Figure 2.1: Generation of deletion / mutation constructs using recombinant PCR

Recombinant PCR may be used in order to generate nucleotide deletions or mutations within a construct. Four primers (P1-P4) are generated with primers P3 and P4 spanning unique restriction sites either side of the region to be deleted / mutated. Primers P1 and P2 are complimentary to each other and contain the nucleotide deletion / mutation (specified by V / Δ). Two initial PCR reactions (A and B) are performed. Reaction A utilises Primers P3 and P1; Reaction B, primers P2 and P4. The resulting PCR products, which contain complimentary sequence originally specified by primers P1 and P2, are then combined in a third Recombinant PCR reaction using Primers primers P3 and P4. This results in the generation of a full-length PCR product containing the mutation / deletion.

2.4.15 Annealing of single-stranded oligonucleotides

Complimentary oligonucleotides for generation of new multiple cloning sites were diluted to 10 ng/ μ l and treated separately with Polynucleotide Kinase (as described). They were then ethanol precipitated, resuspended in 10 μ l H₂O each and combined. Annealing was catalysed by heating to 100 °C (2 min) and slow cooling (100 °C down to 40 °C over 30 min) using a Perkin Elmer DNA Thermal Cycler 480.

2.4.16 Polynucleotide Kinase treatment of DNA

5 μ l DNA was phosphorylated in a 50 μ l reaction volume using 2 μ l Polynucleotide Kinase and 10 μ l 5x T4 DNA ligase buffer (Roche) at 37 °C for 30 min.

2.4.17 Restriction enzyme digestion

Restriction digests were carried out in the buffers and at the temperatures recommended by the manufacturer (restriction enzymes purchased from Roche or, where necessary, New England Biolabs). Double and triple digests were carried out together where the buffers and temperatures were compatible (total restriction enzyme volume in reaction <10%; total reaction volume 10-50 μ l), or the reactions were carried out sequentially with the DNA purified by ethanol precipitation between the digests.

2.4.18 Alkaline Phosphatase treatment of DNA

Digested vectors prepared for ligation were treated with calf intestine alkaline phosphatase (Roche) for 1 hr at 37 °C to dephosphorylate the 5' DNA ends and prevent re-annealing, as per manufacturer's protocol.

2.4.19 DNA ligation

Ligations were carried out at room temperature for 2-3 hr using T4 DNA ligase (Roche) with approximately a 3-fold excess of insert, as per manufacturer's protocol. Control ligations were also set up containing vector DNA alone. The ligated DNA was transformed

into *E. coli* DH5 α and plated out on LB agar plates containing the appropriate antibiotic, as described previously.

2.4.20 Colony PCR screening

Ligation colonies and if present, control colonies, were picked from LB agar plates grown overnight and used to inoculate 1 ml LB medium cultures containing the appropriate antibiotic. After 4-8 hr growth 5 μ l culture was transferred to a PCR tube containing 45 μ l of the PCR mastermix (volumes per colony PCR reaction: 0.25 μ l Taq DNA Polymerase (Invitrogen), 5 μ l 10x Taq buffer, 1.5 μ l MgCl₂, 5 μ l 2 mM dNTP mix (Amersham), 0.25 μ l each primer (100 μ M stock), 32.75 μ l H₂O). PCR was carried out (72 °C elongation temperature) as described previously. 10 μ l PCR product was separated by agarose gel electrophoresis and positive clones identified. The corresponding 1 ml cultures were increased to 5 ml and grown at 37 °C and 220 rpm.

2.4.21 DNA sequencing

Plasmid DNA for sequencing was sent to the Protein and Nucleic Acid Laboratory (University of Leicester, U.K.) and sequenced using an ABI377 Automated Sequencer (Perkin Elmer).

2.5 Biochemical Techniques

2.5.1 Solutions and buffers

4x SDS-PAGE sample buffer: 200 mM Tris-HCl pH 6.8, 40% (v/v) glycerol, 2% (w/v) SDS, 5% (v/v) β -mercaptoethanol, 0.4% (w/v) bromophenol blue, 400 mM dithiothreitol

10x SDS-PAGE running buffer: 250 mM Tris-HCl, 2.5 M glycine, 1% (w/v) SDS

SDS-PAGE stacking gel: 1 ml volume: 680 μ l H₂O, 170 μ l 30% acrylamide mix (National Diagnostics, Hull), 130 μ l 1 M Tris-HCl pH 6.8, 10 μ l 10% (w/v) SDS, 10 μ l 10% (w/v) ammonium persulphate, 1 μ l TEMED (N,N,N',N'-Tetramethylethylenediamine)

% acrylamide in Resolving Gel		6%	8%	12%	15%
Protein Size for Separation (kDa)		150-300	100-250	30-100	10-50
Components	H ₂ O	2,600	2,300	1,600	1,100
	30% acrylamide mix	1,000	1,300	2,000	2,500
	1.5 M Tris-HCl pH 8.8	1,300	1,300	1,300	1,300
	10% (w/v) SDS	50	50	50	50
	10% (w/v) APS	50	50	50	50
	TEMED	4	3	2	2
Volumes (μl) for 5 ml resolving gel					

Table 2.3: Solution compositions for preparing resolving gels for Tris-glycine SDS-Polyacrylamide Gel Electrophoresis

The volumes (in μl) of the components required for the production of 5 ml SDS-PAGE resolving gel at varying percentages of acrylamide are shown. In addition, approximate protein sizes in kilo-Daltons that can be successfully resolved at each acrylamide percentage are indicated.

Coomassie stain: 0.25% (w/v) Coomassie Brilliant Blue R250 in de-stain solution

De-stain solution: 5:5:1 H₂O: methanol: glacial acetic acid

High glycine transfer buffer: 48 mM Tris-HCl, 380 mM glycine, 0.1% (w/v) SDS, 20% (v/v) methano

Fix: 10% (v/v) glacial acetic acid, 10% (v/v) methanol

IPH buffer: 50 mM Tris-HCl pH 8.0, 150 mM NaCl, 0.5% (v/v) NP-40, 1x EDTA-free Complete protease inhibitor tablet (Roche) per 25 ml

RIPA buffer: 20 mM Tris-HCl pH 7.5, 150 mM NaCl, 0.1% (w/v) SDS, 1% (v/v) Triton X-100, 1 mM EDTA

TBST: Tris buffered saline, Tween: 50 mM Tris-HCl pH 7.4, 150 mM NaCl, 0.05% (v/v) Tween-20

Stripping buffer: 62.5 mM Tris-HCl pH 6.7, 100 mM β-mercaptoethanol, 2% SDS

NDTN buffer: 20 mM Tris-HCl pH 8.0, 200 mM NaCl (unless otherwise stated), 0.5% (v/v) NP-40, 1 mM DTT, 1x ETDA-free Complete tablet (Roche) /25 ml buffer

2.5.2 Radiolabelled chemicals

[³⁵S]-Methionine was purchased from Amersham Biosciences (Little Chalfont, Buckinghamshire).

2.5.3 Antibodies

Anti-CBP A-22 and C-20, anti-MOZ N-19, anti-goat IgG FITC and anti-rabbit IgG peroxidase were purchased from Autogen Bioclear (Calne, Wiltshire); and anti-FLAG M2, anti-FLAG M2 affinity gel, anti-mouse IgG FITC, anti-mouse IgG TRITC and anti-rabbit IgG TRITC were from Sigma.

2.5.4 Harvesting adherent cells for reporter assays

Transfected cells to be harvested for reporter assays were washed once with 1x PBS and harvested by scraping in 750 µl 1x PBS and pipetting into micro-centrifuge tubes. The cells were pelleted (5 min, 4,000 rpm) and resuspended in 100 µl 1x Reporter Lysis Buffer

(Applied Biosystems, Bedford, Ma., U.S.A.). Following vigorous vortexing, the cells were frozen at -20 °C.

2.5.5 Harvesting suspension cells for reporter assays

The 2 ml volumes from each transfected well were pipetted into 2 ml microfuge tubes, centrifuged (4,000 rpm, 5 min, 4 °C) and the supernatant replaced with 1 ml 1x PBS. The cells were carefully resuspended and then re-centrifuged. After a second PBS wash the cell pellets were resuspended in 100 µl 1x Reporter Lysis Buffer by vigorous vortexing and stored at -20 °C.

2.5.6 Assay of transfected cells

Harvested cells stored at -20 °C in lysis buffer were centrifuged (8 min, 13,000 rpm, 4 °C) directly from the freezer and placed on ice. Luciferase and β-galactosidase activities were determined using Dual-Light[®] System (Applied Biosystems, Bedford, MA, U.S.A) as described below.

A maximum of 30 cell supernatants were assayed at any one time but where experiments resulted in more than 30 extracts, batches of 24-30 were done sequentially. 5 µl supernatant was placed in two luminometer tubes (Sarstedt, Loughborough, Leicestershire) for each extract to be measured. After aliquoting all the extracts to be measured, 12.5 µl Buffer A was added to each tube at 12 second intervals. 50 µl Buffer B (containing Galacton-Plus[®] substrate diluted 1:100) was added (in the same order as Buffer A) immediately prior to measurement of the luciferase activity (10 second measurement time, Lumat LB 9507 luminometer, Berthold, Redbourn, Hertfordshire). One hour after addition of Buffer A, 50 µl Accelerator was added to each tube and the β-galactosidase activity measured immediately (10 second measurement time). The luciferase:β-galactosidase ratio for each tube was calculated and the average ratio and S.E.M. (standard error of the mean) for each transfection condition determined. Relative Luciferase Activity (RLA), in the absence of ligand where appropriate, was calculated by dividing the average luciferase:β-galactosidase ratio for each condition by that for wells containing reporter DNA alone.

Error bars shown were calculated by dividing the determined S.E.M. by the average luciferase: β -galactosidase ratio for the reporters.

2.5.7 Preparation of cells for immunofluorescence

For immunofluorescence adherent cells grown on coverslips were washed twice (all washes described were in 1x PBS) and fixed with 4% paraformaldehyde (10 min, R.T.). After a further three washes, the cells were permeabilised with 0.2% Triton X-100 in PBS (2 min, R.T.) and washed four times. This was followed by blocking (1 hr, R.T.) in Antibody Dilution Buffer (ADB: 3% BSA in PBS) and incubation with primary antibodies (1:50 dilution for transfected proteins, 1:10 for endogenous CBP, 1 hr, R.T., under aluminium foil). Fluorophore-conjugated secondary antibodies were added (1:100 dilution in ADB, 30 min, R.T., under foil) after a further four washes and removed by three washes. Cells were incubated (5 min, R.T., under foil) in Hoechst 33258 stain (500 ng/ml in PBS) and then a final three washes were carried out. Coverslips were mounted cell-side down on 8 μ l 90% glycerol (v/v) in 1x PBS, and the edges sealed using nail varnish. Slides were stored at 4 °C.

2.5.8 Capturing of immunofluorescence images

Immunofluorescence images were captured using a Zeiss Axioskop2 microscope with the 83,000 filter set (DAPI, FITC, Texas Red filters; Chroma, Brattleboro, VT, U.S.A) and SmartCapture2 software programme (Digital Scientific, Cambridge). Images were processed in Adobe Photoshop (Adobe Systems Incorporated, Uxbridge, Middlesex).

2.5.9 Preparation of whole cell lysates

HEK293 cells incubated for 48 hr following transfection were washed and harvested (by scraping) in 1x PBS. The cells were collected by centrifugation (4,000 rpm, 5 min, 4 °C), resuspended in 1 ml IPH lysis buffer (for co-immunoprecipitation) or 300 μ l RIPA buffer (for western blot) and passed through a 21-gauge needle to shear the DNA. After a 20 min incubation on ice the lysate was centrifuged (13,000 rpm, 10 min, 4 °C) and the

supernatant placed on ice. Lysates for western blot were assayed for protein concentration (as described), and 300 µg protein loaded on a large SDS-PAGE gel.

2.5.10 Protein co-immunoprecipitation

Whole cell supernatants containing 5 mg protein for co-immunoprecipitations were pre-cleared (30 min, 4 °C, rotating wheel) with washed (twice with 1x PBS, twice with IPH buffer) 20 µl Protein-A Sepharose/Protein G-Sepharose (50:50 mix). Bound immune complexes were removed by centrifugation (2,500 rpm, 5 min, 4 °C) and 20 µl washed α-FLAG M2 high affinity bead-conjugated antibody added to the supernatant. The lysates were left rotating overnight (4 °C) before pelleting of immune complexes by gentle centrifugation (2,500 rpm, 5 min, 4 °C), washing three times with Buffer IPH and aspiration down to 20 µl. 40 µl SDS-PAGE sample buffer was added, the sample boiled for 3 min and the bound proteins separated on a 6% SDS PAGE gel.

2.5.11 Protein concentration determination

Protein concentrations of undiluted supernatant and 1:2, 1:5 and 1:10 dilutions were determined using the BCA Protein Assay Kit (Pierce, Rockford, IL. U.S.A). Assays were carried out using the manufacturer-recommended standard protocol (37 °C incubation, 30 min) in microtitre plates with 5 µl standard (0-800 µg/ml BSA) or protein sample and 100 µl assay reagent. Absorbance was measured at 565 nm.

2.5.12 Sodium Dodecyl Sulphate-Polyacrylamide Gel Electrophoresis (SDS-PAGE)

SDS-PAGE gels were prepared with the appropriate percentage resolving gel (as described in Table 2.2) and stacking gel. Polymerisation was catalysed by the addition of ammonium persulphate. Protein extracts (300 µg cell extracts for large gels) were denatured by boiling (3 min) in 1x SDS-PAGE sample buffer immediately prior to loading. Gels were electrophoresised in Biorad Protean II system in 1x SDS-PAGE running buffer at 150 V (mini-gels) or 220 V (large gels).

2.5.13 Coomassie staining of SDS-PAGE gels

Non-radioactively labelled proteins separated on SDS-PAGE gels for visualisation were stained by soaking in Coomassie stain (1 hr, R.T.) followed by transfer to Destain solution (>4hr, R.T.). During destaining, the Destain solution was changed 2-3 times.

2.5.14 Preservation of SDS-PAGE gels

Coomassie-stained SDS-PAGE gels to be preserved were soaked in 1% (v/v) glycerol (>30 min, R.T.), placed on wetted filter paper, covered with saran wrap and dried (80 °C, 1 hr) under vacuum (Biorad Hydrotech Vacuum Pump) using Biorad Model 583 Gel Dryer. After drying, gels were left under vacuum (15 min, R.T.) to cool.

2.5.15 Protein transfer to nitrocellulose membrane

Proteins separated on SDS-PAGE gels for western blotting were transferred to nitrocellulose membranes by wet-blotting overnight at 30 V (4 °C, Biorad Protean II xi Cell) in High Glycine Transfer buffer followed by 1 hr at maximum amps. The membrane was soaked in 0.05% Tween-20 in 1x PBS before visualisation of protein transfer by staining with Ponceau S Solution (Sigma), which was subsequently removed by washing with distilled H₂O.

2.5.16 Western blotting and immunodetection

Nitrocellulose membranes containing immobilised proteins separated by SDS-PAGE were blocked by incubation in 5% dried milk in 1x PBS (1 hr, rocking, R.T.) to prevent further protein binding. Specific bound proteins were detected immunologically. Briefly, primary antibodies were diluted in 1:500 in 3% milk in 1x PBS and incubated with the membrane (1 hr, rocking, R.T.; or overnight, rocking, 4 °C). The membrane was washed three times (5 min, rocking, R.T.) with 0.05% Tween-20 in 1x PBS before addition of secondary HRP-conjugated antibody (1:2000 dilution, 1 hr, rocking, R.T.). Excess/unbound secondary antibody was removed by three washes (5 min, rocking, R.T.) with Tween/PBS solution. For anti-FLAG Western blots 1x TBS was used in place of 1x PBS. Protein:antibody immunocomplexes were detected by ECL+ chemiluminescent detection kit (Amersham).

Membranes were incubated (3-5 min, R.T.) face-down on mixed ECL+ reagents on saran wrap before draining of excess reagent and wrapping in fresh saran wrap. Wrapped blots were placed protein side up in x-ray film cassettes and exposed (10 sec-1 hr) to autoradiography film. If very short exposure times still resulted in over-exposed films, blots were rinsed very briefly in 1x PBS to further remove ECL+ reagent, re-wrapped in saran wrap and exposed again. X-ray films were developed using a DuPont Cronex CX-130 x-ray film developer.

2.5.17 Stripping membranes for re-probing

Membranes to be re-probed with different antibodies were incubated in Stripping Buffer (30 min, shaking, 60 °C) and washed three times with Tween/PBS solution (5 min, rocking, R.T.). They were then blocked and probed as described previously.

2.5.18 Small-scale bacterial expression of GST-tagged proteins

Bacterial colonies from a freshly transformed plate were inoculated into 2.5 ml LB-Ampicillin medium. After 2 hr growth (37 °C) 1 ml was placed in two microfuge tubes. IPTG was added to one to a final concentration of 500 µM (induced culture), and an equal volume of water was added to the other (control culture). The remaining 0.5 ml was kept at 4 °C for future inoculation of large-scale cultures. After a further 3 hr growth (37 °C) the cells were harvested by centrifugation (4,000 rpm, 5 min) and the pellets resuspended in 50 µl SDS-PAGE sample buffer. After boiling, 20 µl was loaded onto a SDS-PAGE mini-gel. Induced cultures were run alongside the appropriate control culture and the presence of an induced protein band of the correct size determined after staining.

2.5.19 Large-scale bacterial expression of GST-tagged proteins

The remaining 0.5 ml from bacterial cultures showing good protein induction during small-scale expression analysis were used to inoculate 10 ml LB-Ampicillin medium (overnight, 37 °C, 220 rpm). The following morning the culture was diluted 1:10 and grown for 1 hr (37 °C, 220 rpm). A 200 µl sample was removed to a microfuge tube (Uninduced), IPTG was added to a final concentration of 500 µM and a second 200 µl sample taken (Induced).

The cultures were incubated for a further 3 hr before harvesting of the bacterial cells by centrifugation (50 ml volume, 4,000 rpm, 10 min, 4 °C) and freezing of the pellet.

2.5.20 Purification of GST-tagged proteins

Induced bacterial pellets from 50 ml culture aliquots were resuspended in NDTN Buffer and sonicated (20 sec on / 40 sec off, 3 cycles, power 12, MSE Soniprep 150, Sanyo). Cell debris was removed by centrifugation (4,000 rpm, 5 min, 4 °C), the supernatant transferred to a 15 ml falcon and a 20 µl sample removed. 100 µl glutathione sepharose beads were washed three times with an equal volume 0.5% milk powder in NDTN Buffer, collected by centrifugation (2,000 rpm, 2 min) and resuspended in 100 µl milk/NDTN. 125 µl bead slurry was added to the cleared 5 ml bacterial supernatant and placed on a rotating wheel at 4 °C for 1 hr. The glutathione beads were collected by centrifugation (2,000 rpm, 2 min, 4 °C) and a 20 µl sample of the aspirated supernatant kept for later analysis. The beads were washed (5 min, rotating wheel, 4 °C) three times with NDTN, resuspended in 1 ml NDTN (20 µl sample taken) and stored at 4 °C.

SDS-PAGE was used to determine the level of GST-fusion protein induction and success of purification. Uninduced and induced cell pellets (Section 2.5.19) were resuspended in 50 µl SDS-PAGE sample buffer and boiled. The cell debris pellet was resuspended in 5 ml NDTN by pipetting and a 20 µl sample taken. This sample along with the post-sonication supernatant sample, glutathione bead-cleared supernatant sample and final bead:GST-fusion sample were mixed with SDS-PAGE sample buffer, boiled and run alongside 20 µl samples of uninduced and induced cell pellets. Relative levels of induced protein at each stage were determined by Coomassie staining of the SDS-PAGE gel.

2.5.21 *In vitro* transcription and translation of expression vector-encoded cDNAs

cDNAs cloned into expression vectors under the control of the T7 promoter were transcribed and translated *in vitro* in a coupled reaction using TNT[®] Coupled Reticulolysate System (Promega). Briefly, 1 µg expression plasmid (containing a T7 promoter) was mixed with 25 µl rabbit reticulolysate, 2 µl TNT reaction Buffer, 1 µl

appropriate T7 RNA Polymerase, 1 μ l amino acid mixture (minus Methionine), [35 S]-Methionine (1.175 mCi/mmol, Amerham), 1 μ l RNasin[®] Ribonuclease Inhibitor (Promega) and nuclease-free water to 50 μ l. The mixture was incubated for 90 min at 30 °C. Samples (1 μ l and 0.1 μ l) of each reaction were loaded onto an SDS-PAGE gel to determine the efficiency of translation. The rest of the IVT was aliquoted into 7 μ l volumes and stored at -80 °C.

2.5.22 GST-pulldown of *in vitro* translated protein

Normalised levels GST-tagged fusion proteins (as determined by SDS-PAGE) were incubated (4 hr, rotating wheel, 4 °C) with *in vitro* translated (IVT) protein in a 1 ml volume of NDTN. Nuclear hormone (10^{-6} M final concentration) was added where appropriate. The beads were washed three times (5 min, rotating wheel, 4 °C), aspirated, dried under vacuum (Savant DNA Speed Vac[®] DNA120), resuspended in 20 μ l SDS-PAGE sample buffer, boiled and run on an SDS-PAGE mini-gel.

2.5.23 Fixing and amplifying radioactive SDS-PAGE gels

Radioactive gels were fixed in 10% (v/v) glacial acetic acid / 10% (v/v) methanol (15 min, rocking, R.T.) and incubated (30 min, rocking, R.T.) in Amplify (Amersham). They were then placed on wetted filter paper, covered by saran wrap and dried down under vacuum as described previously (Section 2.5.14).

2.5.24 Exposure of radioactive gels to x-ray film

Dried radioactive SDS-PAGE gels were placed in x-ray film cassettes and exposed to autoradiography film overnight. Films were processed using a DuPont Cronex CX-130 x-ray film developer.

2.6 Construction of epitope-tagged MOZ and MOZ-TIF2 plasmids

pcDNA3 expression plasmids containing the MOZ and MOZ-TIF2 cDNAs were gifts from Drs. M. Carapeti and D. G. Gilliland (Harvard University, Boston, MA, U.S.A.). In order to generate the MOZ-TIF2 construct Dr. Carapeti extracted RNA from the bone marrow of an AML patient expressing the MOZ-TIF2 protein and generated a cDNA fragment that spanned the fusion breakpoint. This PCR-amplified fragment was ligated to a 5' MOZ fragment from pBS-MOZ and a 3' TIF2 fragment from pSG5-TIF2 (Deguchi *et al.*, 2003). The final product of this two-step ligation was a pcDNA3 construct with MOZ-TIF2 cloned into the unique *EcoRI* site. pcDNA3:MOZ was generated by ligation of the MOZ cDNA from pBS-MOZ into pcDNA3 as an *Apal* fragment.

The construct pcDNA3:MOZ was known to be unstable in the *E.coli* strain DH5 α (Dr. M. Carapeti, personal communication). Therefore, both MOZ and MOZ-TIF2 plasmids were transformed into the *E.coli* SURE[®]2 strain (Stratagene, Texas, U.S.A.) (Section 2.3.8). SURE (Stop Unwanted Rearrangement Events) cells contain deletions in the *uvrC* (UV repair system pathway) and *umuC* (SOS repair pathway) genes to increase stability of long inverted repeats, and *sbcC*, *recB* and *recJ* mutations that reduce rearrangements in Z-DNA structures and confer a recombination-deficient phenotype. Thus, the risk of recombination-mediated deletions of eukaryotic DNA sequences propagated in this strain is greatly reduced. Individual MOZ and MOZ-TIF2 -transformed SURE colonies were cultured, mini-prepped and screened by restriction digest to isolate those that contained an insert of the correct size. Sequence analysis revealed the presence of large 5' and 3' untranslated regions (UTRs) (0.4 kb and 1.5 kb respectively for MOZ, 0.4 kb and 1.6 kb for MOZ-TIF2). In order to remove these UTRs and insert an N-terminal FLAG- or haemagglutinin- (HA) epitope tag, a series of cloning steps were undertaken as described below. Expression of full-length epitope-tagged proteins from the MOZ and MOZ-TIF2 constructs was confirmed by immunofluorescence (Figure 3.1), *in vitro* translation (Figure 4.1) and western blotting (Figure 4.14).

2.6.1 Construction of the vector pcDNA3.0PT

The pcDNA3 vector (Invitrogen, Paisley, Strathclyde) is commonly used for transient and stable expression of cDNAs of interest in mammalian cell lines. The vector contains a multiple cloning cassette (Figure 2.2c) downstream of the cytomegalovirus immediate-early promoter and enhancer, thus allowing a high level of expression of an inserted cDNA. The bovine growth hormone (BGH) polyadenylation signal located 3' of the cloning cassette increases the efficiency of transcription termination and polyadenylation of the transcribed mRNA. The neomycin gene under the control of the SV40 early promoter and polyadenylation signal allows the selection of stable transfectants in mammalian cells, while the SV40 origin contained within the SV40 promoter permits episomal replication of the vector in cell lines that express the SV40 large T antigen. pcDNA3 contains a ColE1 origin that allows its propagation in *E.coli* strains such as DH5 α and SURE[®]2, and the β -lactamase gene, which provides a selection procedure for transformed colonies through resistance to the antibiotic ampicillin. The T7 and SP6 promoters that flank the multiple cloning cassette allow the *in vitro* transcription and translation of a cDNA inserted in either orientation into the cloning cassette.

A new multiple cloning cassette (Figure 2.2b) was designed for pcDNA3 to facilitate construction of epitope-tagged MOZ and MOZ-TIF2 derivatives. Two complimentary oligonucleotides (Primers LE128 and LE129, Appendix 1) were synthesised (PNAACL, University of Leicester), phosphorylated and annealed to give a double-stranded DNA fragment that was ligated into digested pcDNA3 to replace the original multiple cloning site (Figure 2.2c). The fragment was inserted using the *Hind*III and *Apa*I sites present in pcDNA3, which were destroyed by the ligation (Figure 2.2a: Construct pcDNA3.0PT). The insertion of the new cassette was confirmed by sequence analysis of positive clones from the ligation plates.

The new cloning cassette contained *Ksp*I and *Xho*I restriction sites at its 5' end to allow future cloning of the inserted cDNAs into other vectors, and *Apa*I, *Cel*III and *Xba*I sites to allow insertion of the MOZ and MOZ-TIF2 coding sequences as described below.

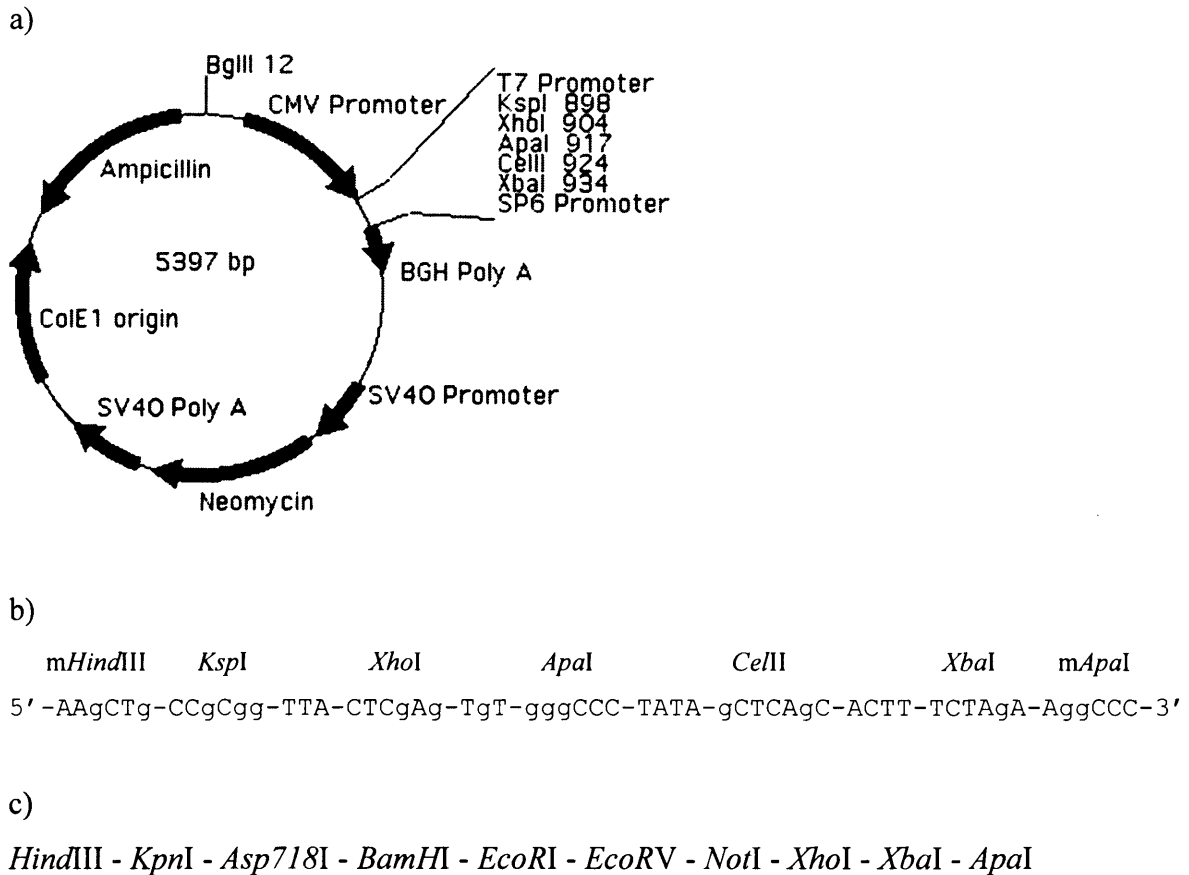


Figure 2.2: pcDNA3.0PT Mammalian Expression Vector

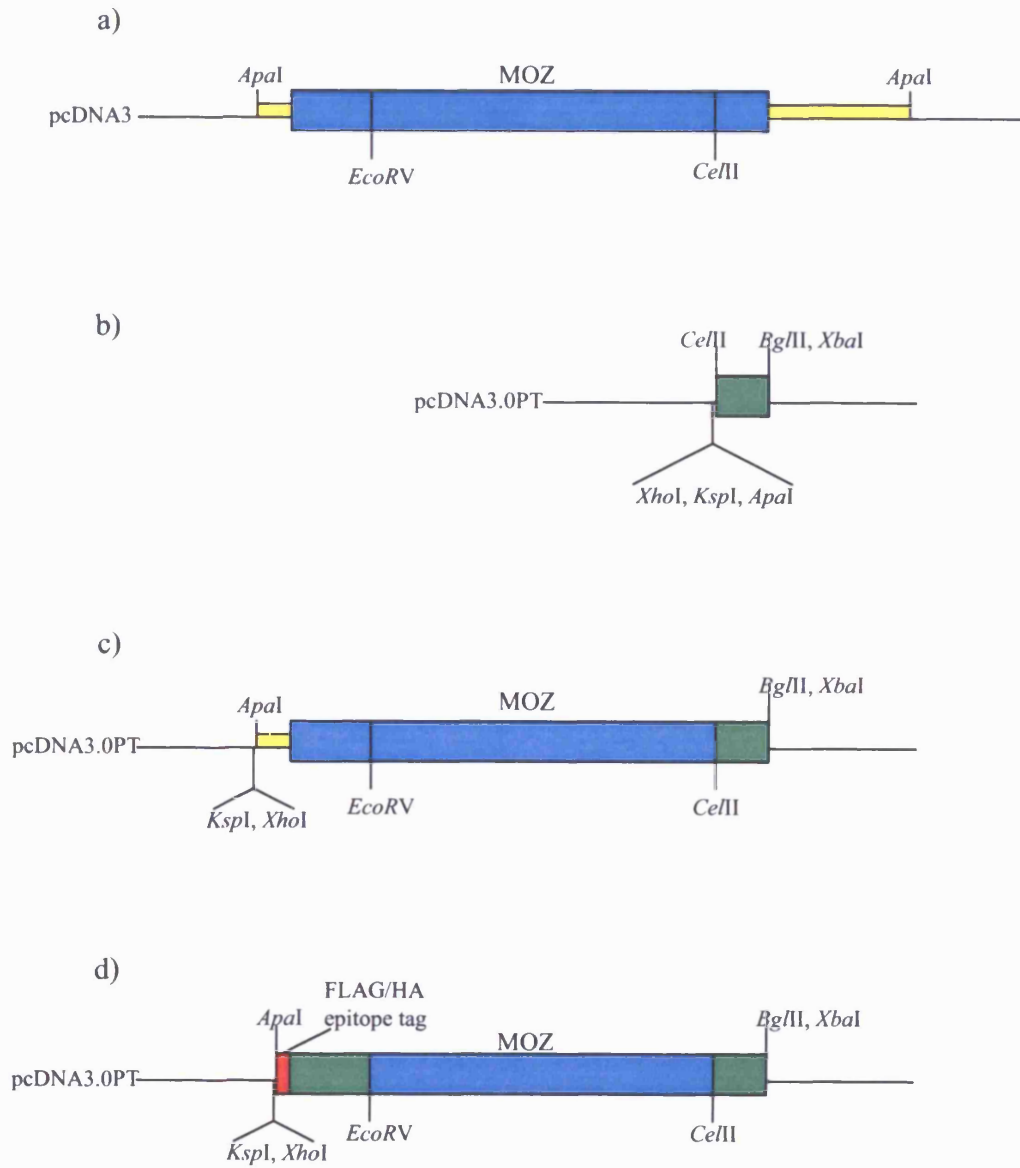
- a) Schematic of the vector pcDNA3.0PT, which was constructed by replacement of the original multiple cloning cassette of pcDNA3 with a new one containing the sites indicated. The new cassette was inserted as a double-stranded phosphorylated *HindIII*-*ApaI* DNA fragment into pcDNA3 digested with these two enzymes. The original *HindIII* and *ApaI* restriction sites were destroyed by the ligation. CMV promoter: nucleotides 209-863; T7 Promoter: 864-882; multiple cloning cassette: 889-945; SP6 Promoter: 951-967; BGH (bovine growth hormone) poly A (adenylation) signal: 970-1201; SV40 Promoter: 1722-2067 incorporating SV40 origin: 1936-2021; neomycin resistance gene: 2103-2897; SV40 poly A signal: 2952-3324; ColE1 origin of replication: 3584-4257; Ampicillin resistance gene β -lactamase: 4402-5262.
- b) Restriction enzyme and nucleotide sequence of the multiple cloning cassette of pcDN3.0PT. *mHindIII* and *mApaI* indicate sites destroyed during the insertion of the new cloning cassette.
- c) Order of restriction enzyme sites in the original pcDNA3 multiple cloning cassette.

2.6.2 pcDNA3.0PT:tag-MOZ

The MOZ cDNA was provided as an *ApaI* fragment in the mammalian expression vector pcDNA3 (Figure 2.3a). In order to remove the 5' and 3' untranslated regions, and insert an N-terminal epitope tag, the sub-cloning was carried out in two stages. Initial steps involved the replacement of the 3' *ApaI* restriction site with *BglII* and *XbaI* sites and removal of the 3' UTR. This was carried out by PCR amplification of 0.6 kb of the 3' end of the coding sequence (Primers LE130 and LE131, Appendix 1) from a unique *CeIII* restriction site (located at codon 1793) to the MOZ termination codon. The 3' primer (LE131, Appendix 1) incorporated an *XbaI* site at its 3' end (to allow cloning into pcDNA3.0PT) immediately preceded by a *BglII* site (to provide a second site for removal of the resulting constructs from pcDNA3.0PT and insertion into other expression vectors). The 600 bp PCR product was digested with *CeIII* and *XbaI*, purified using agarose gel electrophoresis and inserted into pcDNA3.0PT (Figure 2.2a) also digested with these enzymes (Figure 2.3b: Construct pcDNA3.0PT:MOZ 3' *CeIII*). The insertion of the *CeIII-XbaI* fragment into pcDNA3.0PT was initially confirmed by restriction digest of possible positive clones, followed by sequence analysis to confirm no mutations had been incorporated.

A DNA fragment containing the remainder of the MOZ coding sequence (with the 5' UTR still associated) was generated by digestion of pcDNA3:MOZ (Figure 2.3a) with *ApaI* and *CeIII*. The resulting 6.4 kb restriction fragment was purified using agarose gel electrophoresis and inserted into the pcDNA3.0PT:MOZ 3' *CeIII* construct (Figure 2.3b) also digested with these enzymes. The product of the ligation, which was confirmed by restriction digest analysis, was a pcDNA3.0PT:*ApaI-XbaI* construct containing the MOZ 5' UTR and complete coding sequence but no 3' UTR (Figure 2.3c: Construct pcDNA3.0PT:MOZ 5'UTR).

The second stage of MOZ cloning involved the replacement of the 5' UTR with a Kozak sequence for translation initiation, and an epitope tag to allow detection of expressed proteins. The 5' end of the MOZ coding sequence from the start codon to a unique *EcoRV* site (Primer LE205, Appendix 1) located at codon 487 was amplified by PCR. Two



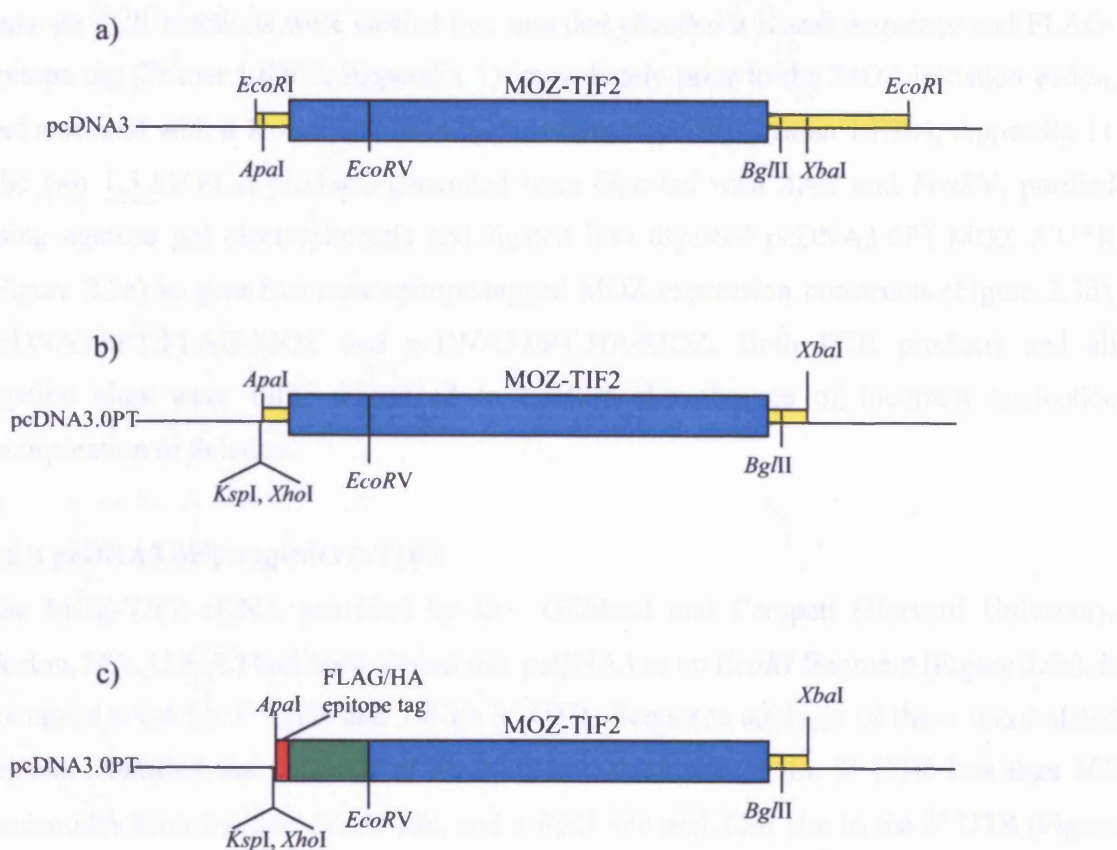


Figure 2.4: Construction of FLAG and HA epitope-tagged MOZ-TIF2 in the pcDNA3.0PT mammalian expression vector.

pcDNA3:MOZ-TIF2 (a) was provided as an *EcoRI* fragment in the expression vector pcDNA3. In order to reduce the size of the untranslated regions (yellow) surrounding the MOZ-TIF2 coding sequence (blue), and insert either a FLAG or HA epitope-tag (red) at the 5' end, a series of cloning steps were undertaken and intermediate constructs generated. Key restriction enzyme sites are indicated. b) The construct pcDNA3.0PT:MOZ-TIF2 5' UTR was generated by insertion of an *Apal*-*XbaI* restriction fragment from pcDNA3:MOZ-TIF2 into pcDNA3.0PT. c) pcDNA3.0PT:FLAG-MOZ-TIF2 and pcDNA3.0PT:HA-MOZ-TIF2 were constructed by the insertion into pcDNA3.0PT:MOZ-TIF2 5'UTR of an *Apal*-*EcoRV* PCR fragment containing the appropriate epitope tag (red) and 5' MOZ sequence (green) from the initiation codon to an internal *EcoRV* site.

separate PCR reactions were carried out: one that encoded a Kozak sequence and FLAG-epitope tag (Primer LE203, Appendix 1) immediately prior to the MOZ initiation codon, and a second with a Kozak and haemagglutinin-epitope tag (Primer LE204, Appendix 1). The two 1.5 kb PCR products generated were digested with *ApaI* and *EcoRV*, purified using agarose gel electrophoresis and ligated into digested pcDNA3.0PT:MOZ 5'UTR (Figure 2.3c) to give two new epitope-tagged MOZ expression constructs (Figure 2.3d), pcDNA3.0PT:FLAG-MOZ and pcDNA3.0PT:HA-MOZ. Both PCR products and all ligation sites were fully sequenced to confirm the absence of incorrect nucleotide incorporation or deletion.

2.6.3 pcDNA3.0PT:tag-MOZ-TIF2

The MOZ-TIF2 cDNA provided by Drs. Gilliland and Carapeti (Harvard University, Boston, MA, U.S.A.) had been cloned into pcDNA3 as an *EcoRI* fragment (Figure 2.4a). It contained a 0.4 kb 5' UTR and 1.6 kb 3' UTR. Sequence analysis of these untranslated regions identified the presence of an *ApaI* restriction site in the 5' UTR less than 100 nucleotides from the first *EcoRI* site, and a *BglIII* site and *XbaI* site in the 3' UTR (Figure 2.4a). The mammalian expression vector pcDNA3 contains a *BglIII* site at nucleotide 12 in its sequence (Figure 2.2a) and therefore this site 250 bp into the MOZ-TIF2 3' UTR could not be used during cloning into pcDNA3.0PT. However, the presence of the *XbaI* site 0.6 kb 3' of the MOZ termination codon allowed the removal of an *ApaI-XbaI* fragment from pcDNA3:MOZ-TIF2 that encompassed the region of the 5' UTR present in the original MOZ construct, the entire coding sequence and 0.6 kb of the 3' UTR. This restriction fragment was purified using agarose gel electrophoresis and inserted into pcDNA3.0PT digested with *ApaI* and *XbaI* to generate the construct pcDNA3.0PT:MOZ-TIF2 5' UTR (Figure 2.4b). The correct insertion of this 6.2 kb fragment was confirmed by restriction digest analysis.

The 5' UTR was removed from the pcDNA:MOZ-TIF2 5' UTR construct (as described for MOZ, Section 2.6.2) by digestion with *ApaI* and *EcoRV*. It was replaced with the purified *ApaI-EcoRV* PCR products containing FLAG- or HA- epitope tag sequences, which were generated during the construction of epitope-tagged MOZ. This ligation resulted in the construction of pcDNA3.0PT:FLAG-MOZ-TIF2 and pcDNA3.0PT:HA-MOZ-TIF2

expression vectors (Figure 2.4c). The absence of nucleotide changes in the region amplified by PCR or at the sites of ligation was confirmed by DNA sequence analysis.

2.7 Yeast Experimental Materials and Methods

2.7.1 Yeast strain

Analysis of LexA-MOZ constructs was carried out in the *Saccharomyces cerevisiae* L40 yeast strain (genotype: *trp1 leu2 his3 ade2 LYS::(lexAop)_{4x}-HIS3 URA3::(LexAop)_{8x}-LacZ*) (Bartel and Fields, 1997).

2.7.2 Solutions

Electroporation buffer: 10 mM Tris-HCl pH 7.5, 1 mM MgCl₂, 270 mM Sucrose

Breaking Buffer: 50 mM Tris-HCl (pH 7.9), 0.4M KCl, 1 Complete Protease Inhibitor tablet (Roche) / 25 ml

LacZ Buffer: 60 mM Na₂HPO₄, 40 mM NaH₂PO₄, 10 mM KCl, 1 mM MgSO₄, 50 mM β-mercaptoethanol, pH 7.0

O-nitrophenyl β D-galactopyranoside (ONPG): 4 mg/ml in LacZ buffer

2.7.3 Yeast growth medium

YPG medium: 1% bacto-yeast extract, 2% bacto-peptone, 2% glucose

Selective Media: 0.67% yeast nitrogen base, 2% glucose, 0.06-0.08% of the appropriate Complete Supplement Media amino acid mix (Bio101 Inc., Carlsbad, Canada).

2.7.4 Solid growth medium

For the generation of solid medium liquid medium was supplemented with 2% bacto-agar (Oxoid Ltd.). 20-25 ml of molten agar medium was poured into each Petri dish and allowed to solidify. Plates were dried for 20 minutes at 37 °C and stored at 4 °C.

2.7.5 Yeast transformations

A 50 ml volume of YPG medium was inoculated from a glycerol stock of *S.cerevisiae* strain L40 and grown overnight at 30°C. This culture was used to inoculate a fresh 50 ml culture of YPG medium to give an optical density (OD) of 0.2 at 600nm. The fresh culture was then incubated at 30°C until it reached an OD of 0.8 before being placed on ice for 1 min. The 50ml culture was split into two and the yeast cells harvested by centrifugation (4,000 rpm, 5 min, 4°C). Each cell pellet was resuspended in 10 ml ice-cold sterile H₂O. A further 35 ml ice-cold sterile H₂O was added, the cells mixed by careful inversion and pelleted once again by centrifugation. Each cell pellet was then resuspended in 25 ml ice-cold electroporation buffer, mixed by inverting gently and the cells re-pelleted by centrifugation. A further wash in 10 ml electroporation buffer was carried out before the two cell pellets were resuspended in a total volume of 1 ml electroporation buffer.

A 50 µl volume of cells was transformed with 1 µg DNA by electroporation at 450 V, 250 µF and 400 Ohms for each LexA construct. Immediately following electroporation 1 ml cold H₂O was added to the cells, which were then transferred to an eppendorf and collected by centrifugation (4,000 rpm, 5 min, 4°C). Following resuspension in 100 µl H₂O the cells were plated on YPD plates lacking tryptophan. They were then incubated at 30°C for 3 days.

2.7.6 Preparation of a yeast cell-free lysate

Colonies from LexA expression vector-transformed yeast plates were used to inoculate 20 ml cultures of selective medium lacking tryptophan. Following an overnight growth at 30 °C the cells were pelleted (4,000 rpm, 5 min, 4 °C) and washed on ice by addition of 1 ml LacZ buffer. The cell suspensions were transferred to eppendorf tubes, re-centrifuged and the cells resuspended in 150 µl LacZ buffer. Acid-washed glass beads (425-600 microns; Sigma) were added until the beads reached a level just below the meniscus of the liquid and the samples placed on ice for 5 min. Following four 30 sec vortexes separated by 30 sec incubations on ice, the cells suspensions were placed on ice for 5 min. Intact cells and cell debris were removed by centrifugation (13,000 rpm, 10 min) and the cell-free lysate transferred to a new eppendorf tube.

2.7.7 Antibodies

A mouse α -LexA (20-12) primary antibody and an α -mouse IgG HRP-conjugated secondary antibody were purchased from Santa Cruz Biotechnology Inc.(Santa Cruz, CA., U.S.A.).

2.7.8 β -galactosidase assay for LacZ expression in yeast

To allow a quantitative determination of the level of β -galactosidase expression in the transformed yeast cells, the specific β -galactosidase activity (nmoles/mg/min) in cell-free lysates was measured. Following the addition of 20 μ l cell-free extract to 500 μ l LacZ buffer present in a cuvette, a 100 μ l volume of ONPG (*O*-nitrophenyl β D-galactopyranoside) was added and the time of addition recorded. 1 M Na₂CO₃ was added (200 μ l) to stop the reaction as soon as the solution turned pale yellow (and the time recorded) or after 30 min if no colour change was visible to the eye. The optical density at 420 nm was recorded and the specific activity of the β -galactosidase enzyme present in each extract calculated according to the following formula:

$$\text{Specific Activity (nmoles/mg/min)} = \frac{\text{OD}_{420\text{nm}}}{0.0045 \times \text{Protein} \times \text{Volume} \times \text{Time}}$$

where Protein is the protein concentration of the cell-free extract in mg/ml, Volume is the extract volume assayed in ml and Time is the reaction time in min. The value 0.0045 is the constant used to calculate nmoles of converted substrate from the measured optical density.

2.8 Construction and analysis of LexA-MOZ fusion proteins

The t(8;16)(p11;p13) chromosomal translocation identified in a patient with the M4/5 subtype of AML was shown to result in the fusion of the CBP gene to a novel gene, termed MOZ (Borrow *et al.*, 1996). An expressed mRNA was detected in the patient that was comprised of the nucleotides encoding residues 266-2440 of CBP following-on in-frame from the sequence encoding residues 1-1546 of MOZ. The presence of this fusion mRNA, which was under the control of the MOZ promoter, suggested that wild-type MOZ might

normally be expressed in haematopoietic cells. However, though it was putatively termed a HAT, no function of MOZ was determined. Therefore, in order to allow the future identification of proteins that interacted with various regions of MOZ using yeast 2-hybrid analysis, LexA fusion constructs were synthesised that spanned the entire MOZ coding sequence. In addition, the equivalent GST fusion proteins were also generated to allow *in vitro* confirmation of any possible interactions.

A schematic diagram explaining the principles of the yeast 2-hybrid system (Bartel and Fields, 1997) is shown in Figure 2.5. The yeast are transformed with expression plasmids for protein fusions of the LexA DNA binding domain, and the VP16 activation domain. The LexA-fusion protein normally contains the protein/domain of interest, termed the “bait”. The VP16 protein fusions, also known as the “prey”, are often formed by the incorporation of a library of cDNA fragments into the expression vector, thus allowing the screening of a large number of sequences for an expressed protein that can interact with the bait. However, they may also be formed by the incorporation of a specific protein domain such as the CBP:SID to allow yeast 2-hybrid analysis of pre-determined interactions (Section 4.3). The expressed LexA-fusion protein binds to LexA binding motifs within the promoters of two reporter genes, but is unable to activate transcription on its own (Figure 2.5a). However, if the prey fusion protein interacts with the bait fusion, the VP16 activation domain is recruited to the promoter, thus inducing transcription of the reporter gene (Figure 2.5b).

2.8.1 Construction of LexA-MOZ expression vectors spanning the entire MOZ sequence

To generate LexA fusion proteins containing functional domains of MOZ, primers were designed that encompassed the predicted domain boundaries as described by Borrow *et al.* (1996), with additional residues at either end to increase the likelihood of correct domain folding. The predicted domains of MOZ are shown schematically in Figure 2.6a, along with the LexA fusions that were constructed. Figure 2.6b details the domains incorporated in each fusion and the primers used for the construction of the LexA (and GST) fusions. All forward primers (Appendix 1) were synthesised with an in-frame *KspI* site to allow cloning of the PCR fragment into the LexA fusion expression plasmid pBTM116mod. The

reverse primers (Appendix 1) LE184, LE185, and LE186 contained a *Bam*HI restriction site; primers (Appendix 1) LE102, LE105, LE176, LE187 AND LE188 incorporated a *Bgl*III site. Following synthesis of the PCR fragments for each fusion, they were digested with *Ksp*I, and *Bam*HI or *Bgl*III as appropriate. Each fragment was then separated by agarose gel electrophoresis, purified from the agarose and cloned into the pBTM116mod. vector, which had been previously digested with *Ksp*I and *Bam*HI and treated with the CIP enzyme. The MOZ PCR fragments were also cloned into the GST-fusion expression vector pGex-DMH to allow the future *in vitro* analysis of any identified interactions. The presence of the correct fragment in each construct was confirmed by DNA sequencing.

2.8.2 Expression analysis of LexA-MOZ fusions in the *S.cerevisiae* strain L40

The LexA-MOZ fusions detailed in Figure 2.6 were constructed in order to allow their use in yeast 2-hybrid studies to identify proteins that interact with specific domains of MOZ. Therefore, to confirm that the fusions were expressed in yeast, they were transformed into the *Saccharomyces cerevisiae* strain L40 (Section 2.7.1). This commonly used yeast strain contains mutations in the genes required for the synthesis of tryptophan (*trp1*), leucine (*leu2*) and adenine (*ade2*). Thus, the removal of these amino acids from the growth medium may be used to ensure the maintenance of transformed vectors, and as a selection mechanism for bait:prey interactions. The LexA-fusion (bait) expression vector pBTM116mod encodes the wild-type *TRP1* gene and thus successful transformation with this vector allows the growth of the yeast in the absence of tryptophan.

Yeast transformations were carried out by electroporation (Section 2.7.5) and the LexA-MOZ transformed yeast selected by growth on plates made from Complete Selective Media lacking tryptophan (CSM -trp plates). Cell-free lysates for each of the LexA-MOZ fusion-transformed yeast were prepared as described (Section 2.7.6). A 70 μ l volume of the lysate was run on a large 12% SDS-PAGE gel, and separated proteins transferred to a nitro-cellulose membrane (Section 2.5.15). Analysis of LexA-fusion protein expression was carried out by western blotting with an α -LexA primary antibody and α -mouse HRP-conjugated secondary antibody. Proteins bands of near the predicted molecular weight

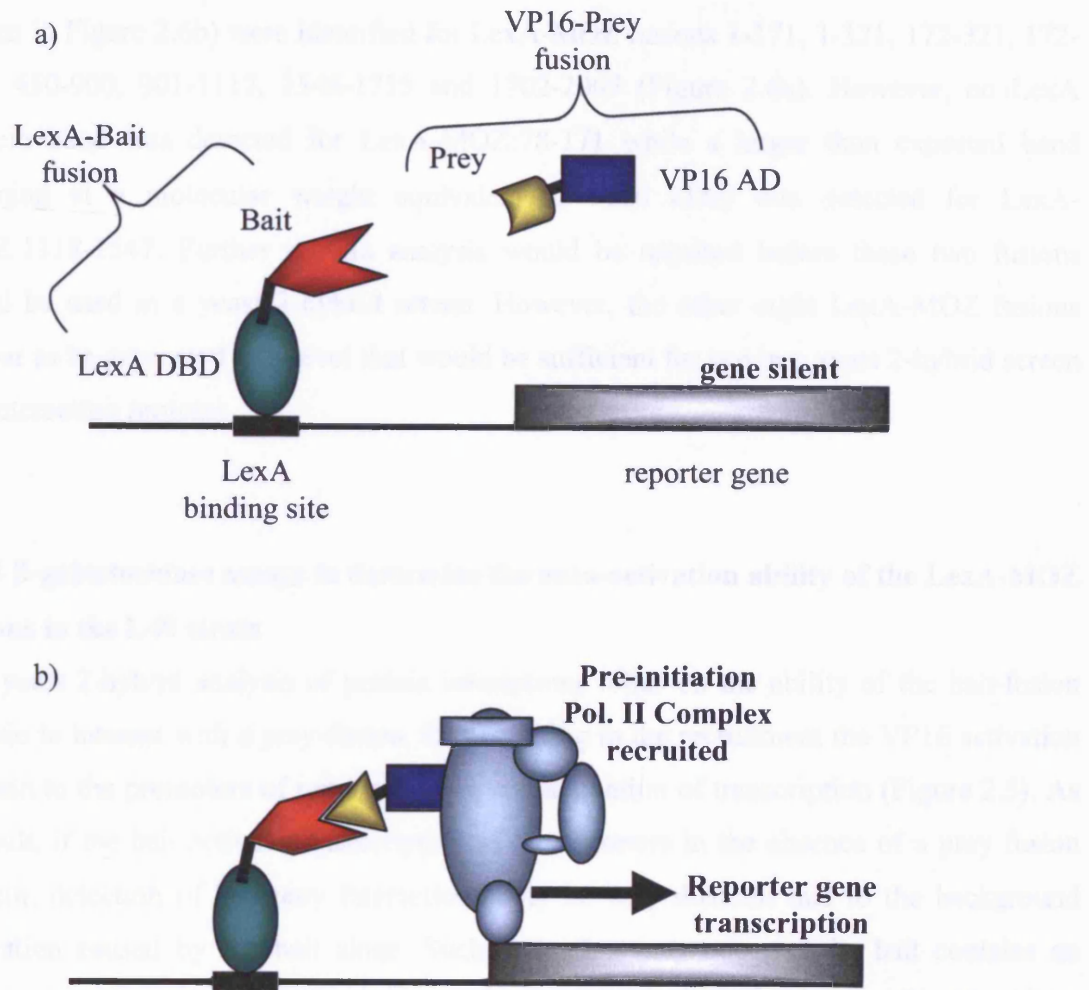


Figure 2.5: Activation of reporter genes by protein interactions using the yeast 2-hybrid system

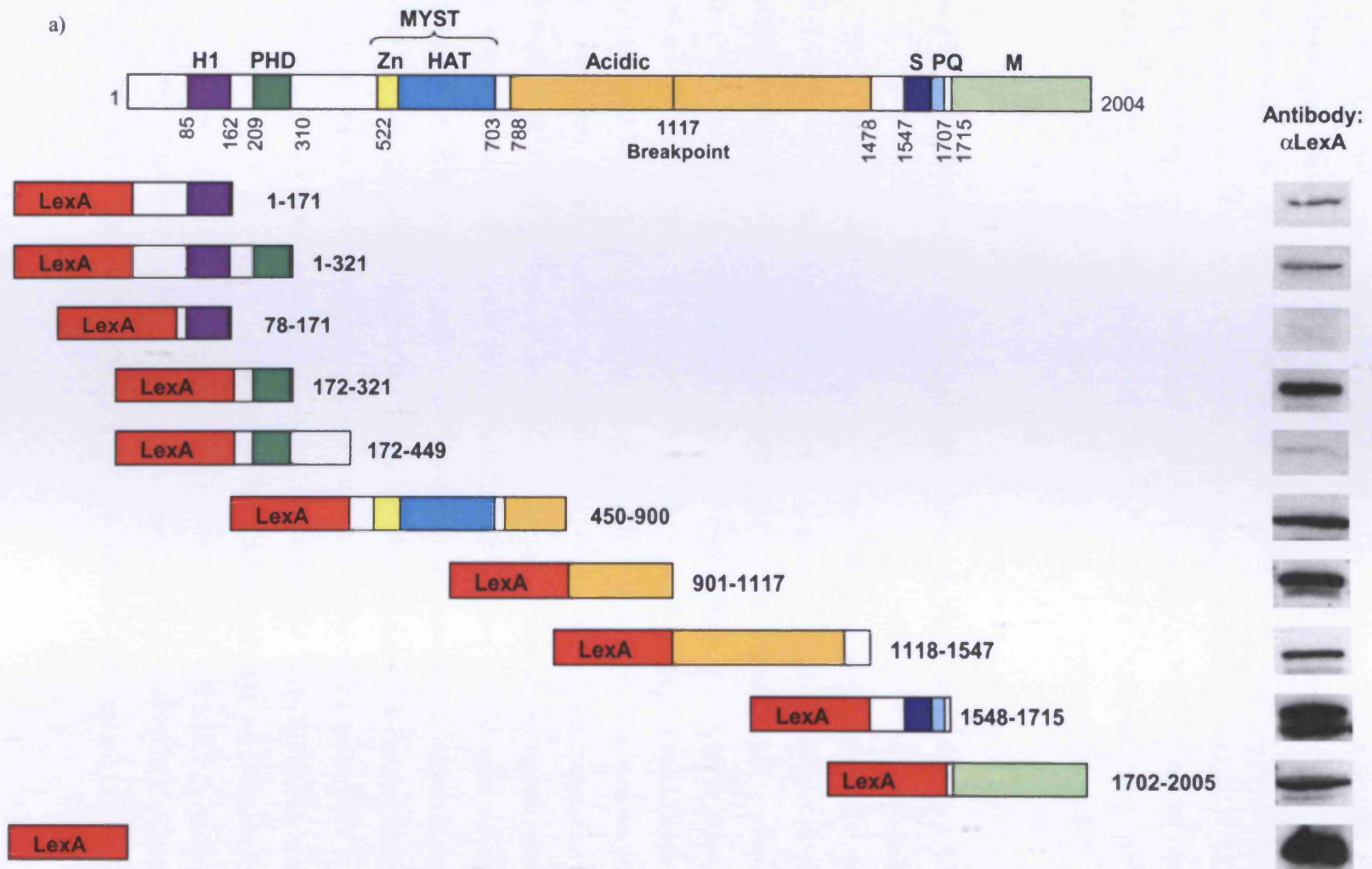
Schematic showing the principle of reporter gene activation by a protein interaction in the yeast 2-hybrid system. a) the protein of interest is expressed in yeast as the bait domain in the LexA-Bait fusion protein, which binds to LexA binding motifs in the promoter of reporter genes through the LexA DNA binding domain (DBD). Proteins (the prey) to be screened for an interaction with the bait are expressed as VP16-prey fusions. b) If a protein interaction between the Bait and Prey occurs the presence of the VP16 activation domain (AD) results in the recruitment of the RNA Polymerase II pre-initiation complex to the promoter and subsequent initiation of reporter gene transcription.

(given in Figure 2.6b) were identified for LexA-MOZ fusions 1-171, 1-321, 172-321, 172-449, 450-900, 901-1117, 1548-1715 and 1702-2005 (Figure 2.6a). However, no LexA protein band was detected for LexA-MOZ:78-171 while a larger than expected band (running at a molecular weight equivalent to ~120 kDa) was detected for LexA-MOZ:1118-1547. Further protein analysis would be required before these two fusions could be used in a yeast 2-hybrid screen. However, the other eight LexA-MOZ fusions appear to be expressed to a level that would be sufficient for use in a yeast 2-hybrid screen for interacting proteins.

2.8.3 β -galactosidase assays to determine the auto-activation ability of the LexA-MOZ fusions in the L40 strain

The yeast 2-hybrid analysis of protein interactions relies on the ability of the bait-fusion protein to interact with a prey-fusion, thus resulting in the recruitment the VP16 activation domain to the promoters of reporter genes, and activation of transcription (Figure 2.5). As a result, if the bait activates transcription of the reporters in the absence of a prey fusion protein, detection of bait:prey interactions may be very difficult due to the background activation caused by the bait alone. Such activation may occur if the bait contains an autonomous transcription activation domain that is functional in yeast cells. Therefore, auto-activation assays were carried out to determine whether any of the LexA-MOZ fusion proteins were able to activate the integrated *LacZ* reporter gene in the absence of a prey-protein fusion. β -galactosidase “auto-activation” assays were carried out using the cell-free lysates generated for the analysis of LexA-MOZ fusion protein expression (Figure 2.6a). A 2 μ l volume of each cell-free extract was assayed for β -galactosidase activity using the colorimetric ONPG (*O*-nitrophenyl β -galactopyranoside) assay, with the generation of the yellow-coloured reaction product, *O*-nitrophenol, measured at a wavelength of 420 nm (Section 2.7.8). The protein concentration of the extract was measured as described (Section 2.5.11) and used to calculate the specific activity (nanomoles product formed per milligram protein per minute) of the β -galactosidase enzyme present (Section 2.7.8).

a)



b)

Construct Name	Forward Primer	Reverse Primer	MOZ Residues Incorporated	Predicted Mr (kDa)	Construct Details
LexA-MOZ:1-171	LE177	LE184	1-171	46	N-terminal residues + H1-like domain
LexA-MOZ:1-321	LE177	LE185	1-321	62	N-terminal residues + H1-like domain + PHD Zinc finger
LexA-MOZ:78-321	LE178	LE185	78-171	37	H1-like domain
LexA-MOZ:172-321	LE179	LE185	172-321	43	PHD Zinc finger domain
LexA-MOZ:172-449	LE179	LE186	172-449	58	PHD Zinc finger + residues to extended MYST domain
LexA-MOZ:450-900	LE173	LE176	450-900	79	extended MYST domain
LexA-MOZ:901-1117	LE180	LE105	901-1117	52	end of extended MYST domain to MOZ-TIF2 break-point
LexA-MOZ:1118-1547	LE181	LE187	1118-1547	75	MOZ-TIF2 break-point to MOZ-CBP break-point
LexA-MOZ:1548-1715	LE182	LE188	1548-1715	44	MOZ-CBP break-point to end of P/Q-rich domain
LexA-MOZ:1702-2005	LE183	LE102	1702-2005	59	Methionine-rich domain + C-terminal residues

Figure 2.6: Construction and expression of LexA-MOZ constructs spanning the entire MOZ sequence

a) Schematic indicating the predicted domain boundaries in MOZ and the LexA-MOZ fusions generated. Also shown is the LexA protein band for each expressed LexA-MOZ fusion protein, as identified by western blotting using α -LexA and α -mouse (HRP-conjugated) antibodies. b) Table detailing the LexA-MOZ constructs generated with residue numbers indicated, the primers used, the predicted molecular weight (Mr) of each fusion protein and a description of the domains contained.

The resulting specific activities are shown in Figure 2.7. The control bars correspond to empty pBTM116mod vector, which expresses the LexA:DBD alone. All ten constructs gave calculated specific activities of less than 0.5 nmoles/mg/min. Thus, none of the LexA-MOZ fusions activated the reporter to a level significantly higher than the LexA DBD alone, indicating that they do not activate transcription in yeast. This finding initially appeared in contrast to that of Champagne *et al.* (1999) that indicated the C-terminal region of MOZ activated transcription in yeast when fused to a LexA DNA binding domain. However, the more recent study by Kitabayashi *et al.* (2001) was in agreement with the results described here as it showed that the individually-expressed amino acid-rich regions were unable to mediate transcriptional activity. Rather, almost the entire region C-terminal to the serine-rich domain was required. Use of the individual LexA-domain fusions in a yeast 2-hybrid screen may thus allow identification of proteins that mediate this activity without the complications of reporter activation in the absence of an interaction.

The finding that the LexA fusion of the MOZ MYST domain was unable to activate transcription was unexpected as MOZ appears to function as a transcriptional coactivator (Kitabayashi *et al.*, 2001a) and domains that mediate histone acetylation are traditionally associated with transcription activation. However, given the lack of requirement of the MYST domain for the coactivation of AML1 transcription by MOZ, it is possible that this domain plays an as yet undetermined non-transcriptional role in MOZ function.

In summary, with the exception of LexA-MOZ:78-171, the LexA-MOZ constructs that span the MOZ residues up to the MOZ-TIF2 breakpoint would be suitable for study in a yeast 2-hybrid screen as when expressed, none activate transcription of the β -galactosidase reporter gene in the L40 yeast strain. Thus, they may be used to identify proteins that interact with the N-terminus of MOZ and thus might be mislocalised by the expression of the MOZ-TIF2 fusion protein. In addition, the LexA constructs spanning the C-terminus of MOZ may be utilised to investigate the proteins that mediate its transcriptional activation activity.

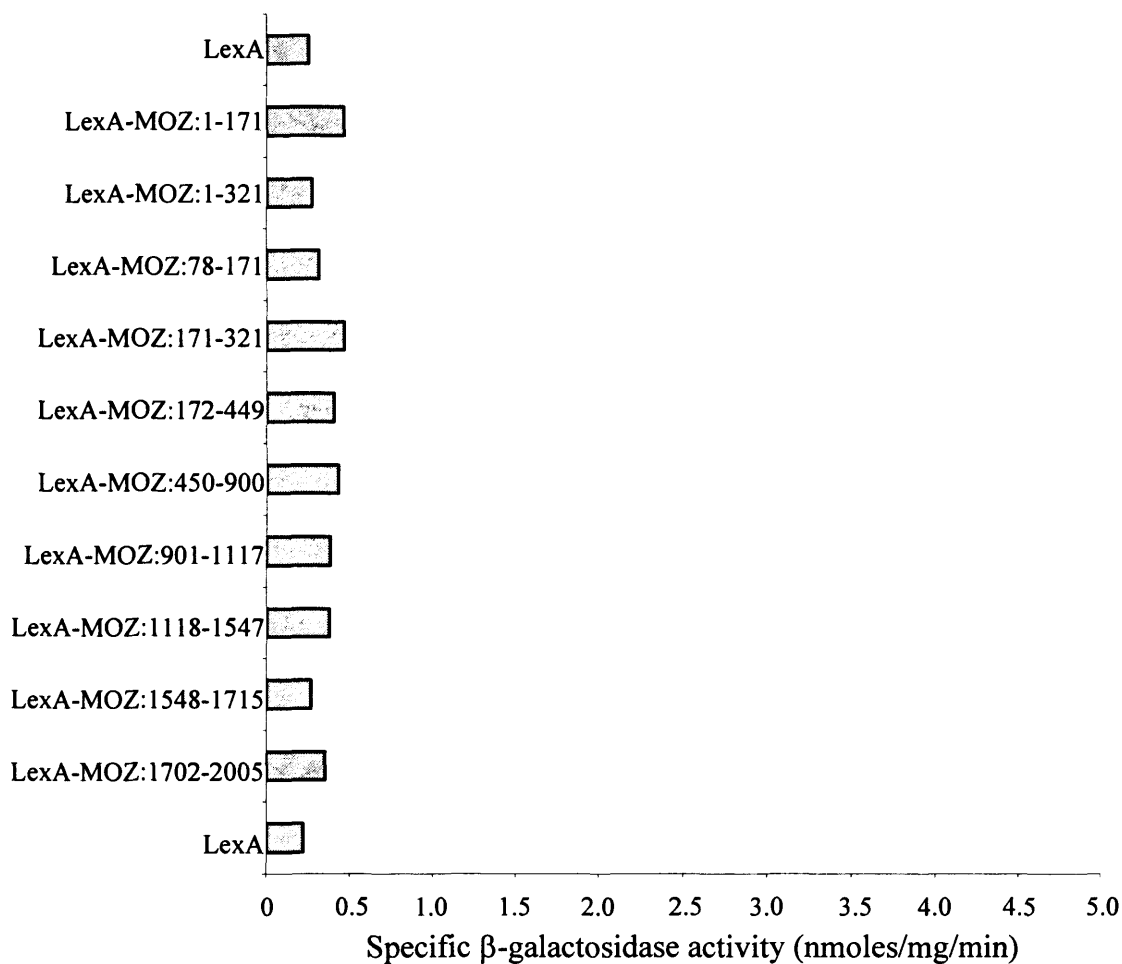


Figure 2.7: β -galactosidase activity in cell-free extracts upon expression of LexA-MOZ constructs

Yeast cell-free protein extracts were assayed for β -galactosidase activity to determine whether the expressed LexA-MOZ fusions activated expression of the *LacZ* gene in the absence of a VP16:AD-Bait fusion. In addition to the ten LexA-MOZ constructs, two control extracts expressing solely the LexA protein were also assayed. β -galactosidase activity was measured using the ONPG assay, and the specific activity (nmol product produced per milligram protein per minute) calculated following determination of the protein concentration of each extract. The data shown is representative of two independent assays carried out using different yeast clones.

Chapter Three:

MOZ-TIF2 inhibits Nuclear Receptor AF2-mediated transcription

3.1 Introduction

The MOZ-TIF2 fusion protein results from a chromosomal inversion *inv(8)(p11,q13)* that has been identified as the only cytogenetic abnormality in two patients with Acute Myeloid Leukaemia (Aguiar *et al.*, 1997; Coulthard *et al.*, 1998; Carapeti *et al.*, 1998a; Carapeti *et al.*, 1999) and three patients that show additional alterations (Liang *et al.*, 1998; Panagopoulos *et al.*, 2000b; Billio *et al.*, 2002). The fusion protein is comprised of the N-terminus of the histone acetyltransferase (HAT) protein MOZ (Borrow *et al.*, 1996; Champagne *et al.*, 2001) and the C-terminal domains of the nuclear receptor (NR) coactivator TIF2 (Voegel *et al.*, 1996; Voegel *et al.*, 1998). Thus, it contains the MOZ histone H1-like, PHD zinc finger and MYST domains along with the AD1, Q-rich and AD2 domains of TIF2 (Introduction Section 1.15). During the preparation of this thesis Deguchi *et al.* (2003) published a study utilising retroviral transduction of murine primary bone marrow cells to investigate the effect of MOZ-TIF2 expression in bone marrow transplant (BMT) assays and serial replating experiments. Transplantation of MOZ-TIF2-transduced bone marrow cells into mice resulted in development of a fatal haematopoietic malignant disease, while in serial replating experiments MOZ-TIF2 expression resulted in immortalisation of myeloid progenitors *in vitro*. This work corroborates the findings that the *inv8(p11,q13)* chromosomal inversion is sufficient to initiate AML in humans (Aguiar *et al.*, 1997; Coulthard *et al.*, 1998; Carapeti *et al.*, 1998a; Carapeti *et al.*, 1999). However, the molecular mechanism by which the MOZ-TIF2 fusion causes this block in myeloid cell differentiation and induces cell proliferation is as yet unknown.

MOZ is a member of the MYST family (Borrow *et al.*, 1996), the proteins of which are characterised by the presence of the MYST domain (Utley and Cote, 2003). The family members share little sequence homology outside of this domain, suggesting that they have diverse cellular functions. However, the majority appear to play a role in the modulation of gene transcription (Utley and Cote, 2003). One member, TIP60, has been shown to interact with NRs, though its function is unclear as it has been reported to have both positive (Gaughan *et al.*, 2001) and negative (Sharma *et al.*, 2000) effects on steroid receptor transactivation. The function of MOZ *in vivo* is, as yet, undetermined. However, MOZ has been reported to act as a coactivator for the haematopoietic transcription factor AML1 (Kitabayashi *et al.*, 2001a; Bristow and Shore, 2003) and to interact with the Runx2 protein (also termed AML3) (Pelletier *et al.*, 2002).

TIF2 (Voegel *et al.*, 1996) is a member of the p160 protein family (Leo and Chen, 2000). These transcriptional coactivators act as platform proteins that recruit chromatin-modifying enzymes to ligand-bound NR complexes. The predominant interaction of TIF2 with NRs is ligand-dependent and is mediated by three LXXLL motifs (Heery *et al.*, 1997) contained within its NR Interaction Domain (NID) (Voegel *et al.*, 1998). Recruitment of the global coactivator CBP, a histone acetyltransferase (HAT) protein (Janknecht, 2002; Blobel, 2002), and CARM1, a histone methyltransferase (HMT) (Ma *et al.*, 2001), to the NR complex by TIF2 occurs through Activation Domains AD1 (Voegel *et al.*, 1998) and AD2 (Chen *et al.*, 1999a) respectively. The histone modifications catalysed by these proteins result in changes in chromatin structure that allows the association of the basal transcription machinery and thus initiation of transcription (Stallcup *et al.*, 2000).

In addition to the translocations that fuse the MOZ gene to the TIF2 gene, MOZ has been identified as the fusion partner of CBP in the translocation t(8;16)(p11;p13) (Borrow *et al.*, 1996) and p300 in the translocation t(8;22)(p11;q13) (Kitabayashi *et al.*, 2001b). The leukaemias that result from these translocations appear to have very similar phenotypes (Borrow *et al.*, 1996; Carapeti *et al.*, 1998a; Kitabayashi *et al.*, 2001b), suggesting that the resulting fusion proteins might mediate their leukaemic effects through identical mechanisms. CBP is a global coactivator utilised by many transcription factors (Janknecht, 2002; Blobel, 2002) including Nuclear Receptors (Chakravarti *et al.*, 1996). However, TIF2 only interacts with a specific set of transcription factor families (Section 1.9), the most studied of which is the Nuclear Receptor super-family (Aranda and Pascual, 2001). Evidence for the role of nuclear receptors in the regulation of myeloid cell differentiation has been provided by studies of the effects of their known ligands *in vivo* and *in vitro* (reviewed in James *et al.*, 1999; Tenen *et al.*, 1997; Collins, 2002). Retinoic acid, vitamin D and PPAR γ ligands have all been reported to inhibit cell growth and induce lineage-specific differentiation of myeloid progenitors, leukaemic blasts and haematopoietic cell lines such as U937 (Olsson and Breitman, 1982; Olsson *et al.*, 1983; Liu *et al.*, 1996a; Liu *et al.*, 1996b; Asou *et al.*, 1999; Pizzimenti *et al.*, 2002). In addition, a study utilising sense and antisense RNA to alter RXR α mRNA levels has shown that this NR mediates retinoic acid-induced growth inhibition in the U937 cell line (Brown *et al.*, 1997), while further work has highlighted the role of RXR in murine myeloid differentiation through targeted expression of a dominant negative RXR β in myeloid cells (Sunaga *et al.*, 1997). These

findings, coupled with the identification of RAR α translocations and mutations that result in acute promyelocytic leukaemia (APL) and non-APL forms of myeloid leukaemia respectively (Zelent *et al.*, 2001; Parrado *et al.*, 2000), suggest an important role for NRs in normal myeloid maturation. Thus, as TIF2 functions to potentiate transcription by NRs primarily (Sheppard *et al.*, 2001; Lee *et al.*, 2003) through recruitment of CBP/p300, one potential mechanism through which the MOZ-TIF2, MOZ-CBP and MOZ-p300 proteins may be similarly leukaemogenic is the disruption of NR-mediated gene expression.

This chapter describes the work carried out to investigate the effects of TIF2, MOZ and MOZ-TIF2 expression on ligand-dependent NR-mediated transcription. To improve construct stability pcDNA3:MOZ and pcDNA3:MOZ-TIF2 expression vectors were re-cloned to remove extensive non-coding 5' and 3' regions as described in Section 2.6. In addition, epitope (FLAG or HA) tags were added to the N-terminus of the coding sequences. All regions of the constructs amplified by PCR during the re-cloning were fully sequenced to confirm no mutations had been incorporated. The epitope-tagged constructs were used in transient transfection experiments of COS-1 cells to investigate their effect on transcriptional activation by fusions of the AF2 domain of NRs to the GAL4 DBD, as described in Section 3.3.

3.2 The sub-nuclear distribution of MOZ-TIF2 is distinct from that of MOZ or TIF2

The p160 family member TIF2 has been shown previously to be a nuclear protein that localises almost exclusively to discrete nuclear speckles in COS-1 cells when over-expressed (Voegel *et al.*, 1996). However, in the HeLa cell-line the exogenous protein forms a predominantly diffuse nucleoplasmic staining with concentration in speckles in only approximately 20% of cells (Baumann *et al.*, 2001 and our unpublished observations). A subset of these speckles in HeLa cells co-localise with PML bodies, though the majority do not and remain to be characterised. The sub-cellular localisation of MOZ and the MOZ-TIF2 fusion protein were unknown.

In order to confirm that FLAG- and HA- tagged MOZ and MOZ-TIF2 proteins were expressed, and to investigate their sub-cellular distributions, COS-1 cells seeded onto glass coverslips were transfected using the calcium phosphate method (Section 2.2.6) with 1 μ g epitope-tagged MOZ or MOZ-TIF2 vector. In addition, pSG5:HA-GRIP1 (gift from Dr. M. R. Stallcup, University of Southern California, U.S.A.), the mouse homologue of TIF2, was transfected to allow comparison of the subcellular localisation of the proteins. 48 hr after transfection, the cells were fixed, permeabilised and incubated with α -HA or α -FLAG antibody and the appropriate TRITC-conjugated secondary antibody (Section 2.5.7). Fixed cells were viewed using a Zeiss Axioskop2 microscope and the location of the nucleus determined using Hoechst 33258 stain, which intercalates in the DNA. The sub-cellular localisations shown were characterised using cells grown in full-medium that contained NR ligands. However, the removal of ligands through the process of dextran/charcoal stripping of the foetal calf serum (Section 2.2.5) had no effect of the subcellular localisation of GRIP1, MOZ or MOZ-TIF2 (personal communication; K. Kindle).

Two representative images are shown for HA-GRIP1, HA-MOZ and HA-MOZ-TIF2 (Figure 3.1). All three HA-tagged proteins were expressed (α -HA) and localised to the nucleus as observed by overlaying (Merge) with the Hoechst 33258 DNA stain (Hoechst). HA-GRIP1 (Figure 3.1a) localised to distinct intranuclear foci, with in some cases a

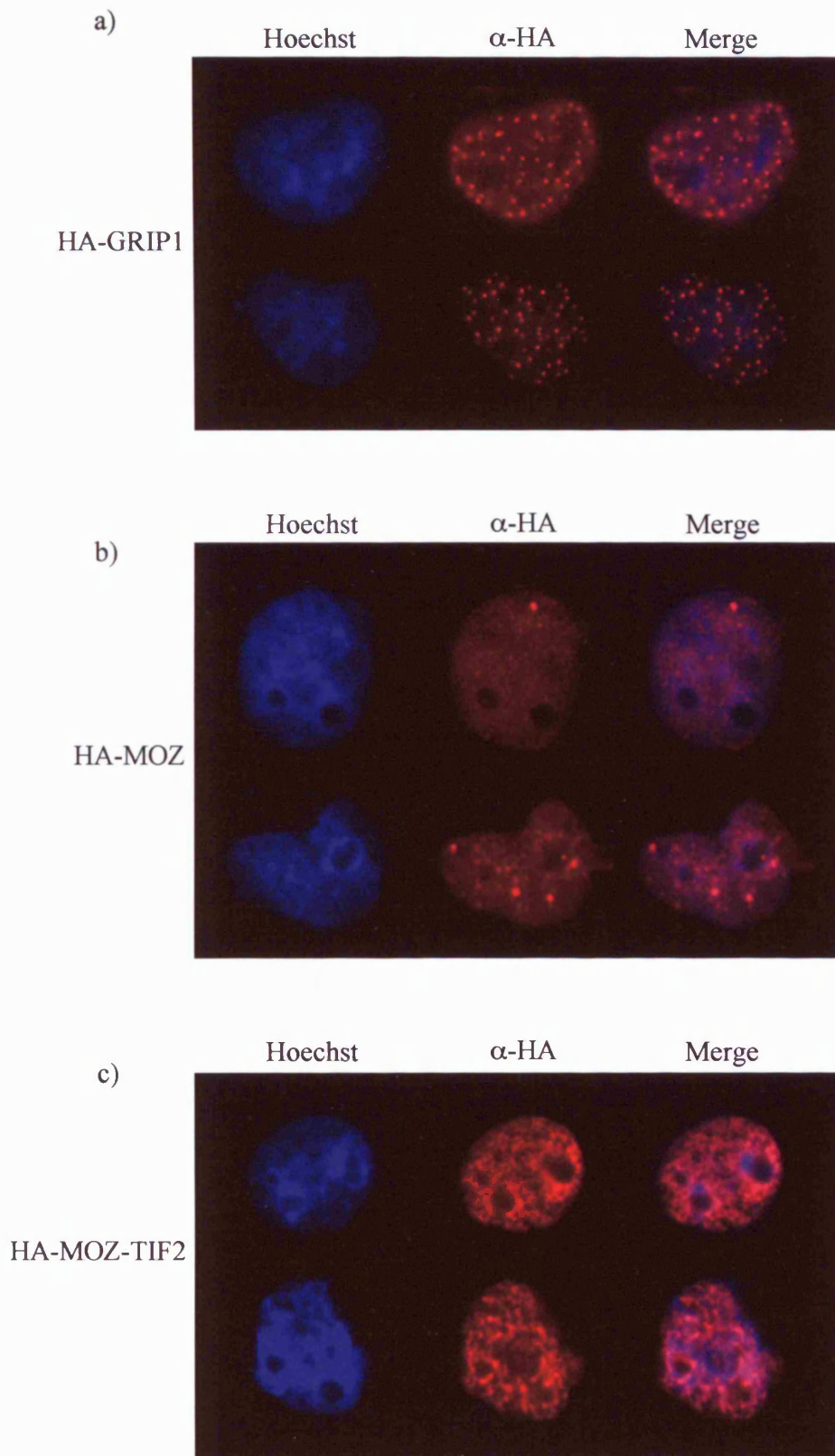
diffuse nucleoplasmic background (upper HA-GRIP1 image), as shown previously (Voegel *et al.*, 1996; Baumann *et al.*, 2001). However, in agreement with the findings of Voegel *et al.* (1996), this localisation of full-length TIF2/GRIP1 to discrete foci was present in all but a small minority of the transfected COS-1 cells.

Visualisation of over-expressed MOZ (Figure 3.1b) indicated that, like GRIP1/TIF2, it gave a speckled nuclear pattern indicating localisation to foci. However, these foci were less uniform than the GRIP1 speckles and did not co-localise with PML bodies (personal communication; K. Kindle). The upper image shows a single nucleus with clearly defined nucleoli that do not stain with either Hoechst or the α -HA antibody. The lower image contains two cell nuclei that partially obscure each other. The nucleoli in these two nuclei are less distinct and show some staining with Hoechst (nucleus on left: nucleoli defined in TRITC (α -HA) channel but not Hoechst) and also with the α -HA antibody (right-hand nucleus: apparent speckle in large nucleolus). However, this apparent nucleolar staining may have been due to the problem of focussing on both nuclei concurrently as they were present in several focal planes. Confocal microscopy and 3D reconstruction showed that MOZ was excluded from nucleoli (personal communication; K. Kindle). The majority of the MOZ foci were smaller and less distinct than those seen with GRIP1. However, a small proportion of cells also contained a few larger foci in their nucleus. In general, a higher diffuse nucleoplasmic background staining was seen with MOZ than GRIP1.

In contrast to GRIP1 and MOZ, epitope-tagged MOZ-TIF2 gave a non-speckled, mesh-like, staining pattern when expressed in COS-1 cells (Figure 3.1c). This result was unexpected given the discrete localisation of the two proteins that form the fusion, and the finding that it is the C-terminus of GRIP1/TIF2 that is essential for its localisation to foci (Baumann *et al.*, 2001). As with MOZ, MOZ-TIF2 staining was non-nucleolar (Figure 3.1c upper image, Figure 4.17 and personal communication K. Kindle).

Figure 3.1 Analysis of the subcellular distribution of HA-tagged GRIP1, MOZ and MOZ-TIF2

COS-1 cells were seeded on glass coverslips in 6-well plates at 1.5×10^5 cells/well and transfected 24 hr later with 1 μ g HA-epitope tagged GRIP1, MOZ or MOZ-TIF2 expression vector. Following a further 24 hr growth in full medium, they were fixed, permeabilised, and incubated with a mouse α -HA monoclonal antibody, followed by an α -mouse TRITC-conjugated secondary antibody and Hoechst 33258 DNA stain. After mounting the slides, protein subcellular localisations were viewed and captured using a Zeiss Axioskop2 microscope. Each image was captured sequentially in the TRITC (α -HA) and Hoechst channels: Hoechst indicates the distribution of DNA; α -HA shows the localisation of the expressed HA-tagged protein; Merge shows an overlay of the Hoechst (blue) and α -HA (red) images. Two different images are shown for each HA-tagged protein: a) HA-GRIP1, b) HA-MOZ and c) HA-MOZ-TIF2.



The subcellular distributions shown are all of over-expressed proteins, and thus may not exactly reflect the localisation of the endogenous proteins. At the time the experiments were performed there were no GRIP1/TIF2 antibodies available that recognised endogenous TIF2 and thus it was not possible to investigate the localisation of this endogenous protein (data not shown and personal communication; K. Kindle). However, during the preparation of this thesis analysis of endogenous MOZ in COS-1 cells using an α -MOZ antibody indicated that it localised to both small and large nuclear foci in a number of different cell lines (personal communication; K. Kindle). Thus the subcellular localisation of over-expressed MOZ (Figure 3.1b) was representative of the endogenous pattern. Studies of the endogenous MOZ-TIF2 protein were not possible as no cells were available from patients with the translocation. Analysis of the subcellular distributions of FLAG-MOZ and FLAG-MOZ-TIF2 using α -FLAG antibody (data not shown) indicated an identical localisation to the HA-tagged proteins.

In summary, the epitope-tagged GRIP1, MOZ and MOZ-TIF2 constructs were all expressed and showed a nuclear localisation. MOZ was present in a speckled nuclear distribution whereas the MOZ-TIF2 leukaemogenic fusion gave a mesh-like pattern. In agreement with previous studies GRIP1/TIF2 was also nuclear (Voegel *et al.*, 1996; Baumann *et al.*, 2001), and localised to distinct nuclear foci in the vast majority of cells (Voegel *et al.*, 1996). This difference in nuclear localisation between the leukaemic fusion and its parent proteins suggests that proteins that interact with the MOZ and TIF2 domains present in MOZ-TIF2 may be mislocalised, potentially interfering with their normal function.

3.3 9-*cis* retinoic acid-dependent activation of a GAL4-responsive reporter by a GAL4-RXR α fusion protein

Nuclear receptors appear to play an important role in haematopoiesis (Section 1.12). NR ligands have been shown to induce differentiation of myeloid progenitors and leukaemic cell-lines (reviewed in Tenen *et al.*, 1997; James *et al.*, 1999; Collins, 2002), while deletion of the NRs themselves (Brown *et al.*, 1997; Sunaga *et al.*, 1997), or their fusion to other proteins (Zelent *et al.*, 2001), results in a block in myeloid cell differentiation. Therefore, as a first step to explore the effect of MOZ-TIF2 and MOZ on ligand-dependent transcription activation by NRs a GAL4-based, calcium phosphate-mediated transient transfection system (Section 2.2.6) coupled with reporter activation assays (Section 2.5.6) was used. GAL4-NR:LBD chimeric proteins, which are comprised of the DNA binding domain (DBD) of the yeast transcription factor GAL4 fused to the ligand-binding domain (LBD) of a nuclear receptor, have been employed in previous studies to investigate ligand-induced AF2-dependent transcription (Folkers and van der Saag, 1995; Voegel *et al.*, 1998; Mak *et al.*, 1999; Sheppard *et al.*, 2001). The fusion protein binds to five GAL4 motifs present upstream of the minimal thymidine kinase promoter in the firefly luciferase reporter p(Gal4)₅-E1b Δ -Luc (gift from Dr. P. Shaw, University of Nottingham). Activation of luciferase transcription occurs upon binding of the nuclear receptor ligand to the LBD contained within the chimeric fusion. The transcriptional activity of the GAL4-fused NR LBD thus controls the level of luciferase expression, which may be determined through direct quantification of luciferase activity in cell-free extracts. Endogenous NR proteins cannot induce luciferase transcription as they are unable to bind the reporter promoter.

In order to confirm that any measured variation in luciferase activity was due to specific changes in luciferase expression and not an overall effect on cellular transcription, translation or protein stability, the constitutively expressed β -galactosidase reporter construct pCH110, driven by the SV40 early promoter, was co-transfected with the luciferase reporter. Transcription of this β -galactosidase reporter was not affected by changes in GAL4-NR transcriptional activity (Figure 3.2b and data not shown). Therefore, the measured β -galactosidase activity could be used to normalise the luciferase values, giving a luciferase/ β -galactosidase ratio. This reporter activity ratio was plotted as Relative Luciferase Activity (RLA) with the ratio for Reporters (in the absence of ligand) set to a value of 1 for all the reporter assay data shown in this study. Data representative of three

independent experiments carried out in triplicate is shown. The plotted error bars indicate the Standard Error of the Mean (S.E.M.) for the triplicate samples. The S.E.M. is calculated by the division of the standard deviation of the samples by the number of samples used to calculate that standard deviation. The standard deviation is a measure of the spread of the data and does not take into account the number of samples used to calculate it. Thus it does not describe the accuracy of the calculated mean. In contrast, the S.E.M. provides an indication of the accuracy of the calculated sample mean as an estimation of the population mean (Tulsa, 1999).

GAL4-RXR α , which consists of a fusion of the retinoid X receptor α LBD (residues 112-467; (Folkers and van der Saag, 1995)) to the GAL4 DBD was examined for its ability to activate the luciferase reporter p(Gal4)₅-E1b Δ -Luc. As shown in Figure 3.2a, when reporters alone (p(Gal4)₅-E1b Δ -Luc + pCH110) were transfected, addition of the ligand 9-*cis* retinoic acid (9-*cis* RA) did not result in an increase in luciferase activity (measured as Relative Light Units) compared to that seen in the absence of ligand. This indicated that any endogenous RXR or RAR proteins that could bind the ligand were not able to activate transcription of the reporter. In contrast, when 100 ng GAL4-RXR α expression vector was co-transfected with reporters and ligand added, luciferase activity increased 5-fold over that seen with reporters alone. This increase was dependent upon the addition of ligand (Figure 3.2a: GAL4-RXR α : “9-*cis* RA” and “No Ligand” bars). β -galactosidase activity (pCH110 reporter) was also measured in the same extracts (Figure 3.2b) to normalise the luciferase data. The resulting ratios were plotted as Relative Luciferase Activity (Figure 3.2c) with the error bars indicating the standard error of the mean (S.E.M.).

Thus in summary, the chimeric protein GAL4-RXR α selectively activates transcription of the luciferase reporter p(Gal4)₅-E1b Δ -Luc in a ligand-dependent manner.

Figure 3.2: Ligand-induced reporter activation by GAL4-RXR α

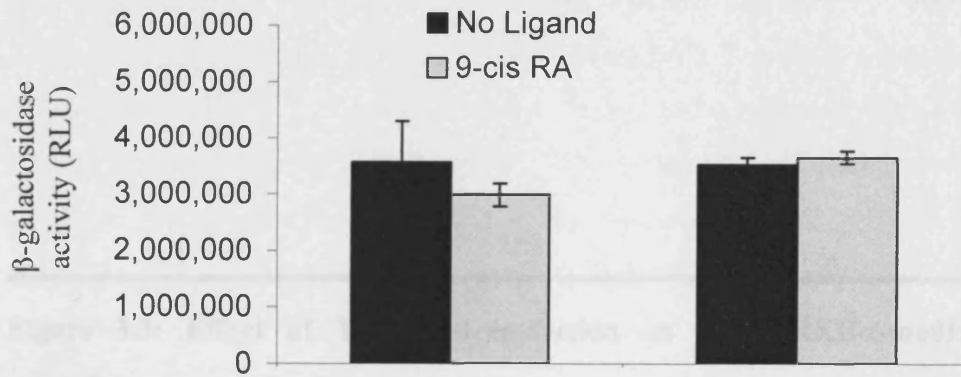
COS-1 cells were transfected with p(Gal4)₅-E1b Δ -Luc luciferase reporter, pCH110 β -galactosidase reporter and GAL4-RXR α expression vector as shown. “-” indicates no DNA transfected; “number” indicates amount of DNA in ng. The ligand 9-*cis* retinoic acid (9-*cis* RA; 1×10^{-7} M), or an equal volume of vehicle (No Ligand), was added as indicated 24 hr after transfection and the cells harvested following a further 24 hr incubation. The luciferase and β -galactosidase activities of each cell-free lysate were measured using a dual assay. The luciferase: β -galactosidase ratios were then calculated and plotted as Relative Luciferase Activity, with the ratio for the reporters p(Gal4)₅-E1b Δ -Luc + pCH110 (No Ligand) set to a value of 1. Error bars show the calculated S.E.M. and indicate the accuracy of each mean.

- a) Effect of 9-*cis* retinoic acid on GAL4-RXR α -mediated expression of the luciferase reporter promoter as determined by measurement of luciferase activity as Relative Light Units (RLU).
 - b) Effect of 9-*cis* RA addition on β -galactosidase expression in the presence of GAL4-RXR α , as determined by measurement of β -galactosidase activity in Relative Light Units (RLU).
 - c) Effect of GAL4-RXR α expression and 9-*cis* RA addition upon the specific induction of the luciferase reporter promoter. Relative Luciferase Activity (RLA) was determined by calculation of luciferase: β -galactosidase ratios, with the ratio for transfection of reporters in the absence of ligand set to a value of 1.
-

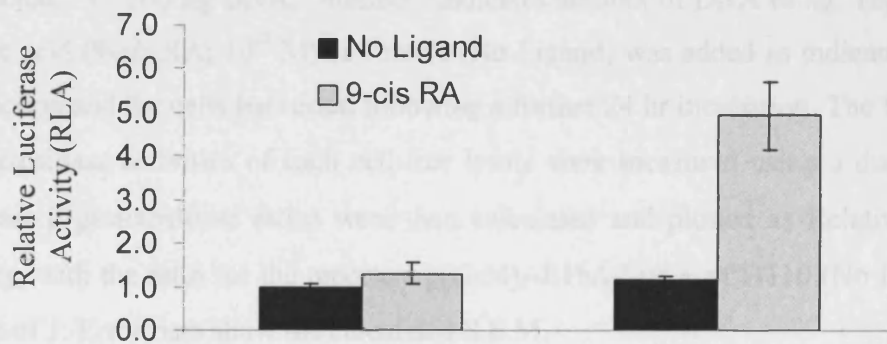
a) Luciferase Activity



b) β -galactosidase Activity



c) Relative Luciferase Activity



p(Gal4) ₅ -E1b Δ -Luc	500	500
pCH110	100	100
GAL4-RXR α	-	100

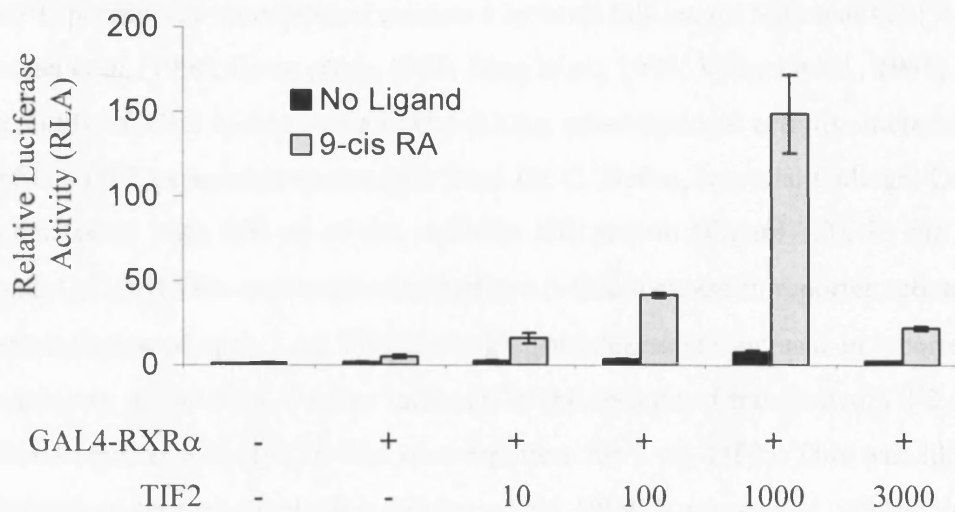


Figure 3.3: Effect of TIF2 co-transfection on GAL4-RXR α -mediated reporter activation

COS-1 cells were transfected with 500 ng p(Gal4)₅-E1b Δ -Luc luciferase reporter, 100 ng pCH110 β -galactosidase reporter and expression vectors as shown. “-” indicates no DNA transfected; “+” 100 ng DNA; “number” indicates amount of DNA in ng. The ligand *9-cis* retinoic acid (*9-cis* RA; 10⁻⁷ M) or vehicle (No Ligand) was added as indicated 24 hr after transfection and the cells harvested following a further 24 hr incubation. The luciferase and β -galactosidase activities of each cell-free lysate were measured using a dual assay. The luciferase: β -galactosidase ratios were then calculated and plotted as Relative Luciferase Activity, with the ratio for the reporters p(Gal4)₅-E1b Δ -Luc + pCH110 (No Ligand) set to a value of 1. Error bars show the calculated S.E.M.

3.4 TIF2 acts as a transcriptional coactivator for GAL4-RXR α

Previous studies have shown that ectopically expressed TIF2, and its mouse homologue GRIP1, potentiates transcription mediated by both full-length NRs and GAL4-NR fusions (Voegel *et al.*, 1996; Hong *et al.*, 1997; Ding *et al.*, 1998; Voegel *et al.*, 1998). To confirm this ability of TIF2 to coactivate GAL4-RXR α transcriptional activity, increasing amounts of pSG5-TIF2 expression vector (gift from Dr. C. Bevan, Imperial College, London) were co-transfected with 100 ng of the chimeric NR protein (Figure 3.3). In the presence of ligand, GAL4-RXR α expression resulted in a 5-fold increase in reporter activation (RLA). Co-transfection of up to 1 μ g TIF2 led to a ligand-dependent increase in reporter activity to a maximum of 148-fold. Further increases in the amount of transfected TIF2 resulted in a reduced reporter activity (20-fold over reporters for 3 μ g TIF2). This was likely due to a phenomenon termed squelching (Meyer *et al.*, 1989; Voegel *et al.*, 1996; Voegel *et al.*, 1998), whereby a large excess of non-NR-bound TIF2 protein sequesters endogenous cofactors required for transcription, thus reducing their association with the active DNA-bound Nuclear Receptor:TIF2 complex. Transfection of HA-GRIP1 was also found to result in the enhancement of GAL4-RXR α -mediated transcription (data not shown), indicating that the HA epitope-tagged mouse homologue acted as a ligand-dependent NR coactivator.

In summary, co-transfection of up to 1 μ g TIF2 resulted in a potent coactivation of reporter transcription mediated by 100 ng GAL4-RXR α . For all further NR reporter assay transfections 100 ng TIF2 was co-transfected as this gave a consistent enhancement of reporter activity over GAL4-RXR α alone.

3.5 GAL4-RXR α transcriptional activity is not enhanced by MOZ

MOZ has been reported to act as a coactivator for AML1, a member of the RUNX family of transcription factors (Kitabayashi *et al.*, 2001a; Bristow and Shore, 2003), indicating that it can play a role in the activation of transcription. TIP60, a MYST homologue of MOZ, has been reported to act as a transcriptional coactivator for the steroid family of nuclear receptors (Gaughan *et al.*, 2001). This activity is dependent upon the LXXLL motif present at the C-terminus of the protein, which mediates interaction with ligand-bound nuclear receptors. MOZ, however, does not contain an LXXLL motif and does not bind the

NR AF2 domain *in vitro* (Section 4.2). In order to investigate whether MOZ could potentiate nuclear receptor-mediated transcription in a ligand-dependent manner, increasing amounts of MOZ expression plasmid DNA were titrated with 100 ng GAL4-RXR α vector (Figure 3.4). Co-transfection of up to 1 μ g MOZ did not enhance NR fusion-mediated transcription in the presence or absence of ligand, whereas transfection of 100 ng TIF2 resulted in a 3.6-fold induction over GAL4-RXR α alone upon 9-*cis* RA addition (Gal4-RXR α : 7-fold over reporters; GAL4-RXR α + TIF2: 25-fold over reporters). This suggests that MOZ does not function as a coactivator for GAL4-RXR α -mediated transcription.

3.6 MOZ-TIF2 does not enhance GAL4-RXR α -mediated transcription

The MOZ-TIF2 fusion protein is comprised of the N terminus of MOZ (residues 1-1117) and C terminus of TIF2 (residues 869-1464) (Carapeti *et al.*, 1998a). As a result, it contains the AD1 and AD2 domains of TIF2, which mediate interaction with CBP and CARM1 respectively. However, the fusion does not contain the LXXLL motif-encoding NID (Heery *et al.*, 1997) located between residues 624 and 869 that mediates TIF2 interaction with NRs (Voegel *et al.*, 1998). To investigate whether the presence of the TIF2-derived AD1 and AD2 coupled to the N terminus of MOZ was sufficient to allow MOZ-TIF2 to act as a coactivator of NR-mediated transcription, titration experiments were carried out in the presence of GAL4-RXR α (Figure 3.5). Co-transfection of up to 3 μ g MOZ-TIF2 plasmid did not result in further enhancement of luciferase expression over that obtained with GAL4-RXR α alone. Indeed, expression of >100 ng MOZ-TIF2 DNA appeared to inhibit the ligand-dependent increase in transcription mediated by GAL4-RXR α down to a level equivalent to that obtained with reporters alone.

This data suggested that MOZ-TIF2 inhibited rather than potentiated GAL4-RXR α fusion-mediated transcription.

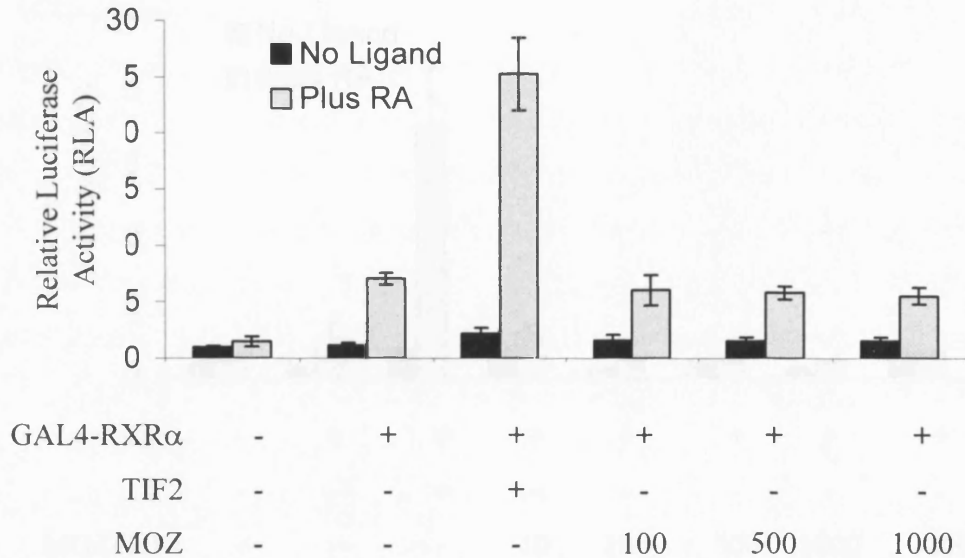


Figure 3.4: Effect of MOZ on GAL4-RXR α transcriptional activity

COS-1 cells were transfected with 500 ng p(Gal4)₅-E1b Δ -Luc luciferase reporter, 100 ng pCH110 β -galactosidase reporter and expression vectors as shown. “-” indicates no DNA transfected; “+” 100 ng DNA; “number” indicates amount of DNA in ng. The ligand 9-*cis* retinoic acid (9-*cis* RA; 10⁻⁷ M) or vehicle (No Ligand) was added as indicated 24 hr after transfection and the cells harvested following a further 24 hr incubation. The luciferase and β -galactosidase activities of each cell-free lysate were measured using a dual assay. The luciferase: β -galactosidase ratios were then calculated and plotted as Relative Luciferase Activity, with the ratio for the reporters p(Gal4)₅-E1b Δ -Luc + pCH110 (No Ligand) set to a value of 1. Error bars show the calculated S.E.M.

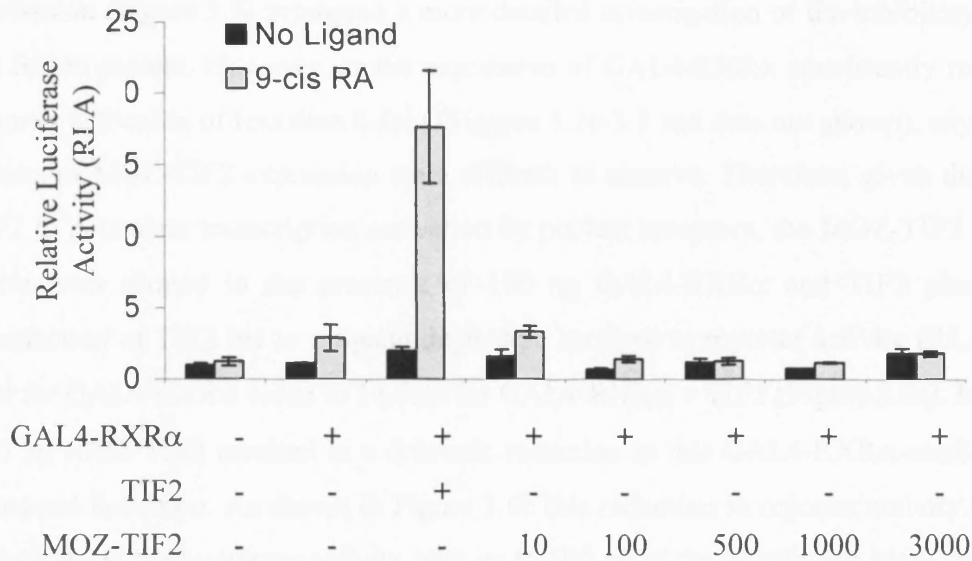


Figure 3.5: Effect of MOZ-TIF2 titration on GAL4-RXR α transcriptional activity

COS-1 cells were transfected with 500 ng p(Gal4)₅-E1b Δ -Luc luciferase reporter, 100 ng pCH110 β -galactosidase reporter and expression vectors as shown. “-” indicates no DNA transfected; “+” 100 ng DNA; “number” indicates amount of DNA in ng. The ligand 9-*cis* retinoic acid (9-*cis* RA; 10⁻⁷ M) or vehicle (No Ligand) was added as indicated 24 hr after transfection and the cells harvested following a further 24 hr incubation. The luciferase and β -galactosidase activities of each cell-free lysate were measured using a dual assay. The luciferase: β -galactosidase ratios were then calculated and plotted as Relative Luciferase Activity, with the ratio for the reporters p(Gal4)₅-E1b Δ -Luc + pCH110 (No Ligand) set to a value of 1. Error bars show the calculated S.E.M.

3.7 MOZ-TIF2 acts as a dominant inhibitor of GAL4-RXR α :TIF2-mediated transcription

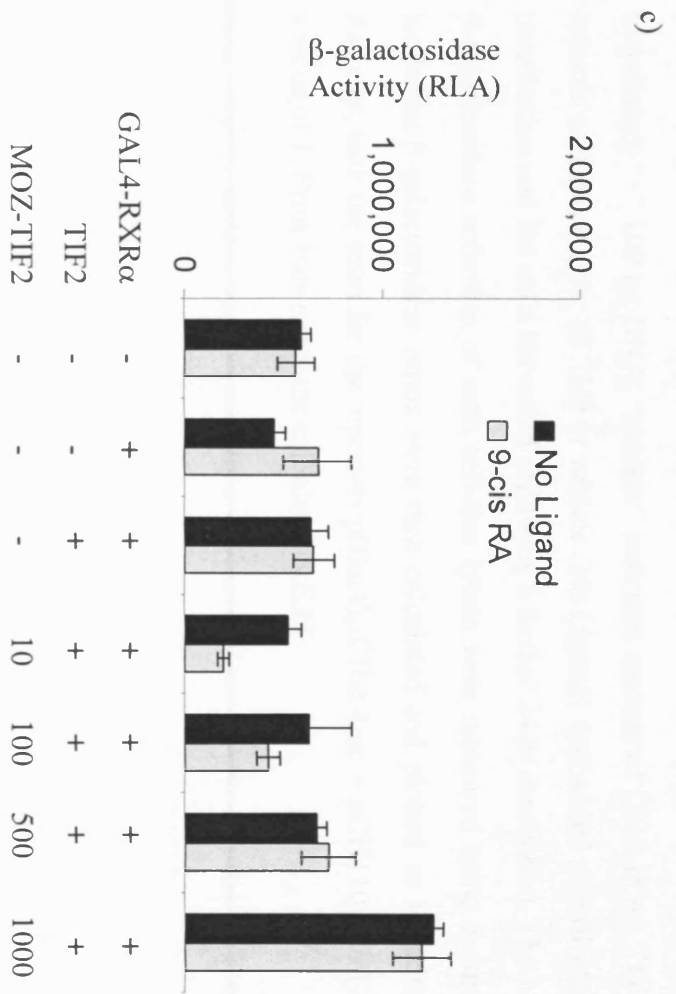
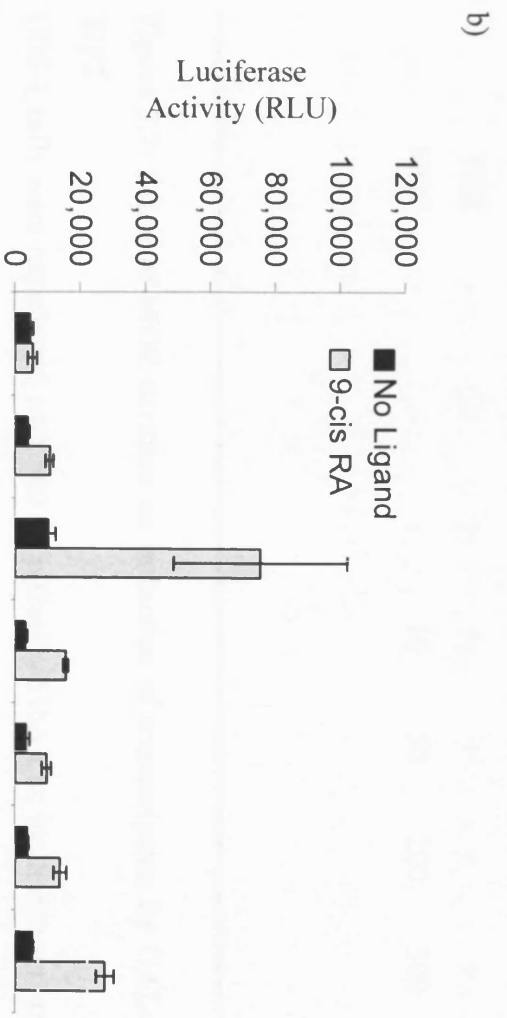
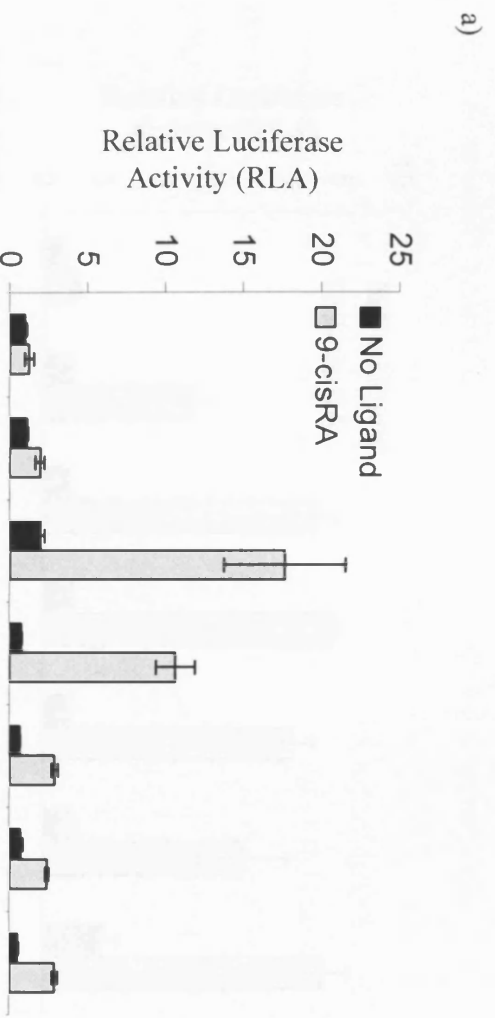
The apparent reduction in ligand-dependent GAL4-RXR α activity upon MOZ-TIF2 expression (Figure 3.5) prompted a more detailed investigation of the inhibitory effects of the fusion protein. However, as the expression of GAL4-RXR α consistently resulted in a reporter activation of less than 8-fold (Figures 3.2c-3.7 and data not shown), any inhibitory effects of MOZ-TIF2 expression were difficult to observe. Therefore, given the ability of TIF2 to potentiate transcription activation by nuclear receptors, the MOZ-TIF2 expression vector was titrated in the presence of 100 ng GAL4-RXR α and TIF2 plasmids. Co-transfection of TIF2 led to a ligand-dependent increase in reporter activity (RLA) from 2-fold for GAL4-RXR α alone to 18-fold for GAL4-RXR α + TIF2 (Figure 3.6a). Inclusion of >10 ng MOZ-TIF2 resulted in a dramatic reduction in this GAL4-RXR α -mediated TIF2-enhanced induction. As shown in Figure 3.6b this reduction in reporter activity was due to a decrease in the luciferase activity with up to 500 ng of the transfected MOZ-TIF2 vector. However, with 1 μ g MOZ-TIF2, both the luciferase (Figure 3.6b) and β -galactosidase (Figure 3.6c) activities increased suggesting that co-expression of high levels of MOZ-TIF2 with TIF2 resulted in a non-NR-specific effect on transcription. As a consequence of this, the amount of MOZ-TIF2 vector transfected was kept below 1 μ g for all further experiments.

In summary, MOZ-TIF2 specifically inhibited GAL4-RXR α /TIF2-mediated transcription when amounts of DNA transfected were kept below 1 μ g.

Figure 3.6: Transfection of MOZ-TIF2 in the presence of GAL4-RXR α and TIF2

COS-1 cells were transfected with 500 ng p(Gal4)₅-E1b Δ -Luc luciferase reporter, 100 ng pCH110 β -galactosidase reporter and expression vectors as shown. “-” indicates no DNA transfected; “+” 100 ng DNA; “number” indicates amount of DNA in ng. The ligand 9-*cis* retinoic acid (9-*cis* RA; 10⁻⁷ M) or vehicle (No Ligand) was added as indicated 24 hr after transfection and the cells harvested following a further 24 hr incubation. The luciferase (b) and β -galactosidase activities (c) of each cell-free lysate were measured using a dual assay and the Relative Luciferase Activity calculated (a). Error bars show the calculated S.E.M.

- a) Effect of MOZ-TIF2 titration on GAL4-RXR α /TIF2-mediated induction of reporter expression. The luciferase: β -galactosidase reporter activity ratios were calculated and plotted as Relative Luciferase Activity (RLA), with the ratio for the reporters p(Gal4)₅-E1b Δ -Luc + pCH110 (No Ligand) set to a value of 1.
 - b) Effect of MOZ-TIF2 titration on induction of luciferase expression as determined by luciferase activity (measured as Relative Light Units: RLU).
 - c) Effect of increasing MOZ-TIF2 on the expression of the constitutive β -galactosidase reporter as determined by measurement of β -galactosidase activity (in RLU).
-



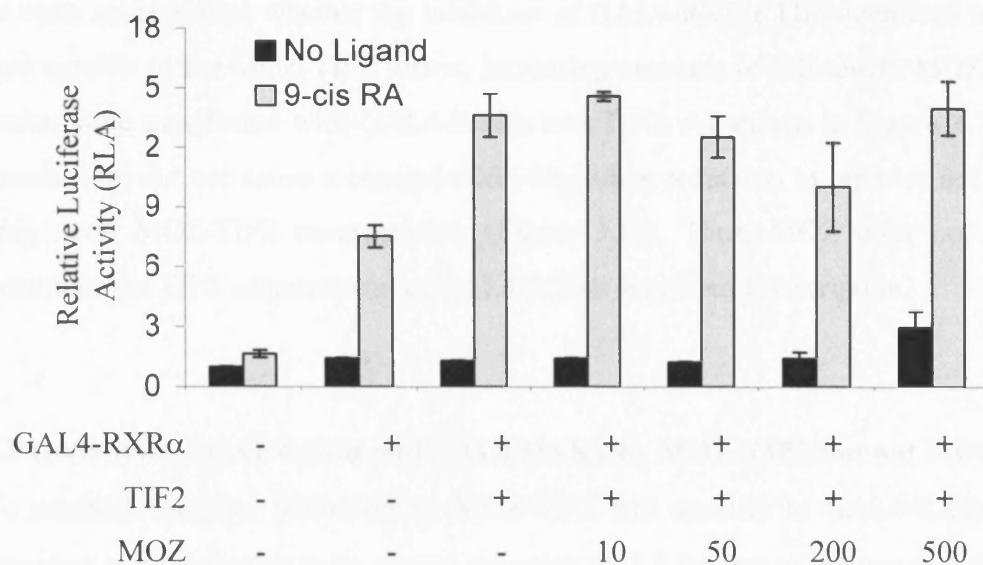


Figure 3.7: Effect of MOZ titration on induction of transcription by GAL4-RXR α + TIF2

COS-1 cells were transfected with 500 ng p(Gal4)₅-E1b Δ -Luc luciferase reporter, 100 ng pCH110 β -galactosidase reporter and expression vectors as shown. “-” indicates no DNA transfected; “+” 100 ng DNA; “number” indicates amount of DNA in ng. The ligand 9-*cis* retinoic acid (9-*cis* RA; 10⁻⁷ M) or vehicle (No Ligand) was added as indicated 24 hr after transfection and the cells harvested following a further 24 hr incubation. The luciferase and β -galactosidase activities of each cell-free lysate were measured using a dual assay. The luciferase: β -galactosidase ratios were then calculated and plotted as Relative Luciferase Activity, with the ratio for the reporters p(Gal4)₅-E1b Δ -Luc + pCH110 (No Ligand) set to a value of 1. Error bars show the calculated S.E.M.

3.8 MOZ does not inhibit GAL4-RXR:TIF2-mediated transcription

In order to determine whether the inhibition of GAL4-RXR α /TIF2-mediated transcription was specific to the MOZ-TIF2 fusion, increasing amounts of full-length MOZ expression vector were transfected with GAL4-RXR α and TIF2. As shown in Figure 3.7, MOZ co-transfection did not cause a concentration-dependent reduction in reporter activity as was seen upon MOZ-TIF2 co-expression (Figure 3.6a). Thus, MOZ does not inhibit nor potentiate the TIF2 enhancement of GAL4-RXR α -mediated transcription.

3.9 Inhibition of GAL4-ER α and GAL4-RAR α by MOZ-TIF2 but not MOZ

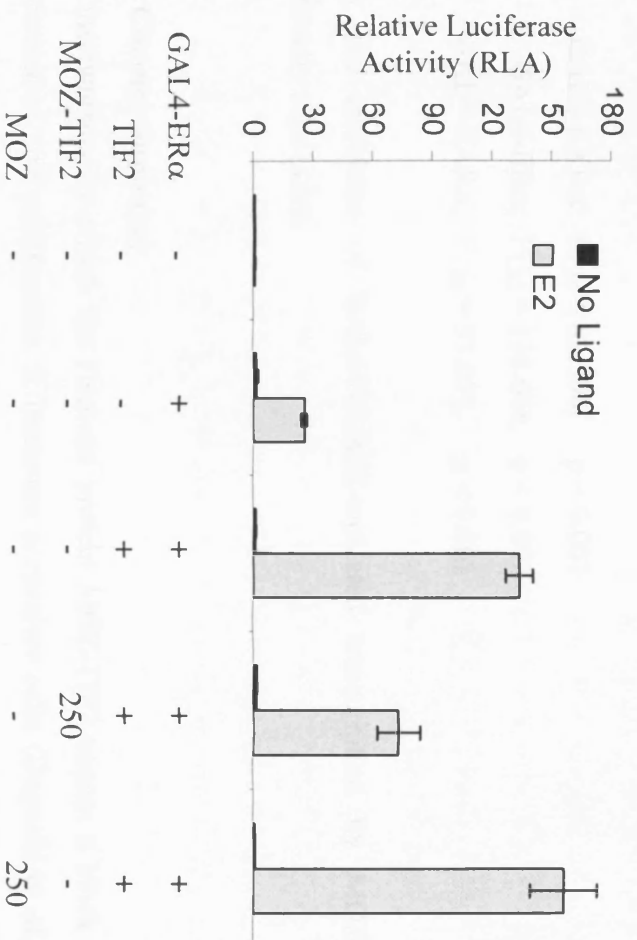
To establish whether inhibition by MOZ-TIF2 was specific to GAL4-RXR α , transient transfection experiments were carried out using GAL4 fusions of the mouse ER α (residues 313-599) and human RAR α (residues 154-462) nuclear receptors (gifts from Dr. M. Parker, Imperial College, London). Upon addition of ligand both GAL4-NR fusions selectively enhanced expression of the luciferase reporter p(Gal4)₅-E1b Δ -Luc, thus giving rise to an increase in reporter activity (Figures 3.8). Activation was further enhanced (from 26-fold to 134-fold for GAL4-ER α , and 50-fold to 155-fold for GAL4-RAR α) by inclusion of 100 ng TIF2 expression vector. Co-transfection of 250 ng MOZ plasmid did not affect reporter induction when compared to transfection of GAL4-NR + TIF2. However, when the MOZ-TIF2 expression vector was co-transfected with GAL4-NR and TIF2 a substantial decrease in reporter activity was seen (134-fold for GAL4-ER α + TIF2 down to 73-fold upon MOZ-TIF2 inclusion; 155-fold down to 91-fold for GAL4-RAR α). This clearly shows that MOZ-TIF2 inhibits the AF2 activity of both Class I and Class II nuclear receptors.

To determine whether the inhibition of GAL4-NR/TIF2-mediated transcription by MOZ-TIF2 was statistically significant, univariate ANalysis Of VAriance (ANOVA) was performed (Brace *et al.*, 2003). Data from ≥ 4 independent experiments for each NR fusion were analysed and in each case co-expression of 250 ng MOZ-TIF2 with GAL4-NR

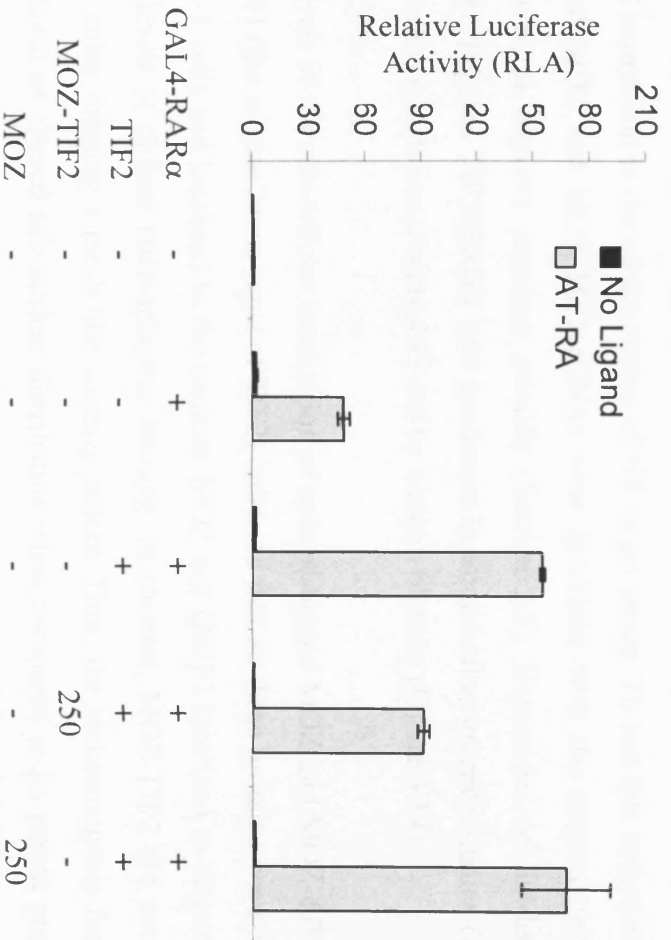
Figure 3.8: Effect of MOZ and MOZ-TIF2 expression on induction of reporter expression by GAL4-ER α and GAL4-RAR α

Co-expression of 250 ng MOZ or MOZ-TIF2 with TIF2 in the presence of a) GAL4-ER α and b) GAL4-RAR α . COS-1 cells were transfected with 500 ng p(Gal4)₅-E1b Δ -Luc luciferase reporter, 100 ng pCH110 β -galactosidase reporter and expression vectors as shown. “-” indicates no DNA transfected; “+” 100 ng DNA; “number” indicates amount of DNA in ng. Ligand (GAL4-ER α : oestradiol, E2; GAL4-RAR α : all-*trans* retinoic acid, AT-RA; 10⁻⁷ M) or vehicle (No Ligand) was added as indicated 24 hr after transfection and the cells harvested following a further 24 hr incubation. The luciferase and β -galactosidase activities of each cell-free lysate were measured using a dual assay. The luciferase: β -galactosidase ratios were then calculated and plotted as Relative Luciferase Activity, with the ratio for the reporters p(Gal4)₅-E1b Δ -Luc + pCH110 (No Ligand) set to a value of 1 for each experiment. Error bars show the calculated S.E.M.

a) GAL4-ER α



b) GAL4-RAR α



and TIF2 was found to have a highly significant effect on the calculated reporter activity (RLA) when compared to expression of the NR fusion with TIF2:

$$\text{GAL4-RXR}\alpha: F_{1,34} = 83.590, \quad p < 0.001$$

$$\text{GAL4-ER}\alpha: F_{1,22} = 138.666, \quad p < 0.001$$

$$\text{GAL4-RAR}\alpha: F_{1,22} = 33.079, \quad p < 0.001$$

Thus, the inhibition of GAL4-NR:AF2-mediated transcription by MOZ-TIF2 was statistically significant.

3.10 Chapter Summary

The mechanisms by which the chimeric protein MOZ-TIF2 causes a block in myeloid differentiation and proliferation of immature progenitor cells (Deguchi *et al.*, 2003) are unknown. However, given the role of the parental protein TIF2 in NR-mediated transcription (Voegel *et al.*, 1998), and the evidence for the importance of NRs and their ligands in haematopoiesis (Introduction Section 1.12), one possible consequence of MOZ-TIF2 expression is the misregulation of NR target genes. To test this hypothesis, epitope-tagged MOZ and MOZ-TIF2 cDNAs were generated with the untranslated sequences removed to improve construct stability (Section 2.6). Expression of full-length MOZ, MOZ-TIF2 and TIF2/GRIP1 was confirmed in immunofluorescence studies (Figure 3.1), by *in vitro* translation (Figure 4.1) and by western blotting (Figure 4.14).

Analysis of the sub-cellular localisation of epitope-tagged MOZ and MOZ-TIF2, and HA-GRIP1 (the murine homologue of TIF2) indicated that all three proteins were expressed in COS-1 cells and localised to the nucleus. MOZ and GRIP1 localised to discrete foci with low levels of diffuse nucleoplasmic staining. In contrast, MOZ-TIF2 did not localise to foci, rather forming a mesh-like staining pattern. Thus, the leukaemogenic fusion protein displayed an altered sub-nuclear distribution when compared to its parent proteins MOZ and TIF2. Analysis of the sub-cellular localisation of MOZ, MOZ-TIF2 and GRIP1 in other cell-types indicated similar patterns to those observed in the COS-1 cell-line (personal communication; K. Kindle).

In order to investigate the effects of expression of TIF2, MOZ and MOZ-TIF2 on ligand-dependent NR-mediated transcription, the constructs were co-transfected with GAL4-NR:LBD fusion proteins in transient transfection experiments. These chimeric fusions are comprised of the DNA binding domain (DBD) of the yeast transcription factor GAL4 fused to the ligand-binding domain (LBD) of a nuclear receptor (Section 3.3). GAL4-RXR α (Figures 3.2-3.7), GAL4-ER α and GAL4-RAR α (Figure 3.8) all activated transcription of a GAL4-responsive luciferase reporter in a ligand-dependent manner as reported by others (Folkers and van der Saag, 1995; Voegel *et al.*, 1998; Mak *et al.*, 1999; Sheppard *et al.*, 2001). This transcriptional activation was enhanced (Figure 3.3 and 3.8) by co-transfection of the p160 coactivator, TIF2/GRIP1, as previously described (Hong *et al.*, 1997; Voegel *et al.*, 1998). In contrast, the MYST protein MOZ was unable to potentiate GAL4-RXR α -mediated transcription (Figure 3.4). The MOZ-TIF2 fusion protein is comprised of the N-terminus of MOZ (residues 1-1117) and C-terminus of TIF2 (residues 869-1464). Thus, it contains the AD1 and AD2 but not NID (residues 624-869) from TIF2. In order to determine whether the combination of MOZ and TIF2-derived domains was sufficient for it to act as an NR coactivator, the fusion was co-transfected with the GAL4-RXR α chimera. No enhancement of reporter activity over that seen with GAL4-RXR α alone was observed (Figure 3.5). This was consistent with the inability of full-length MOZ to act as a coactivator for AF2-mediated transcription, and with the study by Sheppard *et al.* (2001), which showed that a functional NID and AD1 in the TIF2 homologue, SRC1, were essential for enhancement of AF2-mediated transcription. Indeed, the GAL4-RXR α data suggested that MOZ-TIF2 might inhibit rather than enhance transcriptional activation (Figure 3.5).

To investigate the inhibition of GAL4-RXR α -mediated transcription, MOZ and MOZ-TIF2 were co-transfected with the GAL4-NR fusion in the presence of TIF2. As shown in Figures 3.6 and 3.7 MOZ-TIF2 expression, but not MOZ, resulted in a substantial reduction in reporter activity when compared to the transfection of the GAL4-NR fusion + TIF2. This effect on LBD-mediated transcription was further investigated by co-transfection of MOZ-TIF2 with GAL4 fusions of the mouse ER α and human RAR α ligand-binding domains (Figures 3.8a and 3.8b respectively). Both chimeric transcription factors were inhibited by MOZ-TIF2 in a manner similar to GAL4-RXR α . This inhibition by MOZ-TIF2 was shown to be statistically significant for all three GAL4-NR proteins.

The results described here show that the leukaemogenic fusion protein MOZ-TIF2 can act as a dominant inhibitor of ligand-dependent NR-mediated transcription in a transient transfection system. This is in contrast to the two proteins of which it is comprised. TIF2, as described previously (Voegel *et al.*, 1998), enhances NR transcriptional activity, while MOZ has no discernible effect on AF2 function. The inhibition of AF2-mediated NR transcription provides a possible mechanism for the leukaemogenic potential of the fusion as NRs and their ligands appear to play a role in the differentiation of myeloid cells. This is investigated in greater detail in the following chapters, which describe the work carried out to identify possible mechanisms of MOZ-TIF2-mediated inhibition of AF2 activity, and to determine whether this inhibition is relevant to full length receptors in the haematopoietic cell line U937, and to other transcription factors.

Chapter Four:

**The MOZ-TIF2 AD1 domain
is essential for inhibition
of GAL4-RAR α -mediated
transcription**

4.1 Introduction

Ligand-dependent activation of gene transcription by Nuclear Receptors (NRs) requires the recruitment of a number of coactivator complexes to the DNA-bound NR dimer (McKenna and O'Malley, 2002). This recruitment is initiated by the binding of ligand to the NR, which induces a change in the conformation of the NR LBD (Renaud and Moras, 2000). The alteration in structure results in the dissociation of bound co-repressors such as SMRT and NCoR, and exposes a hydrophobic groove that mediates the recruitment of coactivator proteins such as the p160 family (Leo and Chen, 2000). Coactivator association with this surface is mediated by LXXLL motifs present within the coactivator. These motifs form amphipathic α -helices that sit in the NR's hydrophobic groove, thus providing a high affinity ligand-dependent interaction (Heery *et al.*, 1997; Heery *et al.*, 2001; Coulthard *et al.*, 2003).

The analysis of NR coactivator function is an area of considerable interest. It appears that, though both chromatin remodelling and modification complexes are recruited to the promoter of responsive genes by the ligand-bound NR complex, the temporal order of recruitment and relative role of each coactivator may vary with the cell type and gene promoter investigated (Huang *et al.*, 2003; Acevedo and Kraus, 2003; Sharma and Fondell, 2002). However, the p160 coactivator family (Leo and Chen, 2000), which is comprised of three homologous proteins, SRC1, TIF2 (GRIP1) and ACTR (p/CIP, AIB1, RAC3, TRAM-1), appears to be recruited in almost all cases of transcription activation by NRs. These proteins act as bridging factors to recruit chromatin modification enzymes to the NR complex. The association of the p160 proteins with ligand-bound NRs is mediated by the LXXLL motifs present within the coactivator's central NR interaction domain (NID). C-terminal to this domain are the regions that recruit the chromatin modifiers CBP, CARM1 and PRMT1. CBP, a histone acetyltransferase protein that also acts as a bridging factor to the basal transcription machinery (Janknecht, 2002), binds to the p160 AD1 domain via its SRC1-interaction domain (SID) located between residues 2058 and 2130 (Sheppard *et al.*, 2001). CARM1 and PRMT1 are recruited to the NR/p160 complex by the second p160 activation domain, AD2 (Chen *et al.*, 1999a; Koh *et al.*, 2001). These chromatin modifiers act as methyltransferases, methylating the histone H3 and H4 N-terminal tails present in

the nucleosomes surrounding the NR complex (Ma *et al.*, 2001). The addition of these two covalent groups to the histone proteins acts to open up the nucleosomal structure, thus allowing access of the basal transcription machinery, and also provides docking sites for other proteins required for the activation of transcription.

The exact physiological roles of CBP and CARM1 in NR-mediated transcription are still being elucidated (Xu *et al.*, 2001; Dajaj *et al.*, 2002). However, in transient transfection experiments a mutant SRC1 protein comprised of solely the NID and AD1 was able to enhance NR-mediated transcription to the level seen with full-length SRC1 (Sheppard *et al.*, 2001). This, coupled with work published during the preparation of this thesis (Lee *et al.*, 2003), suggests that the recruitment of CBP may provide the main mechanism of enhancement of NR-mediated transcription by the p160 family.

The studies carried out in Chapter 3 of this thesis established that the leukaemogenic fusion protein MOZ-TIF2 inhibited ligand-dependent transcription by both Class I and II NRs in a transient transfection system. This inhibition was most apparent when the p160 protein TIF2 was co-expressed, suggesting that MOZ-TIF2 might act to specifically inhibit the function of this family of coactivators. However, the mechanism of inhibition was unknown. Therefore the experiments described in this chapter were carried out in order to investigate this. Both *in vitro* and *in vivo* studies were used to analyse specific protein interactions with the fusion protein, and mutant MOZ-TIF2 constructs were tested in the transient transfection system to determine the domains required for the inhibition.

4.2 TIF2, but not MOZ nor MOZ-TIF2, interacts with NRs in a ligand-dependent manner *in vitro*

The results described in Chapter 3 indicated that MOZ-TIF2 inhibited ligand-dependent activation of transcription by the AF2 domain of NRs. This transcriptional activity of AF2 is dependent upon the recruitment of the p160 proteins, which interact with the AF2 region present in the ligand-bound NR LBD (Leo and Chen, 2000). The direct interaction between the NR AF2 domain and the p160 protein TIF2 has been demonstrated *in vitro* using the AF2 domains of the ER α , RAR α and RXR α (Voegel *et al.*, 1996). Further work showed that it is mediated by LXXLL motifs present in the TIF2 NID located between residues 624 and 869 (Heery *et al.*, 1997; Voegel *et al.*, 1998). The MOZ-TIF2 leukaemogenic fusion encodes the TIF2 residues 869 to 1464. As a result the fusion protein does not include the NID. Instead, MOZ-TIF2 contains the residues 1-1117 of MOZ. Analysis of the protein sequence of full-length MOZ did not detect LXXLL motifs, in contrast to its MYST homologue TIP60, which contains a single motif at its extreme C-terminus and appears to be able to act as a coactivator for the steroid family of NRs (Gaughan *et al.*, 2001). Thus MOZ and MOZ-TIF2 were not expected to interact with the AF2 domain of NRs. If this were shown to be the case, it would be unlikely that the inhibition of ligand-dependent transcription by MOZ-TIF2 was due to direct binding of the fusion protein to the NR. Thus, to begin to investigate the mechanism of inhibition and confirm the ligand-dependent interaction of TIF2 with the NRs (Voegel *et al.*, 1996), GST-pulldown experiments were carried out with the ER α and RXR α AF2 domains in the presence and absence of ligand.

pcDNA3:TIF2, pcDNA3.0PT:HA-MOZ-TIF2 and pcDNA3.0PT:HA-MOZ were transcribed and translated *in vitro* in the presence of [³⁵S]-methionine to give full-length radiolabelled (IVT) proteins (Section 2.5.21). Synthesis of full-length proteins was confirmed by running 0.1 and 1.0 μ l (of 50 μ l total) of each *in vitro* translation product on an 8% SDS-PAGE gel (Figure 4.1). Estimation of protein size was carried out using the amino acid sequence of each protein (Stothard, 2000). These calculated molecular weights were used to confirm that the radiolabelled protein bands visible on the SDS-PAGE gel migrated at a rate consistent with their expected full-length size. TIF2 was predicted to be 159 kDa, MOZ 226 kDa, and the MOZ-TIF2 fusion 194 kDa. The size of the (non-radiolabelled) protein markers run with the IVT proteins are indicated (Figure 4.1). The

maximum protein size in the Roche Marker was 166 kDa (Figure 4.1b), which correlated well with the predicted size and relative position on the gel of the TIF2 protein. The upper two proteins in the Biorad Prestained Marker (Figure 4.1a) were stated as having molecular weights of 250 kDa and 150 kDa. However, both full-length MOZ and MOZ-TIF2 consistently (data not shown) ran above the upper band, despite having estimated molecular masses of less than 250 kDa. Thus, this marker appeared to result in an over-estimation of the molecular weight of MOZ and MOZ-TIF2 as the correct sequence of each construct had been confirmed during initial cloning and the subsequent re-cloning (Section 2.6).

The TIF2, MOZ and MOZ-TIF2 IVT proteins described above were incubated with glutathione bead-purified GST-ER α :AF2 (Heery *et al.*, 1997) or GST-RXR α :AF2 (gift from Dr. K. Chatterjee, University of Cambridge) in the presence and absence of ligand as described (Section 2.5.22). A lane containing 10% input of the [³⁵S]-labelled protein was included on the SDS-PAGE gels in order to allow estimation of the percentage of labelled protein that interacted with the GST-fusion. As shown in Figure 4.2, TIF2 bound very strongly to both the ER α and RXR α AF2 domains in the presence, but not absence, of the appropriate ligand. This confirmed previous studies (Voegel *et al.*, 1996; Voegel *et al.*, 1998) showing that TIF2 interacts with NR LBDs in a ligand-dependent manner. In contrast, neither MOZ nor the MOZ-TIF2 fusion bound the ER α :AF2 or RXR α :AF2 in the presence or absence of ligand (Figure 4.2). This correlated with the lack of a discernible LXXLL motif in full-length MOZ, and the absence of the TIF2 NR interaction domain in the MOZ-TIF2 fusion. It also ruled out the possibility that other sequences in MOZ or the C-terminus of TIF2 interact with the NR LBD directly.

In summary TIF2, but not MOZ nor MOZ-TIF2, interacted with the AF2 domain of NRs. This suggested that the inhibition of NR:AF2-mediated transcription by MOZ-TIF2 identified in Sections 3.7 and 3.9 was not due to a direct binding of the fusion to the ligand-bound NR complex but rather, was due to an interaction with other factors necessary for transcription.

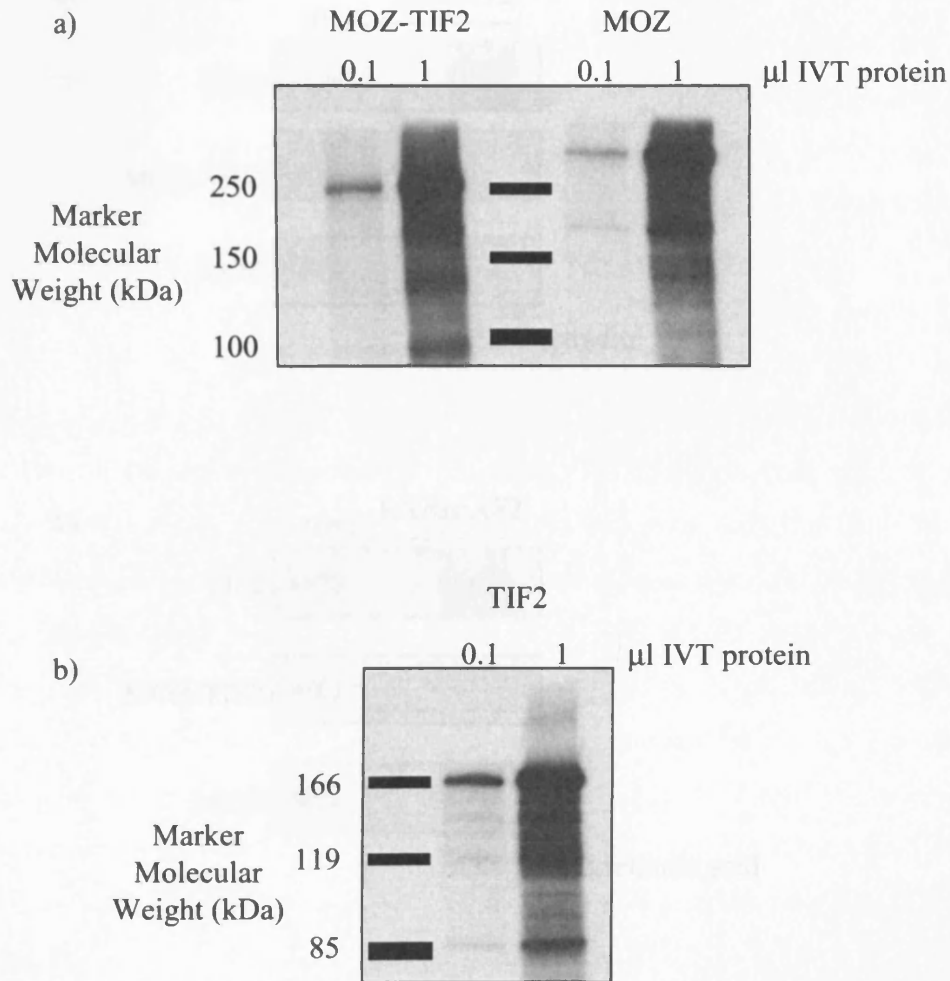


Figure 4.1: SDS-PAGE gels showing [^{35}S]-labelled *in vitro* transcribed and translated MOZ-TIF2, MOZ and TIF2.

pcDNA3.0PT:HA-MOZ-TIF2 and pcDNA3.0PT:HA-MOZ (a), and pcDNA3:TIF2 (b), were *in vitro* transcribed and translated in the presence of [^{35}S]-methionine to give full-length radio-labelled proteins. 0.1 μl and 1 μl of each IVT was run on an 8% SDS-PAGE gel to allow an accurate determination of the size of the predominant protein species synthesised. The sizes of the Molecular Weight Marker (non-radio-labelled) bands are shown.

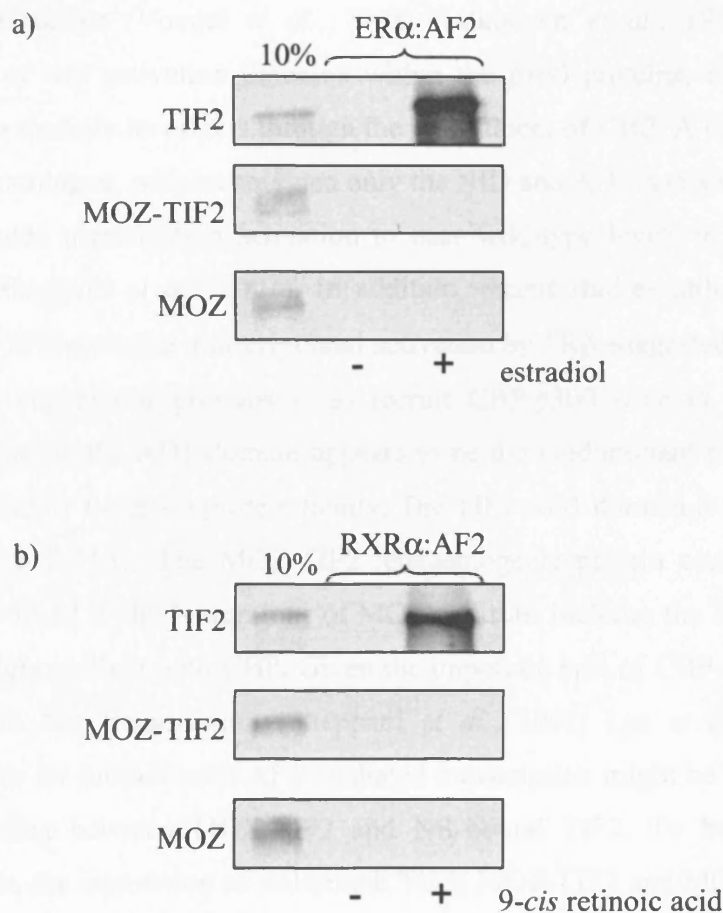


Figure 4.2: GST-pulldown experiments investigating the interaction of TIF2, MOZ-TIF2 and MOZ with the AF2 domain of ER α and RXR α .

Expression of GST-ER α :AF2 and GST-RXR α :AF2 was induced in *E.coli* DH5 α and the GST fusion proteins purified by incubation of the cell-free lysates with glutathione-conjugated beads. *In vitro* transcribed and translated TIF2, MOZ-TIF2 and MOZ were incubated with the GST-ER α :AF2 (a) and GST-RXR α :AF2 (b) -bound beads in the presence of vehicle (-) or ligand (+) as indicated. Bound proteins were separated on an 8% SDS-PAGE gel. A lane showing 10% input of the IVT protein (10%) was included to allow estimation of the percentage of radio-labelled protein bound to the GST fusions.

4.3 TIF2 and MOZ-TIF2 interact strongly with the CBP SID *in vitro*

Published studies (Voegel *et al.*, 1998; Kalkhoven *et al.*, 1998) have identified the presence of two activation domains within the p160 proteins, the first of which, AD1, appears to mediate its effects through the recruitment of CBP. A deletion mutant of SRC1, a TIF2 homologue, which contained only the NID and AD1 domains was able to potentiate NR-mediated transcription activation to near wild-type levels in a transient transfection system (Sheppard *et al.*, 2001). In addition, recent studies utilising *in vitro* chromatin assembly to investigate transcriptional activation by TR β suggested that the primary role of the p160 coactivator proteins is to recruit CBP/p300 (Lee *et al.*, 2003). Thus, CBP recruitment via the AD1 domain appears to be the predominant method of transcriptional coactivation by the p160 protein family. The TIF2 AD1 domain is encompassed within the residues 1010-1131. The MOZ-TIF2 leukaemogenic protein contains the TIF2 residues 869-1464 fused to the N-terminus of MOZ and thus includes the AD1, suggesting that the fusion might interact with CBP. Given the important role of CBP recruitment by the p160 proteins in NR transcription (Sheppard *et al.*, 2001; Lee *et al.*, 2003), one possible mechanism for inhibition of AF2-mediated transcription might be through competition for CBP binding between MOZ-TIF2 and NR-bound TIF2. To begin to investigate this hypothesis, the interaction of full-length TIF2, MOZ-TIF2 and MOZ with the CBP SRC1-Interaction-Domain (SID) (Sheppard *et al.*, 2001) was examined through GST pulldown experiments.

Expression of GST and GST-SID was induced as described (Section 2.5.19), and the GST proteins partially purified through incubation with glutathione beads (Section 2.5.20). The amount of GST protein-beads to be used in the subsequent pulldown experiments was determined by SDS-PAGE gel analysis of the GST-protein levels present. In order to keep the volume of beads equivalent between each sample, washed (non-protein-bound) beads were used. The purified GST-CBP:SID or GST alone (control) beads were incubated with the [³⁵S]-labelled *in vitro* transcribed and translated proteins described in Section 4.2 at various NaCl concentrations of NDTN buffer (Figure 4.3). At 0.2 M NaCl, TIF2, MOZ-TIF2 and MOZ all bound to the SID. However at 0.3 M NaCl, MOZ binding was lost whereas both TIF2 and MOZ-TIF2 bound with equivalent affinity to that seen at 0.2 M. A

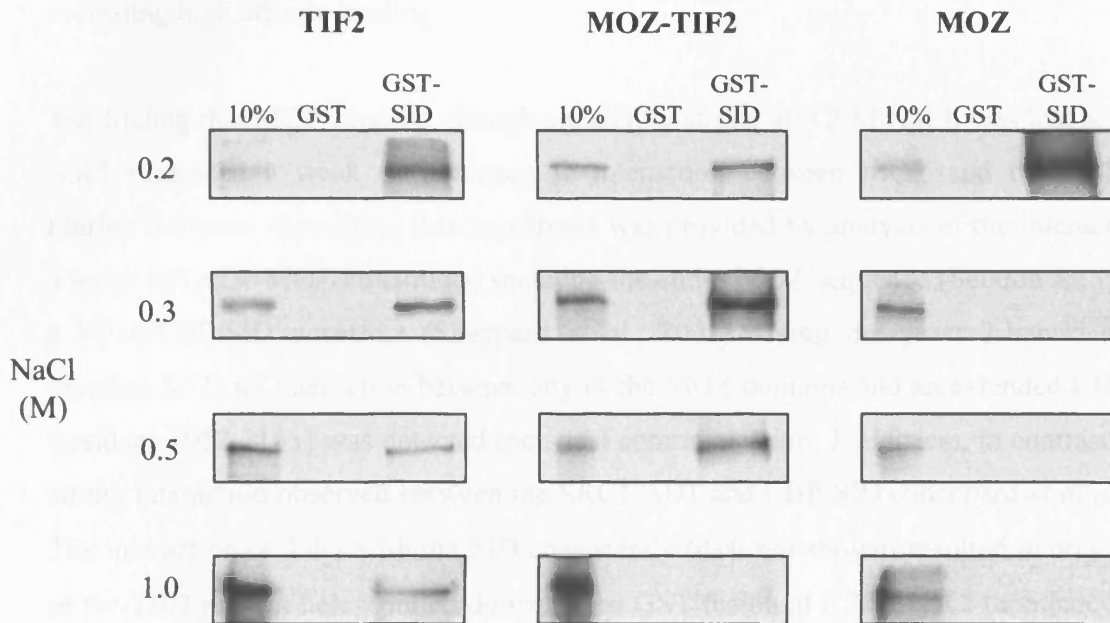


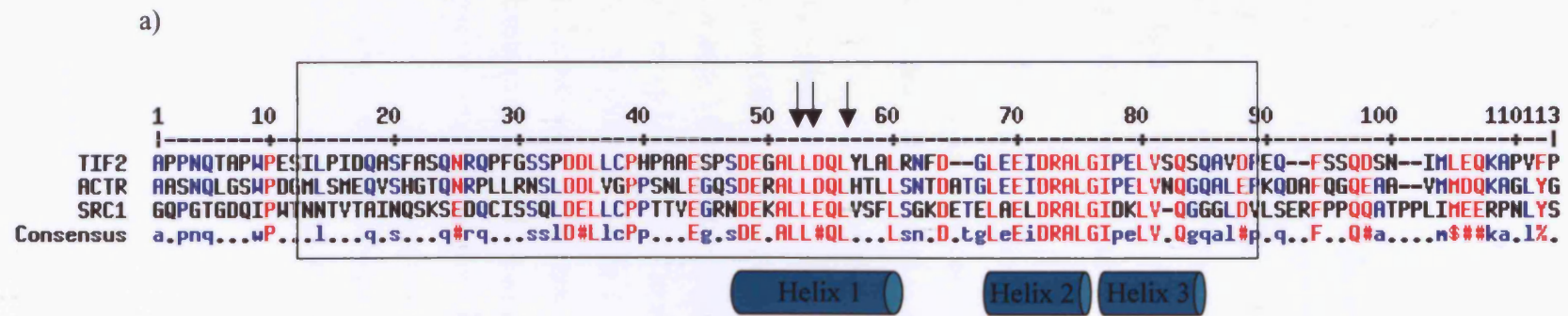
Figure 4.3: GST-pulldown experiments investigating the interaction of TIF2, MOZ-TIF2 and MOZ with the CBP SID at varying NaCl concentrations.

Expression of GST and GST-CBP:SID was induced in *E.coli* DH5 α and the GST fusion proteins purified by incubation of the cell-free lysates with glutathione-conjugated beads. *In vitro* transcribed and translated TIF2, MOZ-TIF2 and MOZ were incubated with the GST or GST-CBP:SID (GST-SID) -bound beads at varying NaCl concentrations (M). Bound proteins were separated on an 8% SDS-PAGE gel. A lane showing 10% input of the IVT protein (10%) was included to allow estimation of the percentage of radio-labelled protein bound to the GST fusions.

further increase in NaCl concentration to 0.5 M did not result in a significant decrease in the strength of TIF2 or MOZ-TIF2 binding. Even at 1.0 M NaCl, a weak interaction of TIF2 and MOZ-TIF2 with the CBP:SID was detected upon longer exposure times, indicating high affinity binding.

The finding that MOZ binding, though apparently strong at 0.2 M NaCl, was lost at 0.3 M NaCl suggested a weak or non-specific interaction between MOZ and the CBP:SID. Further evidence supporting this hypothesis was provided by analysis of the interaction of a series of LexA-MOZ constructs, spanning the entire MOZ sequence (Section 5.13), with a VP16-CBP:SID construct (Sheppard *et al.*, 2001). Using the yeast 2-hybrid system (Section 5.13) no interaction between any of the MOZ domains and an extended CBP:SID (residues 1982-2163) was detected (personal communication, J. Harries), in contrast to the strong interaction observed between the SRC1:AD1 and CBP:SID (Sheppard *et al.*, 2001). The interaction of TIF2 with the SID consistently (data not shown) resulted in only ~10% of the TIF2 protein being pulled down by the GST fusion at 0.2 M NaCl (compare bound protein lane to 10% input). However, increased NaCl concentration up to 0.5 M had no discernible effect on this. Even at 1.0 M NaCl the reduction in the percentage of TIF2 bound was small. This suggested that the interaction of TIF2 with the SID was stable, despite the relatively low percentage of TIF2 that interacted with the GST fusion at low concentrations of NaCl. The reason for this low percentage of TIF2 “pulled-down” in these experiments was unclear. However it was equivalent to that seen in the study of Voegel *et al.* (1998). The amount of MOZ-TIF2 bound by the SID was greater than that of TIF2 at NaCl concentrations less than 1.0 M but this was not the case at this highest concentration, where only a weak interaction of MOZ-TIF2 with the SID was detected. As the sequence encoding CBP interaction was identical in the two proteins the cause of the variation in binding was unclear. However, one possible explanation was that their unique N-termini resulted in differing effects of NaCl concentration on the overall structural stabilities of the IVT proteins.

In summary, TIF2 and MOZ-TIF2, but not MOZ, interact strongly with the CBP:SID *in vitro*. This suggests that one possible mechanism for the inhibition of AF2-mediated transcription is through competition for CBP binding between the leukaemogenic fusion and TIF2.



b)

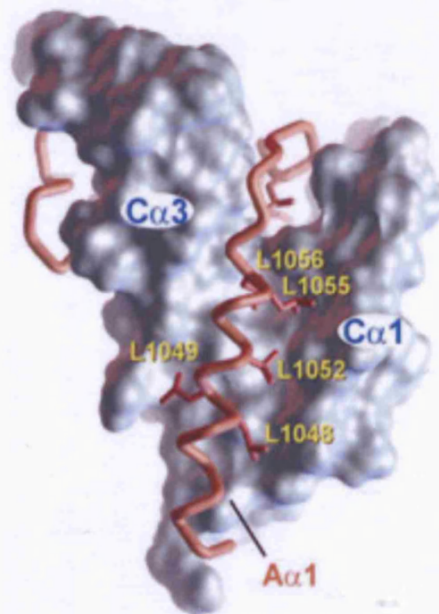


Figure 4.4: Sequence alignment of the AD1 domains from the p160 proteins and NMR structure of the CBP ACTR complex

a) An alignment (Corpet, 1988) of the AD1 domains from TIF2, SRC1 and ACTR. “%” indicates either F or Y; “#” is anyone of N, D, Q or E. Conservation level for UPPERCASE (red) letter in consensus is 90%; conservation level for lowercase (blue) letter in consensus is 50%. The three green helices indicate those present in the ACTR solution structure when in complex with CBP (Demarest *et al.*, 2002). Black box indicates the AD1 region deleted in MOZ-TIF2 Δ AD1; arrows, the leucines mutated to alanines in MOZ-TIF2mAD1. b) Solution structure of the complex of ACTR and CBP reproduced from Demarest *et al.* (2002). The backbone of ACTR (red) is shown with the side-chains of the leucine residues present in ACTR α -helix 1 (A α 1) included. The ACTR backbone is surrounded by a surface representation of CBP, thus highlighting the hydrophobic groove formed by CBP α -helices 1 (C α 1) and 3 (C α 3) in which ACTR α -helix 1 sits. Leucines L1048, L1049 and L1052 correspond to those mutated in the MOZ-TIF2mAD1 construct.

4.4 Deletion of the MOZ-TIF2 AD1

The ability of MOZ-TIF2 to interact with the CBP SID suggested that the inhibition of AF2-mediated transcription might be due to competition for CBP binding between the fusion protein and NR-bound p160 coactivators. Interaction of the p160 proteins with CBP is mediated by their AD1 domain. Therefore, to investigate the role of the MOZ-TIF2 AD1 domain in the inhibition of AF2-mediated transcription, MOZ-TIF2 Δ AD1 constructs were generated in which the sequence that encoded the AD1 was removed by recombinant PCR.

Figure 4.4a shows an alignment (Corpet, 1988) of the TIF2 residues 1028-1134, SRC1 residues 881-992 and ACTR residues 997-1107. The core CBP binding domain in SRC1 had been mapped previously to between residues 926 and 960 (Sheppard *et al.*, 2001). This corresponds to the sequence of greatest conservation between the p160 family members, and aligns to the region of ACTR utilised to determine the solution structure of the CBP:ACTR complex (Demarest *et al.*, 2002). Therefore, in order to remove the AD1 sequence from MOZ-TIF2, two complimentary primers (LE284 and LE285, Appendix A) were designed based upon the TIF2 sequence that encompassed this core region. The primers encoded the TIF2 nucleotide sequence for residues 1035-1040 immediately preceding the sequence for residues 1115-1120. This would result in the deletion of the TIF2 residues 1041-1114 (region deleted indicated by box in Figure 4.4a), which corresponded to residues 1290-1363 in MOZ-TIF2. In addition, two further primers were synthesised: the first spanned the unique *Hind*III restriction enzyme site 1.6 kb 5' of the AD1 domain, and the fourth the unique *Ssp*BI site 0.8 Kb 3' to the AD1 (LE253 and LE255 respectively, Appendix A). Recombinant PCR reactions (Section 2.4.14) were carried out to generate a 2.4 kb PCR product with *Hind*III and *Ssp*BI restriction sites at either end. This PCR fragment was digested with *Hind*III and *Ssp*BI, purified using agarose gel electrophoresis and inserted into digested pcDNA3.0PT:FLAG-MOZ-TIF2 and pcDNA3.0PT:HA-MOZ-TIF2. The resulting epitope-tagged MOZ-TIF2 AD1 deletion expression constructs (Figure 4.5b) were sequenced to confirm the deletion had been incorporated correctly and termed pcDNA3.0PT:FLAG-MOZ-TIF2 Δ AD1 and pcDNA3.0PT:HA-MOZ-TIF2 Δ AD1.

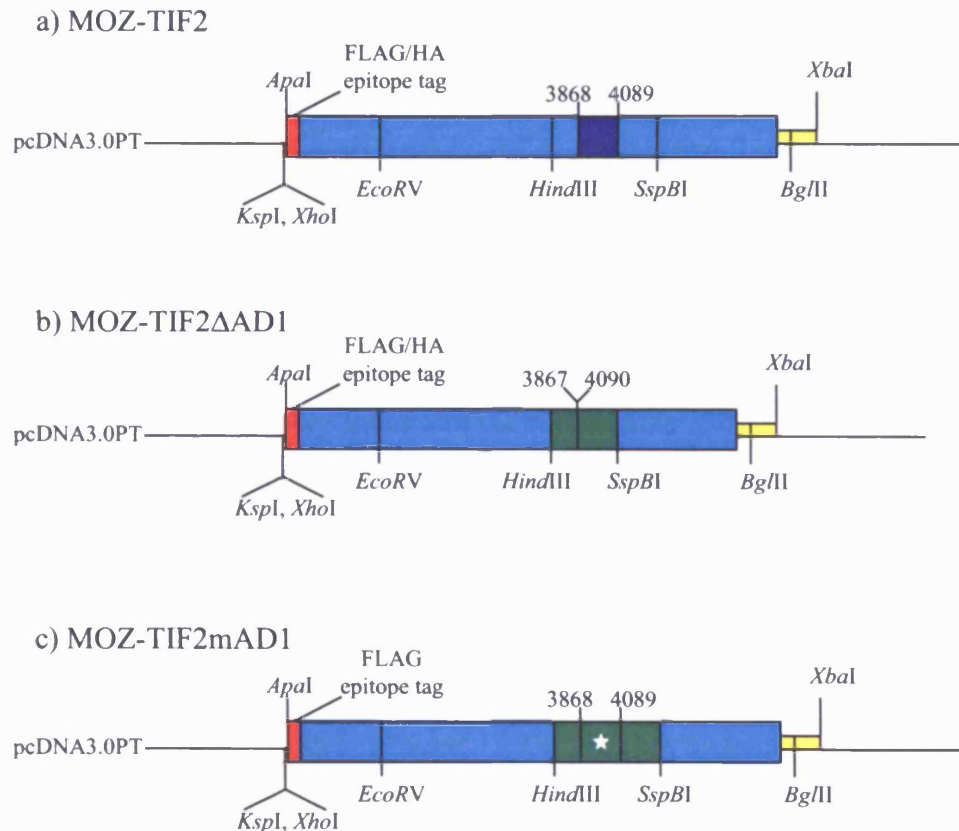


Figure 4.5: Construction of FLAG and HA epitope-tagged MOZ-TIF2 Δ AD1, and FLAG-MOZ-TIF2mAD1, in the pcDNA3.0PT mammalian expression vector.

The AD1 sequence (dark blue) in the epitope-tagged pcDNA3.0PT MOZ-TIF2 construct is shown (a). “Numbers” indicate AD1 nucleotide boundaries in the MOZ-TIF2 coding sequence (light blue); red indicates epitope tag; yellow, the 3’ untranslated region. Key restriction enzyme sites are indicated. b) The epitope-tagged MOZ-TIF2 Δ AD1 constructs were generated by insertion of a *Hind*III-*Ssp*BI recombinant PCR product into pcDNA3.0PT:FLAG-MOZ-TIF2 and pcDNA3.0PT:HA-MOZ-TIF2 constructs also digested with these enzymes. This PCR fragment contained a deletion of the MOZ-TIF2 coding sequence nucleotides 3868-4089, which corresponded to residues 1290-1363 in the MOZ-TIF2 protein sequence. c) pcDNA3.0PT:FLAG-MOZ-TIF2mAD1 was constructed by replacement of the wild-type AD1 sequence with a *Hind*III-*Ssp*BI recombinant PCR fragment in which the nucleotides corresponding to the MOZ-TIF2 leucine residues 1328, 1329 and 1332 had been mutated such that they encoded alanines (denoted by the star).

4.5 Mutation of Leucines 1328, 1329 and 1332 in MOZ-TIF2

Using GST pulldown and co-immunoprecipitation experiments, the study by Voegel *et al.* (1998) showed that mutation of the TIF2 leucine residues 1079, 1080, and 1083 resulted in a considerably weakened, though not completely abrogated, interaction between TIF2 and CBP. Therefore, in addition to the generation of a MOZ-TIF2 construct lacking the complete AD1, a construct was built with the corresponding MOZ-TIF2 residues, leucines 1328, 1329 and 1332, mutated to alanines to determine whether these mutations would result in a loss of the inhibitory activity of the fusion protein. The corresponding leucines in the p160 proteins are indicated in Figure 4.4a by arrows. Subsequent to the generation of this mutant construct, the solution structure of a complex of the ACTR AD1 and CBP SID domains was determined (Demarest *et al.*, 2002). Figure 4.4b (reproduced from Demarest *et al.* 2002, Figure 2c) shows the location of the corresponding leucine residues (L1048, L1049 and L1052) in ACTR in relation to the surface of the CBP domain. The three leucine residues in concert with L1055 and L1056 form the hydrophobic face of the ACTR α -helix 1 ($A\alpha 1$), which sits in a hydrophobic groove generated by the CBP α -helices 1 ($C\alpha 1$) and 3 ($C\alpha 3$).

In order to mutate the three leucines in MOZ-TIF2, two PCR primers were designed that spanned the residues to be mutated and incorporated the following nucleotide changes: codon 1328: ctc→gcc, codon: 1329 ctg→gcg and codon 1332 ctg→gcg (primers LE256 and LE257, Appendix A). These primers were used with those spanning the unique restriction sites *Hind*III and *Ssp*BI (LE253 and LE255, Appendix A) in the MOZ-TIF2 construct to generate a recombinant PCR product (Section 2.4.14). The amplified mutant AD1 domain was cut with *Hind*III and *Ssp*BI, purified by agarose gel electrophoresis and inserted into identically digested pcDNA3.0PT:FLAG-MOZ-TIF2 to generate the construct pcDNA3.0PT:FLAG-MOZ-TIF2mAD1 (Figure 4.5c). The successful incorporation of the nucleotide changes resulting in leucine to alanine mutations was confirmed by DNA sequencing.

4.6 Deletion of the MOZ-TIF2 AD1 results in loss of inhibition of GAL4-RAR α -mediated transcription

The GST pulldown experiments discussed previously indicated that the MOZ-TIF2 fusion protein was able to interact with the CBP SID (Figure 4.3) but not with the AF2 domain of NRs (Figure 4.2). Therefore, it seemed plausible that the dominant inhibition of NR:AF2 transcription identified in Chapter 3 (Figures 3.6 and 3.8) might be due to competition between MOZ-TIF2 and the NR-bound TIF2 for CBP binding. In order to investigate this hypothesis, transient transfection experiments were carried out to determine whether deletion of the MOZ-TIF2 AD1 (Construct pcDNA3.0PT:MOZ-TIF2 Δ AD1), or mutation of the AD1 leucine residues 1328, 1329 and 1332 to alanines (Construct pcDNA3.0PT:HA-MOZ-TIF2mAD1) was sufficient to prevent MOZ-TIF2-mediated inhibition of NR:AF2 transcription. As shown in Figure 4.6, co-transfection of HA-MOZ-TIF2 with GAL4-RAR α and TIF2 resulted in a ~2-fold reduction in reporter activity (RLA) when compared to the transfection of GAL4-RAR α and TIF2 alone. However, co-transfection of 250 or 500 ng MOZ-TIF2 Δ AD1 with GAL4-RAR α and TIF2 did not result in a reduction in the calculated reporter activity (596 and 585 -fold respectively) when compared to transfection of GAL4-RAR α + TIF2 alone (540-fold over reporters). Thus, deletion of the AD1 from the MOZ-TIF2 sequence resulted in the inability of the MOZ-TIF2 AD1 deletion protein to inhibit AF2-mediated transcription. This suggested that the inhibition by MOZ-TIF2 identified in Chapter 3 might be mediated through an interaction with CBP.

In parallel with the study of MOZ-TIF2 Δ AD1, the mutant AD1 construct MOZ-TIF2mAD1 was tested for its ability to inhibit RAR:AF2-mediated transcription (Figure 4.6). The construct contained mutations of three leucine residues (to alanines) within its AD1 that had been suggested previously (Voegel *et al.*, 1998) to play a role in the interaction of TIF2 with CBP. Transfection of 250 ng or 500 ng FLAG-MOZ-TIF2mAD1 construct with the GAL4-NR fusion and TIF2 resulted in a calculated reporter activity (235 and 291 -fold respectively) equivalent to that seen upon MOZ-TIF2 co-transfection (277-fold over reporters). Thus, the AD1 mutant HA-MOZ-TIF2 construct inhibited RAR α

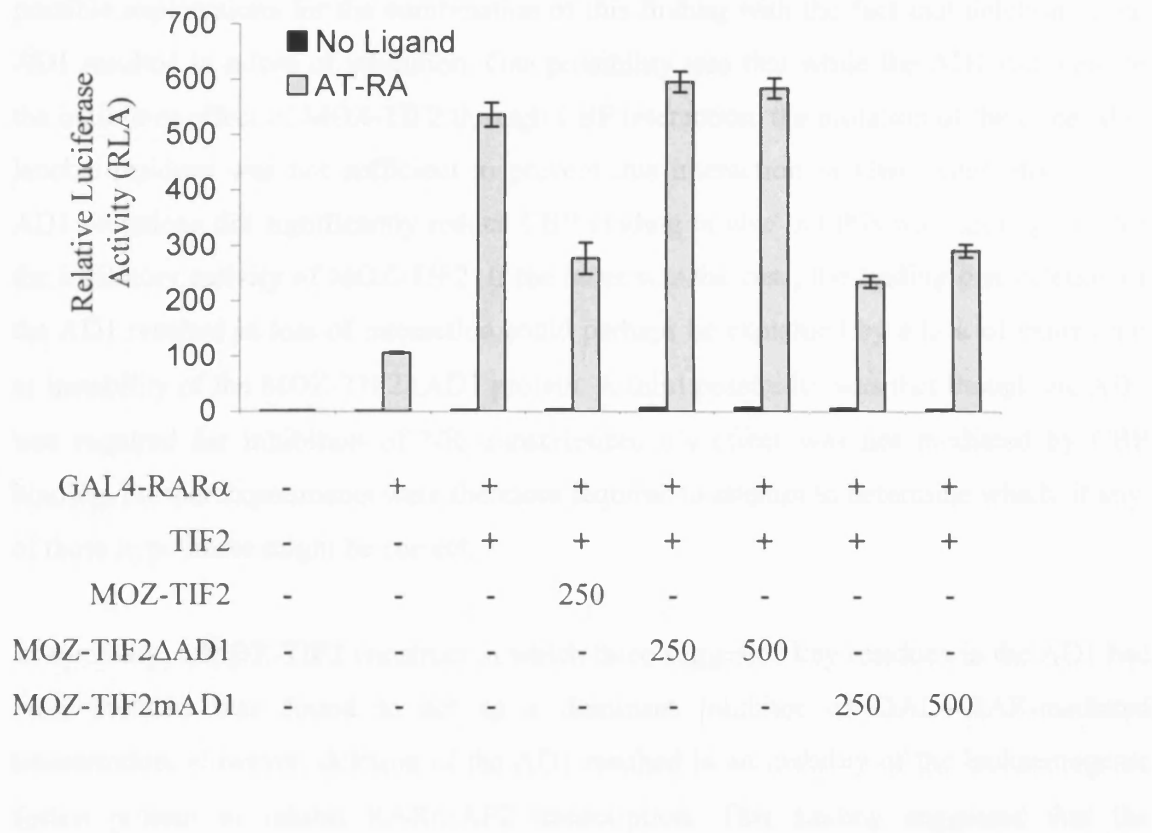


Figure 4.6: Effect of MOZ-TIF2 Δ AD1 and MOZ-TIF2mAD1 on GAL4-RAR α transcriptional activity

COS-1 cells were transfected with 500 ng p(Gal4)₅-E1b Δ -Luc luciferase reporter, 100 ng pCH110 β -galactosidase reporter and expression vectors as shown. “-” indicates no DNA transfected; “+” 100 ng DNA; “number” indicates amount of DNA in ng. The ligand all *trans* retinoic acid (AT-RA) or vehicle (No Ligand) was added as indicated 24 hr after transfection and the cells harvested following a further 24 hr incubation. The luciferase and β -galactosidase activities of each cell-free lysate were measured using a dual assay. The luciferase: β -galactosidase ratios were then calculated and plotted as Relative Luciferase Activity, with the ratio for the reporters p(Gal4)₅-E1b Δ -Luc + pCH110 (No Ligand) set to a value of 1. Error bars show the calculated S.E.M.

AF2-mediated transcription to the same extent as wild-type MOZ-TIF2. There are several possible explanations for the combination of this finding with the fact that deletion of the AD1 resulted in a loss of inhibition. One possibility was that while the AD1 did mediate the inhibitory effect of MOZ-TIF2 through CBP interaction, the mutation of the three AD1 leucine residues was not sufficient to prevent this interaction *in vivo*. Alternatively, the AD1 mutations did significantly reduce CBP binding *in vivo* but this was not required for the inhibitory activity of MOZ-TIF2. If the latter was the case, the finding that deletion of the AD1 resulted in loss of interaction could perhaps be explained by a lack of expression or instability of the MOZ-TIF2 Δ AD1 protein. A third possibility was that though the AD1 was required for inhibition of NR transcription, its effect was not mediated by CBP binding. Further experiments were therefore required to attempt to determine which, if any, of these hypotheses might be correct.

In summary, a MOZ-TIF2 construct in which three suggested key residues in the AD1 had been mutated was found to act as a dominant inhibitor of GAL4-RAR-mediated transcription. However, deletion of the AD1 resulted in an inability of the leukaemogenic fusion protein to inhibit RAR α :AF2 transcription. This finding suggested that the inhibitory activity might be due to interaction of the AD1 domain in MOZ-TIF2 with CBP, thus preventing TIF2-mediated recruitment of CBP to ligand-bound NR complexes.

4.7 Deletion of the AD1 domain from MOZ-TIF2 results in a MOZ-like subnuclear localisation

Transient transfection experiments designed to investigate the role of the MOZ-TIF2 AD1 indicated that deletion of this domain resulted in a loss of inhibition of NR:AF2 transcription (Figure 4.6). In TIF2, the role of this domain is to mediate interaction with CBP (Voegel *et al.*, 1998), suggesting that binding to this global coactivator might be the mechanism by which the MOZ-TIF2 fusion mediated its inhibitory effect. However, a construct in which residues in the AD1 implicated in the TIF2 CBP interaction had been mutated was shown to inhibit AF2-mediated transcription as efficiently as wild-type MOZ-TIF2 (Figure 4.6). One possible explanation for this difference between deletion and mutation of the MOZ-TIF2 AD1 was that the former might result in an unstable protein that did not fold correctly or was degraded rapidly. If this were the case then the MOZ-

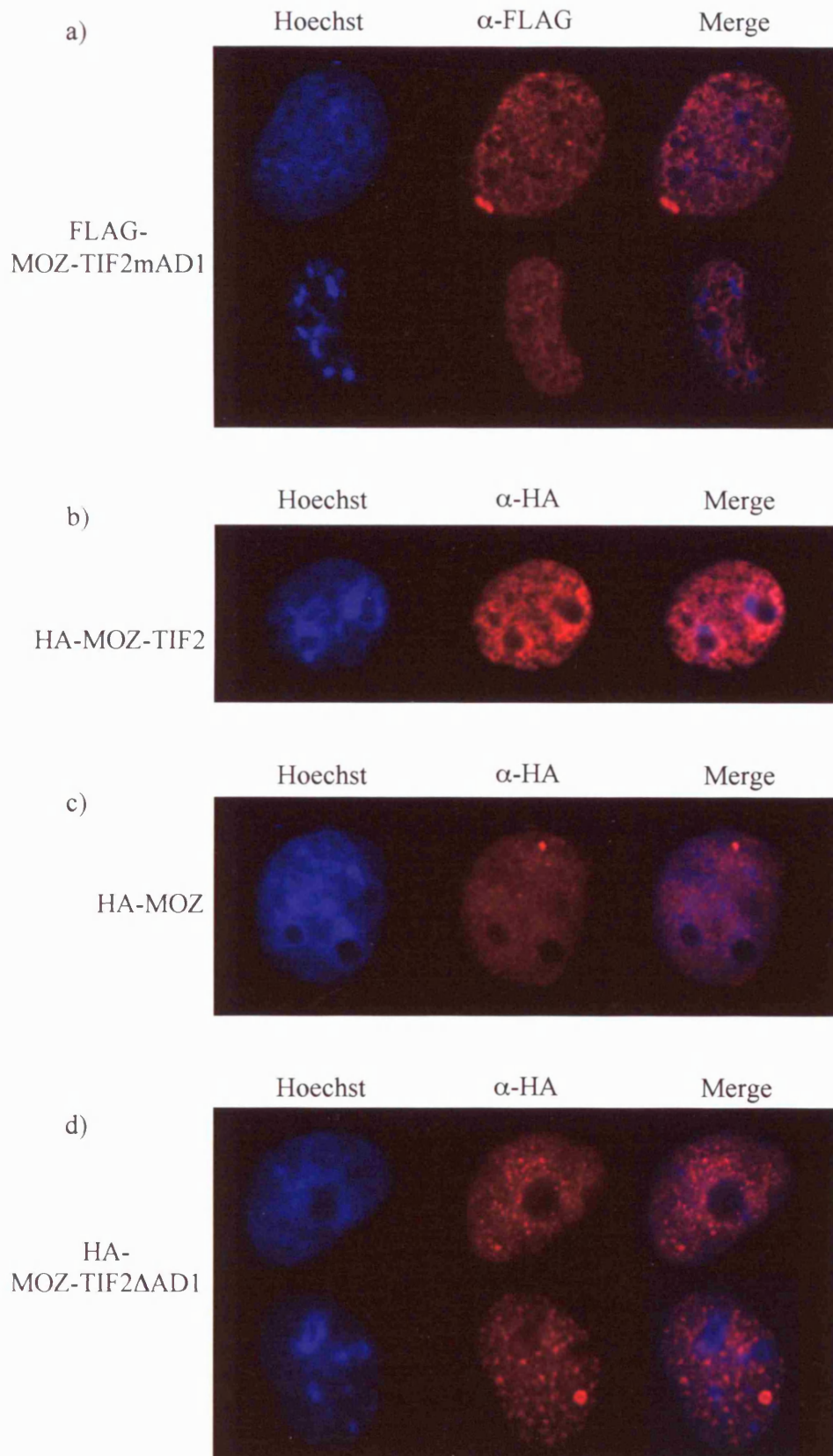
TIF2 Δ AD1 protein would not be able to inhibit NR:AF2 transcription, not because the AD1 was required for this activity, but because a functional protein was not present. Therefore, in an effort to address this, the expression and sub-cellular localisation of MOZ-TIF2 Δ AD1 and MOZ-TIF2mAD1 was investigated through immunofluorescence analysis (Figure 4.7).

COS-1 cells were transfected with 1 μ g HA-MOZ-TIF2 Δ AD1 or FLAG-MOZ-TIF2mAD1 expression construct, fixed, permeabilised, stained with Hoechst 33258 and probed with the appropriate mouse α -epitope primary and a α -mouse secondary antibody. As shown in Figure 4.8 both MOZ-TIF2mAD1 and MOZ-TIF2 Δ AD1 were expressed (red) and co-localised (Merge) with the Hoechst 33258 DNA stain (blue) indicating a nuclear localisation. However, the sub-nuclear distribution of the two mutant constructs appeared to be different from each other. MOZ-TIF2mAD1 (Figure 4.7a) formed a mesh-like pattern indistinguishable from that seen with wild-type MOZ-TIF2 (Figure 4.7b; reproduced from Figure 3.1c). In contrast, MOZ-TIF2 Δ AD1 (Figure 4.7d) did not show a characteristic MOZ-TIF2 distribution, rather appearing to localise in large numbers of variable-sized foci, in a manner indicative of full-length MOZ staining (Figure 4.7c, reproduced from Figure 3.1b). The identification of a differing sub-nuclear localisation for MOZ-TIF2 Δ AD1 compared to wild-type MOZ-TIF2 suggested that the AD1 might play a role in the altered localisation of wild-type MOZ-TIF2 compared to MOZ and TIF2. In addition, it provided a possible explanation for the fact that the deletion construct did not inhibit NR:AF2-mediated transcription. In contrast, the indistinguishable distributions of MOZ-TIF2mAD1 and MOZ-TIF2 correlated nicely with the ability of the mutant fusion protein to inhibit NR:AF2 activity.

In summary, both MOZ-TIF2mAD1 and MOZ-TIF2 Δ AD1 were expressed and localised to the nucleus. However, MOZ-TIF2 Δ AD1 displayed a sub-nuclear distribution distinct from that of MOZ-TIF2 suggesting a role of the AD1 in localisation of the fusion protein in addition to its role in the inhibition of NR:AF2-mediated transcription.

Figure 4.7: Analysis of the subcellular distribution of MOZ-TIF2mAD1 and MOZ-TIF2ΔAD1

COS-1 cells were seeded on glass coverslips in 6-well plates at 1.5×10^5 cells/well and transfected 24 hr later with 1 μ g FLAG-MOZ-TIF2mAD1, HA-MOZ-TIF2, HA-MOZ-TIF2ΔAD1 or HA-MOZ expression vector. Following a further 24 hr growth in full medium, they were fixed, permeabilised, and incubated with a mouse α -FLAG / α -HA monoclonal antibody as appropriate, followed by an α -mouse TRITC-conjugated secondary antibody and Hoechst 33258 DNA stain. After mounting the slides, protein subcellular localisations were viewed and captured using a Zeiss Axioskop2 microscope. Each image was captured sequentially in the TRITC (α -FLAG/ α -HA) and Hoechst channels and then recombined: Hoechst indicates the distribution of DNA, into which the stain intercalates; α -FLAG / α -HA shows the localisation of the expressed FLAG-tagged and HA-tagged proteins; Merge shows an overlay of the Hoechst (blue) and α -FLAG or α -HA (red) images. a) FLAG-MOZ-TIF2mAD1; b) HA-MOZ-TIF2; c) HA-MOZ; d) HA-MOZ-TIF2ΔAD1.



4.8 Construction of truncated MOZ and MOZ-AD1 expression plasmids

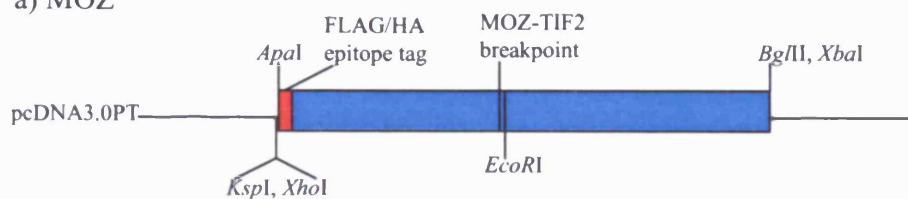
The transient transfection experiments and immunofluorescence studies described above identified the MOZ-TIF2 AD1 as a possible domain involved in both the inhibition of NR:AF2-mediated transcription and the altered localisation of the fusion compared to its parent proteins. This led to the question as to whether the presence of this domain alone fused to the N-terminus of MOZ would be sufficient to reproduce the MOZ-TIF2-mediated inhibition and distinctive sub-nuclear distribution. In order to investigate this, two constructs were built. The first, MOZ-N, was designed as a control that simulated the MOZ truncation in the leukaemogenic fusion, but without the presence of any TIF2-derived sequence. The second, MOZ-AD1, contained solely the minimal AD1 sequence of TIF2 (boxed sequence in Figure 4.4a) fused to the N-terminus of MOZ.

In order to generate a truncated MOZ construct, epitope-tagged full-length MOZ plasmids (pcDNA3.0PT:FLAG-MOZ and pcDNA3.0PT:HA-MOZ) were digested with *EcoRI* and *XbaI* (Figure 4.8a). The *EcoRI* restriction site was located at codon 1136 in MOZ, and the *XbaI* site at the 3' end of the coding sequence. Thus, digestion with these two restriction enzymes resulted in the removal of the sequence encoding residues 1137-2005. This was replaced by a multiple cloning cassette (containing sites for *NotI*, *NheI*, *BamHI*, *BglII* and an in-frame termination codon prior to the *BglII* site) constructed from two phosphorylated and annealed (Section 2.4.15) primers (Primers LE232 and LE233, Appendix A) to allow future construction of other MOZ-protein fusions (Figure 4.8b: Construct pcDNA3.0PT:epitope tag-MOZ-N). The MOZ-N constructs contain 19 additional residues at the C-terminal end of the protein compared to the truncated MOZ found in the MOZ-TIF2 fusion. However, these amino acids are located within the 690-residue MOZ acidic domain in which the breakpoint occurs. Thus, they only extend this domain slightly, which is unlikely to confer additional properties to any fusions built using this construct, although this possibility cannot be formally excluded.

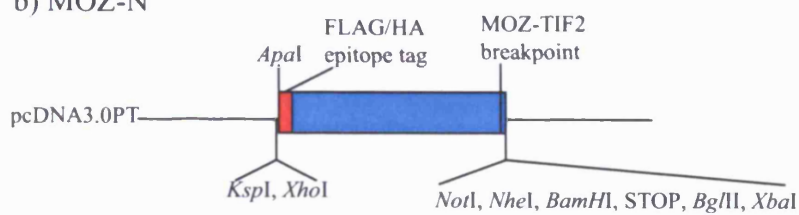
Figure 4.8: Construction of FLAG and HA epitope-tagged MOZ-N and MOZ-AD1 in the pcDNA3.0PT mammalian expression vector.

Schematics of pcDNA3.0PT constructs of epitope-tagged MOZ, MOZ-N, MOZ-AD1 and MOZ-TIF2 are shown with light blue indicating coding sequence; red, the epitope tag; yellow, untranslated regions; green, the AD1 PCR product; and dark blue the MOZ-TIF2 AD1 sequence. a) A schematic of epitope-tagged MOZ is shown with the relative positions of the MOZ-TIF2 breakpoint and *EcoRI* restriction site indicated. b) Epitope-tagged pcDNA3.0PT:MOZ-N were generated by digestion of MOZ with *EcoRI* and *XbaI* and insertion of a multiple cloning site that destroyed the *EcoRI* site and included a termination codon prior to the *BglII* restriction site. c) A PCR product encoding the AD1 sequence of MOZ-TIF2 (boundaries as indicated in d)) was inserted into MOZ digested with *EcoRI* and *XbaI* to generate epitope-tagged pcDNA3.0PT:MOZ-AD1. d) The AD1 sequence (dark blue) in epitope-tagged MOZ-TIF2 construct is shown with “numbers” indicating the AD1 nucleotide boundaries.

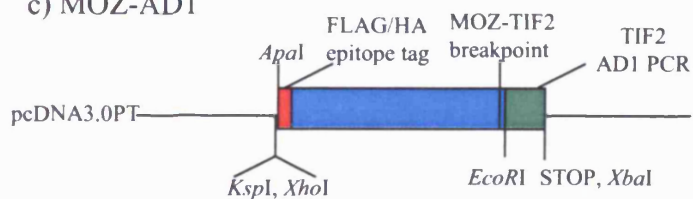
a) MOZ



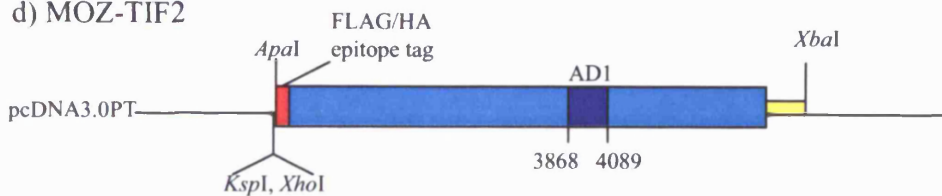
b) MOZ-N



c) MOZ-AD1



d) MOZ-TIF2



In order to construct expression vectors containing the TIF2 AD1 fused to the MOZ N-terminus, primers were designed that amplified the AD1 region (residues 1290-1363) deleted in the MOZ-TIF2 Δ AD1 construct. The boundaries for this deletion had been selected through sequence alignment of the AD1s from the three p160 coactivators (Figure 4.4) as previously described (Section 4.4). The 5' primer (Primer LE214 Appendix A) incorporated an *EcoRI* site at its 5' end and spanned residues 1290-1295 in the MOZ-TIF2 sequence. The reverse 3' primer (Primer LE215, Appendix A) incorporated a termination codon and *XbaI* site at its 5' end and spanned residues 1363-1358. The resulting PCR product was digested with *EcoRI* and *XbaI*, purified by agarose gel electrophoresis and inserted into the identically digested pcDNA3.0PT:FLAG-MOZ and pcDNA3.0PT:HA-MOZ constructs to generate epitope-tagged MOZ-AD1 constructs (Figure 4.8c). The incorporation of the correct AD1 sequence was confirmed by DNA sequencing.

4.9 Expression of a MOZ-AD1 fusion does not result in a MOZ-TIF2 -like inhibition of GAL4-RAR α -mediated transcription

Previous experiments (Figure 4.6) suggested a role for the MOZ-TIF2 AD1 in the inhibition of NR:AF2-mediated transcription by MOZ-TIF2. The construct MOZ-AD1 was therefore designed to investigate whether the presence of solely the minimal AD1 fused to the N-terminus of MOZ was sufficient to reproduce this effect. The MOZ-AD1 fusion and MOZ-N, which simulated the MOZ truncation without additional TIF2 sequence, were individually co-transfected with GAL4-RAR α and TIF2. As shown in Figure 4.9, co-expression of 250 ng MOZ-TIF2 with GAL4-RAR α and TIF2 resulted in a reduction in the Relative Luciferase Activity when compared to GAL4-RAR α + TIF2 alone (195 and 305 -fold over reporters respectively). In contrast, co-transfection of 250 ng or 500 ng MOZ-N with GAL4-RAR α and TIF2 did not result in a marked reduction in the calculated reporter activity (284 and 272 -fold over reporters respectively) compared to GAL4-RAR α + TIF2. The inclusion of 250 ng or 500 ng MOZ-AD1 fusion construct with GAL4-RAR α and TIF2 also did not result in a reduction in reporter activity (312 and 324 -fold respectively) when compared to transfection of the NR fusion and TIF2 alone.

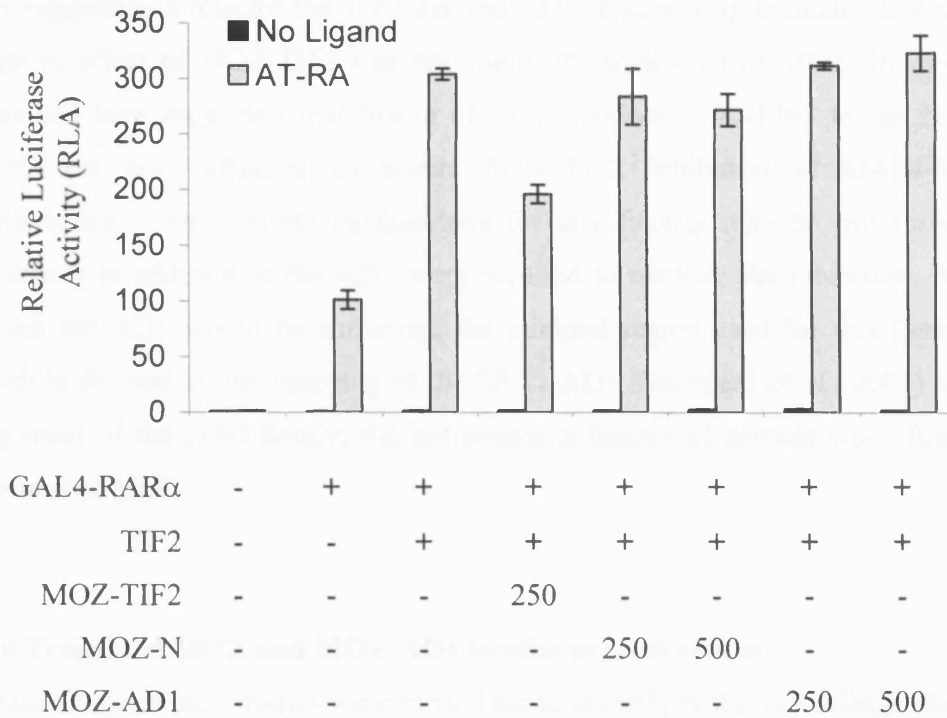


Figure 4.9: Effect of MOZ-N and MOZ-AD1 on GAL4-RAR α transcriptional activity
 COS-1 cells were transfected with 500 ng p(Gal4)₅-E1b Δ -Luc luciferase reporter, 100 ng pCH110 β -galactosidase reporter and expression vectors as shown. “-” indicates no DNA transfected; “+” 100 ng DNA; “number” indicates amount of DNA in ng. The ligand all *trans* retinoic acid (AT-RA) or vehicle (No Ligand) was added as indicated 24 hr after transfection and the cells harvested following a further 24 hr incubation. The luciferase and β -galactosidase activities of each cell-free lysate were measured using a dual assay. The luciferase: β -galactosidase ratios were then calculated and plotted as Relative Luciferase Activity, with the ratio for the reporters p(Gal4)₅-E1b Δ -Luc + pCH110 (No Ligand) set to a value of 1. Error bars show the calculated S.E.M.

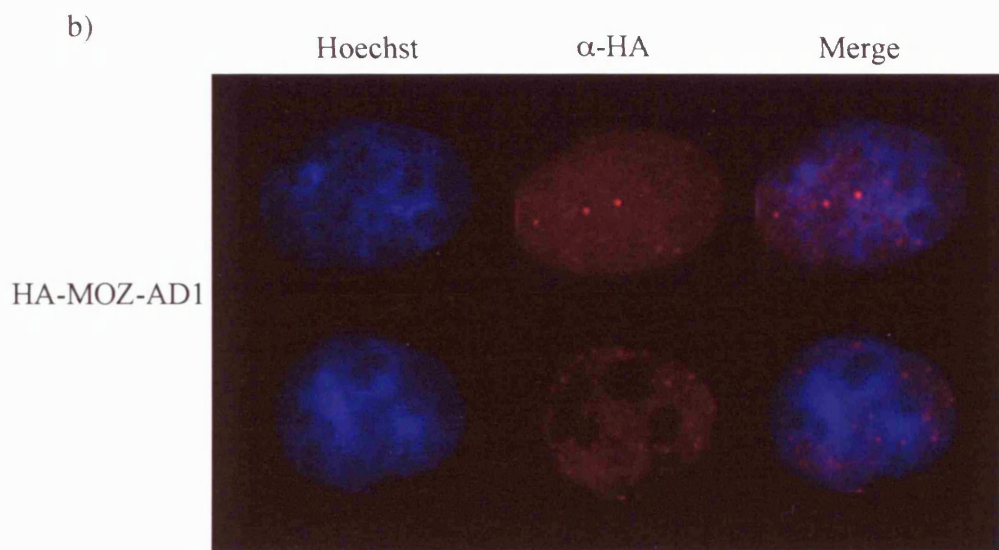
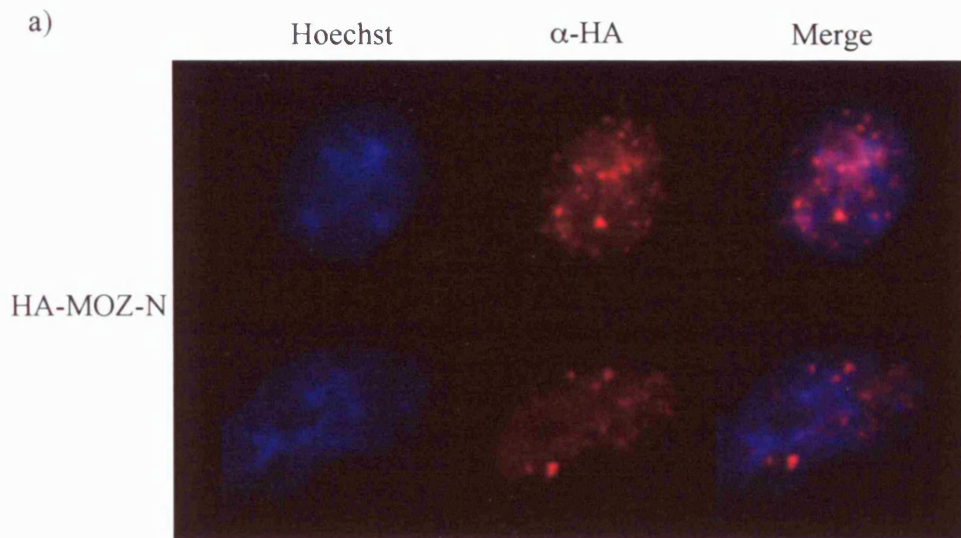
The inability of MOZ-N to inhibit NR:LBD-mediated transcription, combined with the data suggesting a role for the TIF2-derived AD1 (Figure 4.6), indicated that the dominant negative effect of MOZ-TIF2 was not due to the truncation of MOZ. However, the data described here suggested that fusion of TIF2 residues 1290-1363 to the N-terminus of MOZ was not sufficient to mimic MOZ-TIF2 inhibition of GAL4-NR-mediated transcription. Two possible explanations for this finding may be put forward. Firstly, sequences in addition to the AD1 were required to mediate the inhibition. Alternatively, though the AD1 would be sufficient, the minimal region used for this fusion construct, which is defined by the mapping of the SRC1 AD1 (Sheppard *et al.*, 2001) and sequence alignment of the p160 family, did not encode a functional domain when fused to the N-terminus of MOZ.

4.10 Truncated MOZ and MOZ-AD1 localise to nuclear foci

Immunofluorescence studies were carried out to investigate the sub-cellular distributions of the truncated MOZ construct, MOZ-N, and the fusion protein comprised of the TIF2 AD1 fused to the N-terminus of MOZ, MOZ-AD1. COS-1 cells were transfected with 1 µg HA-MOZ-N or HA-MOZ-AD1 and fixed after a 48 hr incubation. Following permeabilisation, staining with Hoechst 33258 and incubation with a mouse α -HA antibody and α -mouse TRITC-conjugated secondary, the cells were viewed using a Zeiss Axioskop2 microscope. As shown in Figure 4.10, both MOZ-N (a) and MOZ-AD1 (b) were expressed, and localised to the nucleus in large numbers of discrete foci. These structures appeared identical to those seen upon full-length MOZ transfection (Figure 4.10c, reproduced from Figure 3.1b), suggesting that a region present in the N-terminus of MOZ mediates its recruitment to these foci. The presence of MOZ-AD1 in MOZ-like foci indicated that the fusion of the AD1 domain to the N-terminus of MOZ was not sufficient to reproduce the altered localisation of MOZ-TIF2. In addition, it showed that MOZ-AD1 was expressed and thus, in combination with transient transfection experiments (Figure 4.9) described above, suggested that the AD1 residues included in the fusion were not sufficient to mediate the dominant inhibition of NR:AF2 transcription seen with MOZ-TIF2.

Figure 4.10: Analysis of the subcellular distribution of MOZ-N and MOZ-AD1

COS-1 cells were seeded on glass coverslips in 6-well plates at 1.5×10^5 cells/well and transfected 24 hr later with 1 μg HA-MOZ-N or HA-MOZ-AD1 expression vector. Following a further 24 hr growth in full medium, they were fixed, permeabilised, and incubated with a mouse α -HA monoclonal antibody, followed by an α -mouse TRITC-conjugated secondary antibody and Hoechst 33258 DNA stain. After mounting the slides, protein subcellular localisations were viewed and captured using a Zeiss Axioskop2 microscope. Each image was captured sequentially in the TRITC (α -HA) and Hoechst channels and then recombined: Hoechst indicates the distribution of DNA, into which the stain intercalates; α -HA shows the localisation of the expressed HA-tagged proteins; Merge shows an overlay of the Hoechst (blue) and α -HA (red) images. Two different images are shown for each of the epitope-tagged protein: a) HA-MOZ-N and b) HA-MOZ-AD1.



4.11 Statistical analysis of the inhibition of GAL4-RAR α by MOZ, MOZ-TIF2 and derivatives

In order to determine whether expression of MOZ-TIF2, MOZ-TIF2 Δ AD1, MOZ-TIF2mAD1, MOZ, MOZ-N or MOZ-AD1 resulted in a significant inhibition of GAL4-RAR α -mediated TIF2-enhanced transcription, a univariate ANalysis Of VAriance (ANOVA) was carried out (Brace *et al.*, 2003) using data from ≥ 3 independent experiments for each construct (Appendix 2.2.3). This analysis indicated that there was a highly significant effect of expression of ≥ 1 of the constructs: $F_{6,93} = 31.285$, $p < 0.001$ (Appendix 2.2.3). Therefore, to identify the constructs whose co-expression resulted in a statistically significant reduction in RLA when compared to GAL4-RAR α + TIF2 alone, a *post-hoc* Bonferroni analysis (Brace *et al.*, 2003) was carried out (Appendix 2.3). Significant differences (Appendix A2.3) were shown to occur upon co-expression of both MOZ-TIF2 ($p < 0.001$) and MOZ-TIF2mAD1 ($p < 0.001$) with GAL4-RAR α and TIF2. In contrast, no significant effect of MOZ-TIF2 Δ AD1 ($p = 0.329$), MOZ ($p = 1.0$), MOZ-N ($p = 0.294$) or MOZ-AD1 ($p = 1.0$) co-expression was identified.

4.12 Deletion of the MOZ-TIF2 AD1 abolishes *in vitro* binding to the CBP SID

Experiments described previously (Section 4.6) showed that transfection of a MOZ-TIF2 construct in which the AD1 domain had been deleted did not result in inhibition of GAL4-RAR α -mediated transcription, suggesting that this domain was required for the inhibitory effects of MOZ-TIF2. The TIF2-derived AD1 mediates interaction of TIF2 with CBP (Voegel *et al.*, 1998) and thus was postulated to be the domain responsible for the MOZ-TIF2 interaction with the CBP SID identified in Figure 4.3. In order to confirm that it was indeed the AD1 domain that mediated this interaction, and not a region of MOZ present in the fusion, MOZ-TIF2 Δ AD1 and MOZ-N were *in vitro* transcribed and translated (Figure 4.11) and used in GST pulldown experiments carried out at 0.3 M NaCl with the GST-CBP:SID fusion (Figure 4.12). MOZ-TIF2 was also *in vitro* translated and used in the pulldown experiments to act as a positive control.

As shown in Figure 4.11a, the IVT MOZ-TIF2 Δ AD1 protein ran slightly faster than full-length MOZ-TIF2. Estimation of protein size (Stothard, 2000) indicated that the deletion protein was 8 kDa smaller than full-length MOZ-TIF2 due to the removal of the AD1. Thus, the small difference evident on the SDS-PAGE gel was consistent with the expected reduction in size due to the deletion of the AD1, suggesting correct translation of the MOZ-TIF2 Δ AD1 protein. MOZ-N, which corresponds to residues 1-1136 of MOZ, *in vitro* transcribed and translated to give a protein that ran at the same speed as the 166 kDa band in the Roche protein marker (Figure 4.11b). This truncated protein had a predicted size of 132 kDa (Stothard, 2000) and thus, as with the MOZ and MOZ-TIF2 IVT proteins (Figure 4.1), appeared to run at a greater molecular weight than expected. However, as sequence analysis had confirmed the correct construction of each MOZ and MOZ-TIF2 plasmid generated, these discrepancies were more likely due to the effect of the amino acid sequence on mobility in the SDS-PAGE gel, rather than any problem with the construct.

The [³⁵S]-methionine labelled proteins were incubated with both glutathione bead-bound GST and GST-CBP:SID and interacting proteins run on an SDS-PAGE gel. As seen previously (Figure 4.3), MOZ-TIF2 selectively bound the GST-CBP:SID beads indicating an interaction with the SID (Figure 4.12). In contrast, neither MOZ-TIF2 Δ AD1 nor MOZ-N bound the GST-CBP:SID or GST itself. This suggested that the MOZ-TIF2 interaction with the CBP:SID was not mediated by the N-terminus of MOZ, but was due to the presence of the TIF2-derived AD1. This correlated with the finding of Voegel *et al.* (1998) that the interaction of TIF2 with CBP is dependent upon the AD1. In addition, it gave credence to the hypothesis that the AD1-dependent dominant inhibition of NR:AF2-mediated transcription by MOZ-TIF2 might be due to the interaction of the fusion protein with CBP.

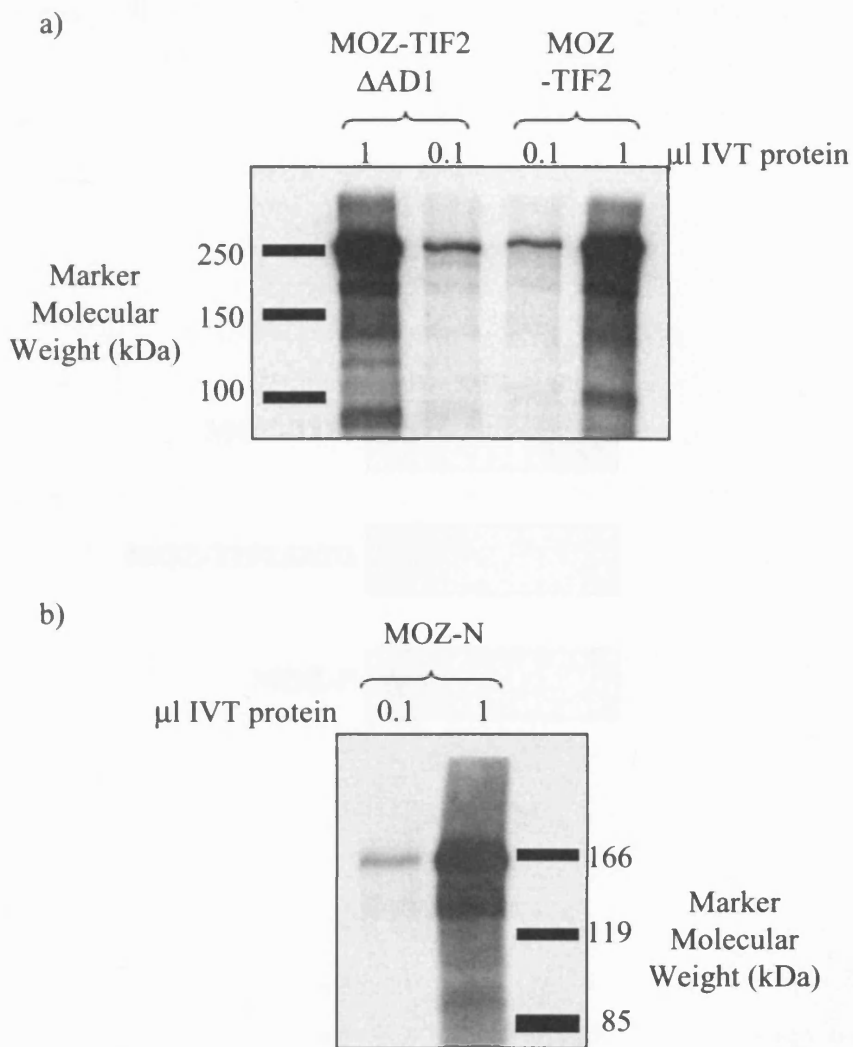


Figure 4.11: SDS-PAGE gels showing [³⁵S]-labelled *in vitro* transcribed and translated MOZ-TIF2ΔAD1, MOZ-TIF2 and MOZ-N.

pcDNA3.0PT:HA-MOZ-TIF2ΔAD1 and pcDNA3.0PT:HA-MOZ-TIF2 (a), and pcDNA3.0PT:MOZ-N (b), were *in vitro* transcribed and translated in the presence of [³⁵S]-methionine to give full-length radio-labelled proteins. 0.1 μl and 1 μl of each IVT was run on an 8% SDS-PAGE gel to allow an accurate determination of the size of the predominant protein species synthesised. The sizes of the Molecular Weight Marker (non-radio-labelled) bands are shown.

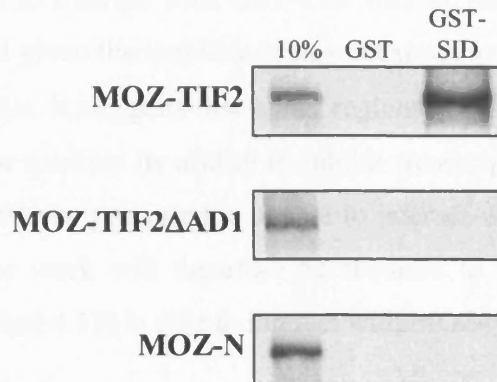


Figure 4.12: GST-pulldown experiments investigating the interaction of MOZ-TIF2, MOZ-TIF2 Δ AD1 and MOZ-N with the CBP SID at 300mM NaCl.

Expression of GST and GST-CBP:SID was induced in *E.coli* DH5 α and the GST fusion proteins purified by incubation of the cell-free lysates with glutathione-conjugated beads. *In vitro* transcribed and translated MOZ-TIF2, MOZ-TIF2 Δ AD1 and MOZ-N were incubated with the GST or GST-CBP:SID (GST-SID) -bound beads at 0.3 M NaCl. Bound proteins were separated on an 8% SDS-PAGE gel. A lane showing 10% input of the IVT protein (10%) was included to allow estimation of the percentage of radio-labelled protein bound to the GST fusions.

During the preparation of this thesis, MOZ-TIF2mAD1 and MOZ-AD1 were analysed for binding to the SID domain of CBP using GST pulldown experiments (personal communication; S. Matsuda & D. Heery). *In vitro* translated MOZ-TIF2mAD1 was found to interact with the GST-CBP:SID protein suggesting that mutation of the three leucine residues was not sufficient to prevent SID binding. This finding correlated with the ability of MOZ-TIF2mAD1 to inhibit AF2-mediated transcription. The MOZ-AD1 fusion protein was also found to interact with GST-CBP:SID *in vitro*, though only weakly. This result was unexpected given the inability of this construct to inhibit the transcriptional activity of the GAL4-RAR α . It suggests that either regions of MOZ-TIF2 in addition to the AD1 are also required to mediate its ability to inhibit transcription activation, or that the minimal MOZ-AD1 construct generated is unable to interact with full-length CBP when expressed *in vivo*. Further work will therefore be required to determine whether full-length CBP (Sections 4.12 and 4.13) is able to interact with MOZ-AD1 *in vitro* and *in vivo*.

4.13 TIF2 and MOZ-TIF2 interact with full length CBP *in vitro*

Pulldown experiments using the CBP SRC1 Interaction Domain (SID) showed a strong *in vitro* interaction with TIF2 and MOZ-TIF2, but not MOZ (Figure 4.3). This MOZ-TIF2 SID interaction was dependent upon on the TIF2-derived AD1, the deletion of which resulted in a loss of binding *in vitro* (Figure 4.12). Transient transfection experiments utilising GAL4-NR fusions suggested that the inhibition of AF2-mediated transcription by MOZ-TIF2 was also dependent on the presence of the AD1 in the fusion (Figure 4.6), and thus, by inference, dependent upon the interaction of the leukaemogenic protein with CBP. However, the work by Kitabayashi *et al.* (2001) identified the presence of both MOZ and CBP in an AML1 complex, though the study did not investigate whether the two HAT proteins interacted directly. This raised the possibility that MOZ might interact with full-length CBP through a domain other than the GST:SID. If this were true, and the region was present in the N-terminus of MOZ, it would allow MOZ-TIF2 to bind full-length CBP through a second site in addition to the AD1, thus reducing the likelihood that the role of the AD1 in inhibition of NR:AF2 transcription was to mediate CBP interaction. Therefore, to determine whether MOZ and MOZ-TIF2 were able to bind to full-length CBP, GST pulldown experiments were carried out using a GST fusion to full-length CBP.

Expression of GST and the GST-CBP full-length construct (gift from Dr. A Harel-Bellan, Centre National de la Recherche Scientifique, Villejuif, France) was induced in *E.coli* DH5 α and the proteins purified from the bacterial extract (Section 2.5.20). However, the purified GST-CBP protein was not visible on Coomassie-stained SDS-PAGE gels (data not shown) suggesting a very low level of expression. This was not unexpected given the large size of the fusion (predicted Mr: 292 kDa; (Stothard, 2000)) as *E.coli* only have two ORFs that encode >200 kDa proteins and do not express endogenous proteins of >250 kDa (Medigue *et al.*, 1993). In spite of the very low level of GST-CBP protein expressed, pulldown experiments were attempted at 0.2 M NaCl with the bacterial extract-incubated glutathione beads to determine whether any interaction with MOZ, MOZ-TIF2 or their derivatives could be detected.

As shown in Figure 4.13, TIF2 and MOZ-TIF2 selectively bound beads incubated with the bacterial cell extract in which GST-CBP expression had been induced. In contrast, MOZ and MOZ-N did not interact with the incubated glutathione beads. Given the presence of the GST-tag at the N-terminus of the GST-CBP fusion protein, and the location of the SID (to which TIF2 and MOZ-TIF2 bound) near the C-terminus, it seemed likely that a near full-length GST-CBP protein had been induced and was bound to the glutathione-conjugated beads. This suggested therefore that either MOZ did not interact with full-length CBP directly, or that any such interaction was too weak to detect using this system.

Deletion of the AD1 domain from MOZ-TIF2 (MOZ-TIF2 Δ AD1) resulted in a loss of binding to the GST-CBP full-length fusion indicating that this domain was required for interaction of the leukaemogenic protein with CBP. This data was in accordance with the finding that the N-terminus of MOZ was unable to interact with CBP under these conditions, and with the work by Voegel *et al.* (1998) and Kalkhoven *et al.* (1998) identifying the AD1 as the only region of TIF2 / SRC1 that interacted with CBP. It also supports the hypothesis that the inhibition of NR:AF2 transcription by MOZ-TIF2 might be mediated through the interaction of the AD1 with full-length CBP.

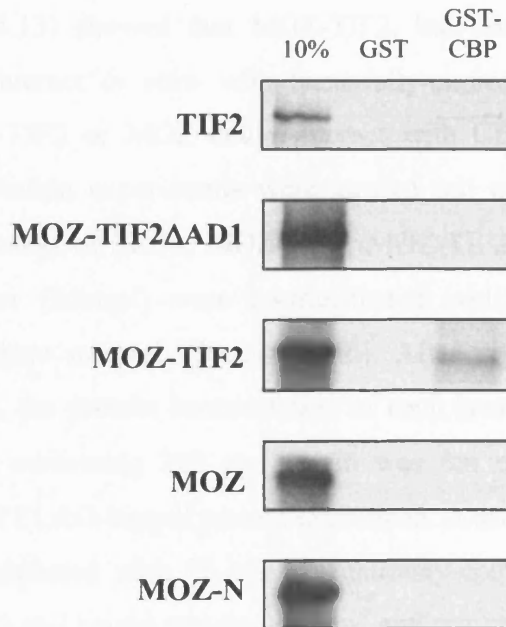


Figure 4.13: GST-pulldown experiments investigating the interaction of TIF2, MOZ-TIF2ΔAD1, MOZ-TIF2, MOZ and MOZ-N with a GST-CBP fusion.

Expression of GST and GST-CBP full-length was induced in *E.coli* DH5α and the GST fusion proteins purified by incubation of the cell-free lysates with glutathione-conjugated beads. *In vitro* transcribed and translated TIF2, MOZ-TIF2ΔAD1, MOZ-TIF2, MOZ and MOZ-N were incubated with the GST or GST-CBP -bound beads at 0.2 M NaCl. Bound proteins were separated on an 8% SDS-PAGE gel. A lane showing 10% input of the IVT protein (10%) was included to allow estimation of the percentage of radio-labelled protein bound to the GST fusions.

4.14 MOZ-TIF2, but not MOZ-TIF2 Δ AD1, binds CBP in co-immunoprecipitation experiments

GST pulldown experiments with both the CBP:SID (Figures 4.3 and 4.12) and full-length CBP (Figure 4.13) showed that MOZ-TIF2, but not MOZ-TIF2 Δ AD1 nor full-length MOZ, could interact *in vitro* with bacterially-expressed CBP. In order to investigate whether MOZ-TIF2 or MOZ could interact with CBP in mammalian cell lysates, co-immunoprecipitation experiments were carried out using HEK293 cells. FLAG-tagged pcDNA3 constructs of SRC1, MOZ-TIF2, MOZ-TIF2 Δ AD1, MOZ or MOZ-N or empty pcDNA3 vector (control) were co-transfected with pSG5-CBP full-length using the calcium phosphate method (Section 2.2.6). After preparation of the whole cell lysate (Section 2.5.9), the protein concentration of each lysate was determined (Section 2.5.11) and a volume containing 300 μ g protein was run on a 8% SDS-PAGE gel to allow confirmation of FLAG-tagged protein expression. A second lysate volume containing 5 mg protein was incubated with FLAG M2 antibody-conjugated sepharose beads overnight (Section 2.5.10) and bound proteins isolated and run on a 6% SDS-PAGE gel to detect co-immunoprecipitated proteins.

The proteins separated in the SDS-PAGE gels were transferred to nitrocellulose membranes (Section 2.5.15) and probed for the presence of FLAG-tagged proteins (8% gel) and full-length CBP (6% gel) (Section 2.5.16). As shown in Figure 4.14, FLAG-MOZ appeared to be expressed at a very high level compared to the other FLAG-tagged proteins. Expression of MOZ-TIF2, MOZ-TIF2 Δ AD1 and MOZ-N was low, though they were comparable with each other. However, FLAG-SRC1 was not detected in this experiment, though the presence of both HA-GRIP1 (data not shown) and FLAG-SRC1 (personal communication, K. Kindle) was shown by western blotting in other experiments. The identification of immunoprecipitated MOZ-TIF2 Δ AD1, in conjunction with the evidence for expression from the immunofluorescence studies (Figure 4.7) suggested the lack of inhibition of NR:AF2 transcription by MOZ-TIF2 Δ AD1 (Figure 4.6) was not due to a lack of expressed or soluble protein. Thus, it appeared likely that the inability of the MOZ-TIF2 deletion protein to inhibit NR transcription was due to the removal of the AD1.

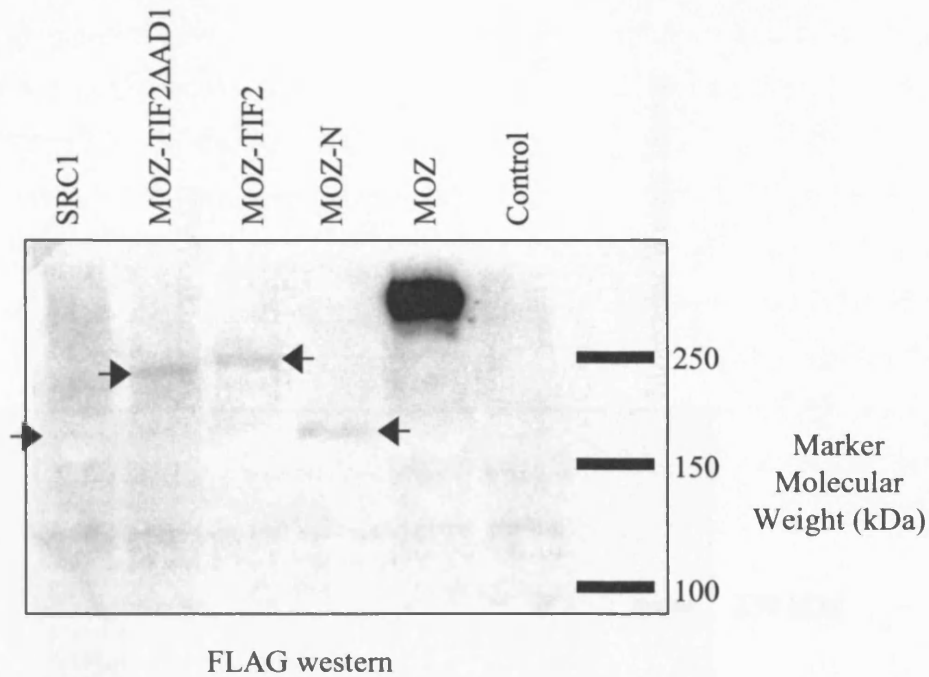


Figure 4.14: Western blot for expression of FLAG-tagged SRC1, MOZ-TIF2ΔAD1, MOZ-TIF2, MOZ-N and MOZ in transfected HEK293 cells.

HEK293 cells were co-transfected with pSG5-CBP and either a FLAG-tagged expression construct (SRC1, MOZ-TIF2ΔAD1, MOZ-TIF2, MOZ-N or MOZ) or empty pcDNA3.0PT vector (Control). Cells were harvested 48 hr after transfection and a cell-free lysate prepared. 300 μ g protein was run on an 8% SDS-PAGE gel and then transferred to a nitrocellulose membrane. Following blocking, the membrane was incubated with an HRP-conjugated α -FLAG antibody and protein:antibody immunocomplexes detected using chemiluminescence.

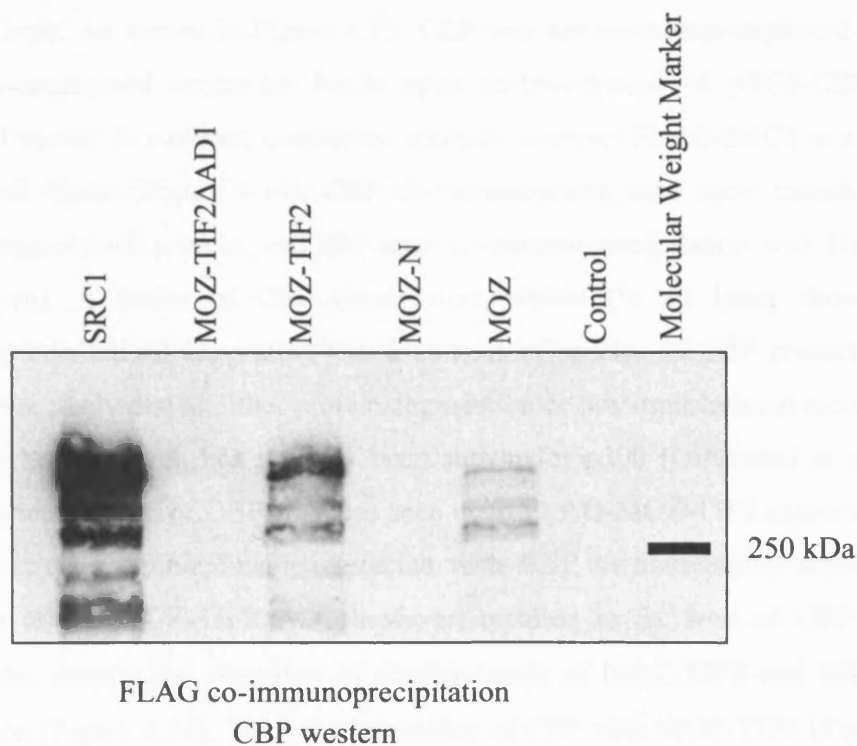


Figure 4.15: Western blot for presence of CBP after immunoprecipitation of FLAG-tagged SRC1, MOZ-TIF2ΔAD1, MOZ-TIF2, MOZ-N and MOZ in transfected HEK293 cells.

HEK293 cells were co-transfected with pSG5-CBP and either a FLAG-tagged expression construct (SRC1, MOZ-TIF2ΔAD1, MOZ-TIF2, MOZ-N or MOZ) or empty pcDNA3.0PT vector (Control). Cells were harvested 48 hr after transfection and a cell-free lysate prepared. A volume containing 5 mg protein was incubated overnight with bead-conjugated α -FLAG antibody. Bound proteins were run on a 6% SDS-PAGE gel and transferred to a nitrocellulose membrane. Following blocking, the membrane was incubated with a rabbit α -CBP (A-22, C-20) antibody mix and an HRP-conjugated α -rabbit antibody. Protein:antibody immunocomplexes were detected using chemiluminescence.

Analysis of CBP interaction with the FLAG-tagged proteins through co-immunoprecipitation was carried out using a mix of the CBP antibodies A-22 and C-20 (Santa Cruz). As shown in Figure 4.15, CBP was not immunoprecipitated by FLAG M2 antibody-conjugated sepharose beads upon co-transfection of pSG5-CBP with empty pcDNA3 vector. In contrast, despite the inability to detect FLAG-SRC1 in a western of the whole cell lysate (Figure 4.14), CBP co-immunoprecipitated upon transfection with the FLAG-tagged p160 protein, and also upon co-immunoprecipitation with HA-GRIP1 (data not shown). A series of CBP bands were visible (in all lanes showing CBP co-immunoprecipitation) suggesting that a number of species of CBP protein were present. These were likely due to either protein degradation or post-translational modifications such as sumoylation, which has recently been shown for p300 (Girdwood *et al.*, 2003). Co-immunoprecipitation of CBP was also seen upon FLAG-MOZ-TIF2 expression, indicating that the leukaemogenic fusion interacted with CBP in mammalian whole cell lysates. Deletion of the MOZ-TIF2 AD1 however, resulted in the loss of CBP bands on the membrane, despite the detection of similar levels of MOZ-TIF2 and MOZ-TIF2 Δ AD1 expression (Figure 4.14). Thus, the interaction of CBP with MOZ-TIF2 in mammalian cell extracts appeared to be mediated by the MOZ-TIF2 AD1.

The presence of immunoprecipitated CBP in the FLAG-MOZ lane was also noted (Figure 4.15). The co-immunoprecipitation of CBP by MOZ was clearly less than that seen with either SRC1 or MOZ-TIF2. Thus, given the much higher level of expression of MOZ in the cell lysate (Figure 4.14), this “interaction” did not appear to be very strong in comparison with that of the p160 protein and MOZ-TIF2. One explanation for this weak interaction was suggested by the work of Kitabayashi *et al.* (2001), who identified the presence of both MOZ and CBP in an AML1 complex. Thus, the co-immunoprecipitation of CBP by full-length MOZ might not have been due to a direct interaction of the two proteins, but rather be due to the immunoprecipitation of a MOZ complex that also contained CBP. No immunoprecipitation of CBP was visible upon FLAG-MOZ-N transfection (Figure 4.15). This truncated MOZ construct was expressed at a much lower level than full-length MOZ, though comparable to MOZ-TIF2 and MOZ-TIF2 Δ AD1 (Figure 4.14). Two plausible explanations thus arise for the difference in CBP co-immunoprecipitation by MOZ and MOZ-N. Firstly, the hypothesised indirect MOZ interaction with CBP might not have been mediated through the N-terminus of MOZ, and

therefore not be relevant to MOZ-TIF2. Alternatively, the MOZ N-terminus might mediate (either directly or indirectly) CBP interaction but too weakly for a detectable level of CBP to be immunoprecipitated by the low level of expressed MOZ-N protein. However, given the equivalent level of expression of MOZ-N and MOZ-TIF2 and yet the significantly different amounts of CBP co-immunoprecipitated, any weak “interaction” between CBP and the MOZ sequence in MOZ-TIF2 would be completely out-weighted by the strong AD1-mediated interaction with CBP.

In summary, this data indicates that MOZ-TIF2, but not MOZ nor a MOZ-TIF2 AD1 deletion construct, bound full-length CBP in cell-free mammalian lysates.

4.15 TIF2, but not MOZ, partially co-localises with CBP speckles

The GST pulldown and co-immunoprecipitation experiments described previously showed that TIF2 interacted strongly with full-length CBP *in vitro* (Figure 4.13) and that SRC1 (Figure 4.15) and GRIP1 (data not shown), interacted with CBP in cell-free lysates. In contrast, interaction of MOZ with full-length CBP was not seen *in vitro* using GST pulldown experiments (Figure 4.13), and only a weak interaction was detected by co-immunoprecipitation of cell free lysates (Figure 4.15). *In vivo*, CBP has been shown to localise to discrete speckles termed PML bodies (also termed PODs or ND-10s) (Doucas *et al.*, 1999; Boisvert *et al.*, 2001), and GRIP1 partially co-localises with these CBP-containing bodies when over-expressed (Baumann *et al.*, 2001). Therefore, to confirm this partial co-localisation, and to determine whether the MOZ speckles co-localised with CBP, immunofluorescence analysis of endogenous CBP distribution was carried out in cells expressing GRIP1 or MOZ.

In both untreated and mock-transfected COS-1 cells endogenous CBP (red) was localised to a small number of discrete nuclear foci (Figure 4.16a α -CBP). These foci were identified as PML bodies by co-staining for endogenous PML (personal communication, K. Kindle). Transfection of 1 μ g HA-GRIP1 expression plasmid resulted in the accumulation of GRIP1 in a large number of nuclear speckles (Figure 4.16b α -HA). Co-staining of these cells with α -CBP antibodies (Figure 4.16b) showed that some of these GRIP1 foci partially co-localised with the CBP-containing PML bodies as indicated by the

white arrows (Figure 4.16b Merge). This finding was in accordance with that of Baumman *et al.* (2001), who showed both adjacency and partial co-localisation of exogenous GRIP1 and endogenous CBP speckles. As with GRIP1, transfection of MOZ resulted in the accumulation of the exogenous protein in a large number of foci (Figure 4.16c α -HA). However, no co-localisation was seen between these speckles and those containing CBP (Figure 4.16c Merge) suggesting MOZ and CBP localise to discrete bodies within the nucleus. Thus, though both exogenous GRIP1/TIF2 and MOZ accumulated in a large numbers of speckles, only GRIP1/TIF2 partially co-localised with CBP-containing PML bodies.

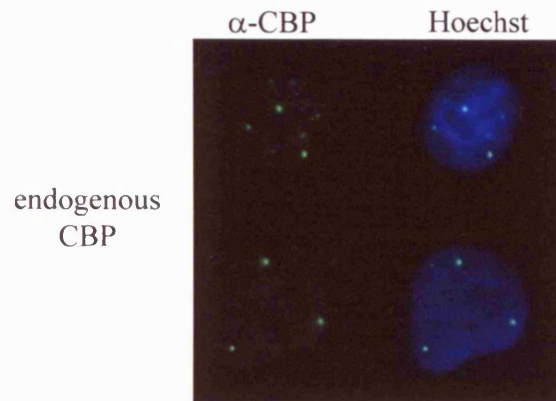
4.16 MOZ-TIF2 expression results in the loss of CBP foci

Analysis of the subcellular localisation of GRIP1 (TIF2), MOZ and MOZ-TIF2 (Figure 3.1) indicated that, in contrast to the wild-type proteins, MOZ-TIF2 was not localised to nuclear foci but formed a mesh-like, nuclear pattern. This altered distribution appeared to be dependent upon the presence of the AD1 domain in the MOZ-TIF2 fusion, as deletion of the AD1 resulted in localisation to foci (Figure 4.7). Given the ability of the AD1 domain to mediate interaction of MOZ-TIF2 with full-length CBP *in vitro* (Figure 4.13) and in cell-free lysates (Figure 4.15), it appeared likely that MOZ-TIF2 might interact with CBP *in vivo*. However, as endogenous CBP normally localises to discrete speckles (Figure 4.16a) that are PML bodies (personal communication; K. Kindle) and MOZ-TIF2 forms a non-speckled mesh-like nuclear pattern, such an interaction might result in an altered CBP distribution. Therefore, in order to investigate whether MOZ-TIF2 expression affected the nuclear distribution of endogenous CBP, COS-1 cells were transfected with 1 μ g MOZ-TIF2 expression plasmid and stained for both endogenous CBP and the exogenous fusion protein.

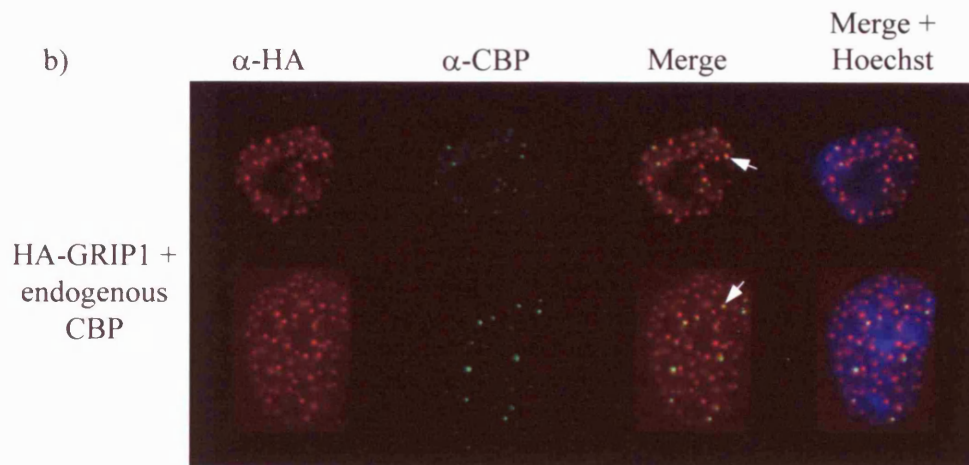
Figure 4.16: Analysis of the subcellular distributions of GRIP1 and MOZ in relation to endogenous CBP

COS-1 cells were seeded on glass coverslips in 6-well plates at 1.5×10^5 cells/well and either, transfected 24 hr later with 1 μ g HA-GRIP1 or HA-MOZ expression vector, or left untreated. Following a further 24 hr growth in full medium, they were fixed and permeabilised. Slides from non-transfected wells were incubated with a rabbit α -CBP antibody followed by a α -rabbit FITC-conjugated secondary antibody. Slides from transfected wells were incubated with rabbit α -CBP and mouse α -HA antibodies, followed by α -rabbit FITC and α -mouse TRITC-conjugated secondary antibodies. All slides were incubated with the Hoechst 33258 DNA stain. After mounting the slides, protein subcellular localisations were viewed and captured using a Zeiss Axioskop2 microscope. Images were captured sequentially in the FITC (green; α -CBP), TRITC (red; α -HA; Figures b and c) and Hoechst (blue) channels and then recombined. α -CBP indicates the distribution of endogenous CBP; α -HA shows the localisation of the expressed HA-tagged proteins; Merge shows an overlay of the FITC and TRITC images; Merge + Hoechst, the signal from all three channels with the Hoechst stain (blue) indicating the distribution of DNA. Two different images are shown for each of transfection conditions examined: a) endogenous CBP; b) HA-GRIP1 with endogenous CBP and c) HA-MOZ with endogenous CBP.

a)



b)



c)

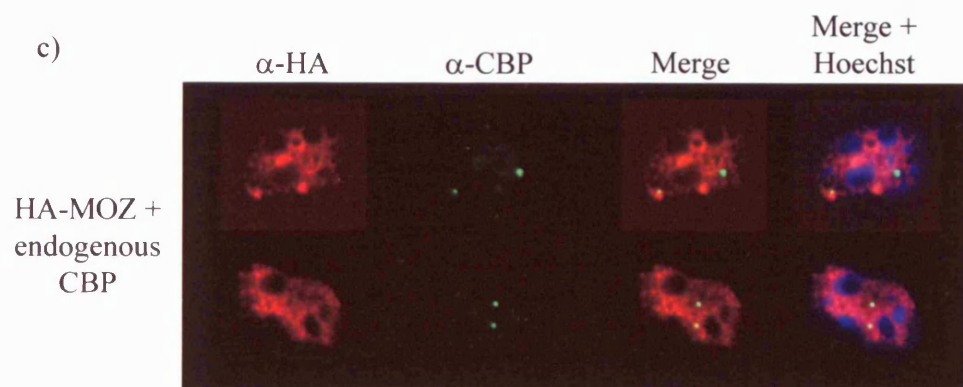
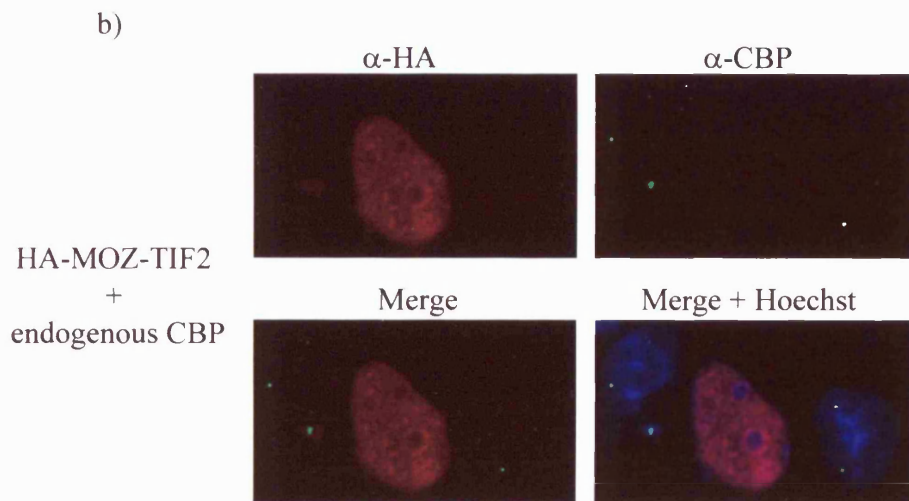
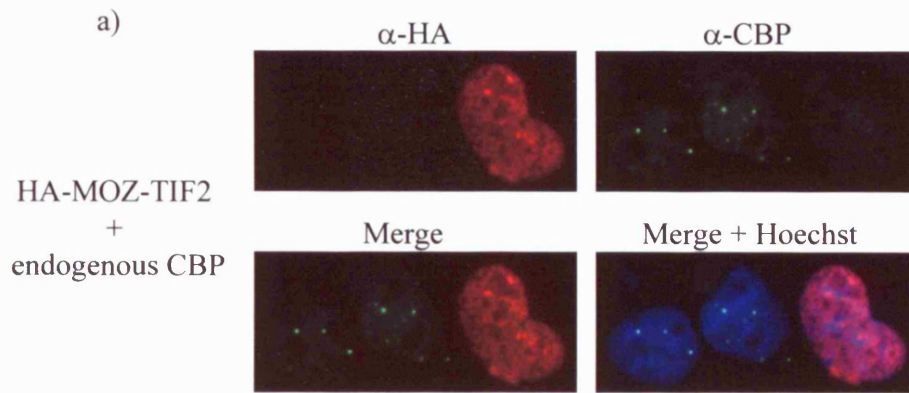


Figure 4.17: Analysis of the effect of MOZ-TIF2 expression on the subcellular distribution of endogenous CBP

COS-1 cells were seeded on glass coverslips in 6-well plates at 1.5×10^5 cells/well and transfected 24 hr later with 1 μg HA-MOZ-TIF2 expression vector. Following a further 24 hr growth in full medium, they were fixed, permeabilised and incubated with rabbit α -CBP and mouse α -HA antibodies, followed by α -rabbit FITC and α -mouse TRITC -conjugated secondary antibodies. The slides were then incubated with the Hoechst 33258 DNA stain and mounted. Protein subcellular localisations were viewed and captured using a Zeiss Axioskop2 microscope. Each image was captured sequentially in the TRITC (red; α -HA), FITC (green; α -CBP) and Hoechst (blue) channels and then recombined. α -HA shows the localisation of the expressed HA-tagged proteins; α -CBP indicates the distribution of endogenous CBP; Merge shows an overlay of the TRITC and FITC images; Merge + Hoechst, the signal from all three channels with the Hoechst stain (blue) indicating the distribution of DNA. Two images are shown as a) and b).



As described previously, MOZ-TIF2-expressing cells showed a mesh-like staining pattern for the exogenous protein (Figure 4.17 α -HA). However, in a substantial proportion of these cells (Figure 4.17 α -CBP), CBP did not localise to discrete foci but showed a very faint diffuse staining. This was in contrast to the surrounding non-expressing cells (nuclei indicated by blue Hoechst stain), which all showed a normal staining pattern for CBP. Thus, the lack of CBP speckles in transfected cells was not due to a problem with the CBP stain. Further analysis indicated that intact PML bodies were present in MOZ-TIF2-expressing cells (personal communication, Dr. K. Kindle). Thus the loss of CBP from speckles was not due to the disruption of the PML bodies themselves.

The data described here thus shows that expression of MOZ-TIF2 results in the depletion of CBP from PML bodies in a considerable proportion of COS-1 cells.

4.17 Deletion of the MOZ-TIF2 AD1 prevents the fusion protein-mediated loss of CBP foci

To further investigate the effect of MOZ-TIF2 on endogenous CBP localisation in COS-1 cells, the AD1 mutant (FLAG-MOZ-TIF2mAD1) and AD1 deletion (HA-MOZ-TIF2 Δ AD1) expression constructs (Figure 4.5), along with truncated HA-MOZ and the HA-MOZ-AD1 fusion (Figure 4.8), were transfected and the cells stained for CBP (Figure 4.18).

As seen previously (Figure 4.7), MOZ-TIF2mAD1 formed a nuclear distribution indistinguishable from MOZ-TIF2 (Figure 4.18a α -HA). Preliminary experiments co-staining these cells with α -CBP antibodies indicated further similarities with MOZ-TIF2 based on their effects on CBP localisation. FLAG-MOZ-TIF2mAD1 appeared to mislocalise CBP (Figure 4.18a α -CBP) in a manner identical to wild-type MOZ-TIF2 (Figure 4.17). Two cells are shown, the upper contains no CBP foci but rather shows a very faint diffuse CBP stain. The lower shows a single large green speckle. However, careful visualisation under the microscope suggested this was not a CBP speckle but rather, appeared to be an artefact due to staining of a non-cellular object on the slide.

In contrast to MOZ-TIF2 and MOZ-TIF2mAD1, the AD1 deletion protein MOZ-TIF2 Δ AD1 localised to foci similar to those seen with MOZ (Figure 4.18b α -HA). As shown in the α -CBP and Merge images in Figure 4.18b, CBP foci were present in COS-1 cells expressing MOZ-TIF2 Δ AD1, indicating a normal CBP localisation to PML bodies. Thus, the expression of the MOZ-TIF2 AD1 deletion construct, MOZ-TIF2 Δ AD1, did not appear to affect the subcellular distribution of CBP. This inability to deplete CBP from PML bodies correlated well with the inability of MOZ-TIF2 Δ AD1 to inhibit NR:AF2-mediated transcription or bind CBP *in vitro* and in cell-free extracts.

The effect of expression of the truncated MOZ construct, MOZ-N, and the MOZ-AD1 fusion on CBP localisation was also investigated. Both constructs had been shown previously to localise to MOZ-like foci (Figure 4.10) rather than in a MOZ-TIF2-like pattern, and neither inhibited NR:AF2-mediated transcription (Figure 4.9). Co-staining for CBP indicated that the expression of either MOZ-N (Figure 4.19a α -CBP) or the MOZ-AD1 fusion (Figure 4.19b α -CBP) did not result in the loss of CBP foci. Thus, neither exogenous protein appeared to affect CBP localisation. This finding supported the hypothesis that the truncation of MOZ was not sufficient to mediate the effects of MOZ-TIF2. In addition, it provided further evidence suggesting that the addition of the AD1 residues 1041 to 1114 from MOZ-TIF2 to the N-terminus of MOZ was not sufficient to mimic the effects of full-length MOZ-TIF2 *in vivo*, despite the ability to bind CBP *in vitro*.

In summary, the ability of MOZ-TIF2 to deplete CBP from PML bodies was dependent on the presence of its AD1 domain. However, fusion of the AD1 residues 1041-1114 to the N-terminus of MOZ did not result in redistribution of CBP. This suggested that either this domain alone was not sufficient to mediate the effect, or that fusion solely of residues of the AD1 to MOZ-N did not allow the domain to attain a conformation that was conducive to an interaction with CBP *in vivo*.

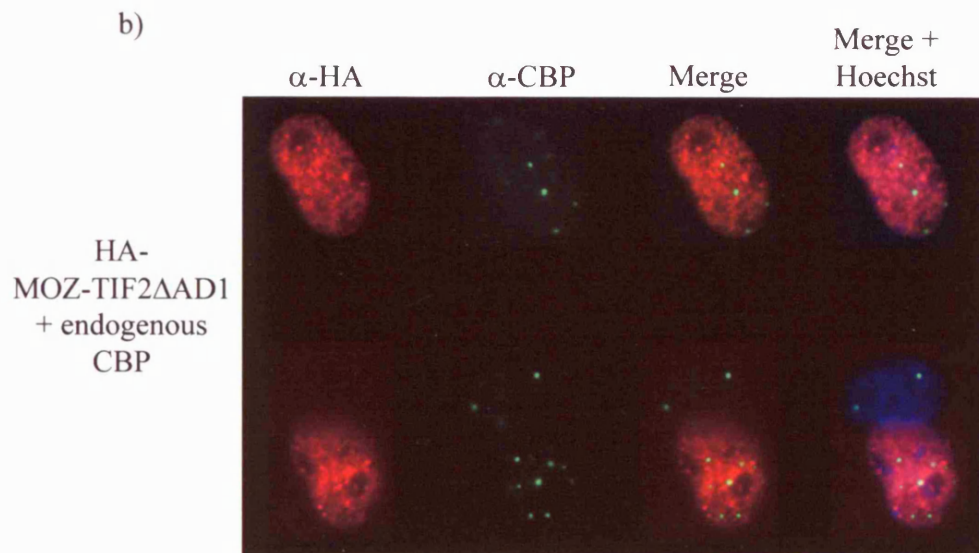
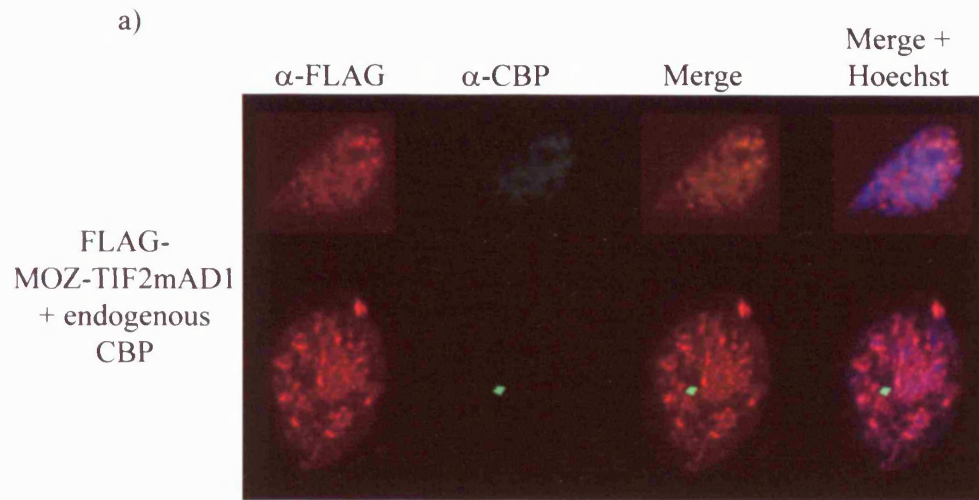


Figure 4.18: Analysis of the effect of MOZ-TIF2mAD1 and MOZ-TIF2 Δ AD1 on the subcellular distribution of endogenous CBP

COS-1 cells were seeded on glass coverslips in 6-well plates at 1.5×10^5 cells/well and transfected 24 hr later with 1 μ g FLAG-MOZ-TIF2mAD1 or HA-MOZ-TIF2 Δ AD1 expression vector. Following a further 24 hr growth in full medium, they were fixed, permeabilised and incubated with mouse α -FLAG or α -HA antibody as appropriate, rabbit α -CBP antibody, and α -mouse TRITC and α -rabbit FITC -conjugated secondary antibodies. The slides were then incubated with the Hoechst 33258 DNA stain and mounted. Protein subcellular localisations were viewed and captured using a Zeiss Axioskop2 microscope. Each image was captured sequentially in the TRITC (red; α -FLAG in a); α -HA in b)), FITC (green; α -CBP) and Hoechst (blue) channels and then recombined. α -FLAG and α -HA show the localisation of the expressed FLAG- and HA-tagged proteins respectively; α -CBP indicates the distribution of endogenous CBP; Merge shows an overlay of the TRITC and FITC images; Merge + Hoechst, the signal from all three channels with the Hoechst stain (blue) indicating the distribution of DNA. Two images are shown for a) FLAG-MOZ-TIF2mAD1 with endogenous CBP; and b) HA-MOZ-TIF2 Δ AD1 with endogenous CBP.

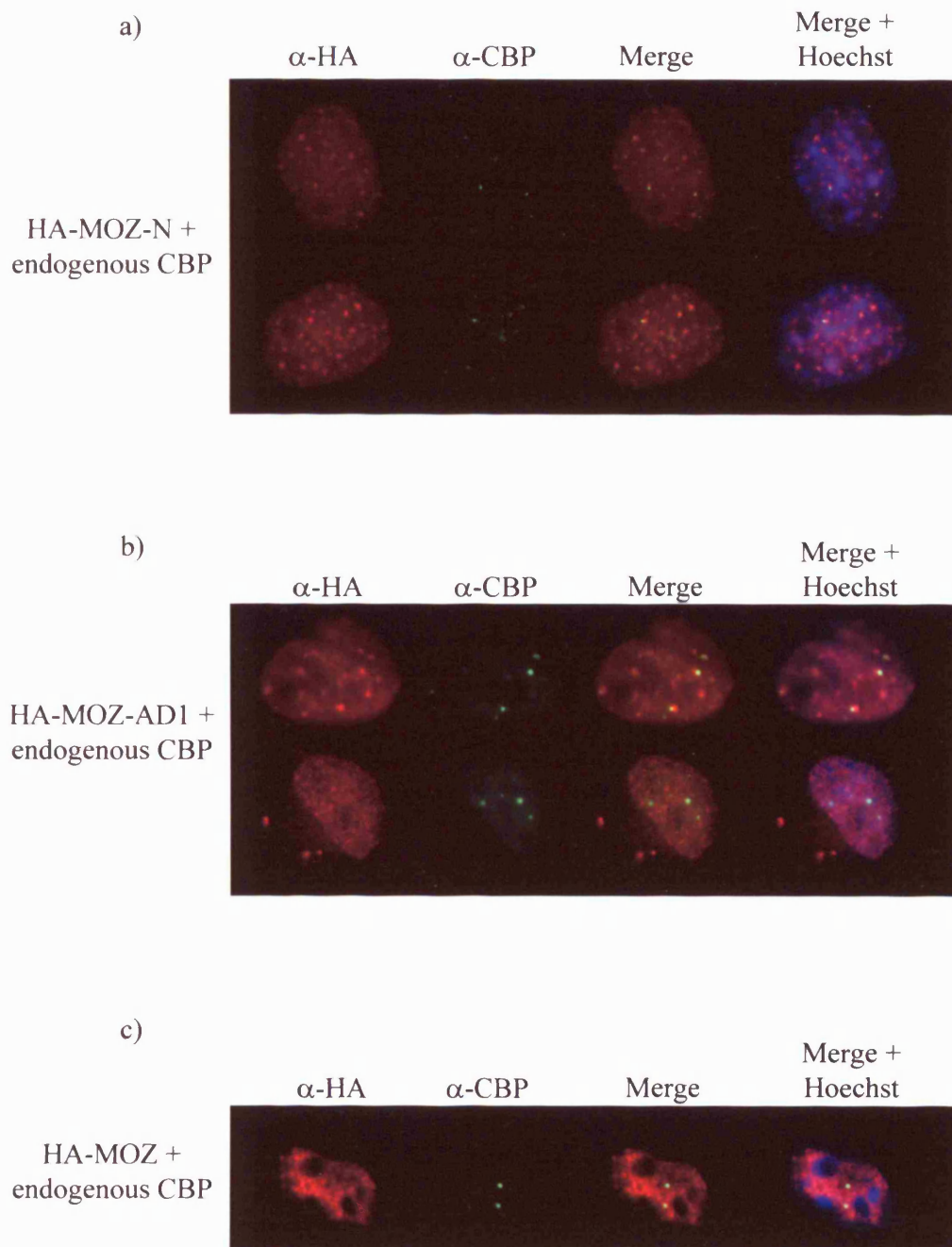


Figure 4.19: Analysis of the effect of MOZ-N and MOZ-AD1 expression on the subcellular distribution of endogenous CBP

COS-1 cells were seeded on glass coverslips in 6-well plates at 1.5×10^5 cells/well and transfected 24 hr later with 1 μ g HA-MOZ-N or HA-MOZ-AD1 expression vector. Following a further 24 hr growth in full medium, they were fixed, permeabilised and incubated with rabbit α -CBP and mouse α -HA antibodies, followed by α -rabbit FITC and α -mouse TRITC -conjugated secondary antibodies. The slides were then incubated with the Hoechst 33258 DNA stain and mounted. Protein subcellular localisations were viewed and captured using a Zeiss Axioskop2 microscope. Each image was captured sequentially in the TRITC (red; α -HA), FITC (green; α -CBP) and Hoechst (blue) channels and then recombined. α -HA shows the localisation of the expressed HA-tagged proteins; α -CBP indicates the distribution of endogenous CBP; Merge shows an overlay of the TRITC and FITC images; Merge + Hoechst, the signal from all three channels with the Hoechst stain (blue) indicating the distribution of DNA. Two images are shown: a) HA-MOZ-N with endogenous CBP; and b) HA-MOZ-AD1 with endogenous CBP.

4.18 Chapter Summary

The experiments discussed in Chapter 3 suggested that the leukaemogenic fusion protein MOZ-TIF2 inhibited the ligand-dependent activation of gene transcription by both Class I and Class II Nuclear Receptors. Therefore, the work described here attempted to ascertain a mechanism for this inhibition. In order to determine whether MOZ-TIF2 could interact with the NR (AF2-containing) ligand-binding domain *in vitro*, GST pulldown experiments were used. Full-length TIF2, MOZ and MOZ-TIF2 were *in vitro* transcribed and translated in the presence of [³⁵S]-methionine. These radiolabelled proteins were incubated with GST fusions of the ER α and RXR α in both the presence and absence of the appropriate ligand. As previously published (Voegel *et al.*, 1996), TIF2 interacted with both GST fusions in a ligand-dependent manner. However, neither MOZ nor the MOZ-TIF2 fusion protein bound either NR. This was not unexpected given the absence of the TIF2 NR Interaction Domain (NID) in the fusion, and the lack of discernible LXXLL motifs, which mediate NR:LBD binding, in MOZ or the C-terminus of TIF2. Thus, it appeared unlikely that the inhibition of NR-mediated transcription by MOZ-TIF2 was due to the binding of the leukaemogenic fusion to NRs *in vivo*.

The MOZ-TIF2 fusion protein is comprised of the N-terminus of MOZ (residues 1-1117), a MYST family protein, and the C-terminus of TIF2 (residues 869-1464), a p160 coactivator. As a result, the fusion contains Activation Domain 1 (AD1) and 2 (AD2) from the TIF2 sequence. The role of these two domains in the p160 proteins is to mediate recruitment of the chromatin modifiers CBP and CARM1 to the ligand-bound NR complex. Given that the MOZ-TIF2 protein was unable to interact with NRs directly, it was postulated that the inhibition of NR-mediated transcription identified in Chapter 3 might have been due to the binding of the leukaemogenic fusion to these downstream coactivators, thus preventing their recruitment to the NR complex by the p160 proteins. In order to investigate whether the MOZ-TIF2 fusion could bind to CBP, GST pulldown experiments were utilised. Initial studies investigated the interaction of TIF2, MOZ and MOZ-TIF2 with a GST fusion of residues 2058-2130 from CBP. This region has been termed the SID and shown to be the minimal sequence of CBP required to bind the p160 proteins (Sheppard *et al.*, 2001). Experiments carried out at a NaCl concentration of 0.2 M indicated that TIF2, MOZ and MOZ-TIF2 all bound to the CBP:SID. However, increasing the NaCl concentration to 0.3 M resulted in a complete loss of MOZ binding,

while having no effect on the interaction of TIF2 or MOZ-TIF2. Both of these IVT proteins were shown to be capable of SID interaction up to a NaCl concentration of 1 M, suggesting they bound the SID with high affinity. In summary therefore, both TIF2 and MOZ-TIF2 interacted strongly with the CBP:SID, whereas MOZ appeared to bind in a weak, possibly non-specific manner.

To determine whether the inhibition of NR-transcription by MOZ-TIF2 might be mediated through the TIF2-derived AD1 domain, two constructs were designed. The first deleted the minimal AD1 sequence from the fusion, as defined by sequence alignment to SRC1, the AD1 of which has been closely mapped (Sheppard *et al.*, 2001). The second construct mutated three AD1 leucine residues, which had previously been implicated in the interaction of TIF2 with CBP (Voegel *et al.*, 1998). Transient transfection experiments carried out using these two constructs indicated that the deletion, but not mutation, of the MOZ-TIF2 AD1 resulted in a loss of inhibition. Immunofluorescence analysis showed that both constructs were expressed, suggesting the lack of inhibition by MOZ-TIF2 Δ AD1 was not due to a lack of expression. In addition, the immunofluorescence data indicated that the sub-nuclear distribution of MOZ-TIF2 Δ AD1 was more like that of MOZ than the wild-type MOZ-TIF2 fusion, suggesting the AD1 plays a role in its localisation. However, the MOZ-TIF2 mutant AD1 construct, MOZ-TIF2mAD1, localised to a pattern indistinguishable from that of wild-type MOZ-TIF2. Subsequent to the construction of MOZ-TIF2mAD1, the solution structure of a complex of the ACTR:AD1 and CBP:SID domains was published (Demarest *et al.*, 2002). Analysis of the structure indicated that, in contrast to the p160 interaction with ligand-bound NRs, the interface between the two protein domains was not mediated by a short amphipathic α -helical sequence in the p160 protein but rather, was due to synergistic folding of extensive hydrophobic regions from both proteins. Thus, the mutation of the three leucines to alanines may not have a significant effect on the formation of the complex between the p160 AD1 and CBP SID domains. This hypothesis would therefore provide a possible explanation for the finding that mutation of the three leucines was not sufficient to alter the properties of the MOZ-TIF2 construct.

To investigate whether fusion of the AD1 sequence alone to the N-terminus of MOZ was sufficient for inhibition of NR transcription, two constructs were generated. The first, MOZ-N simulated the truncation of MOZ found in the MOZ-TIF2 fusion. The second, MOZ-AD1 fused the minimal AD1 sequence (deleted in MOZ-TIF2 Δ AD1) to the MOZ N-terminus. Transient transfection experiments indicated that neither construct was able to inhibit GAL4-RAR α -mediated transcription, though both proteins were expressed, as shown by immunofluorescence analysis. Two possible explanations for the inability of MOZ-AD1 to inhibit NR transcription may be put forward. It is possible that, though the AD1 is necessary for inhibition, additional TIF2 sequences are also required. Alternatively, given that only the minimal AD1 sequence that had deleted in MOZ-TIF2 Δ AD1 was fused to the N-terminus of MOZ, it is possible that the fusion protein was not able to fold *in vivo* into a functional CBP-binding domain, though recent studies (personal communication, S. Matsuda) have shown that an interaction does occur with the CBP SID *in vitro*. During the preparation of this thesis, Deguchi *et al.* (2003) published a study on the leukaemogenic properties of MOZ-TIF2 in the mouse. Their work indicated that expression of a MOZ-TIF2 construct that was truncated after the AD1 domain resulted in a construct that retained the ability to cause acute myeloid leukaemia in a murine bone marrow transplant assay. Thus, it would appear that the TIF2 Q-rich and AD2 sequences are not essential for transformation. However a MOZ-TIF2 AD1 deletion construct was unable to cause AML in this system, indicating that the AD1 is required.

The study by Kitabayashi *et al.* (2002) identified the presence of both MOZ and CBP in an AML1 complex. Therefore, to determine whether MOZ could interact with CBP through a region other than the SID, pulldown experiments were carried out using a GST fusion to full-length CBP. Despite the inability to detect this GST-fusion protein on SDS-PAGE gels, the experiments showed that TIF2 and MOZ-TIF2 selectively bound beads incubated with the bacterial cell extract in which expression had been induced. In contrast, MOZ, MOZ-N and MOZ-TIF2 Δ AD1 did not bind. Thus, it appeared that full-length MOZ and CBP do not interact directly, and that the interaction of MOZ-TIF2 with CBP full-length is mediated by the TIF2-derived AD1 domain.

To confirm the interaction of MOZ-TIF2 with CBP in mammalian cell extracts, co-immunoprecipitation experiments were carried out. These showed that TIF2 and MOZ-TIF2 bound CBP *in vivo*. In contrast no interaction of MOZ-TIF2 Δ AD1 with CBP was detected. CBP was found to co-immunoprecipitate with full-length MOZ. However, given the finding that CBP and MOZ are present in an AML1 complex (Kitabayashi *et al.*, 2001a) this result was not unexpected as an interaction identified through co-immunoprecipitation may not be direct, but rather be mediated through the presence of a common binding partner (for example AML1). This possibly indirect CBP MOZ interaction appeared unlikely to play a role in the immunoprecipitation of CBP by MOZ-TIF2 as no such effect was seen with MOZ-N.

The final experiments discussed in this chapter investigated the effect of MOZ-TIF2 expression on CBP distribution within the cell nucleus. Endogenous CBP has been shown previously to localise to speckles termed PML bodies (Doucas *et al.*, 1999; Boisvert *et al.*, 2001). This speckled staining pattern of CBP was confirmed, and co-transfection of GRIP1, MOZ, MOZ-N and MOZ-AD1 shown to have no effect on CBP localisation. However, the two constructs, MOZ-TIF2 and MOZ-TIF2mAD1, both of which were shown to inhibit ligand-dependent transcription activation by NRs, appeared to reduce the association of CBP with these PML bodies, though the PML bodies themselves were not disrupted as shown by anti-PML staining (personal communication, K. Kindle).

In conclusion therefore, the experiments described in this chapter suggest that the inhibition of ligand-dependent NR-mediated transcription by MOZ-TIF2 requires its AD1 domain. This finding correlates with the study by Deguchi *et al.* (2003) that indicates the AD1 is essential for the leukaemogenic properties of MOZ-TIF2. The AD1 also appears to be involved in the unique sub-nuclear localisation of the fusion protein as deletion of the AD1 results in a MOZ-like distribution. In addition, the work described here shows that the AD1 mediates the interaction of MOZ-TIF2 with CBP both *in vitro* and in cell-free extracts. This interaction appears to result in the reduced association of CBP with PML bodies, in which it normally resides. The mislocalisation of CBP may result in a reduction in the CBP that can be recruited to NR complexes by the p160 proteins, thus providing one possible mechanism for the inhibition of NR-mediated transcription by MOZ-TIF2.

The studies described thus far have investigated the inhibition of transcription by transiently expressed GAL4-NR proteins. These transcription factor fusions allow analysis into effects on ligand-dependent transcription of a GAL4-responsive reporter. Therefore, in order to investigate the effects of MOZ-TIF2 on endogenous NRs using a more physiologically relevant model, the studies described in the following chapter utilised the haematopoietic cell line U937. In addition, given the ability of a number of transcription factors to bind the CBP SID (Lin *et al.*, 2001; Matsuda *et al.*, 2003), and the role of MOZ in AML1-mediated transcription, preliminary experiments are described that investigate whether the leukaemogenic fusion protein can inhibit the activity of other transcription factors.

Chapter Five:

**Effect of MOZ-TIF2 on
transcription activation by
endogenous Nuclear Receptors in
U937 cells, and on exogenously
expressed p53, ETS-2 and AML1**

5.1 Introduction

The experiments discussed in Chapter 3 describe the inhibition of NR-mediated, ligand-dependent transcription activation by the MOZ-TIF2 leukaemogenic fusion protein. Those detailed in Chapter 4 showed that this inhibition required the presence of the MOZ-TIF2 AD1 domain, which mediates the interaction of MOZ-TIF2 with CBP. However, this ability to inhibit NR transcription was identified in the COS-1 cell line through the use of over-expressed fusions of NR ligand-binding domains to the GAL4 DNA binding domain. Therefore, in order to investigate the effects of MOZ-TIF2 using a more physiologically relevant model, transient transfection reporter experiments were carried out in the U937 haematopoietic cell line, which phenotypically resembles monocytic blasts (Sundstrom and Nilsson, 1976). U937 cells have been shown to express endogenous NRs, which appear to mediate the cell growth inhibition and differentiation activities in this cell line of NR ligands such as retinoic acid, troglitazone and vitamin D3 (Botling *et al.*, 1996; Brown *et al.*, 2000; Pizzimenti *et al.*, 2002; James *et al.*, 1999). Thus, the use of these cells allowed the analysis of the effects of MOZ-TIF2 expression on activation of reporters by endogenous NRs in a haematopoietic cell line.

The mechanism of NR-mediated transcription inhibition by MOZ-TIF2 was investigated in Chapter 4 of this thesis using various mutant constructs. These experiments highlighted a requirement for the TIF2-derived AD1 domain of MOZ-TIF2, which mediates binding to CBP. The interaction of CBP with the AD1 occurs through the CBP SID (Sheppard *et al.*, 2001). This domain of CBP has been shown to be required for its interaction with a number of diverse transcription factors including p53, Tax, E1A, IRF3 and ETS-2 (Scoggin *et al.*, 2001; Livengood *et al.*, 2002; Lin *et al.*, 2001; Matsuda *et al.*, 2003). Thus, given the ability of MOZ-TIF2 to bind the SID and inhibit NR-mediated transcription, it appeared possible that the fusion protein might act as an inhibitor of other transcription factors that utilise SID interactions during CBP recruitment. In order to determine whether MOZ-TIF2 might inhibit the transcriptional activity of non-NR transcription factors that recruit CBP through its SID, preliminary studies were carried out using two such proteins, p53 and ETS-2.

The tumour suppressor protein p53 has been shown to play a crucial role in protecting against cancer (Vousden and Lu, 2002). It acts as the focal point for a large range of signalling pathways that respond to oncogenic alterations or abnormal cell proliferation. Upon activation, p53 induces the expression of genes involved in cell growth arrest and/or apoptosis. The global coactivator CBP/p300 is involved both in the regulation of p53 and in mediating its induction of gene transcription (Grossman, 2001; Livengood *et al.*, 2002). p53 binds to three separate regions of CBP/p300 (Figure 1.8): the KIX domain, the C/H3 domain and the SID, with the SID appearing to play an important role in the recruitment of CBP/p300 to target promoters during p53-mediated activation of reporter gene transcription (Livengood *et al.*, 2002). As a result, MOZ-TIF2 interaction with the CBP SID domain could potentially lead to an inhibition of p53-mediated transcription.

ETS-2 is a member of the ETS transcription factor family that contain an evolutionarily conserved DNA binding domain (Oikawa and Yamada, 2003). The ETS family members have a wide range of functions that include transcription activation of genes involved in cell proliferation, and also activation of apoptosis-related genes. Induction of gene expression by ETS proteins is regulated by the Ras-MAP Kinase signalling pathways, thus allowing control of ETS-target genes in response to extra-cellular stimuli. Some members such as ETS-2 are ubiquitously expressed, while others are restricted to particular cell lineages; PU.1 for example, which is required for normal myeloid differentiation, is exclusively expressed in B-cells, macrophages and neutrophils. ETS-2, which has been shown to cooperate with PU.1 during the activation of myeloid-specific promoters (Ross *et al.*, 1998; Sevilla *et al.*, 2001), recruits CBP/p300 during transcription activation through interaction with the C/H1 and SID (Jayaraman *et al.*, 1999; Lin *et al.*, 2001). MOZ-TIF2 expression may therefore affect ETS-2-mediated transcription by preventing an interaction with the CBP SID domain.

The report that the MOZ protein acts as a coactivator for the haematopoietic transcription factor AML1 provided the first clue to the physiological function of this MYST family protein (Kitabayashi *et al.*, 2001a). Both MOZ and CBP were identified in an AML1 complex in co-immunoprecipitation experiments, and were shown to acetylate histones and AML1 *in vitro*. Kitabayashi *et al.* (2001) also investigated the effect of the MOZ-CBP leukaemogenic fusion protein on AML1-mediated transcription, and showed that it inhibited the ability of CBP, but not MOZ, to act as a coactivator for this transcription factor. Given the essential role of AML1 in haematopoiesis (Lutterbach and Hiebert, 2000; Skalnik, 2002; Michaud *et al.*, 2003), this suggested that MOZ fusions might affect AML1-mediated, in addition to NR-mediated, transcription in these cells. The phenotypes of the leukaemias resulting from MOZ-TIF2 and MOZ-CBP fusions are very similar, suggesting a possible common mechanism of leukaemogenesis. Therefore, the final set of transient transfection experiments discussed in this thesis describes preliminary investigations into the effects of MOZ and MOZ-TIF2 on AML1-mediated transcription activation.

MOZ has been shown to interact with both AML1 and its homologue Runx2 (AML3) (Kitabayashi *et al.*, 2001a; Pelletier *et al.*, 2002) and to act as a coactivator for AML1 (Kitabayashi *et al.*, 2001a; Bristow and Shore, 2003). However, no other direct protein interactions have as yet been confirmed. As a result, the final sections of this chapter describe the construction and analysis of a series of LexA-MOZ fusions spanning the entire MOZ sequence. Although there was insufficient time to carry out a yeast 2-hybrid screen, these constructs have been characterised for their suitability for such a screen, which will be carried out by others in the laboratory. Expression of the LexA-MOZ fusions in yeast was confirmed by western analysis, and the ability of each construct to auto-activate transcription in the absence of a prey-fusion protein (Figure 5.15) checked using β -galactosidase assays. In addition, the equivalent GST fusion constructs were generated to allow the future *in vitro* confirmation of any identified interactions from such a screen.

5.2 Activation of RARE and PPRE luciferase reporters by endogenous NRs in the U937 haematopoietic cell line

The U937 line was derived from the pleural effusion (escape of fluid from blood vessels into the lung cavity) of a patient with a histiocytic lymphoma (malignant tumour of reticular tissue comprised of predominantly abnormal macrophages) (Sundstrom and Nilsson, 1976). This established suspension cell line contains a large number of chromosomal abnormalities (Lee *et al.*, 2002). However, it resembles cells of monocytic origin that can be induced to terminally differentiate into monocytes (Olsson and Breitman, 1982). Thus, it provides a model system in which to investigate the effects of expression of a fusion protein implicated in Acute Myeloid Leukaemia. Nuclear hormones such as retinoic acid (James *et al.*, 1999) and PPAR γ ligands (Asou *et al.*, 1999; Pizzimenti *et al.*, 2002) have been shown to inhibit the proliferation of U937 cells and/or promote differentiation. These effects appear to be mediated, at least in part, through the activation of endogenous nuclear receptors (Botling *et al.*, 1996; Brown *et al.*, 1997; Asou *et al.*, 1999). Thus, the experiments described below were carried out in order to determine whether these endogenous NRs could activate transcription of transiently transfected luciferase reporters.

Two luciferase reporters were transfected into U937 cells by electroporation (Section 2.2.7) to determine whether they could be activated by endogenous NRs upon addition of the appropriate ligand. The first, pRep4-RARE (gift from Dr. A. Zelent, Institute of Cancer Research) was a retinoic acid-responsive reporter; the second, p(PPRE)₃-tk-Luc (gift from Dr. S. Ali, Imperial College, London), was comprised of three copies of the consensus PPAR γ binding site upstream of the minimal thymidine kinase promoter and luciferase reporter, and thus luciferase transcription should be initiated in response to PPAR γ ligands. In addition to transfection of 4 μ g of one of the luciferase reporters, 1 μ g of the β -galactosidase reporter pEF-BOS (gift from Dr. C Bevan, Imperial College, London) was co-transfected to allow normalisation of the luciferase values measured. Due to the large numbers of cells required for each individual electroporation (1×10^8), each transfection condition was tested in duplicate, rather than triplicate. Ligand (pRep4-RARE: all-*trans* retinoic acid and 9-*cis* retinoic acid; p(PPRE)₃-tk-Luc: rosiglitazone and 9-*cis* retinoic acid; final concentrations 10^{-7} M) or an equivalent volume of vehicle was added three hours after electroporation and the cells harvested as described (Section 2.5.5). Luciferase and β -

galactosidase activities were determined in duplicate and the luciferase: β -galactosidase ratio calculated. As with the COS-1 transient transfections, the ratios were plotted as Relative Luciferase Activities (RLA) with the ratio for Reporters (in the absence of ligand) set to a value of 1. Data representative of two independent experiments is shown. The error bars indicate the Standard Error of the Mean (S.E.M.) for the duplicate samples and provides an indication of the accuracy of the calculated mean.

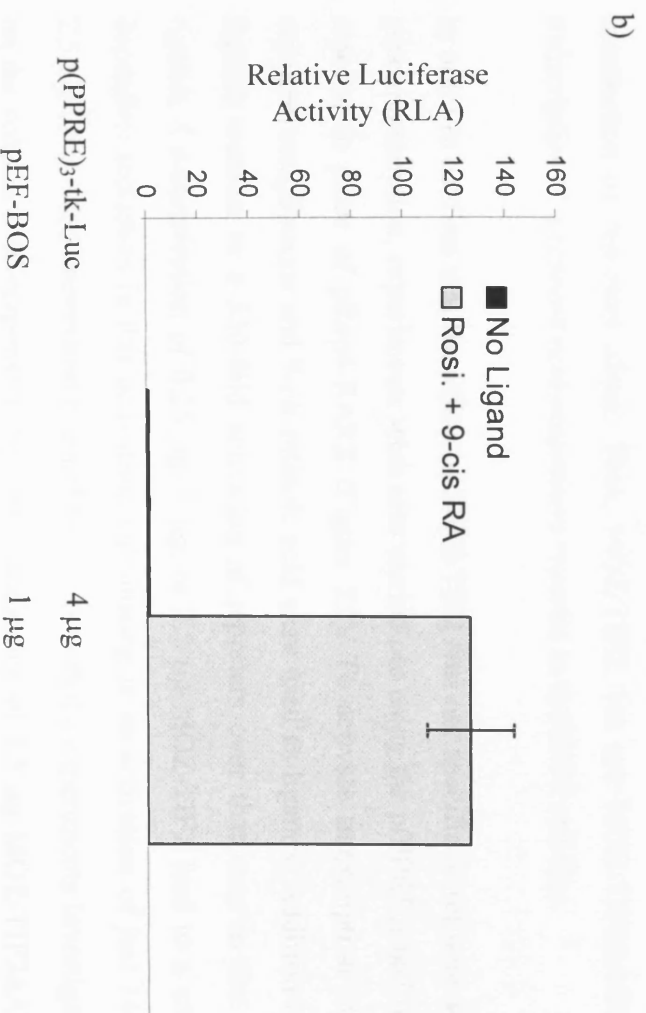
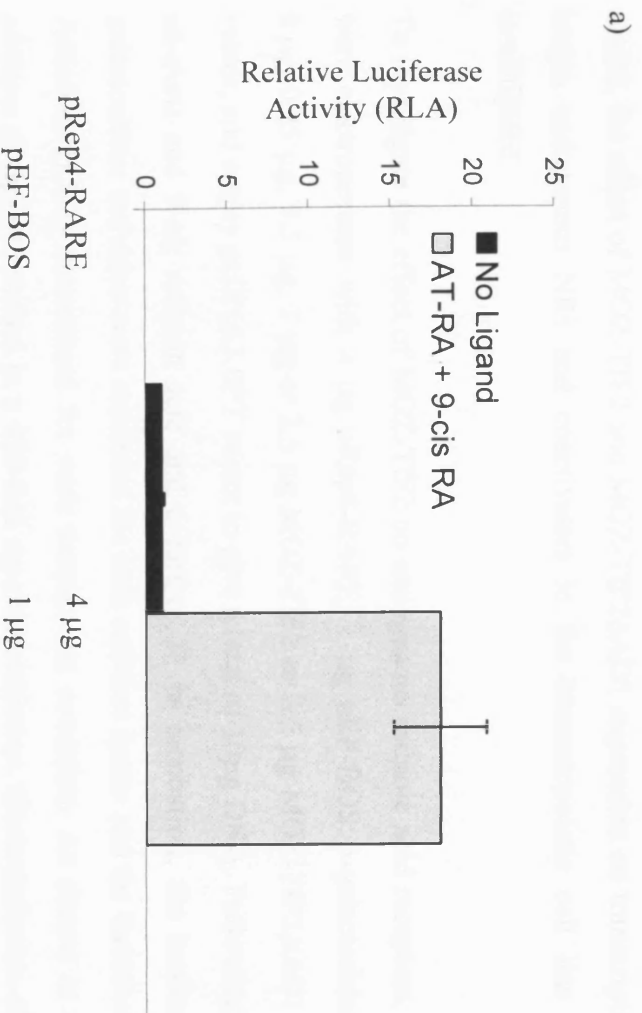
As shown in Figure 5.1a, addition of all-*trans* retinoic acid and 9-*cis* retinoic acid resulted in activation of the pRep4-RARE luciferase reporter. Given the absence of co-transfected NR expression plasmids this ligand-dependent activation was likely due to the activity of endogenous RAR and RXR nuclear receptors. A ligand-dependent activation of luciferase activity was also seen (Figure 5.1b) following electroporation of the reporter p(PPRE)₃-tk-Luc and addition of rosiglitazone (a PPAR γ ligand) and 9-*cis* retinoic acid (RXR ligand). Thus, the U937 cell line is able to activate transcription of luciferase reporters containing either RAR response elements or PPAR γ response elements in a ligand-dependent manner. It is likely that this activation was mediated through endogenous NRs and therefore the U937 cell line provides a suitable model system in which to test the effect of the leukaemogenic fusion MOZ-TIF2 on NR-mediated transcription.

5.3 MOZ-TIF2 inhibition of NR-mediated transcription in the U937 cell line is dependent upon the AD1 domain

Experiments described in Chapter 3 of this thesis showed that the leukaemogenic fusion protein MOZ-TIF2 inhibited transcriptional activation mediated by the ligand-binding domain of NRs (Figures 3.6 and 3.8). This inhibition was dependent upon the presence of the AD1 in the fusion protein (Figure 4.6), which mediates the interaction of MOZ-TIF2 with CBP both *in vitro* (Figure 4.13) and in mammalian cell-free extracts (Figure 4.15). The transient transfection experiments used to investigate the effect of MOZ-TIF2 on NR-mediated transcription were carried out in the COS-1 cell line due to the ease with which they could be transfected, and the relatively low level of activity of endogenous coactivator proteins (our laboratory, unpublished observations). In addition, the experiments utilised

Figure 5.1: Activation of pRep4-RARE and p(PPRE)₃-tk-Luc luciferase reporters in the haematopoietic U937 cell line by addition of NR ligands

U937 cells were transfected in duplicate with 1 µg pEF-BOS β-galactosidase reporter and 4 µg of either pRep4-RARE (a) or p(PPRE)₃-tk-Luc luciferase reporter (b). Vehicle (No Ligand bars) or the ligands (final concentration of 10⁻⁷ M) all-*trans* retinoic acid (AT-RA) and 9-*cis* retinoic acid (9-*cis* RA) were added for a), and vehicle (No Ligand) or rosiglitazone (Rosi.) and 9-*cis* retinoic acid (9-*cis* RA) for b), 3 hr after electroporation. The cells were harvested following a further 21 hr incubation. Luciferase and β-galactosidase activities of each cell-free lysate were measured using a dual assay. The luciferase:β-galactosidase ratios were then calculated and plotted as Relative Luciferase Activity, with the ratio in the absence of ligand set to a value of 1. Error bars show the calculated S.E.M.



GAL4-NR:LBD fusions to investigate the effect on ligand-dependent transcription by NRs. Therefore, in order to extend these findings to a more physiologically relevant cellular model, the effect of MOZ-TIF2 and MOZ-TIF2 Δ AD1 expression on transcription by full-length endogenous NRs and coactivators in the haematopoietic cell line U937 was investigated.

To investigate the effect of MOZ-TIF2 on endogenous retinoic acid receptors, U937 cells were electroporated with 4 μ g pRep4-RARE, 1 μ g pEF-BOS β -galactosidase reporter, 0 μ g, 0.25 μ g, 0.5 μ g, 1 μ g or 2.5 μ g MOZ-TIF2 or 2.5 μ g MOZ-TIF2 Δ AD1 expression vector, and empty pcDNA3.0PT vector to give a total of 10 μ g DNA. Following addition of all-*trans* and 9-*cis* retinoic acid and a further 21 hr incubation, the luciferase and β -galactosidase activities were measured for each cell-free lysate and the Relative Luciferase Activities (RLA) determined for each transfection condition. As shown in Figure 5.2, addition of ligand resulted in a 450-fold reporter activation. Co-transfection of increasing amounts of MOZ-TIF2 expression plasmid resulted in a reduction in this activation down to 150-fold with 2.5 μ g DNA. In contrast, electroporation of 2.5 μ g MOZ-TIF2 Δ AD1 expression plasmid did not result in a change in reporter activation when compared to the transfection of reporters alone. Thus, MOZ-TIF2, but not MOZ-TIF2 Δ AD1, inhibited transcription of a retinoic acid-responsive reporter in the U937 cell line.

In order to confirm that the effect of MOZ-TIF2 was not specific to retinoic acid-induced gene transcription, experiments were also carried out using the p(PPRE)₃-tk-Luc luciferase reporter in place of pRep4-RARE (Figure 5.3). To activate transcription of the PPRE reporter, rosiglitazone and 9-*cis* retinoic acid were used as ligands. Addition of these NR ligands resulted in a 530-fold activation of reporters over that seen in the absence of ligands. Co-transfection of 0.25 μ g, 1 μ g, or 2.5 μ g MOZ-TIF2 lead to a concentration dependent reduction in this activation, culminating in an activation of just 140-fold with 2.5 μ g MOZ-TIF2 expression plasmid DNA. As with the experiments investigating effects on the retinoic acid-responsive reporter, transfection of 2.5 μ g MOZ-TIF2 Δ AD1 did not result in a reduction in reporter activity, indicating that this construct did not inhibit ligand-induced transcription.

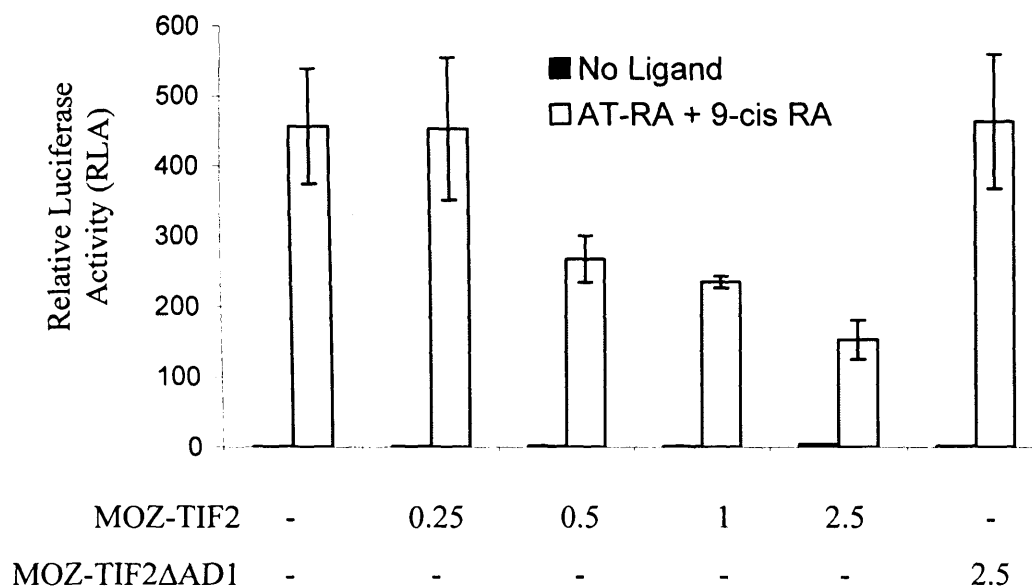


Figure 5.2: Effect of MOZ-TIF2 and MOZ-TIF2ΔAD1 on ligand-induced activation of the pRep4-RARE luciferase reporter in the U937 cell line.

U937 cells were electroporated in duplicate with 4 μg pRep4-RARE, 1 μg pEF-BOS and the expression plasmids shown (“-” indicates no DNA and “number” amount of DNA in μg). Vehicle (No Ligand bars) or the ligands (final concentration of 10^{-7} M) all-*trans* retinoic acid (AT-RA) and 9-*cis* retinoic acid (9-*cis* RA) were added 3 hr after electroporation and the cells harvested following a further 21 hr incubation. Luciferase and β-galactosidase activities of each cell-free lysate were measured using a dual assay. The luciferase:β-galactosidase ratios were then calculated and plotted as Relative Luciferase Activity, with the ratio in the absence of ligand set to a value of 1. Error bars show the calculated S.E.M.

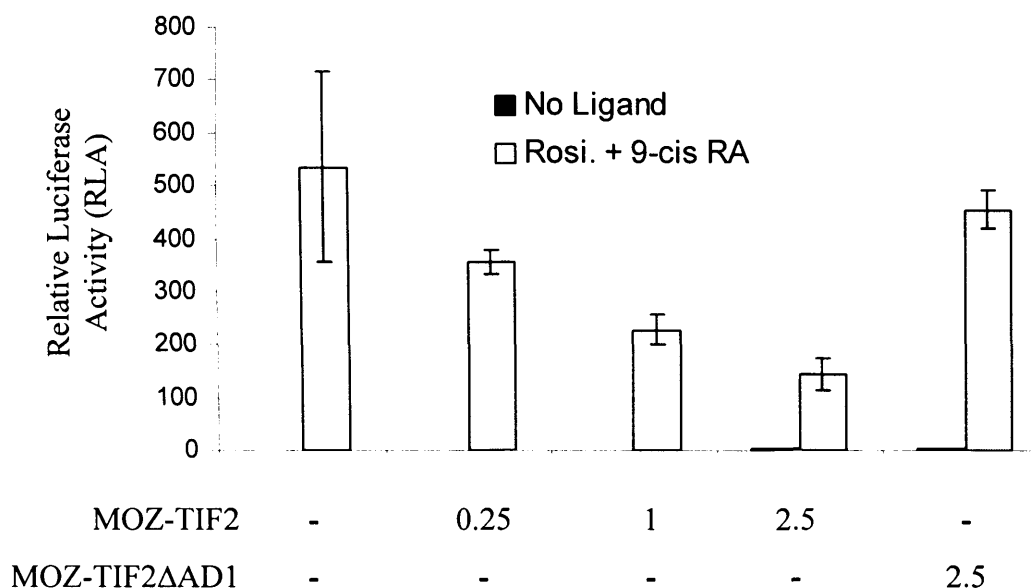


Figure 5.3: Effect of MOZ-TIF2 and MOZ-TIF2ΔAD1 on ligand-induced activation of the p(PPRE)₃-tk-Luc luciferase reporter in the U937 cell line.

U937 cells were electroporated in duplicate with 4 μg p(PPRE)₃-tk-Luc, 1 μg pEF-BOS and the expression plasmids shown (“-” indicates no DNA and “number” amount of DNA in μg). Vehicle (No Ligand bars) or the ligands (final concentration of 10⁻⁷ M) rosiglitazone (Rosi.) and 9-*cis* retinoic acid (9-*cis* RA) were added 3 hr after electroporation and the cells harvested following a further 21 hr incubation. Luciferase and β-galactosidase activities of each cell-free lysate were measured using a dual assay. The luciferase:β-galactosidase ratios were then calculated and plotted as Relative Luciferase Activity, with the ratio in the absence of ligand set to a value of 1. Error bars show the calculated S.E.M.

In summary therefore, these experiments have shown that the leukaemogenic protein MOZ-TIF2 inhibits transcription mediated by the ligands of NRs in the haematopoietic cell line U937. Given the absence of transfected nuclear receptor or coactivator expression plasmids, this suggests that the fusion protein inhibits transcription activation by endogenous NRs and coactivators in haematopoietic cells. The inability of the MOZ-TIF2 Δ AD1 construct to replicate this inhibition further implies that the AD1 present in MOZ-TIF2 is required for this activity.

5.4 Activation of luciferase reporter gene expression by p53

Experiments described in Chapter 4 showed that the leukaemogenic fusion protein MOZ-TIF2 bound to full-length CBP both *in vitro* (Figure 4.13) and in mammalian cell-free extracts (Figure 4.15). This interaction was mediated by the TIF2-derived AD1 domain, which binds to the CBP SID (Figures 4.3 and 4.12). As a result, the apparent requirement for the AD1 in inhibition of NR-mediated transcription by MOZ-TIF2 (Figures 4.6, 5.2 and 5.3) suggested that MOZ-TIF2 might mediate its effects through an interaction with CBP that prevented its recruitment to active NR complexes. A number of transcription factors utilise SID interactions to recruit CBP/p300 during the activation of transcription, and thus might also be affected by the ability of MOZ-TIF2 to bind this region of CBP. The tumour suppressor protein p53 provides one such example. Although it binds CBP/p300 through three discrete regions of the global coactivator, transcription activation by p53 appears to require a specific interaction with the SID (Livengood *et al.*, 2002). Thus, expression of the leukaemogenic fusion protein MOZ-TIF2 might act to inhibit p53-mediated transcription, thus reducing the ability of this crucial protein to induce apoptosis in response to uncontrolled cell proliferation.

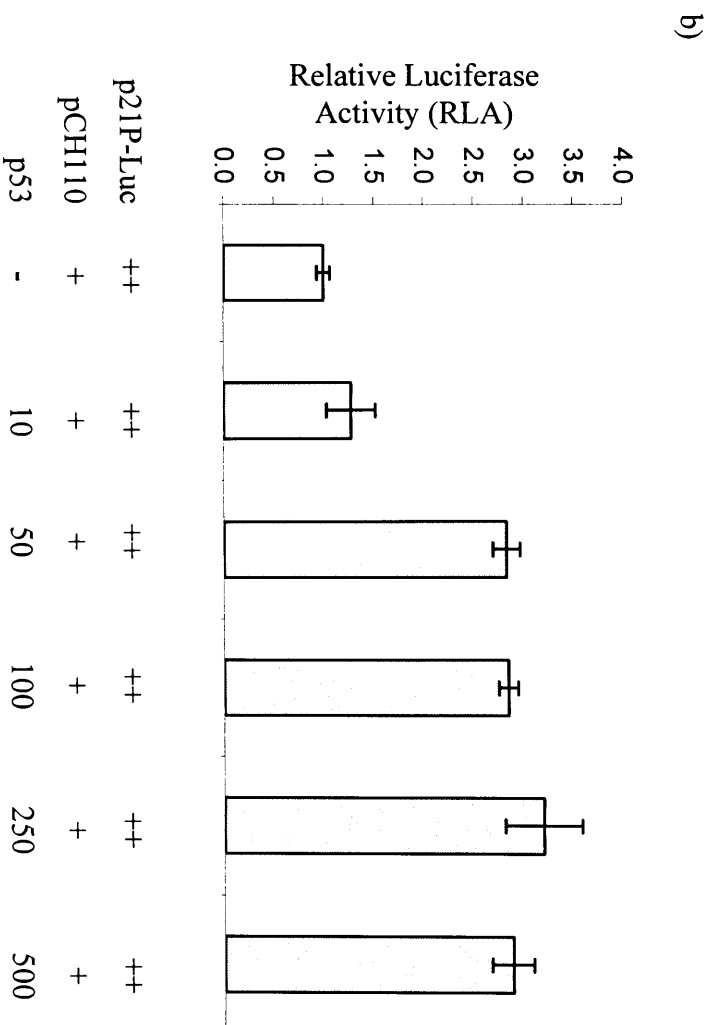
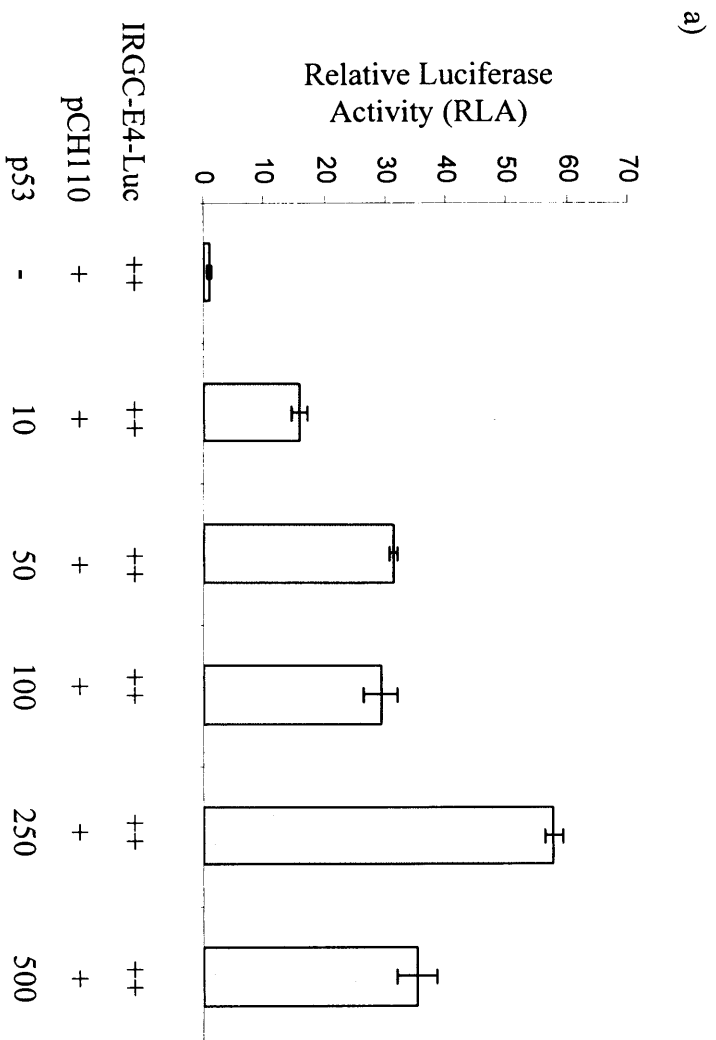
To allow analysis of the effects of MOZ-TIF2 on p53-mediated transcription, transient transfection experiments were carried out in the HeLa cell line grown in 10% foetal calf serum. The HeLa line was derived from a cervical carcinoma, and is positive for the

Human Papillomavirus 18 (HPV-18). Thus, though these cells express endogenous wild-type p53 it is rapidly degraded due to the presence of the E6 oncoprotein encoded by the HPV-18 virus (Scheffner *et al.*, 1990). As a result, activation of p53-responsive reporters in these cells is very low in the absence of transfected p53, thus allowing investigation of p53-mediated transcription through exogenous expression. Two luciferase reporters were investigated to determine whether co-transfection of a p53 expression plasmid resulted in an increase in luciferase expression and thus activity. The p21P-Luc luciferase reporter (Datto *et al.*, 1995) was comprised of a 2.4kb fragment of the p21 promoter that contains two p53 binding sites. The p21 protein mediates p53-induced growth arrest by acting as an inhibitor of cyclin-dependent kinases, which are required for cell cycle progression. The second p53-responsive reporter, IRGC-E4-Luc, contains a consensus p53 binding sequence fused upstream of the adenovirus E4 promoter's TATA-box and the Luciferase gene (gift from Dr. X. Liu, University of California, Riverside, USA).

The expression construct pcDNA3:p53 (gift from Dr. Liu) was titrated with 100 ng pCH110 β -galactosidase reporter and 500 ng of either IRGC-E4-Luc or p21P-Luc luciferase reporter to confirm that it could activate luciferase reporter transcription. Transfection of 10 ng p53 with the IRGC synthetic promoter resulted in a 16-fold activation of the luciferase promoter compared to reporters alone (Figure 5.4a). This activation was enhanced to a maximum of 58-fold (250 ng p53 expression vector) by increasing amounts of transfected p53. In contrast, while expression of luciferase from the p21P-Luc reporter was stimulated by p53 transfection in a concentration-dependent manner, the maximal determined reporter activity was just 3.2-fold (Figure 5.4b). Due to the low level of p21P-Luc activation by p53 in this cell line, the effect of MOZ-TIF2 expression on p53-mediated transcription was investigated using the IRGC-E4-Luc luciferase reporter activated by 50 ng p53.

Figure 5.4: Activation of the IRGC-E4-Luc and p21P-Luc luciferase reporters by p53 expression in the HeLa cell line

HeLa cells grown in 10% foetal calf serum were transfected in triplicate with 100 ng pCH110 β -galactosidase reporter, either 500 ng IRGC-E4-Luc (a) or p21P-Luc (b) luciferase reporter, and p53 expression plasmid as shown (“-” indicates no DNA, “+” 100 ng DNA, “++” 500ng DNA, and “number” amount of DNA in ng). The cells were harvested 48 hr after transfection and luciferase and β -galactosidase activities of each cell-free lysate measured using a dual assay. The luciferase: β -galactosidase ratios were then calculated and plotted as Relative Luciferase Activity, with the ratio upon transfection of reporters alone set to a value of 1. Error bars show the calculated S.E.M.



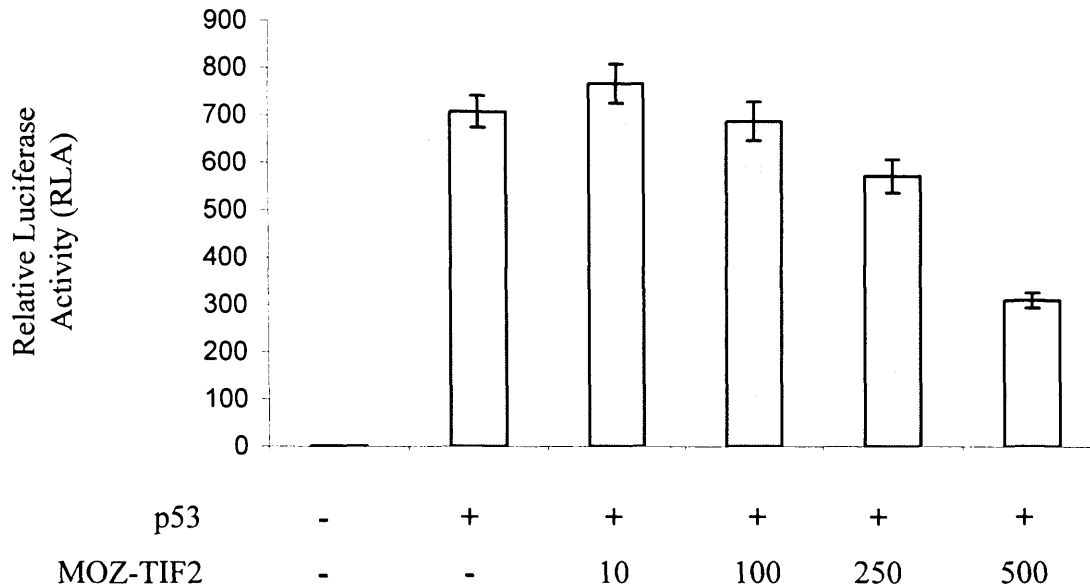


Figure 5.5: Effect of MOZ-TIF2 expression on activation of the IRGC-E4-Luc luciferase reporter by p53 in the HeLa cell line

HeLa cells were transfected in triplicate with 100 ng pCH110 β -galactosidase reporter, 500 ng IRGC-E4-Luc luciferase reporter and expression plasmids as shown (“-” indicates no DNA, “+” 50 ng DNA, and “number” amount of DNA in ng). The cells were harvested 48 hr after transfection and luciferase and β -galactosidase activities of each cell-free lysate measured using a dual assay. The luciferase: β -galactosidase ratios were then calculated and plotted as Relative Luciferase Activity, with the ratio upon transfection of reporters alone set to a value of 1. Error bars show the calculated S.E.M.

5.5 Inhibition of p53-mediated transcription of the IRGC-E4-Luc luciferase reporter by MOZ-TIF2

To investigate the effects of MOZ-TIF2 expression on p53-mediated transcription, transient transfection experiments were carried out using the IRGC-E4-Luc luciferase reporter. MOZ-TIF2 expression constructs were titrated with 100 ng pCH110, 500 ng IRGC-E4-Luc and 50 ng pcDNA3:p53 (Figure 5.5). Transfection of p53 with reporters resulted in a 700-fold activation of reporter activity. Co-transfection of MOZ-TIF2 with p53 and the reporters gave rise to a concentration-dependent reduction in RLA down to minimum of 300-fold with 500 ng MOZ-TIF2. Thus, MOZ-TIF2 expression resulted in the inhibition of p53-mediated transcription in transient transfection experiments carried out in the HeLa cell line. Further experiments have confirmed that this inhibition also occurs with exogenous p53 expressed in the p53^{-/-} cell line SaOS2 (personal communication, H. Collins). However, additional experiments are required to investigate the mechanism of inhibition, and determine whether MOZ-TIF2 inhibits transcription activation by endogenous wild-type p53 in haematopoietic cells. However in summary, the experiments described here indicate that MOZ-TIF2 expression results in the inhibition of p53-mediated transcription in luciferase reporter assays.

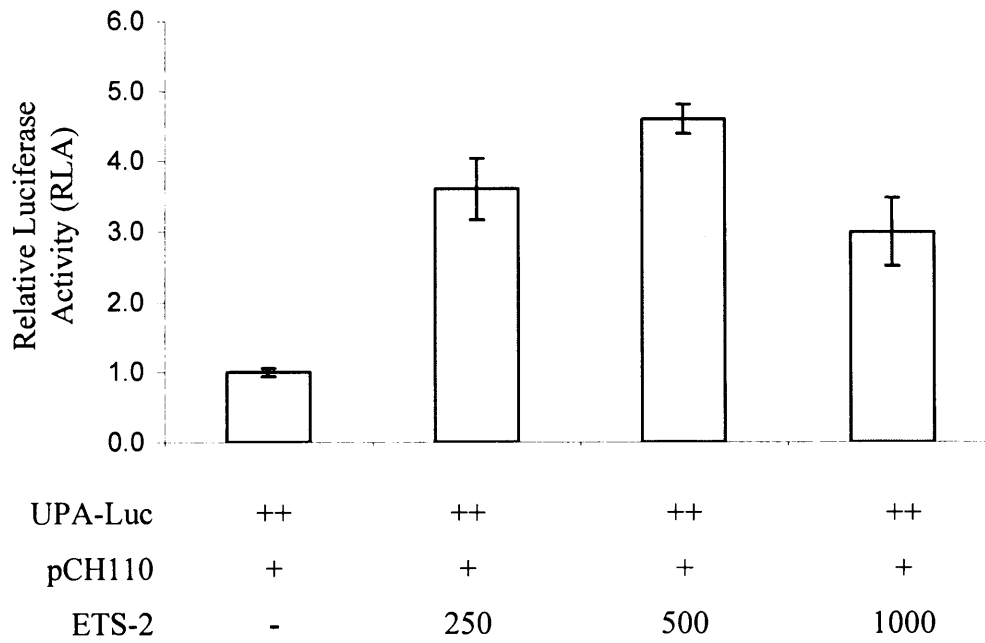
5.6 Activation of luciferase reporters by the ETS-2 transcription factor

ETS-2 is a member of the ETS transcription factor family that induces gene expression in response to a wide range of stimuli (Oikawa and Yamada, 2003). Activation of gene transcription by a number of the family members involves the recruitment of CBP/p300, and for ETS-2 this recruitment is mediated by binding to two discrete regions in the global coactivators: the C/H1 domain and the SID (Figure 1.8). ETS-2 has been shown to act in concert with the haematopoietic ETS protein PU.1 during the induction of responsive genes required for myeloid cell differentiation (Ross *et al.*, 1998; Sevilla *et al.*, 2001). GST pulldown studies in this laboratory (Matsuda *et al.*, 2003) have indicated that binding of ETS-2 and SRC1 to the CBP SID domain is mutually exclusive. In addition, co-transfection of ETS-2 results in an inhibition of ER α /SRC1-mediated reporter

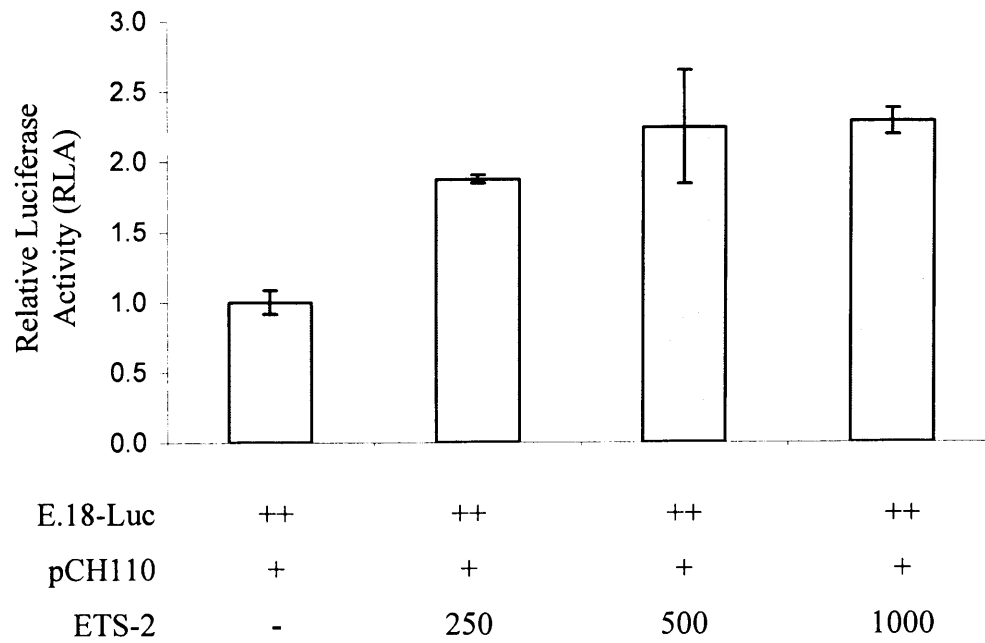
Figure 5.6: Activation of the UPA-Luc and E.18-Luc luciferase reporters by ETS-2 expression in the COS-1 cell line

COS-1 cells were transfected in triplicate with 100 ng pCH110 β -galactosidase reporter, either 500 ng UPA-Luc (a) or E.18-Luc (b) luciferase reporter, and ETS-2 expression plasmid as shown (“-” indicates no DNA, “+” 100 ng DNA, “++” 500ng DNA, and “number” amount of DNA in ng). The cells were harvested 48 hr after transfection and luciferase and β -galactosidase activities of each cell-free lysate measured using a dual assay. The luciferase: β -galactosidase ratios were then calculated and plotted as Relative Luciferase Activity, with the ratio upon transfection of reporters alone set to a value of 1. Error bars show the calculated S.E.M.

a)



b)



transcription, suggesting that competition for limiting amounts of CBP within a cell may result in negative crosstalk between different transcription factors. The ability of MOZ-TIF2 to inhibit NR and p53-mediated transcription, both of which recruit CBP through its SID, suggested that transcriptional activation by ETS-2 might also be affected by expression of the leukaemogenic fusion protein. In order to investigate this, the luciferase reporters E.18-Luc and UPA-Luc (gifts from Dr. M. Ostrowski, Ohio State University, USA) were investigated to determine whether luciferase expression could be induced by co-transfection of ETS-2, and whether such activation would be inhibited by MOZ-TIF2 expression.

Luciferase expression from the E.18-Luc reporter was driven by a consensus ETS-response element fused to the c-fos promoter (with the latter's two internal ETS-binding sites destroyed). The UPA-Luc reporter consisted of the ETS-response element from the urokinase plasminogen activator-1 (UPA) promoter fused to the proximal UPA promoter to drive expression of the luciferase reporter gene.

FNpcDNA3:ETS-2 (gift from Dr. Ostrowski, Ohio State University, USA) was titrated in transient transfection experiments of COS-1 cells in the presence of 100 ng pCH110 β -galactosidase and 500 ng of either E.18-Luc or UPA-Luc (Figure 5.6). Stimulation of the E.18-Luc reporter by ETS-2 in this cell line was very weak, with a maximal reporter activity obtained of just 2.3-fold with 1 μ g ETS-2 expression plasmid (Figure 5.6a). Co-transfection of the ETS-2 construct with the UPA-Luc reporter resulted in a 3.6-fold activation with 250 ng ETS-2 and 4.6-fold with 500 ng. The calculated reporter activation with 1 μ g ETS-2 was less than that seen with the lower amounts of transfected ETS-2 DNA, possibly due to squelching, as has been shown to occur with NRs and their coactivators (Meyer *et al.*, 1989).

In summary, ETS-2 expression resulted in a weak induction of luciferase activity with both the E.18-Luc and UPA-Luc reporters. The calculated reporter activity upon co-transfection of 250 ng ETS-2 was greater with the UPA-Luc luciferase reporter than with the E.18-Luc reporter. Therefore this luciferase reporter was used to test the effects of MOZ-TIF2 expression on transcription mediated by ETS-2.

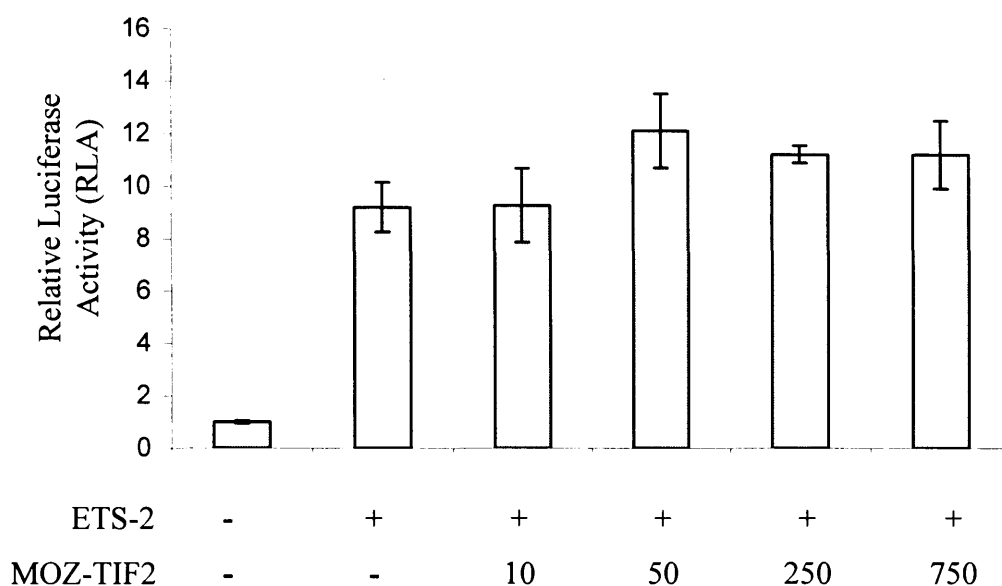


Figure 5.7: Effect of MOZ-TIF2 expression on activation of the UPA-Luc luciferase reporter by ETS-2 in the COS-1 cell line

COS-1 cells were transfected in triplicate with 100 ng pCH110 β -galactosidase reporter, 500 ng UPA-Luc luciferase reporter and expression plasmids as shown (“-” indicates no DNA, “+” 250 ng DNA, and “number” amount of DNA in ng). The cells were harvested 48 hr after transfection and luciferase and β -galactosidase activities of each cell-free lysate measured using a dual assay. The luciferase: β -galactosidase ratios were then calculated and plotted as Relative Luciferase Activity, with the ratio upon transfection of reporters alone set to a value of 1. Error bars show the calculated S.E.M.

5.7 MOZ-TIF2 does not appear to inhibit ETS2-mediated reporter gene transcription

Transient transfection experiments described previously have shown that expression of MOZ-TIF2 resulted in an inhibition of transcription mediated by GAL4-NR fusions in COS-1 cells (Sections 3.7 and 3.9), endogenous NRs in the haematopoietic cell line U937 (Section 5.3), and p53 in HeLa cells (Section 5.5). Experiments investigating the inhibition of NR-mediated transcription suggested that this effect was due to the presence of the AD1 domain in the fusion, which interacts with the SID of the global coactivator CBP (Section 4.11). Given that ETS-2 also utilises a SID interaction during recruitment of CBP for transcription activation (Jayaraman *et al.*, 1999; Lin *et al.*, 2001), MOZ-TIF2 was co-transfected with 250 ng ETS-2, 500ng of the luciferase reporter UPA-Luc and 100 ng β -galactosidase reporter pCH110, to determine whether expression of the fusion inhibited ETS-2 mediated transcription. As shown in Figure 5.7, transfection of ETS-2 resulted in a 9-fold activation of luciferase activity. Titration of up to 750 ng MOZ-TIF2 expression vector did not lead to a reduction in this value, suggesting that MOZ-TIF2 was unable to inhibit the induction of reporter expression by ETS-2.

In summary, therefore, MOZ-TIF2 does not appear to inhibit the transcriptional activity of ETS-2 in transient transfection assays. MOZ-TIF2 expression in these experiments was not confirmed. However, given that the cell line, transfection conditions and constructs used during the ETS-2 experiments were identical to those for the NR experiments, and that epitope-tagged MOZ may be detected via immunofluorescence in COS-1 cells, there is no evidence to suggest MOZ-TIF2 would not be expressed when transfected here.

5.8 Activation of the luciferase reporter pT109-Luc by AML1

During this investigation into the effects of the leukaemogenic fusion protein MOZ-TIF2 on NR-mediated transcription and other transcription factors that utilise the SID domain of CBP, a paper was published describing the presence of both MOZ and CBP in an AML1 complex (Kitabayashi *et al.*, 2001a). AML1 is a transcription factor that plays a key role in the early development of all haematopoietic lineages (Lutterbach and Hiebert, 2000; Skalnik, 2002; Michaud *et al.*, 2003). Therefore, the interaction of MOZ with AML1 suggested a possible role of this MYST family protein in haematopoietic cells. Both MOZ

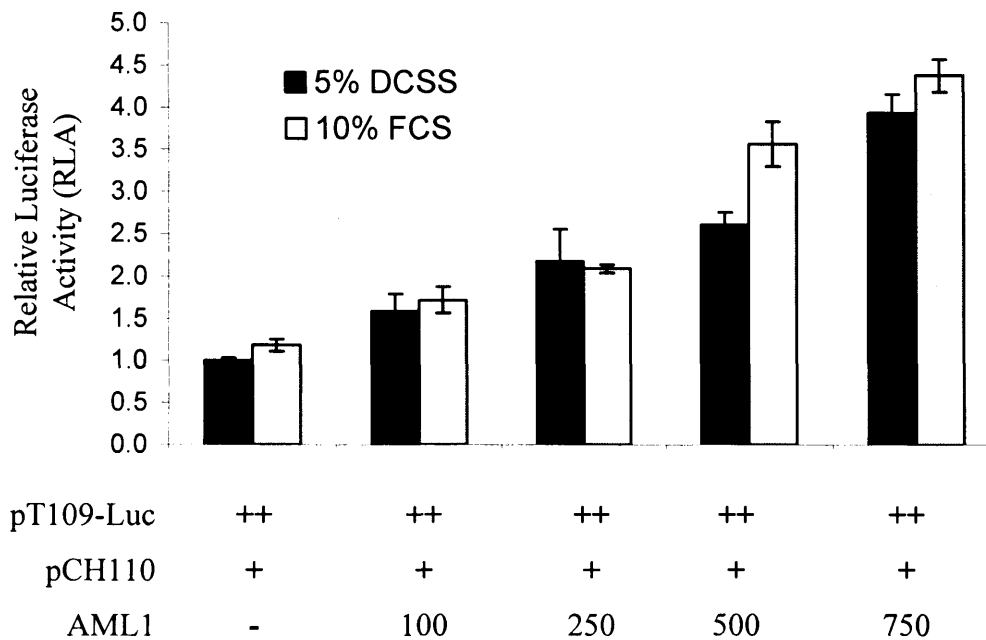


Figure 5.8: Activation of the pT109-Luc luciferase reporter by AML1 in COS-1 cells grown in 5% dextran/charcoal-stripped serum or 10% foetal calf serum

COS-1 cells grown in either 5% dextran/charcoal-stripped foetal calf serum (DCSS) or 10% foetal calf serum (FCS) were transfected in triplicate with 100 ng pCH110 β -galactosidase reporter, 500 ng pT109-Luc luciferase reporter and the pSG5-AML1 expression plasmid as shown (“-” indicates no DNA, “+” 100 ng DNA, “++” 500 ng DNA, and “number” amount of DNA in ng). The cells were harvested 48 hr after transfection and luciferase and β -galactosidase activities of each cell-free lysate measured using a dual assay. The luciferase: β -galactosidase ratios were then calculated and plotted as Relative Luciferase Activity, with the ratio upon transfection of reporters alone set to a value of 1. Error bars show the calculated S.E.M.

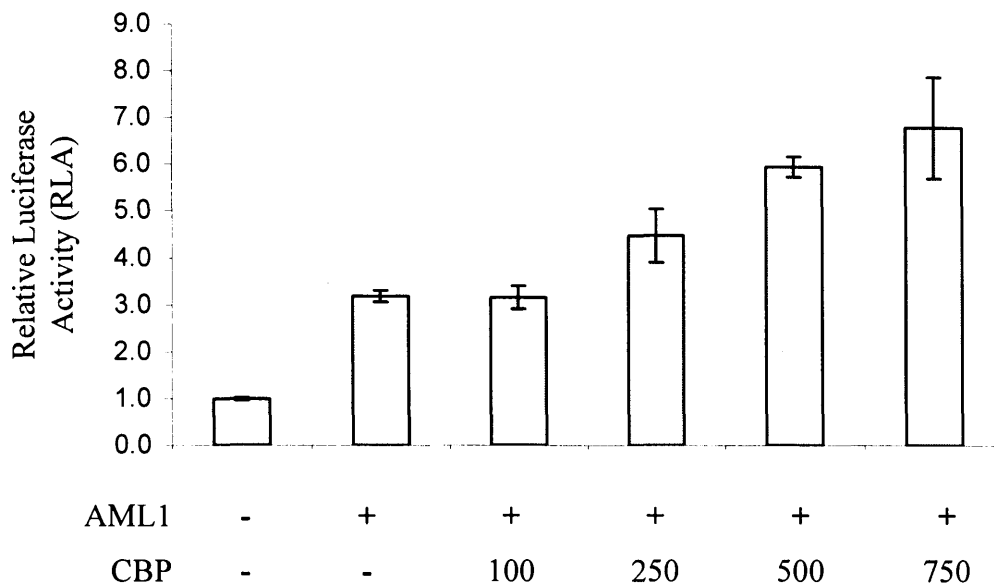


Figure 5.9: Effect of CBP on activation of the pT109-Luc luciferase reporter by AML1 in the COS-1 cell line

COS-1 cells grown in 10% foetal calf serum (FCS) were transfected in triplicate with 100 ng pCH110 β -galactosidase reporter, 500 ng pT109-Luc luciferase reporter and AML1 and CBP expression plasmids as shown (“-” indicates no DNA, “+” 500 ng DNA, and “number” amount of DNA in ng). The cells were harvested 48 hr after transfection and luciferase and β -galactosidase activities of each cell-free lysate measured using a dual assay. The luciferase: β -galactosidase ratios were then calculated and plotted as Relative Luciferase Activity, with the ratio upon transfection of reporters alone set to a value of 1. Error bars show the calculated S.E.M.

and CBP were shown to acetylate histones and AML1 *in vitro*, and act as coactivators for AML1-mediated transcription *in vivo* (Kitabayashi *et al.*, 2001a). In addition, the effect of expression of the MOZ-CBP leukaemogenic fusion on AML1 transcription was investigated. MOZ-CBP was shown to inhibit the ability of CBP, but not MOZ, to act as a coactivator for AML1. Thus, it appeared possible that fusions involving the MOZ gene might lead to leukaemia, at least in part, through the inhibition of normal AML1 function in myeloid cells. In order to confirm the ability of MOZ and CBP to act as coactivators for AML1, and to determine whether MOZ-TIF2 might inhibit this activity, an AML1-responsive transient reporter activation system was set up. Experiments were carried out in triplicate with error bars indicating the accuracy of the means of the triplicate values.

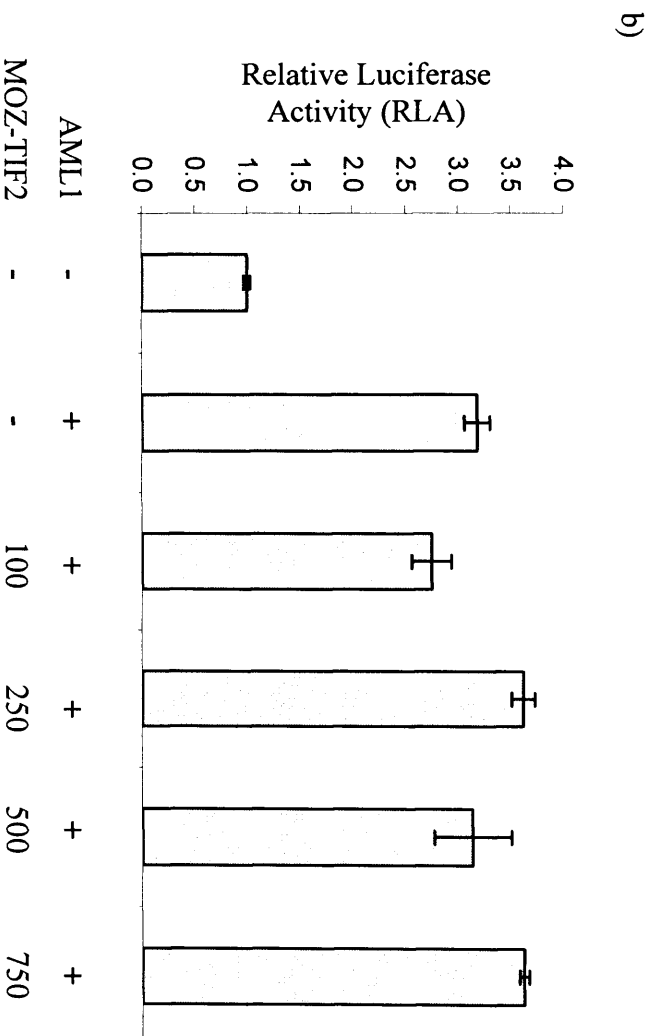
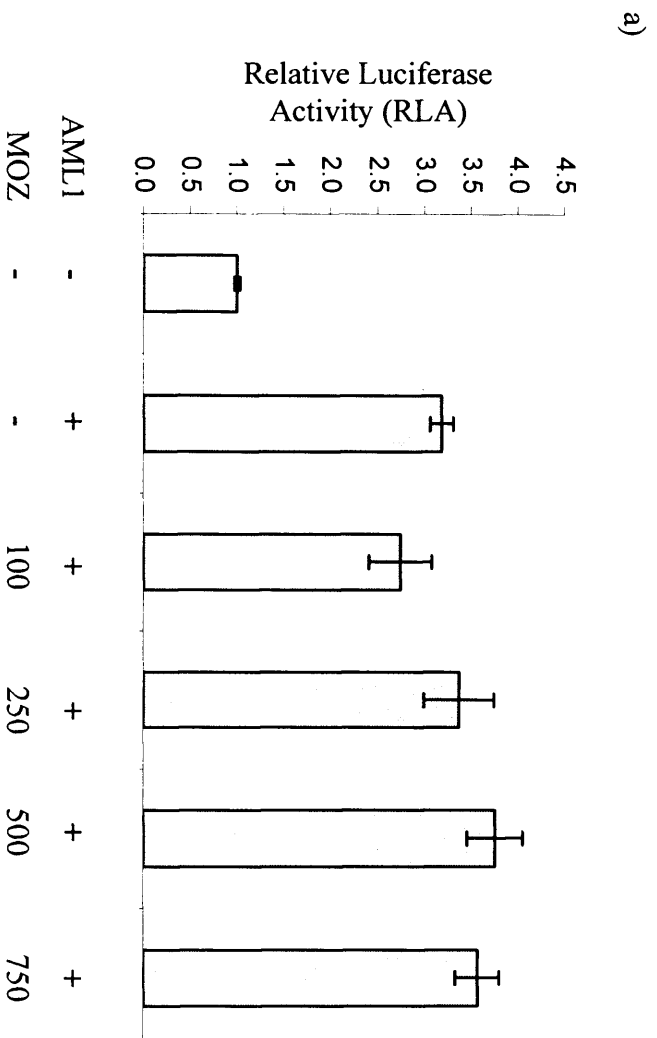
The transcription factor AML1 was tested for its ability to activate the luciferase reporter pT109-Luc, which contains three consensus AML1 binding sites (gifts from Dr. A Zelent, Institute of Cancer Research, London). AML1 titrations were carried out (Figure 5.8) in the presence of either 10% foetal calf serum (FCS) or 5% dextran-charcoal stripped serum (DCSS) to confirm that the presence/absence of ligands had no effect on AML1-mediated transcription. Increasing amounts of transfected AML1 DNA resulted in a small, though measurable increase in fold activation when compared to reporters alone, with a maximal reporter activity of 4-fold with 750 ng AML1. This concentration-dependent activation did not vary appreciably with the serum used. Therefore, all further AML1 transfections were carried out in the presence of 10% FCS, and used 500 ng AML1, as this gave a measurable activation of reporter activity over background.

5.9 CBP, but not MOZ nor MOZ-TIF2, activates AML1-mediated transcription

CBP, MOZ and MOZ-TIF2 were titrated with 500ng AML1 to determine whether their co-expression affected AML1-mediated transcription. As shown in Figure 5.9, addition of 100 ng - 750 ng CBP resulted in an increase in reporter activity when compared to transfection of AML1 alone. In contrast however, neither MOZ (Figure 5.10a) nor MOZ-TIF2 (Figure 5.10b) were able to act as a coactivators for AML1 in this system as co-transfection with either of these expression plasmids did not result in an appreciable increase in reporter activity over that seen with AML1. The finding that MOZ did not act

Figure 5.10: Effect of MOZ and MOZ-TIF2 on activation of the pT109-Luc luciferase reporter by AML1 in the COS-1 cell line

COS-1 cells grown in 10% foetal calf serum (FCS) were transfected in triplicate with 100 ng pCH110 β -galactosidase reporter, 500 ng pT109-Luc luciferase reporter and AML1 and MOZ (a) or MOZ-TIF2 (b) expression plasmids as shown (“-” indicates no DNA, “+” 500 ng DNA, and “number” amount of DNA in ng). The cells were harvested 48 hr after transfection and luciferase and β -galactosidase activities of each cell-free lysate measured using a dual assay. The luciferase: β -galactosidase ratios were then calculated and plotted as Relative Luciferase Activity, with the ratio upon transfection of reporters alone set to a value of 1. Error bars show the calculated S.E.M.



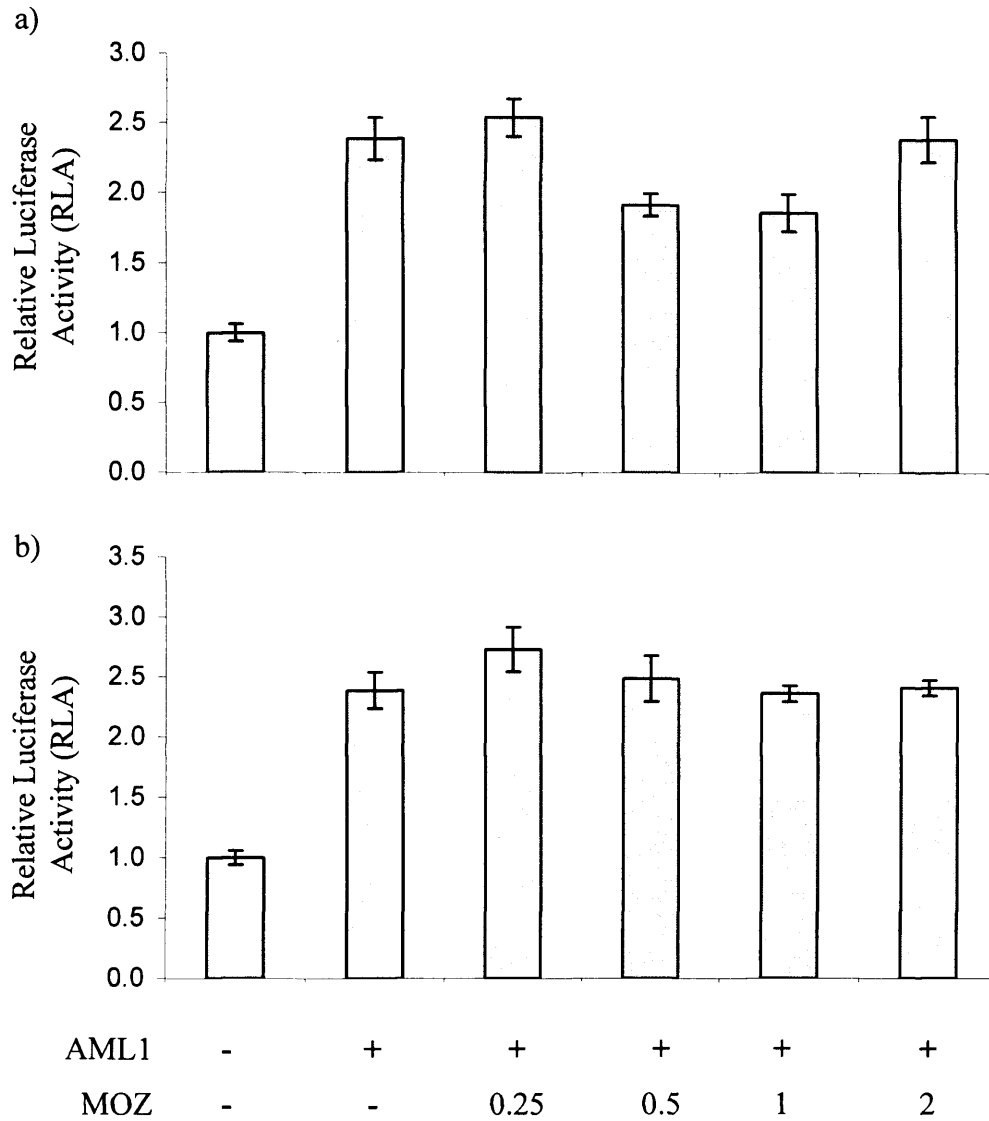


Figure 5.11: Effect of MOZ on pT109-Luc luciferase reporter activation by AML1

COS-1 cells were transfected in triplicate with 100 ng pCH110 β -galactosidase reporter, 500 ng pT109-Luc luciferase reporter and AML1 and FLAG-MOZ (a) or HA-MOZ (b) expression plasmids as shown (“-” indicates no DNA, “+” 0.5 μ g DNA, and “number” amount of DNA in μ g). The cells were harvested 48 hr after transfection and luciferase and β -galactosidase activities of each cell-free lysate measured using a dual assay. The luciferase: β -galactosidase ratios were then calculated and plotted as Relative Luciferase Activity, with the ratio upon transfection of reporters alone set to a value of 1. Error bars show the calculated S.E.M.

as a coactivator for AML1 was in contrast to the published data of Kitabayashi *et al.* (2001) and Bristow *et al.* (2003). Therefore, in order to confirm this data, additional titrations of up to 2 μ g MOZ were carried out using both FLAG and HA epitope-tagged constructs (Figure 5.11). Even at 2 μ g transfected expression vector, MOZ did not potentiate AML1-mediated transcription. Given the ability to detect epitope-tagged MOZ protein upon construct transfection (Figure 3.1, 4.14 and 4.16), the reason for this discrepancy is unknown. It is possible however, that the inability of MOZ to act as a coactivator in COS-1 cells may be due to the lack of expression of additional proteins whose interaction with MOZ is required for its activity. Indirect evidence for such a hypothesis is provided by the finding that coactivation by MOZ does not require the MYST domain (Kitabayashi *et al.*, 2001a), suggesting it must be mediated through protein interactions rather than its enzymatic activity.

In summary therefore, CBP, but not MOZ nor MOZ-TIF2, acts as a coactivator for AML1-mediated transcription activation of the pT109-Luc luciferase reporter in the COS-1 cell line.

5.10 Co-transfection of MOZ-TIF2 with CBP results in a potentiation of AML1/CBP-mediated transcription

The study by Kitabayashi *et al.* (2001) suggested that the leukaemogenic fusion MOZ-CBP inhibited the ability of CBP to act as a coactivator for AML1. Therefore, transfection experiments were carried out in order to investigate the effect of co-transfection of MOZ-TIF2 on AML1/CBP-mediated transcription. As shown in Figure 5.12 transfection of CBP, but not MOZ-TIF2, resulted in an enhancement of reporter activity above that seen with AML1 alone, as seen previously (Figures 5.9 and 5.10). Upon co-transfection of MOZ-TIF2 with CBP the measured reporter activity increased from 5.9-fold (CBP + AML1) to 14-fold (MOZ-TIF2 + CBP + AML1). This suggested that MOZ-TIF2 could act in synergy with CBP to enhance AML1-mediated transcription, despite its inability to act as a coactivator for AML1 when expressed alone.

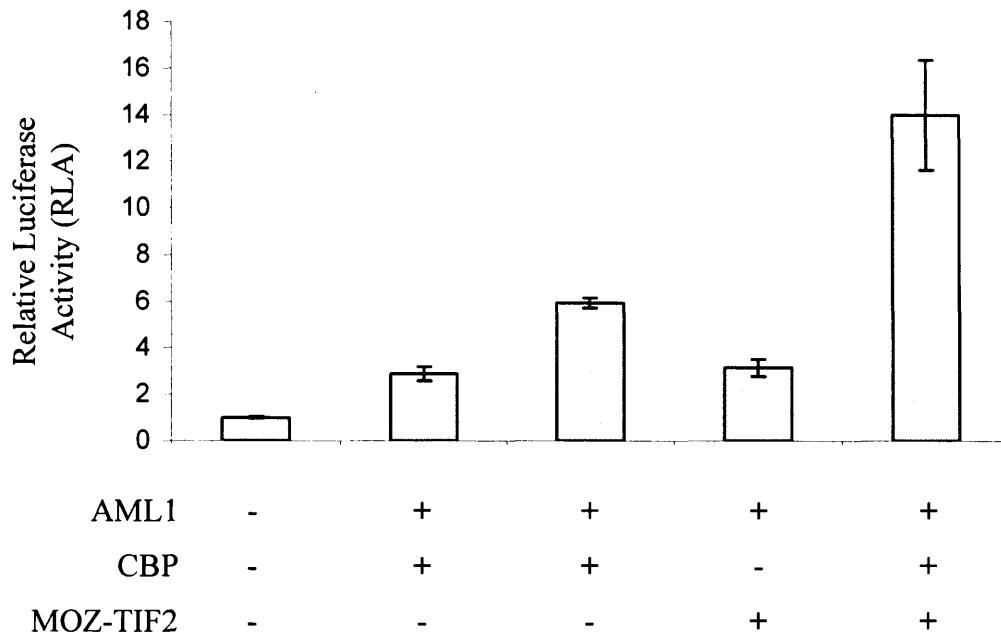


Figure 5.12: Effect of MOZ-TIF2 on AML1/CBP-mediated activation of the pT109-Luc luciferase reporter

COS-1 cells were transfected in triplicate with 100 ng pCH110 β -galactosidase reporter, 500 ng pT109-Luc luciferase reporter and combinations of 500ng AML1, CBP and MOZ-TIF2 as shown (“-” indicates no DNA, “+” 500 ng DNA). The cells were harvested 48 hr after transfection and luciferase and β -galactosidase activities of each cell-free lysate measured using a dual assay. The luciferase: β -galactosidase ratios were then calculated and plotted as Relative Luciferase Activity, with the ratio upon transfection of reporters alone set to a value of 1. Error bars show the calculated S.E.M.

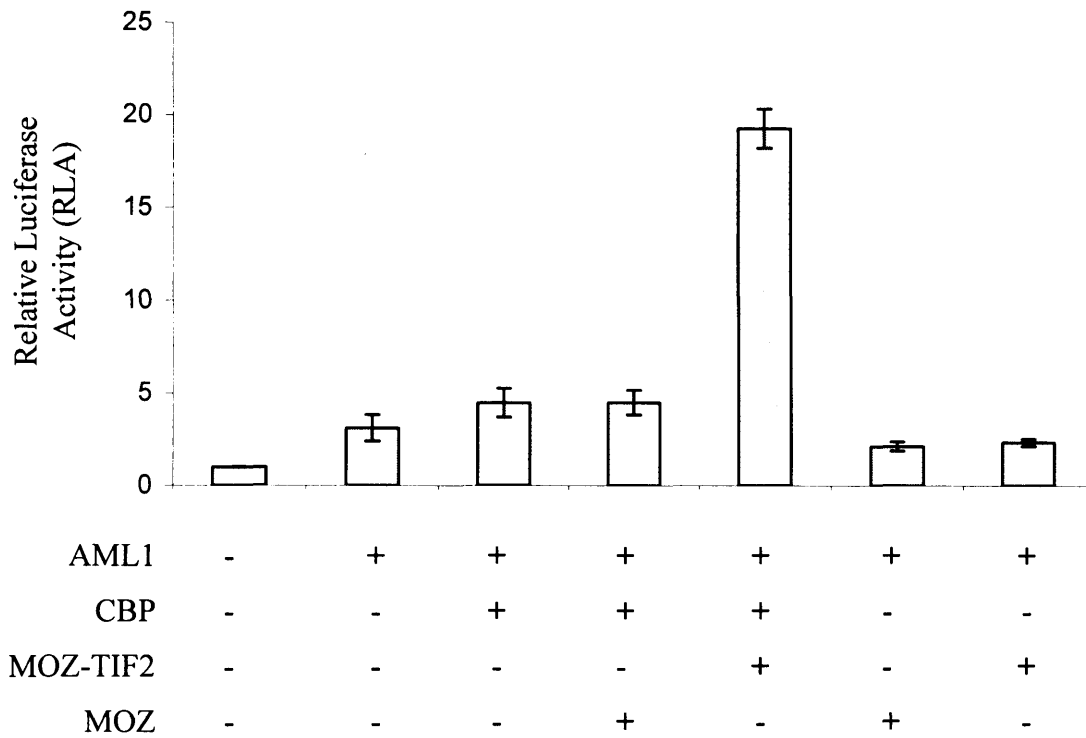


Figure 5.13: Effect of CBP, MOZ and MOZ-TIF2 co-transfection on AML1-mediated activation of the pT109-Luc luciferase reporter

COS-1 cells were transfected in triplicate with 100 ng pCH110 β -galactosidase reporter, 500 ng pT109-Luc luciferase reporter and combinations of 500ng AML1, CBP, MOZ and MOZ-TIF2 as shown (“-” indicates no DNA, “+” 500 ng DNA). The cells were harvested 48 hr after transfection and luciferase and β -galactosidase activities of each cell-free lysate measured using a dual assay. The luciferase: β -galactosidase ratios were then calculated and plotted as Relative Luciferase Activity, with the ratio upon transfection of reporters alone set to a value of 1. Error bars show the calculated S.E.M.

5.11 MOZ does not enhance AML1/CBP-mediated transcription

The study by Kitabayashi *et al.* (2001) suggested that MOZ and CBP could function independently as coactivators of AML1-mediated transcription, and also coactivate synergistically. Given the inability to show MOZ-mediated enhancement of AML1 transcription in COS-1 cells (Figure 5.11), MOZ was co-transfected with CBP to determine whether it could enhance AML1/CBP transcription in a manner similar to MOZ-TIF2 (Figure 5.12). As shown in Figure 5.13, CBP expression with AML1 resulted in an enhancement of AML1-mediated transcription. However, no further increase in activation was seen upon MOZ co-transfection, indicating that MOZ was unable to act as a coactivator for AML1-mediated transcription either alone or in concert with CBP, in this system.

5.12 MOZ-TIF2 enhancement of AML1/CBP-mediated transcription requires the AD1 domain

To begin to investigate the mechanism of MOZ-TIF2-mediated enhancement of AML1/CBP transcription, MOZ-TIF2 or MOZ-TIF2 Δ AD1 were co-transfected with CBP and AML1. As shown in Figure 5.14, MOZ-TIF2 acted in synergy with CBP to activate AML1-mediated transcription. However, MOZ-TIF2 Δ AD1 was not able to enhance AML1/CBP transcription, indicating that the effect of MOZ-TIF2 co-expression with CBP required the presence of the MOZ-TIF2 AD1 domain. This finding suggests that, though MOZ-TIF2 is unable to act as a coactivator for AML1 in this system, the presence of CBP may allow its recruitment to the active AML1 complex through a CBP:SID MOZ-TIF2:AD1 interaction. However, the mechanism by which MOZ-TIF2 acts to enhance CBP activity remains to be elucidated. Further experiments will be required to determine whether domains from MOZ present in MOZ-TIF2 are also required, or whether wild-type TIF2 can enhance AML1/CBP-mediated transcription without the presence of MOZ sequence.

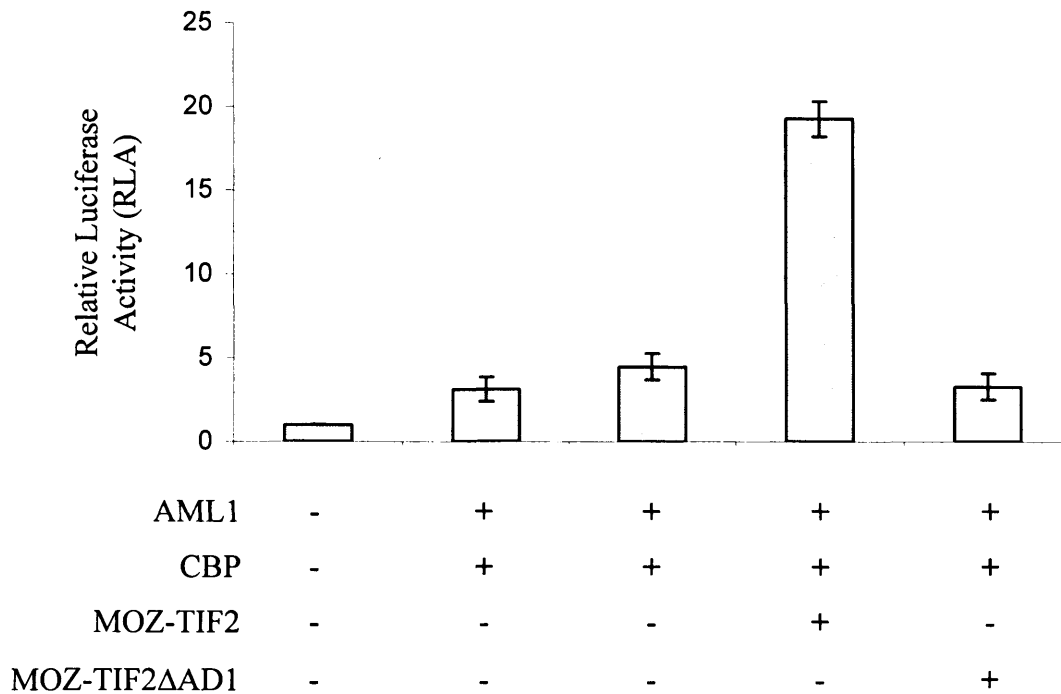


Figure 5.14: Effect of MOZ-TIF2 or MOZ-TIF2ΔAD1 co-transfection on AML1/CBP-mediated activation of the pT109-Luc luciferase reporter

COS-1 cells were transfected in triplicate with 100 ng pCH110 β -galactosidase reporter, 500 ng pT109-Luc luciferase reporter and 500ng AML1, CBP, MOZ-TIF2 and MOZ-TIF2ΔAD1 as shown (“-” indicates no DNA, “+” 500 ng DNA). The cells were harvested 48 hr after transfection and luciferase and β -galactosidase activities of each cell-free lysate measured using a dual assay. The luciferase: β -galactosidase ratios were then calculated and plotted as Relative Luciferase Activity, with the ratio upon transfection of reporters alone set to a value of 1. Error bars show the calculated S.E.M.

In summary, these preliminary experiments suggest that MOZ-TIF2 is unable to act as a coactivator of AML1 transcription when expressed alone. However, it can enhance the ability of CBP to act as an AML1 coactivator when they are co-expressed. This activity requires the presence of the MOZ-TIF2 AD1 domain. In contrast to the studies by Kitabayashi *et al.* (2001), MOZ was unable to act as a coactivator for AML1-mediated transcription, either alone or in concert with CBP, using this transient transfection system. Given this discrepancy, and the publication of a second study showing MOZ enhancement of AML1-mediated transcription during the preparation of this thesis (Bristow and Shore, 2003), further work will be required to investigate the role of MOZ in AML1 transcription.

5.13 Chapter Summary

The experiments described in Chapter 3 of this thesis showed that the MOZ-TIF2 leukaemogenic fusion protein, which is generated by the chromosomal translocation *inv8(p11;q13)*, inhibits the AF2 transcriptional activity of NRs. Those discussed in Chapter 4 suggested that this inhibition required the MOZ-TIF2 AD1 domain, which mediates interaction of the fusion protein with the SID domain of CBP. The transcription inhibition studies were carried out in the COS-1 cell line using GAL4-NR fusions. Therefore, the initial experiments described in this chapter were undertaken to determine whether the inhibitory effects seen in the COS-1 cells were relevant to transcription activation in the haematopoietic cell line U937. This line phenotypically resembles cells of monocytic origin and has been shown previously to express endogenous NRs. Thus, its use allowed an analysis of the effect of transient expression of MOZ-TIF2 on activation of luciferase reporters by endogenous NRs in a cell line reminiscent of AML blasts.

Two luciferase reporters were tested in U937 cells and shown to be activated in response to NR ligands (Figure 5.1). pRep4-RARE was a retinoic acid-responsive luciferase reporter, while activation of p(PPRE)₃-tk-Luc occurred upon addition of the PPAR γ ligand rosiglitazone and RXR ligand 9-*cis* retinoic acid. Co-transfection of increasing amounts of MOZ-TIF2 expression plasmid with either luciferase reporter resulted in a concentration-dependent reduction in luciferase activity (Figures 5.2 and 5.3), suggesting an inhibition of luciferase expression. In contrast, co-transfection of the deletion construct MOZ-TIF2 Δ AD1 did not affect luciferase activity (Figures 5.2 and 5.3). Thus, expression of

MOZ-TIF2, but not MOZ-TIF2 Δ AD1, appeared to inhibit transcription activation by endogenous NRs and coactivators in a haematopoietic cell line. This suggests that the leukaemogenic properties of the chromosomal translocation inv8(p11;q13) might in part be due to the inhibition of transcription of genes regulated by NRs that are required for normal differentiation. In addition, the inability of the MOZ-TIF2 Δ AD1 construct to replicate this inhibition suggests that the MOZ-TIF2 domain required for CBP binding plays an essential role in the mechanism of inhibition.

The finding that the AD1 domain of MOZ-TIF2 was essential for the inhibition of NR transcription suggested that an interaction with the SID domain of CBP might be required for the MOZ-TIF2-mediated effect. Given the requirement for SID binding by the p160 coactivators during NR-mediated transcription and the apparent ability of MOZ-TIF2 to result in the alteration of CBP localisation, it seemed plausible that the MOZ-TIF2 protein may sequester CBP through the SID, thus preventing its interaction with NR complexes. A number of other transcription factors also utilise interactions with the SID domain to recruit CBP during transcription activation (Jayaraman *et al.*, 1999; Lin *et al.*, 2001; Livengood *et al.*, 2002; Scoggin *et al.*, 2001). Thus, expression of the MOZ-TIF2 fusion protein might be predicted to interfere with their transcriptional activity, in addition to affecting NR-mediated transcription. In order to investigate this, preliminary transient reporter studies were carried out using two such factors, p53 and ETS-2. MOZ-TIF2 was found to have no effect on ETS-2-mediated transcription (Figure 5.7). However, an inhibitory effect was seen when MOZ-TIF2 was co-transfected with p53 (Figure 5.5). p53 plays a crucial role in protecting cells against cell stress and uncontrolled proliferation through activating transcription of cell cycle inhibitors such as p21 in response to cell stress (Vousden and Lu, 2002). Thus, an inhibitory effect of MOZ-TIF2 on p53-mediated transcription might facilitate the avoidance of apoptosis-induction that must occur MOZ-TIF2-expressing blasts.

A study published in 2001 by Kitabayashi *et al.* described the identification of the MOZ protein in a complex with AML and CBP. This work suggested that both MOZ and CBP acted as coactivators for the AML1 protein, which is a master regulator of haematopoiesis (Lutterbach and Hiebert, 2000). In addition, experiments using a MOZ-CBP construct indicated that expression of the MOZ-CBP fusion protein resulted in an inhibition of CBP

enhancement of AML1-mediated transcription. Given the similarities in the leukaemic phenotypes of cells expressing MOZ-CBP and MOZ-TIF2 fusions, it appeared possible that their mechanism of leukaemogenesis might be similar. Therefore, preliminary transient transfection experiments were carried out to determine whether the MOZ-TIF2 fusion would inhibit AML1-mediated transcription. A reporter assay system was set up involving activation of the pT109-Luc luciferase reporter by AML1 in COS-1 cells (Figure 5.8). Using this system, CBP was shown to act as a coactivator for AML1 (Figure 5.9). However, no coactivator function of MOZ was detected (Figure 5.10a and 5.11), in contrast to the studies by Kitabayashi *et al.* (2001) and Bristow *et al.* (2003), which showed a consistent coactivator function of MOZ in AML1-driven reporter assays. This discrepancy suggests that there may be cell line-specific effects and therefore further work will be required to confirm these findings in haematopoietic cells such as the U937 line. Titrations of MOZ-TIF2 indicated that this fusion did not act as a coactivator for AML1 when transfected alone (Figure 5.10b). However, co-transfection of MOZ-TIF2 with CBP and AML1 resulted in an enhancement of AML1/CBP-mediated transcription, suggesting that the MOZ-TIF2 fusion could act as a coactivator in the presence of CBP (Figure 5.12). This activity was shown to require the presence of the MOZ-TIF2 AD1 domain (Figure 5.14), though further studies will be required to determine which other regions of MOZ-TIF2 are essential for this coactivator function.

Taken together, these results confirm the negative effect of MOZ-TIF2 on NR activity, extending it to endogenous factors in a haematopoietic cell line, and shed light on other factors, such as p53, which may be inhibited by the presence of MOZ-TIF2. In addition, the preliminary studies using AML1 suggest that MOZ-TIF2 could potentially increase the activity of some transcription factors.

Chapter Six:

Discussion

6.1 Function of MOZ

The leukaemogenic chromosomal inversion inv8(p11;q13) that gives rise to Acute Myeloid Leukaemia-M5 (AML) was shown in 1998 to result in the fusion of the MOZ gene to the TIF2 gene (Carapeti *et al.*, 1998b). The function of MOZ was unknown, though it was associated with a distinct subtype of AML characterised by its fusion to the CBP gene (Borrow *et al.*, 1996). At the outset of this study it was assumed that MOZ might be a transcriptional regulator due to the presence of the MYST domain, which had been shown to mediate histone acetylation when present in other proteins (reviewed in Utley and Cote, 2003). Although the ability of MOZ to acetylate histone H3 lysine 14 and Histone H4 lysines 5, 8, 12 and 16 has been demonstrated (Kitabayashi *et al.*, 2001a), the physiological role *in vivo* remains to be established. Some evidence for a role in transcription has been suggested by the Kitabayashi *et al.* (2001) and Bristow *et al.* (2003) studies of transcription activation by AML1. However, the MYST domain, and thus HAT activity, was not required for MOZ-mediated coactivation of AML1 (Kitabayashi *et al.*, 2001a) suggesting MOZ has other, as yet undetermined, functions in the cell. Indeed, experiments described in this study were unable to detect an effect of MOZ on transcription by AML1 or NRs, though a cell-type or promoter-specific effect (e.g. a requirement for additional cofactors absent in our experiments) cannot be ruled out. Thus, at present, the evidence in support of MOZ acting as a transcriptional modulator is weak. Further studies such as RNAi, gene expression profiling and gene knockout in mice will be required to provide insight into the physiological function of MOZ.

6.2 TIF2, Nuclear Receptors and a potential role in haematopoiesis

TIF2 was first identified as a Nuclear Receptor (NR) cofactor (Voegel *et al.*, 1996) that functioned as a platform protein to recruit the global coactivator and histone acetyltransferase (HAT) CBP/p300 (Voegel *et al.*, 1998). Studies (reviewed in Collins and Tsai, 1996; Tenen *et al.*, 1997) investigating the role of NR proteins (Brown *et al.*, 1997; Sunaga *et al.*, 1997) and their ligands (Olsson and Breitman, 1982; Olsson *et al.*, 1983; Liu *et al.*, 1996a; Liu *et al.*, 1996b) have suggested a role for Nuclear Receptors in the normal differentiation pathways of haematopoietic cells. In addition, the RAR α gene had been identified as the common fusion partner of several leukaemogenic translocations that result in the M3 subtype of AML (reviewed in Parrado *et al.*, 1999; Zelent *et al.*, 2001). Thus,

cellular alterations that affect NR transcription might also be expected to affect normal haematopoietic processes. Given the role of TIF2 as an NR coactivator, the identification of the MOZ-TIF2 fusion implied that the ability of NRs to mediate haematopoietic differentiation might be compromised in cells in which it was expressed. However, as the transcriptional targets (if any) of MOZ were unknown, it was possible that the pathways involving MOZ might also be affected by expression of the leukaemogenic fusion protein. In addition, as TIF2 interacts with CBP, CARM1 and potentially other factors, a third possibility remained that other pathways requiring these proteins might be compromised in cells expressing MOZ-TIF2. As a result, the studies described here focussed on the activation of transcription by NRs. However, preliminary investigations were also carried out of the effects of MOZ-TIF2 expression on AML1, p53 and ETS-2 -mediated transcription.

6.3 Effect of MOZ-TIF2 on Nuclear Receptor-mediated transcription

In order to begin to investigate the effect of expression of epitope-tagged MOZ-TIF2 and MOZ constructs on ligand-dependent NR-mediated transcription, GAL4-NR fusion proteins were employed in a transient transfection system. These fusion proteins were comprised of the ligand-binding domain of RXR α , ER α or RAR α fused to the DNA-binding domain of GAL4. Thus, all three proteins bound a GAL4-responsive luciferase and were able to induce luciferase expression upon addition of their appropriate ligand. Preliminary experiments indicated that neither MOZ nor MOZ-TIF2 were able to potentiate transcription by these GAL4-NR fusions at concentrations at which TIF2 had a significant effect, suggesting they were unable to act as ligand-dependent NR coactivators. These studies however, suggested that MOZ-TIF2 might function to inhibit NR transcription. Therefore, to investigate this further, MOZ-TIF2 was co-expressed with TIF2 and the GAL4-NR fusions. Upon inclusion of MOZ-TIF2, but not MOZ, a significant inhibition of GAL4-NR-mediated, TIF2-enhanced, transcription was seen, indicating that MOZ-TIF2 inhibited NR-mediated transcription in this transient system.

To allow determination of the mechanism by which MOZ-TIF2 affected ligand-dependent transcription by GAL4-NR fusions, *in vitro* interaction studies were carried out. These indicated that the MOZ-TIF2 fusion protein was unable to interact with the ligand-binding domain of either ER α or RXR α . This finding was not unexpected given the absence of the

TIF2 NR interaction domain in the MOZ-TIF2 fusion protein, and indicated that MOZ-TIF2 was unable to bind the NR LBD through additional sequences in MOZ, or the C-terminus of TIF2. In contrast to the NR studies, MOZ-TIF2 (but not MOZ) was shown to interact with full-length CBP and specifically, its SID (SRC1-interaction domain). Thus, it appears likely that the inhibition of NR-mediated transcription is due to interaction with, and possible sequestration of, CBP, rather than interaction with the Nuclear Receptors themselves.

6.4 Role of the AD1 in MOZ-TIF2 function

A series of deletion constructs were generated to allow further investigation of the inhibition of ligand-dependent NR-mediated transcription by MOZ-TIF2. The domains required for interaction of TIF2, and its homologue SRC1, with CBP had been previously identified (Voegel *et al.*, 1998; Kalkhoven *et al.*, 1998) and more recently mapped in fine detail (Sheppard *et al.*, 2001). Therefore, two constructs were initially designed in order to investigate the role of the AD1 (CBP-interaction) domain in the MOZ-TIF2 fusion protein. The first construct generated, MOZ-TIF2 Δ AD1, was designed to remove the minimal AD1 sequence from MOZ-TIF2. Analysis of this deletion construct indicated that it was unable to inhibit NR-mediated transcription, or bind CBP. This, coupled with the immunofluorescence analysis and *in vitro* translation that confirmed expression of the full-length deletion protein, suggested that the AD1 sequence was required for MOZ-TIF2 inhibition of ligand-dependent NR-mediated transcription.

The second AD1 construct, MOZ-TIF2mAD1, involved the mutation of three leucines present within the TIF2-derived AD1 sequence. Mutation of these leucines had been shown to result in the reduced binding of TIF2 to CBP, and also lead to a reduction in the ability of full-length TIF2 to act as a coactivator for GAL4-ER α (Voegel *et al.*, 1998). However, when the construct MOZ-TIF2mAD1 was co-transfected with GAL4-NR and TIF2, it resulted in a level of inhibition indistinguishable from wild-type MOZ-TIF2. This finding was unexpected as it suggested that the AD1 might not mediate the inhibitory effect of MOZ-TIF2. However, when reviewed in parallel with the MOZ-TIF2 Δ AD1 data, the most likely explanation for this anomaly appeared to be that the leucine to alanine mutations were not sufficient to inhibit the interaction with CBP *in vivo*. Indeed, the study

by Voegel *et al.* (1998) had suggested that this might be the case based upon analysis of their *in vivo* results. Evidence supporting this hypothesis was subsequently provided by the publication of the solution structure of a complex of the CBP SID and ACTR AD1 domains (Demarest *et al.*, 2002). The structure indicated that binding of the p160 protein to CBP was mediated by a large heterodimerisation interface generated by the two domains. This was in contrast to the interaction of the p160 coactivators with NRs, which is mediated by the binding of leucines present within a small isolated p160 amphipathic α -helix to the NR LBD (Heery *et al.*, 1997). Thus, the minimal mutation of three leucines to alanines in Helix 1 of the AD1 does not appear sufficient to destabilise an interaction involving such a large binding surface. During the preparation of this thesis, it was confirmed in our laboratory using GST pulldown experiments that MOZ-TIF2mAD1 binds the CBP SID *in vitro* (personal communication; S. Matsuda and D. Heery). Thus the mutation is indeed unable to prevent the interaction of MOZ-TIF2 with CBP.

In order to investigate further the role of the AD1 in inhibition of NR transcription by MOZ-TIF2, two additional constructs were designed. The first, MOZ-N, was equivalent to the truncation of MOZ in the MOZ-TIF2 protein. This construct did not affect NR transcription, or bind CBP, confirming that TIF2 sequences were required for both of these events. The second construct, termed MOZ-AD1, fused solely the minimal AD1 sequence (corresponding to that removed in the MOZ-TIF2 Δ AD1 construct) to the N-terminus of MOZ. When analysed in the GAL4-NR luciferase experiments the MOZ-AD1 construct was unable to inhibit NR transcription, suggesting that either TIF2 sequences in addition to the AD1 were required for inhibition of NR-mediated transcription, or that the MOZ-AD1 protein was unable to fold into a conformation that allowed significant interaction with CBP. During the preparation of this thesis MOZ-AD1 was shown to bind weakly to the CBP SID *in vitro* (personal communication; S. Matsuda). Further study will therefore be required to determine whether the inability of MOZ-AD1 to inhibit NR-mediated transcription is due a lack of interaction with CBP *in vivo*.

The initial transfection experiments described in this thesis were carried out in the COS-1 monkey kidney cell-line due to the ease with which these cells could be transfected, and the low level of activity of endogenous NR coactivator proteins (our laboratory, unpublished observations). In addition, the NR experiments were carried out using LBD

fusions to the GAL4 DNA-binding domain to allow analysis of the effect of MOZ-TIF2 expression on multiple NRs. Therefore, in order to relate the findings described thus far to the haematopoietic system, an analysis of the effect of MOZ-TIF2 expression on NR-mediated transcription in the haematopoietic cell line U937, which phenotypically resembles cells of monocytic origin, was carried out. U937 cells express endogenous NRs and coactivators and thus transfection of an NR-responsive luciferase reporter and addition of the appropriate ligand is sufficient to mediate a high level of luciferase expression. These suspension cells may be transfected by electroporation, though the number of cells required is very high due to the cell death that occurs during the procedure, and the efficiency of transfection is very low (personal communication; S. Matsuda). However, a study of the effect of MOZ-TIF2 or MOZ-TIF2 Δ AD1 co-transfection on NR-mediated activation of luciferase constructs was carried out. Two luciferase reporters were used; one that was activated in response to the addition of retinoic acid, and a second that was induced by addition of rosiglitazone, a PPAR γ ligand. Co-transfection of MOZ-TIF2, but not MOZ-TIF2 Δ AD1, with either luciferase construct resulted in an inhibition of luciferase induction. Thus, MOZ-TIF2, but not a deletion construct in which the AD1 had been removed, inhibits NR-mediated transcription in a haematopoietic cell line. This suggests that expression of MOZ-TIF2 in normal myeloid precursors might result in inhibition of gene expression controlled by NRs, and thus affect the normal differentiation of these haematopoietic cells. Further work is required to determine whether the stable expression of MOZ-TIF2 is sufficient to prevent NR ligand-induced differentiation of leukaemic cell lines or haematopoietic cells. To this end, a collaborative study is currently underway to generate haematopoietic stem cells stably expressing MOZ-TIF2 and determine the effect of such expression on cell survival and differentiation.

6.5 The mechanism of MOZ-TIF2 inhibition of NR transcription correlates with the ability of the fusion protein to immortalise haematopoietic cells

During the preparation of this thesis, a study was published by Deguchi *et al.* (2003) investigating the effects of MOZ-TIF2 on normal murine bone marrow cells. Expression of MOZ-TIF2 in primitive murine myeloid progenitors resulted in cell immortalisation, thus allowing sustained proliferation in serial replating experiments and subsequently, in suspension cultures in the presence of exogenous Interleukin-3. This initial requirement for

IL-3 indicated that MOZ-TIF2 must cooperate with the IL-3 signalling pathway in order to immortalise haematopoietic progenitors. Introduction of MOZ-TIF2-transduced bone marrow cells into mice resulted in the development of a fatal haematopoietic malignant disease with a latency of 90 days. Upon transplantation of bone marrow into secondary recipients the latency period was reduced to 35-42 days. This reduction in latency upon transplantation, combined with the initial requirement for IL-3 for growth of MOZ-TIF2-transduced bone marrow cells in suspension culture, suggested secondary mutations are likely required in order for the haematopoietic disease to progress to a fully malignant phenotype. Such a mutation in the tyrosine kinase FLT3 has been described in a patient with the MOZ-TIF2 translocation (Billio *et al.*, 2002) and is recognised as a requirement for a number of leukaemias resulting from chromosomal translocations (Kelly and Gilliland, 2002).

The domains of MOZ-TIF2 that were required for MOZ-TIF2-induced transformation of bone marrow progenitors were also analysed in the study by Deguchi *et al.* (2003). Deletion analysis confirmed that the TIF2 AD1 domain and MOZ MYST domain were required, but that the MOZ-derived PHD zinc fingers were not. In addition, Deguchi *et al.* (2003) tested the effect of mutation of the AD1 domain. In contrast to the mutant described in this thesis, eight residues contained within two of the three LXXLL motifs present in the core of the AD1 sequence were mutated. These mutations were sufficient to prevent binding to an extended CBP SID *in vitro* (in contrast to our three leucine mutation construct) and resulted in a loss in the immortalisation ability of the construct. Thus, it appears that a more severe mutation of the AD1 than was used in the GAL4-NR transcription experiments could be sufficient to affect the ability of MOZ-TIF2 to bind CBP and thus inhibit NR-mediated transcription. Further work will be required to design and test this construct and confirm whether this is indeed the case.

The final construct examined by Deguchi *et al.* (2003), MOZ-CID (CBP-interaction domain), was generated by restriction enzyme digestion and subsequent self-ligation that placed the TIF2 sequence C-terminal to the AD1 domain out of frame. This construct was found to immortalise cells in a manner similar to full-length MOZ-TIF2 suggesting that the TIF2 sequence 3' of the AD1 (CID) is not required for immortalisation. This initially appears in contrast to the findings described in this thesis where no effect of MOZ-AD1

was detected in transfection experiments. However, the MOZ-AD1 construct tested for its ability to inhibit NR-mediated transcription was comprised solely of the minimal AD1 sequence fused to MOZ, whereas the MOZ-CID construct described by Deguchi *et al.* (2003) contained significantly more TIF2 sequence N-terminal to the AD1, and indeed some sequence C-terminal to it. Thus, it is possible that this extended construct may be able to adopt a conformation *in vivo* that is not stable when solely the minimal AD1 sequence is attached to the MOZ sequence. The MOZ-CID construct does however confirm that the TIF2 AD2 domain, and therefore CARM1 interaction, is not required for leukaemogenesis.

In summary, the study by Deguchi *et al.* (2003) indicated that expression of MOZ-TIF2 in haematopoietic progenitor cells resulted in their immortalisation, and the development of a fatal haematopoietic disease when the cells were subsequently introduced into irradiated mice. This disease development was dependent upon the presence of the MOZ MYST domain and the TIF2-derived AD1, but not other sequences of TIF2. This requirement for the AD1 correlates well with the findings described in this thesis indicating that inhibition of NR-mediated transcription by MOZ-TIF2 requires this domain. Given that NRs play a role in myeloid cell differentiation it is possible that one mechanism through which the AD1 mediates its effects is inhibition of NR transcription. Clearly however, the finding that the MOZ MYST domain is also required indicates that other mechanisms are involved as this domain would not be expected to directly affect NR-mediated transcription. To confirm this, a MOZ-TIF2 construct containing mutations that inactivate its HAT activity must be tested for its ability to inhibit NR-mediated transcription.

6.6 MOZ-TIF2 forms a mesh-like nuclear localisation pattern and mislocalises CBP

In order to confirm expression of the epitope-tagged MOZ, MOZ-TIF2 and derivative constructs utilised during the research described here, immunofluorescence analysis of transfected cells was carried out. These studies indicated that MOZ-TIF2 formed a mesh-like nuclear staining pattern that was distinct from the speckled localisations of both MOZ and TIF2. The localisation of MOZ-TIF2mAD1 was found to be indistinguishable from that of MOZ-TIF2. In contrast, MOZ-TIF2 Δ AD1 and MOZ-AD1 patterns were indicative of MOZ. Thus, it appeared that the ability of the constructs to inhibit NR-mediated

transcription correlated with their sub-nuclear localisation. Given the ability of MOZ-TIF2 to bind full-length CBP *in vitro* and *in vivo* (in contrast to MOZ which appeared to bind CBP *in vivo* in a weak, possibly indirect manner) experiments were carried out to determine whether MOZ-TIF2 expression affected the localisation of endogenous CBP in COS-1 cells. In the presence of exogenous MOZ or TIF2, endogenous CBP localised to discrete nuclear speckles that were identified as PML bodies (personal communication; K. Kindle). However, upon transfection of MOZ-TIF2, but not MOZ-TIF2 Δ AD1, CBP was lost from these speckles and showed a diffuse staining pattern. Thus, expression of MOZ-TIF2 resulted in the mislocalisation of CBP in an AD1-dependent manner. This mislocalisation was also seen when MOZ-TIF2mAD1, but not MOZ-AD1, was transfected, suggesting that the ability to inhibit NR-mediated transcription correlated with interaction with, and mislocalisation of, CBP. These findings provided further evidence that the mutation of the three leucine residues present within the AD1 domain was not sufficient to prevent an interaction of MOZ-TIF2 with CBP and in addition, suggested that the minimal AD1 sequence fused to MOZ in the MOZ-AD1 construct was unable to interact with CBP *in vivo*.

To confirm the ability of MOZ-TIF2 to interact with, and mislocalise, CBP *in vivo*, additional immunofluorescence studies have been carried out by Dr. K. Kindle (Troke *et al.*, 2003). Analysis of the percentage of cells containing CBP speckles when either mock-transfected or MOZ-, MOZ-TIF2- or MOZ-TIF2 Δ AD1- transfected was carried out by Z-sectioning. This technique involves analysing multiple horizontal focal planes through each cell to determine whether speckles are present anywhere within the cell. These experiments indicated that the expression of MOZ-TIF2, but not MOZ or MOZ-TIF2 Δ AD1, resulted in the statistically significant complete loss of CBP from PML bodies in 42% of expressing cells (Chi-square analysis, $\chi^2(2) = 13.12$, $p < 0.005$), though the PML bodies themselves remained intact. In addition, the direct interaction of MOZ-TIF2 with CBP *in vivo* was confirmed by FRET photobleach analysis using CFP-CBP as the donor and YFP-MOZ-TIF2 or YFP-MOZ-TIF2 Δ AD1 as the acceptor proteins (Troke *et al.*, 2003). Fluorescence resonance energy transfer (FRET) involves the absorption of the emitted energy from the CFP domain by the YFP fluorophore (Day *et al.*, 2001). This absorption may only occur if the two fluorophores are within 10 nm of each other, thus indicating very close association and probable interaction of the partner domains. If such

absorption occurs, it results in a reduced level of emitted light at the CFP emission wavelength. However, if the acceptor protein (YFP-MOZ-TIF2) is photobleached by a high intensity of light at its absorption spectrum, it will subsequently be unable to absorb the light emitted by the CFP and thus the amount of light detected at the CFP emission wavelength will increase.

Prior to the FRET analysis, the YFP-MOZ-TIF2 and YFP-MOZ-TIF2 Δ AD1 proteins were examined for their ability to inhibit NR-mediated transcription, and their sub-cellular localisation was confirmed. YFP-MOZ-TIF2, but not YFP-MOZ-TIF2 Δ AD1, inhibited NR-mediated transcription (data not shown), and both proteins localised to patterns indicative of their corresponding non-fluorescently tagged proteins (personal communication; K. Kindle). Thus, the addition of the fluorescent tag did not appear to affect the MOZ-TIF2 constructs. FRET photobleaching experiments using YFP-MOZ-TIF2 gave a calculated FRET efficiency of $33.7\% \pm 7.0\%$ while those in which YFP-MOZ-TIF2 Δ AD1 was expressed with CFP-CBP gave a reduced FRET efficiency of $15.2\% \pm 6.9\%$ (Trope *et al.*, 2003). Statistical analysis confirmed that this reduction was significant ($p < 0.001$, $n = 25$). Thus, MOZ-TIF2 interacts directly with CBP in live cells and the AD1 domain mediates this interaction.

In conclusion therefore, MOZ-TIF2 interacts with CBP in live cells and leads to its mislocalisation from PML bodies. This interaction is mediated by the TIF2-derived AD1 domain present in the leukaemogenic fusion protein. This domain also appears to mediate the ability of MOZ-TIF2 to inhibit transcription by endogenous NRs and coactivators in haematopoietic cells, suggesting that it might function by sequestering CBP and preventing recruitment of the global coactivator to active NR complexes.

6.7 Effect of MOZ-TIF2 expression on transcription activation by p53 and ETS-2

The studies discussed thus far indicated that the interaction of MOZ-TIF2 with CBP is mediated by their AD1 and SID domains respectively. This interaction results in the inhibition of NR-mediated transcription, likely through the sequestration of CBP from active NR complexes to which it would normally be recruited by the p160 proteins. Recent studies have indicated that a number of other transcription factors mediate binding to CBP

in part through the SID domain (Scoggin *et al.*, 2001; Livengood *et al.*, 2002; Lin *et al.*, 2001; Matsuda *et al.*, 2003). This finding has led to the theory of competition for limiting CBP within the cell and thus cross-talk between different signalling pathways attempting to activate gene expression (Matsuda *et al.*, 2003). Given the ability of MOZ-TIF2 to inhibit NR-mediated transcription, it appeared possible that the leukaemogenic fusion protein might also affect other NRs that recruit CBP through an interaction with the SID. In order to investigate this hypothesis, two such transcription factors were analysed in preliminary experiments to determine whether their ability to activate transcription was affected by MOZ-TIF2.

The ETS-2 protein is a member of the ETS transcription factor family (Oikawa and Yamada, 2003) that includes the PU.1 protein, with which it cooperates to activate transcription in myeloid cells (Ross *et al.*, 1998; Sevilla *et al.*, 2001). In contrast to NRs, which solely bind the CBP SID, two domains within the global coactivator, the C/H1 and SID (Jayaraman *et al.*, 1999; Lin *et al.*, 2001), mediate ETS-2 interaction with CBP. In preliminary experiments MOZ-TIF2 expression did not inhibit ETS-2-mediated transcription of a luciferase reporter construct. Thus MOZ-TIF2 does not appear to inhibit transcription by the ETS-2 protein. This finding was unexpected given the ability of MOZ-TIF2 to bind the SID. However, analysis of the ETS-2 interaction with CBP has indicated that the only one of the two ETS-2 binding sites in CBP is required for CBP to function as a coactivator for ETS-2 (Jayaraman *et al.*, 1999). Thus, though MOZ-TIF2 might act to inhibit ETS-2 recruitment of CBP via the SID, an interaction of ETS-2 with the C/H1 would be sufficient to recruit CBP to the gene promoter. This hypothesis leads to the interesting supposition that through ETS-2 interaction with the CBP C/H1 domain, and MOZ-TIF2 binding to the SID, MOZ-TIF2 might actually be recruited to active ETS-2 complexes. Further studies utilising co-immunoprecipitation experiments would be required to investigate this and determine whether it might affect normal cell signalling control of ETS-2 transcription.

p53 plays a crucial role as a tumour suppressor protein acting downstream of a number of signalling pathways that respond to oncogenic alterations or uncontrolled cell proliferation (Vousden and Lu, 2002). p53 binds to 3 separate regions within CBP (Grossman, 2001; Livengood *et al.*, 2002) but in contrast to ETS-2, specifically mediates its transcriptional

activation activity through recruitment of CBP to target promoters via interaction with the SID (Livengood *et al.*, 2002). Preliminary studies indicated that expression of MOZ-TIF2 resulted in a reduction in transcription activation by exogenously expressed p53 in the HeLa cell line. This finding has been confirmed by additional studies carried out in the p53-negative cell line SAOS-2 (personal communication; H. Collins). Further work is ongoing to confirm the domains required for this activity. However, investigations into this finding are likely to provide significant further insights into the mechanism by which haematopoietic cells expressing MOZ-TIF2 are able to overcome the apoptotic signals that usually accompany uncontrolled cell proliferation and/or a block in differentiation.

In summary therefore, it appears that the ability of MOZ-TIF2 to bind the SID domain of CBP results in the inhibition of transcription by factors such as NRs or p53 that require this interaction for transcription activation. However, other transcription factors such as ETS-2 that utilise multiple interactions for CBP recruitment do not appear to be affected by competition with MOZ-TIF2 for SID binding.

6.8 Summary Model for the effect of MOZ-TIF2 expression on NR- and p53-mediated transcription

A schematic summarising one possible mechanism by which MOZ-TIF2 might inhibit Nuclear Receptor- and p53- mediated transcription is shown in Figure 6.1. Activation of transcription by NRs (Figure 6.1a) and p53 (Figure 6.1c) is mediated in part through the recruitment of CBP via its C-terminal SRC1 Interaction Domain (SID) (Sheppard *et al.*, 2001; Livengood *et al.*, 2002). However, expression of MOZ-TIF2 appears to result in the sequestration of CBP due to the interaction of the MOZ-TIF2 AD1 domain with the CBP SID. Thus, an interaction between CBP and the active DNA-bound NR or p53 complex is prevented and full transcription activation does not occur (Figure 6.1b and d). This sequestration of CBP by MOZ-TIF2 is reflected by a loss of CBP from PML bodies, as shown by the immunofluorescence studies discussed in Section 6.6.

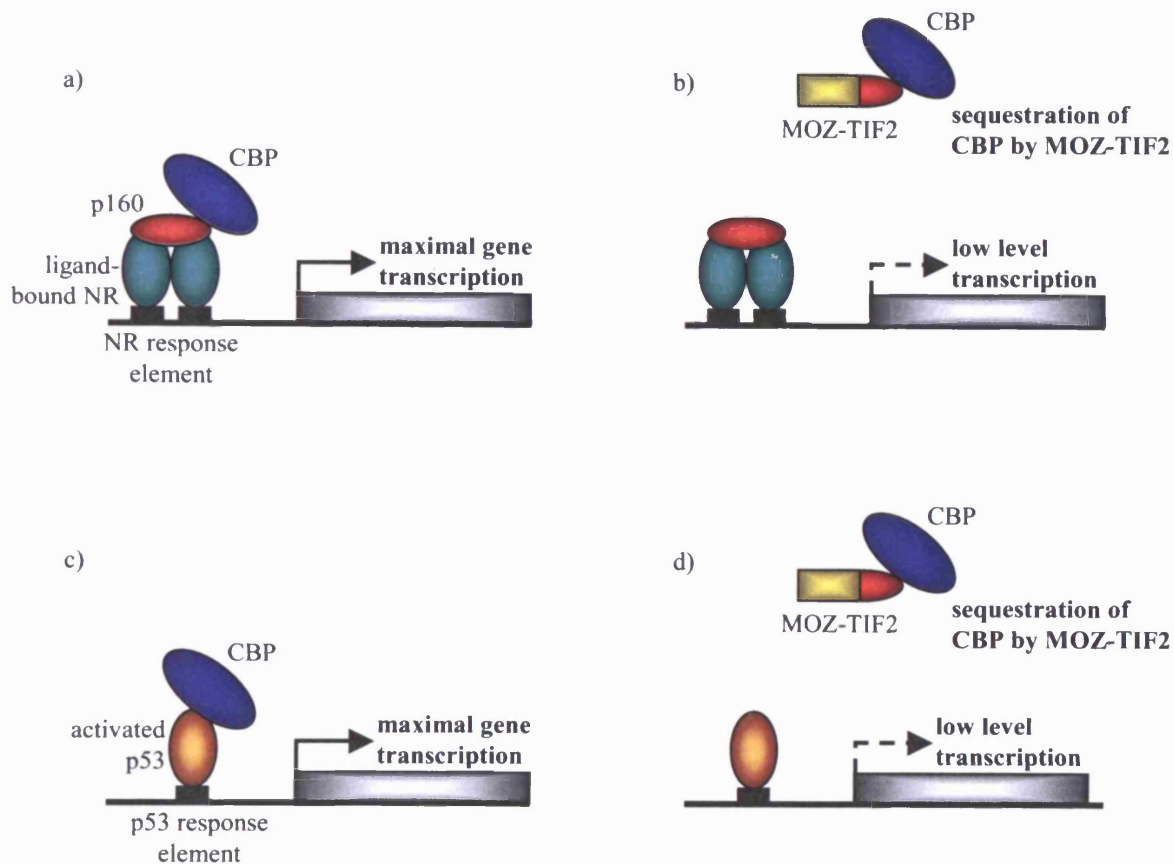


Figure 6.1: Proposed model for the inhibition of NR- and p53- mediated transcription by MOZ-TIF2

Schematic describing a model whereby expression of MOZ-TIF2 results in sequestration of CBP and a reduction in transcription activation by NRs and p53. a) in the presence of ligand the NR dimer binds a p160 coactivator protein, which recruits CBP to the DNA-bound NR complex. CBP recruitment results in the strong activation of transcription of the responsive gene. b) MOZ-TIF2 expression leads to CBP sequestration through an interaction of the MOZ-TIF2 AD1 with the CBP SID, thus preventing the recruitment of CBP to the active NR complex and a reduced level of transcription activation. c) Active p53 induces transcription through the recruitment of CBP via the latter's SID domain. d) MOZ-TIF2 sequestration of CBP mediated by an AD1 SID interaction prevents CBP recruitment to the DNA-bound p53, thus resulting in a reduction in transcription of the p53-responsive gene.

6.9 MOZ-TIF2 as a coactivator for AML1-mediated transcription

During the course of this PhD research, Kitabayashi *et al.* (2001) published a study identifying MOZ as an AML1-interacting protein, and suggesting that MOZ acts as a coactivator of AML1-mediated transcription. The publication also showed that MOZ-CBP acted as an inhibitor of AML1 transcription through the inhibition of CBP, but not MOZ, coactivation. In addition, a second publication this year (Bristow and Shore, 2003) has provided further evidence that MOZ acts as a coactivator for AML1. Given the similarities in the leukaemic phenotypes of MOZ-CBP and MOZ-TIF2 translocations, it appeared possible that MOZ-TIF2 might function in a manner similar to the MOZ-CBP fusion in inhibiting AML1-mediated transcription. The ability of MOZ and CBP to act as coactivators of AML1 transcription, and the effect of MOZ-TIF2 expression, was therefore investigated in COS-1 cells using an AML1-responsive luciferase reporter. In contrast to the findings of Kitabayashi *et al.* (2001) and Bristow *et al.* (2003), in the experiments carried out here MOZ did not function as a coactivator for AML1, though potentiation by CBP was confirmed. This result will require further investigation utilising other reporter constructs and cell lines as discussed in Section 6.2. Given the ability to detect MOZ expression in COS-1 cells by immunofluorescence analysis it is unlikely that this inability to replicate MOZ coactivation of AML1 was due to a lack of expression. It is possible however that the ability of MOZ to act as a coactivator for AML1 is dependent upon its interaction with currently unidentified proteins that are not expressed in COS-1 cells. Kitabayashi *et al.* (2001) showed that coactivation by MOZ was not dependent upon the MYST domain and thus the ability of MOZ to act as a bridging factor to other proteins does appear to be the most likely method of coactivation. To allow further analysis of such an activity, LexA constructs spanning the MOZ sequence have been generated and will allow the future identification of such proteins in a yeast 2-hybrid screen.

The effect of MOZ-TIF2 expression on AML1-mediated transcription was investigated both when co-transfected with AML1 alone, and with AML1 in the presence CBP. Co-transfection of MOZ-TIF2 had no effect on the level of transcription activation by AML1. However, when MOZ-TIF2 was expressed with both AML1 and CBP a significant increase in luciferase activity was seen when compared to that resulting from transfection of CBP with AML1. This indicated that in contrast to MOZ-CBP, which inhibits the ability of CBP to act as a coactivator of AML1, MOZ-TIF2 acted in synergy with CBP resulting

in an increase in transcription. Experiments utilising the deletion construct MOZ-TIF2 Δ AD1 showed that the AD1 domain is required for this activity as its deletion prevented MOZ-TIF2 acting as a coactivator in the presence of CBP. Thus, though the mechanism by which this potentiation occurs is unknown, it appears that the AD1 domain might allow CBP to recruit MOZ-TIF2 to the AML1 complex.

In summary, these experiments investigating the effect of MOZ and MOZ-TIF2 on AML1 transcription suggest that MOZ is unable to act as an AML1 coactivator in COS-1 cells. However, when co-expressed with CBP, MOZ-TIF2 acts to potentiate AML1-mediated transcription. The mechanism by which this coactivation occurs is unclear, though it involves the AD1 domain that mediates MOZ-TIF2 binding to CBP.

6.10 Concluding Remarks

In the last six years translocations involving the MOZ gene, and its close homologue MORF, have been identified as the cause of a distinct subtype of Acute Myeloid Leukaemia. These leukaemic fusions all appear to result in the generation of a fusion protein containing the N-terminus of MOZ/MORF fused to a second coactivator. The first of these C-terminal fusion partners to be identified was the global coactivator CBP, but subsequently the coactivators TIF2 and p300 were also shown to be fused to MOZ. The physiological role of MOZ is unknown but the function of TIF2 as a NR-specific coactivator lead to the study detailed here investigating the effect of the MOZ-TIF2 fusion protein on NR-mediated transcription. MOZ-TIF2 was found to act as an inhibitor of NR transcription which, given the role of Nuclear Receptors and their ligands in haematopoiesis, may provide one mechanism by which MOZ-TIF2 blocks myeloid cell differentiation. MOZ-TIF2 appears to inhibit Nuclear Receptor transcription through binding to, and sequestration of, CBP. CBP functions as a global coactivator and thus this finding suggested that MOZ-TIF2 could potentially affect the activity of a number of transcription factors. The studies described in this thesis indicate that this is indeed the case

with MOZ-TIF2 expression affecting transcription activation by p53 and AML1, both factors crucial to correct haematopoietic differentiation. Clearly, extensive research is required to further these preliminary findings. However, these results may help long-term in the determination of the mechanisms by which normal haematopoietic differentiation is regulated, and also aid in the identification of possible methods of treatment for leukaemogenic translocations involving coactivators such as MOZ, TIF2 and CBP.

Appendix One:

Oligonucleotides

Oligonucleotide Number	Oligonucleotide Sequence (5' - 3')
LE102	AAAAAgATCTTCATCTTgTCATgTAAgg
LE105	AAAAAgATCTTCAATCAgCATCATCTgACTC
LE128	AgCTgCCgCggTACTCgAgTgTgggCCCTATAgCTC AgCACTTTCTAgAAggCC
LE129	TTCTAgAAAgtgCTgAgCTATAgggCCCACACTC gAgTAACCgCggC
LE130	AAAATCTAgAAgATCTTCATCTTCTCATgTAAggTCC
LE131	ggACTggCTCAgCTggCTCC
LE173	AAAACCgCggTCAgATTggCCCACAgAC
LE176	AAAAAgATCTTCATCCATATTgTTCCTgAgg
LE177	AAAACCgCggATggTAAACTCgCAAACC
LE178	AAAACCgCgggggCgAATAgCACTTCC
LE179	AAAACCgCggAAAgCAACCAACgTgg
LE180	AAAACCgCgggAATgTggggAgAAATC
LE181	AAAACCgCgggACACTCCTATCTTAAAgC
LE182	AAAACCgCggAgCggCTTCAgTgACCTg
LE183	AAAACCgCggCTgTCACAgTgTAgTATg
LE184	AAAaggATCCTCAAgTgTTgAgCCgATAAAg
LE185	AAAaggATCCTCATTgTAgAAgTTTTc

Oligonucleotide Number	Oligonucleotide Sequence (5' - 3')
LE186	AAAAGgATCCTCAAgtgCTTgATTTCCTg
LE187	AAAAAgATCTTCAgTCCACCACCTgCTgAg
LE188	AAAAAgATCTTCAAaggAgCTggggTgAAAC
LE203	AAAAGggCCCCACCATggACTACAaggACgACgACg ATAAggggATggTAAAACTCgCAAAC
LE204	AAAAGggCCCCACCATgTACCCATACgATgTTCCTgATT ATgCggggATggTAAAACTCgCAAAC
LE205	gTTCTTggATATCACg
LE214	AAAAGaATTCTCTgCCTATAgACCAggCg
LE215	AAAATCTAgACTATggATCTACTgCTTggCT
LE232	AATTTgggCggCCgCgAATTCgCTAgCggATCCTgAAgATCTT
LE233	CTAgAAgATCTTCAggATCCgCTAgCgAATTCgCggCCgCCCA
LE253	CACATggCAAAGCTTCAgCTg
LE255	gTTgTTACTgTACATgCTggTg
LE256	AgTgATgAgggAgCTgCCgCggACCAggCgTATCTggCCTTgCgg
LE257	CCgCAAaggCCAgATACgCCTggTCCgCggCAgCTCCCTCATCACT
LE284	CCATggCCTgAAAgCATCgAACAgTTCTCAAgtCag
LE285	CTgACTTgAgAACTgTTCgATgCTTTCaggCCATgg

Appendix Two:

Statistical analysis of the inhibition of GAL4-RAR α

A.2.1 Introduction

Experiments investigating the effect of expression of MOZ, MOZ-TIF2 and their derivatives on GAL4-RAR α -mediated, TIF2-potentiated transcription were analysed using the statistical package SPSS v11.5.0 (SPSS Inc., Chicago, Ill., U.S.A.). In order to allow non-biased assessment of the significance of inhibition, the entered data were grouped by experiment in addition to the grouping by DNA. The effect of experiment on the RLA (relative luciferase activity) values was investigated (A2.1.2) prior to the analysis of whether there was a significant difference between the DNA groups (2.1.3). In order to determine the DNA groups between which significant differences in RLA values occurred, a *post-hoc* Bonferroni Test was carried out.

A2.2 Univariate analysis of variance

A2.2.1 Between-subjects factors

DNA Value Label	Full DNA Name	Number of Data Points
TIF2	TIF2	23
MT	MOZ-TIF2	24
MT Δ	MOZ-TIF2 Δ AD1	8
MTm	MOZ-TIF2mAD1	9
M	MOZ	12
M-N	MOZ-N	15
M-AD1	MOZ-AD1	9

A2.2.2 Levene's test of equality of error variances

Dependent variable = RLA (relative luciferase activity)

F	df 1	df 2	Significance
.611	6	93	0.721

Tests the null hypothesis that the error variance of the dependent variable is equal across the groups. The significance is 0.721 and therefore there is no evidence of a difference between the population variances in each group. Thus, the data can be examined by Analysis of Variance.

A2.2.3 Test of between-subjects effects

Source	Type III Sum of Squares	df	Mean Square	F	Significance
Corrected Model	4.878 ^a	6	.813	31.285	0.000
Intercept	60.309	1	60.309	2320.881	0.000
DNA	4.878	6	.813	31.285	0.000
Error	2.417	93	.026		
Total	75.736	100			
Corrected Total	7.294	99			

a. R squared - 0.669 (Adjusted R Squared = 0.647)

The determined significance (shown in bold) was <0.001 and therefore there was a significant variation between the DNA groups.

A2.3 *Post hoc* Bonferroni statistical test

Dependent Variable: RLA

Comparison Groups		Mean Difference (DNA1-DNA2)	Standard Error	Significance
DNA1	DNA2			
TIF2	MT	0.43234448	0.04703750	0.00000000
	MT Δ	-0.16286084	0.06616629	0.32936456
	MTm	0.55869664	0.06338036	0.00000000
	M	0.03939295	0.05740429	1.00000000
	M-N	0.14033636	0.05349918	0.21380946
	M-AD1	0.06570704	0.06338036	1.00000000
MT	TIF2	-0.43234448	0.04703750	0.00000000
	MT Δ	-0.59520532	0.06580960	0.00000000
	MTm	0.12635216	0.06300789	1.00000000
	M	-0.39295153	0.05699278	0.00000001
	M-N	-0.29200811	0.05305739	0.00000687
	M-AD1	-0.36663743	0.06300789	0.00000175
MT Δ	TIF2	0.16286084	0.06616629	0.32936456
	MT	0.59520532	0.06580960	0.00000000
	MTm	0.72155747	0.07832909	0.00000000
	M	0.20225379	0.07357737	0.15087640
	M-N	0.30319720	0.07057293	0.00089633
	M-AD1	0.22856788	0.07832909	0.09274775
MTm	TIF2	-0.55869664	0.06338036	0.00000000
	MT	-0.12635216	0.06300789	1.00000000
	MT Δ	-0.72155747	0.07832909	0.00000000
	M	-0.51930369	0.07108249	0.00000000
	M-N	-0.41836027	0.06796786	0.00000039
	M-AD1	-0.49298959	0.07599038	0.00000009
M	TIF2	-0.03939295	0.05740429	1.00000000
	MT	0.39295153	0.05699278	0.00000001
	MT Δ	-0.20225379	0.07357737	0.15087640
	MTm	0.51930369	0.07108249	0.00000000
	M-N	0.10094341	0.06243247	1.00000000
	M-AD1	0.02631410	0.07108249	1.00000000
M-N	TIF2	-0.14033636	0.05349918	0.21380946
	MT	0.29200811	0.05305739	0.00000687
	MT Δ	-0.30319720	0.07057293	0.00089633
	MTm	0.41836027	0.06796786	0.00000039
	M	-0.10094341	0.06243247	1.00000000
	M-AD1	-0.07462932	0.06796786	1.00000000
M-AD1	TIF2	-0.06570704	0.06338036	1.00000000
	MT	0.36663743	0.06300789	0.00000175
	MT Δ	-0.22856788	0.07832909	0.09274775
	MTm	0.49298959	0.07599038	0.00000009
	M	-0.02631410	0.07108249	1.00000000
	M-N	0.07462932	0.06796786	1.00000000

Based on observed means:

“bold” indicates mean difference is significant at the 0.001 level.

A2.4 Conclusions

The Levene's Test of Equality of Error Variances indicated that grouping the data by experiment did not result in a significant difference in the group variances. Therefore, the data were suitable for statistical analysis using ANOVA to determine whether there were significant differences between the RLA values obtained upon transfection of the constructs. A Univariate Analysis of Variance indicated that there was indeed a highly significant difference between the DNA groups and therefore a *Post Hoc* Bonferroni Test was carried out to determine the groups that varied significantly from each other. Each group was compared with every other and significant differences in the means indicated in "bold".

Co-transfection of MOZ-TIF2 or MOZ-TIF2mAD1 with TIF2 resulted in a significant difference in the mean RLA value when compared to transfection of TIF2 alone with GAL4-RAR α . In contrast, no significant differences were obtained (when compared to TIF2) upon co-transfection of MOZ-TIF2 Δ AD1, MOZ, MOZ-N or MOZ-AD1. Thus, MOZ, MOZ-N and the minimal MOZ-AD1 construct were unable to inhibit NR transcription. However, MOZ-TIF2 expression resulted in a significant inhibition of GAL4-RAR α -mediated, TIF2-enhanced transcription. This effect was lost upon deletion of the AD1 from the fusion construct. However, the mutation of the 3 leucine residues to alanines in the AD1 did not affect the ability of the protein to inhibit NR transcription.

Bibliography

Acevedo, M. L., and Kraus, W. L. (2003). Mediator and p300/CBP-steroid receptor coactivator complexes have distinct roles, but function synergistically, during estrogen receptor alpha-dependent transcription with chromatin templates. *Molecular and Cellular Biology* 23, 335-348.

Aguiar, R. C., Chase, A., Coulthard, S., Macdonald, D. H., Carapeti, M., Reiter, A., Sohal, J., Lennard, A., Goldman, J. M., and Cross, N. C. (1997). Abnormalities of chromosome band 8p11 in leukemia: two clinical syndromes can be distinguished on the basis of MOZ involvement. *Blood* 90, 3130-3135.

Allard, S., Utley, R. T., Savard, J., Clarke, A., Grant, P., Brandl, C. J., Pillus, L., Workman, J. L., and Cote, J. (1999). NuA4, an essential transcription adaptor/histone H4 acetyltransferase complex containing Esa1p and the ATM-related cofactor Tra1p. *EMBO Journal* 18, 5108-5119.

Anzick, S. L., Kononen, J., Walker, R. L., Azorsa, D. O., Tanner, M. M., Guan, X. Y., Sauter, G., Kallioniemi, O. P., Trent, J. M., and Meltzer, P. S. (1997). AIB1, a steroid receptor coactivator amplified in breast and ovarian cancer. *Science* 277, 965-968.

Aranda, A., and Pascual, A. (2001). Nuclear hormone receptors and gene expression. *Physiological Reviews* 81, 1269-1304.

Asou, H., Verbeek, W., Williamson, E., Elstner, E., Kubota, T., Kamada, N., and Koeffler, H. P. (1999). Growth inhibition of myeloid leukemia cells by troglitazone, a ligand for peroxisome proliferator activated receptor gamma, and retinoids. *International Journal of Oncology* 15, 1027-1031.

Bannister, A. J., and Kouzarides, T. (1996). The CBP coactivator is a histone acetyltransferase. *Nature* 384, 641-643.

Bannister, A. J., Schneider, R., and Kouzarides, T. (2002). Histone methylation: Dynamic or static? *Cell* 109, 801-806.

Barlev, N. A., Liu, L., Chehab, N. H., Mansfield, K., Harris, K. G., Halazonetis, T. D., and Berger, S. L. (2001). Acetylation of p53 activates transcription through recruitment of coactivators/histone acetyltransferases. *Molecular Cell* 8, 1243-1254.

Bartel, P. L., and Fields, S. (1997). *The Yeast Two-Hybrid System* (New York, Oxford University Press).

Baumann, C. T., Ma, H., Wolford, R., Reyes, J. C., Maruvada, P., Lim, C., Yen, P. M., Stallcup, M. R., and Hager, G. L. (2001). The glucocorticoid receptor interacting protein 1 (GRIP1) localizes in discrete nuclear foci that associate with ND10 bodies and are enriched in components of the 26S proteasome. *Molecular Endocrinology* 15, 485-500.

- Becker, P. B., and Horz, W. (2002). ATP-dependent nucleosome modeling. *Annual Review of Biochemistry* 71, 247-273.
- Belandia, B., and Parker, M. G. (2000). Functional interaction between the p160 coactivator proteins and the transcriptional enhancer factor family of transcription factors. *Journal of Biological Chemistry* 275, 30801-30805.
- Berger, S. L. (2002). Histone modifications in transcriptional regulation. *Current Opinion in Genetics and Development* 12, 142-148.
- Bevan, C. L., Hoare, S., Claessens, F., Heery, D. M., and Parker, M. G. (1999). The AF1 and AF2 domains of the androgen receptor interact with distinct regions of SRC1. *Molecular and Cellular Biology* 19, 8383-8392.
- Billio, A., Steer, E. J., Pianezze, G., Svaldi, M., Casin, M., Amato, B., Coser, P., and Cross, N. C. (2002). A further case of acute myeloid leukaemia with inv(8)(p11q13) and MOZ-TIF2 fusion. *Haematologica* 87, ECR15.
- Bird, A. W., Yu, D. Y., Pray-Grant, M. G., Qiu, Q. F., Harmon, K. E., Megee, P. C., Grant, P. A., Smith, M. M., and Christman, M. F. (2002). Acetylation of histone H4 by Esa1 is required for DNA double-strand break repair. *Nature* 419, 411-415.
- Blobel, G. A. (2002). CBP and p300: versatile coregulators with important roles in hematopoietic gene expression. *Journal of Leukocyte Biology* 71, 545-556.
- Bohlander, S. K. (2000). Fusion genes in leukemia: an emerging network. *Cytogenetics and Cell Genetics* 91, 52-56.
- Boisvert, F. M., Kruhlak, M. J., Box, A. K., Hendzel, M. J., and Bazett-Jones, D. P. (2001). The transcription coactivator CBP is a dynamic component of the promyelocytic leukemia nuclear body. *Journal of Cell Biology* 152, 1099-1106.
- Borden, K. L. B. (2002). Pondering the promyelocytic leukemia protein (PML) puzzle: Possible functions for PML nuclear bodies. *Molecular and Cellular Biology* 22, 5259-5269.
- Borrow, J., Stanton, V. P., Jr., Andresen, J. M., Becher, R., Behm, F. G., Chaganti, R. S., Civin, C. I., Disteche, C., Dube, I., Frischauf, A. M., et al. (1996). The translocation t(8;16)(p11;p13) of acute myeloid leukaemia fuses a putative acetyltransferase to the CREB-binding protein. *Nature Genetics* 14, 33-41.

- Botling, J., Oberg, F., Torma, H., Tuohimaa, P., Blauer, M., and Nilsson, K. (1996). Vitamin D3- and retinoic acid-induced monocytic differentiation: interactions between the endogenous vitamin D3 receptor, retinoic acid receptors, and retinoid X receptors in U-937 cells. *Cell Growth and Differentiation* 7, 1239-1249.
- Brace, M., Kemp, R., and Snelgar, R. (2003). *SPSS for Psychologists*, 2nd edn, Palgrave Macmillan).
- Brady, M. E., Ozanne, D. M., Gaughan, L., Waite, I., Cook, S., Neal, D. E., and Robson, C. N. (1999). Tip60 is a nuclear hormone receptor coactivator. *Journal of Biological Chemistry* 274, 17599-17604.
- Bristow, C. A. P., and Shore, P. (2003). Transcriptional regulation of the human MIP-1 alpha promoter by RUNX1 and MOZ. *Nucleic Acids Research* 31, 2735-2744.
- Brown, C. E., Lechner, T., Howe, L., and Workman, J. L. (2000). The many HATs of transcription coactivators. *Trends in Biochemical Sciences* 25, 15-19.
- Brown, T. R. P., Stonehouse, T. J., Branch, J. S., Brickell, P. M., and Katz, D. R. (1997). Stable transfection of U937 cells with sense or antisense RXR- alpha cDNA suggests a role for RXR-alpha in the control of monoblastic differentiation induced by retinoic acid and vitamin D. *Experimental Cell Research* 236, 94-102.
- Carapeti, M., Aguiar, R. C., Goldman, J. M., and Cross, N. C. (1998a). A novel fusion between MOZ and the nuclear receptor coactivator TIF2 in acute myeloid leukemia. *Blood* 91, 3127-3133.
- Carapeti, M., Aguiar, R. C., Watmore, A. E., Goldman, J. M., and Cross, N. C. (1999). Consistent fusion of MOZ and TIF2 in AML with inv(8)(p11q13). *Cancer Genetics and Cytogenetics* 113, 70-72.
- Carapeti, M., Aguiar, R. C. T., Chase, A., Goldman, J. M., and Cross, N. C. P. (1998b). Assignment of the steroid receptor coactivator-1 (SRC-1) gene to human chromosome band 2p23. *Genomics* 52, 242-244.
- Chaffanet, M., Gressin, L., Preudhomme, C., Soenen-Cornu, V., Birnbaum, D., and Pebusque, M. J. (2000). MOZ is fused to p300 in an acute monocytic leukemia with t(8;22). *Genes, Chromosomes and Cancer* 28, 138-144.
- Chakravarti, D., LaMorte, V. J., Nelson, M. C., Nakajima, T., Schulman, I. G., Juguilon, H., Montminy, M., and Evans, R. M. (1996). Role of CBP/p300 in nuclear receptor signalling. *Nature* 383, 99-103.
- Champagne, N., Bertos, N. R., Pelletier, N., Wang, A. H., Vezmar, M., Yang, Y., Heng, H. H., and Yang, X. J. (1999). Identification of a human histone acetyltransferase related to monocytic leukemia zinc finger protein. *Journal of Biological Chemistry* 274, 28528-28536.

- Champagne, N., Pelletier, N., and Yang, X. J. (2001). The monocytic leukemia zinc finger protein MOZ is a histone acetyltransferase. *Oncogene* 20, 404-409.
- Chan, H. M., and La Thangue, N. B. (2001). p300/CBP proteins: HATs for transcriptional bridges and scaffolds. *Journal of Cell Science* 114, 2363-2373.
- Chen, D., Ma, H., Hong, H., Koh, S. S., Huang, S. M., Schurter, B. T., Aswad, D. W., and Stallcup, M. R. (1999a). Regulation of transcription by a protein methyltransferase. *Science* 284, 2174-2177.
- Chen, H., Lin, R. J., Schiltz, R. L., Chakravarti, D., Nash, A., Nagy, L., Privalsky, M. L., Nakatani, Y., and Evans, R. M. (1997). Nuclear receptor coactivator ACTR is a novel histone acetyltransferase and forms a multimeric activation complex with P/CAF and CBP/p300. *Cell* 90, 569-580.
- Chen, H., Lin, R. J., Xie, W., Wilpitz, D., and Evans, R. M. (1999b). Regulation of hormone-induced histone hyperacetylation and gene activation via acetylation of an acetylase. *Cell* 98, 675-686.
- Chen, S. L., Wang, S. C. M., Hosking, B., and Muscat, G. E. O. (2001). Subcellular localization of the steroid receptor coactivators (SRCs) and MEF2 in muscle and rhabdomyosarcoma cells. *Molecular Endocrinology* 15, 783-796.
- Cheung, J., and Smith, D. F. (2000). Molecular chaperone interactions with steroid receptors: an update. *Molecular Endocrinology* 14, 939-946.
- Chevillard-Briet, M., Trouche, D., and Vandell, L. (2002). Control of CBP coactivating activity by arginine methylation. *EMBO Journal* 21, 5457-5466.
- Christiaens, V., Bevan, C. L., Callewaert, L., Haelens, A., Verrijdt, G., Rombauts, W., and Claessens, F. (2002). Characterization of the two coactivator-interacting surfaces of the androgen receptor and their relative role in transcriptional control. *Journal of Biological Chemistry* 277, 49230-49237.
- Chrivia, J. C., Kwok, R. P. S., Lamb, N., Hagiwara, M., Montminy, M. R., and Goodman, R. H. (1993). Phosphorylated CREB binds specifically to the nuclear-protein CBP. *Nature* 365, 855-859.
- Collins, S. J. (2002). The role of retinoids and retinoic acid receptors in normal hematopoiesis. *Leukemia* 16, 1896-1905.
- Collins, S. J., and Tsai, S. (1996). Retinoic acid receptors in hematopoiesis. *Current Topics in Microbiology and Immunology* 211, 7-15.

- Corpet, F. (1988). Multiple sequence alignment with hierarchical clustering. *Nucleic Acids Research* 16, 10881-10890.
- Coulthard, S., Chase, A., Orchard, K., Watmore, A., Vora, A., Goldman, J. M., and Swirsky, D. M. (1998). Two cases of inv(8)(p11q13) in AML with erythrophagocytosis: a new cytogenetic variant. *British Journal of Haematology* 100, 561-563.
- Coulthard, V. H., Matsuda, S., and Heery, D. M. (2003). An extended LXXLL motif sequence determines the nuclear receptor binding specificity of TRAP220. *Journal of Biological Chemistry* 278, 10942-10951.
- Cress, W. D., and Seto, E. (2000). Histone deacetylases, transcriptional control, and cancer. *Journal of Cellular Physiology* 184, 1-16.
- Datto, M. B., Li, Y., Panus, J. F., Howe, D. J., Xiong, Y., and Wang, X. F. (1995). Transforming growth factor beta induces the cyclin-dependent kinase inhibitor p21 through a p53-independent mechanism. *Proceedings of the National Academy of Sciences of the United States of America* 92, 5545-5549.
- Daujat, S., Bauer, U. M., Shah, V., Turner, B., Berger, S., and Kouzarides, T. (2002). Crosstalk between CARM1 methylation and CBP acetylation on histone H3. *Current Biology* 12, 2090-2097.
- Day, R. N., Periasamy, A., and Schaufele, F. (2001). Fluorescence resonance energy transfer microscopy of localized protein interactions in the living cell nucleus. *Methods* 25, 4-18.
- Deguchi, K., Ayton, P. M., Carapeti, M., Kutok, J. L., Snyder, C. S., Williams, I. R., Cross, N. C. P., Glass, C. K., Cleary, M. L., and Gilliland, D. G. (2003). MOZ-TIF2-induced acute myeloid leukemia requires the MOZ nucleosome binding motif and TIF2-mediated recruitment of CBP. *Cancer Cell* 3, 259-271.
- Demarest, S. J., Martinez-Yamout, M., Chung, J., Chen, H. W., Xu, W., Dyson, H. J., Evans, R. M., and Wright, P. E. (2002). Mutual synergistic folding in recruitment of CBP/p300 by p160 nuclear receptor coactivators. *Nature* 415, 549-553.
- Dhalluin, C., Carlson, J. E., Zeng, L., He, C., Aggarwal, A. K., and Zhou, M. M. (1999). Structure and ligand of a histone acetyltransferase bromodomain. *Nature* 399, 491-496.
- Dillon, N., and Festenstein, R. (2002). Unravelling heterochromatin: competition between positive and negative factors regulates accessibility. *Trends in Genetics* 18, 252-258.
- Dilworth, F. J., and Chambon, P. (2001). Nuclear receptors coordinate the activities of chromatin remodeling complexes and coactivators to facilitate initiation of transcription. *Oncogene* 20, 3047-3054.

- Ding, X. F., Anderson, C. M., Ma, H., Hong, H., Uht, R. M., Kushner, P. J., and Stallcup, M. R. (1998). Nuclear receptor-binding sites of coactivators glucocorticoid receptor interacting protein 1 (GRIP1) and steroid receptor coactivator 1 (SRC-1): multiple motifs with different binding specificities. *Molecular Endocrinology* 12, 302-313.
- Doucas, V., Tini, M., Egan, D. A., and Evans, R. M. (1999). Modulation of CREB binding protein function by the promyelocytic (PML) oncoprotein suggests a role for nuclear bodies in hormone signaling. *Proceedings of the National Academy of Sciences of the United States of America* 96, 2627-2632.
- Eckner, R., Ewen, M. E., Newsome, D., Gerdes, M., DeCaprio, J. A., Lawrence, J. B., and Livingston, D. M. (1994). Molecular cloning and functional analysis of the adenovirus E1A-associated 300-kD protein (p300) reveals a protein with properties of a transcriptional adaptor. *Genes and Development* 8, 869-884.
- Enver, T., and Greaves, M. (1998). Loops, lineage, and leukemia. *Cell* 94, 9-12.
- Ernst, P., Wang, J., and Korsmeyer, S. J. (2002). The role of MLL in hematopoiesis and leukemia. *Current Opinion in Hematology* 9, 282-287.
- Featherstone, M. (2002). Coactivators in transcription initiation: here are your orders. *Current Opinion in Genetics and Development* 12, 149-155.
- Fischle, W., Wang, Y. M., and Allis, C. D. (2003). Histone and chromatin cross-talk. *Current Opinion in Cell Biology* 15, 172-183.
- Folkers, G. E., and van der Saag, P. T. (1995). Adenovirus E1A functions as a cofactor for retinoic acid receptor beta (RAR beta) through direct interaction with RAR beta. *Molecular and Cellular Biology* 15, 5868-5878.
- Gaughan, L., Brady, M. E., Cook, S., Neal, D. E., and Robson, C. N. (2001). Tip60 is a coactivator specific for class I nuclear hormone receptors. *Journal of Biological Chemistry* 276, 46841-46848.
- Giguere, V. (1999). Orphan nuclear receptors: From gene to function. *Endocrine Reviews* 20, 689-725.
- Giraud, S., Bienvenu, F., Avril, S., Gascan, H., Heery, D. M., and Coqueret, O. (2002). Functional interaction of STAT3 transcription factor with the coactivator NCoA/SRC1a. *Journal of Biological Chemistry* 277, 8004-8011.
- Girdwood, D., Bumpass, D., Vaughan, O. A., Thain, A., Anderson, L. A., Snowden, A. W., Garcia-Wilson, E., Perkins, N. D., and Hay, R. T. (2003). p300 transcriptional repression is mediated by SUMO modification. *Molecular Cell* 11, 1043-1054.

- Grossman, S. R. (2001). p300/CBP/p53 interaction and regulation of the p53 response. *European Journal of Biochemistry* 268, 2773-2778.
- Guidez, F., and Zelent, A. (2001). Role of nuclear receptor corepressors in leukemogenesis. *Current Topics in Microbiology and Immunology* 254, 165-185.
- Hans, F., and Dimitrov, S. (2001). Histone H3 phosphorylation and cell division. *Oncogene* 20, 3021-3027.
- Hayashi, Y., Honma, Y., Niitsu, N., Taki, T., Bessho, F., Sako, M., Mori, T., Yanagisawa, M., Tsuji, K., and Nakahata, T. (2000). SN-1, a novel leukemic cell line with t(11;16)(q23;p13): myeloid characteristics and resistance to retinoids and vitamin D-3. *Cancer Research* 60, 1139-1145.
- Heery, D. M., Hoare, S., Hussain, S., Parker, M. G., and Sheppard, H. (2001). Core LXXLL motif sequences in CREB-binding protein, SRC1, and RIP140 define affinity and selectivity for steroid and retinoid receptors. *Journal of Biological Chemistry* 276, 6695-6702.
- Heery, D. M., Kalkhoven, E., Hoare, S., and Parker, M. G. (1997). A signature motif in transcriptional coactivators mediates binding to nuclear receptors. *Nature* 387, 733-736.
- Hoffman, R. (2000). *Hematology: basic principle and practice*, 3rd edn, Churchill Livingstone).
- Hong, H., Kohli, K., Garabedian, M. J., and Stallcup, M. R. (1997). GRIP1, a transcriptional coactivator for the AF-2 transactivation domain of steroid, thyroid, retinoid, and vitamin D receptors. *Molecular and Cellular Biology* 17, 2735-2744.
- Horn, P. J., and Peterson, C. L. (2002). Molecular biology: chromatin higher order folding: wrapping up transcription. *Science* 297, 1824-1827.
- Huang, Z. Q., Li, J. W., Sachs, L. M., Cole, P. A., and Wong, J. M. (2003). A role for cofactor-cofactor and cofactor-histone interactions in targeting p300, SWI/SNF and Mediator for transcription. *EMBO Journal* 22, 2146-2155.
- Iizuka, M., and Smith, M. M. (2003). Functional consequences of histone modifications. *Current Opinion in Genetics and Development* 13, 154-160.
- Ikura, T., Ogryzko, V. V., Grigoriev, M., Groisman, R., Wang, J., Horikoshi, M., Scully, R., Qin, J., and Nakatani, Y. (2000). Involvement of the TIP60 histone acetylase complex in DNA repair and apoptosis. *Cell* 102, 463-473.

Jacquemin, P., Hwang, J. J., Martial, J. A., Dolle, P., and Davidson, I. (1996). A novel family of developmentally regulated mammalian transcription factors containing the TEA/ATTS DNA binding domain. *Journal of Biological Chemistry* 271, 21775-21785.

James, S. Y., Williams, M. A., Newland, A. C., and Colston, K. W. (1999). Leukemia cell differentiation: cellular and molecular interactions of retinoids and vitamin D. *General Pharmacology* 32, 143-154.

Janknecht, R. (2002). The versatile functions of the transcriptional coactivators p300 and CBP and their roles in disease. *Histology and Histopathology* 17, 657-668.

Jason, L. J. M., Moore, S. C., Lewis, J. D., Lindsey, G., and Ausio, J. (2002). Histone ubiquitination: a tagging tail unfolds? *Bioessays* 24, 166-174.

Jayaraman, G., Srinivas, R., Duggan, C., Ferreira, E., Swaminathan, S., Somasundaram, K., Williams, J., Hauser, C., Kurkinen, M., Dhar, R., et al. (1999). p300/cAMP-responsive element-binding protein interactions with ETS-1 and ETS-2 in the transcriptional activation of the human stromelysin promoter. *Journal of Biological Chemistry* 274, 17342-17352.

John, S., Howe, L., Tafrov, S. T., Grant, P. A., Sternglanz, R., and Workman, J. L. (2000). The something about silencing protein, SAS3, is the catalytic subunit of NuA3, a yTAF(II)30-containing HAT complex that interacts with the Spt16 subunit of the yeast CP (Cdc68/Pob3)-FACT complex. *Genes and Development* 14, 1196-1208.

Jones, P. L., and Shi, Y. B. (2003). N-CoR-HDAC corepressor complexes: roles in transcriptional regulation by nuclear hormone receptors. *Current Topics in Microbiology and Immunology* 274, 237-268.

Kalkhoven, E., Valentine, J. E., Heery, D. M., and Parker, M. G. (1998). Isoforms of steroid receptor coactivator 1 differ in their ability to potentiate transcription by the oestrogen receptor. *EMBO Journal* 17, 232-243.

Kastner, P., Lawrence, H. J., Waltzinger, C., Ghyselinck, N. B., Chambon, P., and Chan, S. (2001). Positive and negative regulation of granulopoiesis by endogenous RAR alpha. *Blood* 97, 1314-1320.

Kelly, L. M., and Gilliland, D. G. (2002). Genetic's of myeloid leukemias. *Annual Review of Genomics and Human Genetics* 3, 179-198.

Kitabayashi, I., Aikawa, Y., Nguyen, L. A., Yokoyama, A., and Ohki, M. (2001a). Activation of AML1-mediated transcription by MOZ and inhibition by the MOZ-CBP fusion protein. *EMBO Journal* 20, 7184-7196.

Kitabayashi, I., Aikawa, Y., Yokoyama, A., Hosoda, F., Nagai, M., Kakazu, N., Abe, T., and Ohki, M. (2001b). Fusion of MOZ and p300 histone acetyltransferases in acute monocytic leukemia with a t(8;22)(p11;q13) chromosome translocation. *Leukemia* 15, 89-94.

Kitabayashi, I., Yokoyama, A., Shimizu, K., and Ohki, M. (1998). Interaction and functional cooperation of the leukemia-associated factors AML1 and p300 in myeloid cell differentiation. *EMBO Journal* 17, 2994-3004.

Koh, S. S., Chen, D., Lee, Y. H., and Stallcup, M. R. (2001). Synergistic enhancement of nuclear receptor function by p160 coactivators and two coactivators with protein methyltransferase activities. *Journal of Biological Chemistry* 276, 1089-1098.

Kornberg, R. D., and Lorch, Y. L. (1999). Twenty-five years of the nucleosome, fundamental particle of the eukaryote chromosome. *Cell* 98, 285-294.

Kouzarides, T. (2002). Histone methylation in transcriptional control. *Current Opinion in Genetics and Development* 12, 198-209.

Kraus, W. L., and Lis, J. T. (2003). PARP goes transcription. *Cell* 113, 677-683.

Kung, A. L., Rebel, V. I., Bronson, R. T., Ch'ng, L. E., Sieff, C. A., Livingston, D. M., and Yao, T. P. (2000). Gene dose-dependent control of hematopoiesis and hematologic tumor suppression by CBP. *Genes and Development* 14, 272-277.

Lee, J. Y., Lee, C. H., Shim, S. H., Seo, H. K., Kyhm, J. H., Cho, S., and Cho, Y. H. (2002). Molecular cytogenetic analysis of the monoblastic cell line U937: karyotype clarification by G-banding, whole chromosome painting, microdissection and reverse painting, and comparative genomic hybridization. *Cancer Genetics and Cytogenetics* 137, 124-132.

Lee, K. C., Li, J. W., Cole, P. A., Wong, J. M., and Kraus, W. L. (2003). Transcriptional activation by thyroid hormone receptor-beta involves chromatin remodeling, histone acetylation, and synergistic stimulation by p300 and steroid receptor coactivators. *Molecular Endocrinology* 17, 908-922.

Lemon, B., and Tjian, R. (2000). Orchestrated response: a symphony of transcription factors for gene control. *Genes and Development* 14, 2551-2569.

Leo, C., and Chen, J. D. (2000). The SRC family of nuclear receptor coactivators. *Gene* 245, 1-11.

Leroy, P., Krust, A., Zelent, A., Mendelsohn, C., Garnier, J. M., Kastner, P., Dierich, A., and Chambon, P. (1991). Multiple Isoforms of the Mouse Retinoic Acid Receptor Alpha Are Generated by Alternative Splicing and Differential Induction by Retinoic Acid. *EMBO Journal* 10, 59-69.

Li, H., Gomes, P. J., and Chen, J. D. (1997). RAC3, a steroid/nuclear receptor-associated coactivator that is related to SRC-1 and TIF2. *Proceedings of the National Academy of Sciences of the United States of America* 94, 8479-8484.

Li, J. W., Lin, Q. S., Yoon, H. G., Huang, Z. Q., Strahl, B. D., Allis, C. D., and Wong, J. M. (2002). Involvement of histone methylation and phosphorylation in regulation of transcription by thyroid hormone receptor. *Molecular and Cellular Biology* 22, 5688-5697.

Li, J. W., O'Malley, B. W., and Wong, J. M. (2000). p300 requires its histone acetyltransferase activity and SRC-1 interaction domain to facilitate thyroid hormone receptor activation in chromatin. *Molecular and Cellular Biology* 20, 2031-2042.

Liang, J., Prouty, L., Williams, B. J., Dayton, M. A., and Blanchard, K. L. (1998). Acute mixed lineage leukemia with an inv(8)(p11q13) resulting in fusion of the genes for MOZ and TIF2. *Blood* 92, 2118-2122.

Lin, C. H., Hare, B. J., Wagner, G., Harrison, S. C., Maniatis, T., and Fraenkel, E. (2001). A small domain of CBP/p300 binds diverse proteins: solution structure and functional studies. *Molecular Cell* 8, 581-590.

Liu, M., Lavarone, A., and Freedman, L. P. (1996a). Transcriptional activation of the human p21(WAF1/CIP1) gene by retinoic acid receptor. Correlation with retinoid induction of U937 cell differentiation. *Journal of Biological Chemistry* 271, 31723-31728.

Liu, M., Lee, M. H., Cohen, M., Bommakanti, M., and Freedman, L. P. (1996b). Transcriptional activation of the Cdk inhibitor p21 by vitamin D-3 leads to the induced differentiation of the myelomonocytic cell line U937. *Genes and Development* 10, 142-153.

Livengood, J. A., Scoggin, K. E. S., Van Orden, K., McBryant, S. J., Edayathumangalam, R., Laybourn, P. J., and Nyborg, J. K. (2002). p53 transcriptional activity is mediated through the SRC1-interacting domain of CBP/p300. *Journal of Biological Chemistry* 277, 9054-9061.

Look, A. T. (1997). Oncogenic transcription factors in the human acute leukemias. *Science* 278, 1059-1064.

Luger, K. (2003). Structure and dynamic behavior of nucleosomes. *Current Opinion in Genetics and Development* 13, 127-135.

- Lutterbach, B., and Hiebert, S. W. (2000). Role of the transcription factor AML-1 in acute leukemia and hematopoietic differentiation. *Gene* 245, 223-235.
- Ma, H., Baumann, C. T., Li, H. W., Strahl, B. D., Rice, R., Jelinek, M. A., Aswad, D. W., Allis, C. D., Hager, G. L., and Stallcup, M. R. (2001). Hormone-dependent, CARM1-directed, arginine-specific methylation of histone H3 on a steroid-regulated promoter. *Current Biology* 11, 1981-1985.
- Ma, H., Hong, H., Huang, S. M., Irvine, R. A., Webb, P., Kushner, P. J., Coetzee, G. A., and Stallcup, M. R. (1999). Multiple signal input and output domains of the 160-kilodalton nuclear receptor coactivator proteins. *Molecular and Cellular Biology* 19, 6164-6173.
- Mak, H. Y., Hoare, S., Henttu, P. M., and Parker, M. G. (1999). Molecular determinants of the estrogen receptor-coactivator interface. *Molecular and Cellular Biology* 19, 3895-3903.
- Mangelsdorf, D. J., Thummel, C., Beato, M., Herrlich, P., Schutz, G., Umesono, K., Blumberg, B., Kastner, P., Mark, M., Chambon, P., and et al. (1995). The nuclear receptor superfamily: the second decade. *Cell* 83, 835-839.
- Matsuda, S., Harries, J. C., Kindle, K. B., Viskaduraki, M., Troke, P. J. F., and Heery, D. M. (2003). Diverse nuclear proteins compete with Steroid Receptor Coactivator (SRC1) for interaction with CREB-binding protein. In preparation.
- McInerney, E. M., Rose, D. W., Flynn, S. E., Westin, S., Mullen, T. M., Kronen, A., Inostroza, J., Torchia, J., Nolte, R. T., Assa-Munt, N., et al. (1998). Determinants of coactivator LXXLL motif specificity in nuclear receptor transcriptional activation. *Genes and Development* 12, 3357-3368.
- McKenna, N. J., and O'Malley, B. W. (2002). Combinatorial control of gene expression by nuclear receptors and coregulators. *Cell* 108, 465-474.
- Medigue, C., Viari, A., Henaut, A., and Danchin, A. (1993). Colibri - a functional database for the Escherichia Coli genome. *Microbiology Reviews* 57, 623-654.
- Melnick, A., and Licht, J. D. (1999). Deconstructing a disease: RAR alpha, its fusion partners, and their roles in the pathogenesis of acute promyelocytic leukemia. *Blood* 93, 3167-3215.
- Merika, M., Williams, A. J., Chen, G. Y., Collins, T., and Thanos, D. (1998). Recruitment of CBP/p300 by the IFN beta enhanceosome is required for synergistic activation of transcription. *Molecular Cell* 1, 277-287.
- Meyer, M. E., Gronemeyer, H., Turcotte, B., Bocquel, M. T., Tasset, D., and Chambon, P. (1989). Steroid-hormone receptors compete for factors that mediate their enhancer function. *Cell* 57, 433-442.

- Michaud, J., Scott, H. S., and Escher, R. (2003). AML1 interconnected pathways of leukemogenesis. *Cancer Investigation* 21, 105-136.
- Moras, D., and Gronemeyer, H. (1998). The nuclear receptor ligand-binding domain: structure and function. *Current Opinion in Cell Biology* 10, 384-391.
- Nakajima, T., Uchida, C., Anderson, S. F., Lee, C. G., Hurwitz, J., Parvin, J. D., and Montminy, M. (1997). RNA helicase A mediates association of CBP with RNA polymerase II. *Cell* 90, 1107-1112.
- Nolte, R. T., Wisely, G. B., Westin, S., Cobb, J. E., Lambert, M. H., Kurokawa, R., Rosenfeld, M. G., Willson, T. M., Glass, C. K., and Milburn, M. V. (1998). Ligand binding and coactivator assembly of the peroxisome proliferator-activated receptor-gamma. *Nature* 395, 137-143.
- Nucifora, F. C., Sasaki, M., Peters, M. F., Huang, H., Cooper, J. K., Yamada, M., Takahashi, H., Tsuji, S., Troncoso, J., Dawson, V. L., et al. (2001). Interference by Huntingtin and atrophin-1 with CBP-mediated transcription leading to cellular toxicity. *Science* 291, 2423-2428.
- Ogryzko, V. V., Schiltz, R. L., Russanova, V., Howard, B. H., and Nakatani, Y. (1996). The transcriptional coactivators p300 and CBP are histone acetyltransferases. *Cell* 87, 953-959.
- Oikawa, T., and Yamada, T. (2003). Molecular biology of the Ets family of transcription factors. *Gene* 303, 11-34.
- Olsson, I., Gullberg, U., Ivhed, I., and Nilsson, K. (1983). Induction of Differentiation of the Human Histiocytic Lymphoma Cell-Line U-937 by ¹-Alpha,25-Dihydroxycholecalciferol. *Cancer Research* 43, 5862-5867.
- Olsson, I. L., and Breitman, T. R. (1982). Induction of Differentiation of the Human Histiocytic Lymphoma Cell-Line U-937 by Retinoic Acid and Cyclic Adenosine 3'-5'- Monophosphate-Inducing Agents. *Cancer Research* 42, 3924-3927.
- Omate, S. A., Tsai, S. Y., Tsai, M. J., and Omalley, B. W. (1995). Sequence and characterization of a coactivator for the steroid-hormone receptor superfamily. *Science* 270, 1354-1357.
- Osada, S., Sutton, A., Muster, N., Brown, C. E., Yates, J. R., Sternglanz, R., and Workman, J. L. (2001). The yeast SAS (something about silencing) protein complex contains a MYST-type putative acetyltransferase and functions with chromatin assembly factor ASF1. *Genes and Development* 15, 3155-3168.

- Panagopoulos, I., Fioretos, T., Isaksson, M., Samuelsson, U., Billstrom, R., Strombeck, B., Mitelman, F., and Johansson, B. (2001). Fusion of the MORF and CBP genes in acute myeloid leukemia with the t(10;16)(q22;p13). *Human Molecular Genetics* 10, 395-404.
- Panagopoulos, I., Isaksson, M., Lindvall, C., Bjorkholm, M., Ahlgren, T., Fioretos, T., Heim, S., Mitelman, F., and Johansson, B. (2000a). RT-PCR analysis of the MOZ-CBP and CBP-MOZ chimeric transcripts in acute myeloid leukemias with t(8;16)(p11;p13). *Genes, Chromosomes and Cancer* 28, 415-424.
- Panagopoulos, I., Teixeira, M. R., Micci, F., Hammerstrom, J., Isaksson, M., Johansson, B., Mitelman, F., and Heim, S. (2000b). Acute myeloid leukemia with inv(8)(p11q13). *Leukemia and Lymphoma* 39, 651-656.
- Panagopoulos, L., Isaksson, M., Lindvall, C., Hagemeijer, A., Mitelman, F., and Johansson, B. (2003). Genomic characterization of MOZ/CBP and CBP/MOZ chimeras in acute myeloid leukemia suggests the involvement of a damage- repair mechanism in the origin of the t(8;16)(p11;p13). *Genes, Chromosomes and Cancer* 36, 90-98.
- Parker, D., Ferreri, K., Nakajima, T., Morte, V. J. L., Evans, R., Koerber, S. C., Hoeger, C., and Montminy, M. R. (1996). Phosphorylation of CREB at Ser-133 induces complex formation with CREB-binding protein via a direct mechanism. *Molecular and Cellular Biology* 16, 694-703.
- Parrado, A., Chomienne, C., and Padua, R. A. (2000). Retinoic acid receptor alpha (RAR alpha) mutations in human leukemia. *Leukemia and Lymphoma* 39, 271-282.
- Parrado, A., West, R., Jordan, D., Bastard, C., McKenna, S., Whittaker, J. A., Bentley, P., White, D., Chomienne, C., and Padua, R. A. (1999). Alterations of the retinoic acid receptor alpha (RAR alpha) gene in myeloid and lymphoid malignancies. *British Journal of Haematology* 104, 738-741.
- Pelletier, N., Champagne, N., Stifani, S., and Yang, X. J. (2002). MOZ and MORF histone acetyltransferases interact with the Runt- domain transcription factor Runx2. *Oncogene* 21, 2729-2740.
- Petrij, F., Giles, R. H., Dauwerse, H. G., Saris, J. J., Hennekam, R. C. M., Masuno, M., Tommerup, N., Vanommen, G. J. B., Goodman, R. H., Peters, D. J. M., and Breuning, M. H. (1995). Rubinstein-Taybi Syndrome caused by mutations in the transcriptional coactivator CBP. *Nature* 376, 348-351.
- Pizzimenti, S., Laurora, S., Briatore, F., Ferretti, C., Dianzani, M. U., and Barrera, G. (2002). Synergistic effect of 4-hydroxynonenal and PPAR ligands in controlling human leukemic cell growth and differentiation. *Free Radical Biology and Medicine* 32, 233-245.
- Rachez, C., and Freedman, L. P. (2001). Mediator complexes and transcription. *Current Opinion in Cell Biology* 13, 274-280.

- Reese, J. C. (2003). Basal transcription factors. *Current Opinion in Genetics and Development* 13, 114-118.
- Reid, J. L., Iyer, V. R., Brown, P. O., and Struhl, K. (2000). Coordinate regulation of yeast ribosomal protein genes is associated with targeted recruitment of ESA1 histone acetylase. *Molecular Cell* 6, 1297-1307.
- Reifsnnyder, C., Lowell, J., Clarke, A., and Pillus, L. (1996). Yeast SAS silencing genes and human genes associated with AML and HIV-1 Tat interactions are homologous with acetyltransferases. *Nature Genetics* 14, 42-49.
- Renaud, J. P., and Moras, D. (2000). Structural studies on nuclear receptors. *Cellular and Molecular Life Sciences* 57, 1748-1769.
- Rohde, J. R., and Cardenas, M. E. (2003). The tor pathway regulates gene expression by linking nutrient sensing to histone acetylation. *Molecular and Cellular Biology* 23, 629-635.
- Ross, I. L., Yue, X., Ostrowski, M. C., and Hume, D. A. (1998). Interaction between PU.1 and another Ets family transcription factor promotes macrophage-specific basal transcription initiation. *Journal of Biological Chemistry* 273, 6662-6669.
- Roth, S. Y., Denu, J. M., and Allis, C. D. (2001). Histone acetyltransferases. *Annual Review of Biochemistry* 70, 81-120.
- Sanjuan, R., and Marin, I. (2001). Tracing the origin of the compensasome: Evolutionary history of DEAH helicase and MYST acetyltransferase gene families. *Molecular Biology and Evolution* 18, 330-343.
- Scheffner, M., Werness, B. A., Huibregtse, J. M., Levine, A. J., and Howley, P. M. (1990). The E6 oncoprotein encoded by Human Papillomavirus Type-16 and Type-18 promotes the degradation of p53. *Cell* 63, 1129-1136.
- Scoggin, K. E. S., Ulloa, A., and Nyborg, J. K. (2001). The oncoprotein Tax binds the SRC-1-interacting domain of CBP/p300 to mediate transcriptional activation. *Molecular and Cellular Biology* 21, 5520-5530.
- Sevilla, L., Zaldumbide, A., Carlotti, F., Dayem, M. A., Pognonec, P., and Boulukos, K. E. (2001). Bcl-x(L) expression correlates with primary macrophage differentiation, activation of functional competence, and survival and results from synergistic transcriptional activation by ETS-2 and PU.1. *Journal of Biological Chemistry* 276, 17800-17807.
- Shang, Y., Hu, X., DiRenzo, J., Lazar, M. A., and Brown, M. (2000). Cofactor dynamics and sufficiency in estrogen receptor-regulated transcription. *Cell* 103, 843-852.

Sharma, D., and Fondell, J. D. (2002). Ordered recruitment of histone acetyltransferases and the TRAP/Mediator complex to thyroid hormone-responsive promoters in vivo. *Proceedings of the National Academy of Sciences of the United States of America* 99, 7934-7939.

Sharma, M., Zarnegar, M., Li, X., Lim, B., and Sun, Z. (2000). Androgen receptor interacts with a novel MYST protein, HBO1. *Journal of Biological Chemistry* 275, 35200-35208.

Sheppard, H. M., Harries, J. C., Hussain, S., Bevan, C., and Heery, D. M. (2001). Analysis of the steroid receptor coactivator 1 (SRC1)-CREB binding protein interaction interface and its importance for the function of SRC1. *Molecular and Cellular Biology* 21, 39-50.

Skalnik, D. G. (2002). Transcriptional mechanisms regulating myeloid-specific genes. *Gene* 284, 1-21.

Spencer, T. E., Jenster, G., Burcin, M. M., Allis, C. D., Zhou, J. X., Mizzen, C. A., McKenna, N. J., Onate, S. A., Tsai, S. Y., Tsai, M. J., and Omalley, B. W. (1997). Steroid receptor coactivator-1 is a histone acetyltransferase. *Nature* 389, 194-198.

Stallcup, M. R., Chen, D., Koh, S. S., Ma, H., Lee, Y. H., Li, H., Schurter, B. T., and Aswad, D. W. (2000). Cooperation between protein-acetylating and protein-methylating coactivators in transcriptional activation. *Biochemical Society Transactions* 28, 415-418.

Stothard, P. (2000). The sequence manipulation suite: JavaScript programs for analyzing and formatting protein and DNA sequences. http://www.bioinformatics.org/sms/prot_mw.html.

Strahl, B. D., and Allis, C. D. (2000). The language of covalent histone modifications. *Nature* 403, 41-45.

Sun, T., and Wu, E. (2001). Acute monoblastic leukemia with t(8;16): a distinct clinicopathologic entity. Report of a case and review of the literature. *American Journal of Hematology* 66, 207-212.

Sunaga, S., Maki, K., Lagasse, E., Blanco, J. C. G., Ozato, K., Miyazaki, J., and Ikuta, K. (1997). Myeloid differentiation is impaired in transgenic mice with targeted expression of a dominant negative form of retinoid X receptor beta. *British Journal of Haematology* 96, 19-30.

Sundstrom, C., and Nilsson, K. (1976). Establishment and characterization of a human histiocytic lymphoma cell line (U-937). *International Journal of Cancer* 17, 565-577.

Takeshita, A., Cardona, G. R., Koibuchi, N., Suen, C. S., and Chin, W. W. (1997). TRAM-1, a novel 160-kDa thyroid hormone receptor activator molecule, exhibits distinct properties from steroid receptor coactivator-1. *Journal of Biological Chemistry* 272, 27629-27634.

Tenen, D. G., Hromas, R., Licht, J. D., and Zhang, D. E. (1997). Transcription factors, normal myeloid development, and leukemia. *Blood* 90, 489-519.

Torchia, J., Rose, D. W., Inostroza, J., Kamei, Y., Westin, S., Glass, C. K., and Rosenfeld, M. G. (1997). The transcriptional coactivator p/CIP binds CBP and mediates nuclear-receptor function. *Nature* 387, 677-684.

Troke, P. J. F., Kindle, K. B., Matsuda, S., Collins, H. M., and Heery, D. M. (2003). The leukaemogenic fusion protein MOZ-TIF2 inhibits nuclear receptor-mediated transcription and mislocalises CBP from PML bodies. In preparation.

Tsukiyama, T. (2002). The in vivo functions of ATP-dependent chromatin-remodelling factors. *Nature Reviews Molecular Cell Biology* 3, 422-429.

Tulsa, O. K. (1999). *Electronic Statistics Textbook* (Statsoft, Inc.)
<http://www.statsoft.com/textbook/stathome.html>.

Utley, R. T., and Cote, J. (2003). The MYST family of histone acetyltransferases. *Current Topics in Microbiology and Immunology* 274, 203-236.

Voegel, J. J., Heine, M. J., Tini, M., Vivat, V., Chambon, P., and Gronemeyer, H. (1998). The coactivator TIF2 contains three nuclear receptor-binding motifs and mediates transactivation through CBP binding-dependent and -independent pathways. *EMBO Journal* 17, 507-519.

Voegel, J. J., Heine, M. J., Zechel, C., Chambon, P., and Gronemeyer, H. (1996). TIF2, a 160 kDa transcriptional mediator for the ligand-dependent activation function AF-2 of nuclear receptors. *EMBO Journal* 15, 3667-3675.

Vousden, K. H., and Lu, X. (2002). Live or let die: the cell's response to p53. *Nature Reviews Cancer* 2, 594-604.

Wadgaonkar, R., Phelps, K. M., Haque, Z., Williams, A. J., Silverman, E. S., and Collins, T. (1999). CREB-binding protein is a nuclear integrator of nuclear factor- κ B and p53 signaling. *Journal of Biological Chemistry* 274, 1879-1882.

Watson, J. D., and Crick, F. H. C. (1953a). Genetical implications of the structure of deoxyribonucleic acid. *Nature* 171, 964-967.

Watson, J. D., and Crick, F. H. C. (1953b). Molecular structure of nucleic acids. *Nature* 171, 737-738.

Xu, J. M., and Li, Q. T. (2003). Review of the in vivo functions of the p160 steroid receptor coactivator family. *Molecular Endocrinology* 17, 1681-1692.

Xu, W., Chen, H. W., Du, K. Y., Asahara, H., Tini, M., Emerson, B. M., Montminy, M., and Evans, R. M. (2001). A transcriptional switch mediated by cofactor methylation. *Science* 294, 2507-2511.

Yang, X. J., Ogryzko, V. V., Nishikawa, J., Howard, B. H., and Nakatani, Y. (1996). A p300/CBP-associated factor that competes with the adenoviral oncoprotein E1A. *Nature* 382, 319-324.

Zelent, A., Guidez, F., Melnick, A., Waxman, S., and Licht, J. D. (2001). Translocations of the RAR alpha gene in acute promyelocytic leukemia. *Oncogene* 20, 7186-7203.

Zhu, J., and Emerson, S. G. (2002). Hematopoietic cytokines, transcription factors and lineage commitment. *Oncogene* 21, 3295-3313.